Towards an efficient treatment and valorization of plastic-waste : hydrogen production by plastic electrolysis

Nicolas Grimaldos Osorio

N°d'ordre NNT : 2022LYSE1148

THESE DE DOCTORAT DE L'UNIVERSITE DE LYON

opérée au sein de

l'Université Claude Bernard Lyon 1

Ecole Doctorale de Chimie de Lyon
N°ED206

Spécialité de doctorat : Chimie

Discipline : Electrochimie et Matériaux

Soutenue publiquement le 21/07/2022, par :

NICOLAS GRIMALDOS OSORIO

Vers un traitement et une valorisation efficace des déchets plastiques : Production d'hydrogène par électrolyse

Devant le jury composé de :

Baranova, Elena	Professeure (uOttawa, Canada)	Rapporteure
De Lucas Consuegra, Antonio	Professeur (UCLM, Spain)	Rapporteur
Gil Villarino, Sonia	Maître de Conférences (UCBL, France)	Examinatrice
Monteil, Vincent	Directeur de Recherche (CP2M, France)	Président
Rieu, Mathilde	Professeure assistante (EMSE, France)	Examinatrice
Tsampas, Michail (Mihalis)	Chercheur (DIFFER, Netherlands)	Examinateur
Vernoux, Philippe	Directeur de Recherche (IRCELYON, France)	Directeur de thèse
Caravaca, Angel	Chargé de Recherche (IRCELYON, France)	Co-directeur de thèse (Invité)
Passananti, Monica	Professeure Associée (UNITO, Italy)	Directrice de thèse
Sordello, Fabrizio	Professeur Assistant (UNITO, Italy)	Co-directeur de thèse (Invité)

N°d'ordre NNT : 2022LYSE1148

UNIVERSITÉ CLAUDE BERNARD LYON 1

ECOLE DOCTORALE DE CHIMIE DE LYON (N°ED206)

UNIVERSITÀ DEGLI STUDI DI TORINO

DOTTORATO DI RICERCA IN SCIENZE CHIMICHE E DEI MATERIALI (35° CICLO)

DOCTORAL THESIS

Doctoral specialty: Chemistry
Discipline: Electrochemistry and Materials

Publicly defended on 21/07/2022, by:

NICOLAS GRIMALDOS OSORIO

Towards an efficient treatment and valorisation of plastic-wastes: Hydrogen production by electrolysis

---

Before the jury composed by:

Baranova, Elena	Professor (uOttawa, Canada)	Rapporteur
De Lucas Consuegra, Antonio	Professor (UCLM, Spain)	Rapporteur
Gil Villarino, Sonia	Associate Professor (UCBL, France)	Examiner
Monteil, Vincent	Research Director (CP2M, France)	Examiner
Rieu, Mathilde	Assistant Professor (EMSE, France)	Examiner
Tsampas, Michail (Mihalis)	Researcher (DIFFER, Netherlands)	Examiner
Vernoux, Philippe	Research Director (IRCELYON, France)	Supervisor
Caravaca, Angel	Researcher (IRCELYON, France)	Co-supervisor (Invited)
Passananti, Monica	Associate Professor (UNITO, Italy)	Supervisor
Sordello, Fabrizio	Assistant Professor (UNITO, Italy)	Co-supervisor (Invited)

N°d'ordre NNT : 2022LYSE1148

THESE DE DOCTORAT DE L'UNIVERSITE DE LYON

opérée au sein de

l'Université Claude Bernard Lyon 1

Ecole Doctorale de Chimie de Lyon
N°ED206

Spécialité de doctorat : Chimie

Discipline : Electrochimie et Matériaux

Soutenue publiquement le 21/07/2022, par :

NICOLAS GRIMALDOS OSORIO

Vers un traitement et une valorisation efficace des déchets plastiques : Production d'hydrogène par électrolyse

Devant le jury composé de :

Baranova, Elena	Professeure (uOttawa, Canada)	Rapporteure
De Lucas Consuegra, Antonio	Professeur (UCLM, Spain)	Rapporteur
Gil Villarino, Sonia	Maître de Conférences (UCBL, France)	Examinatrice
Monteil, Vincent	Directeur de Recherche (CP2M, France)	Examinateur
Rieu, Mathilde	Professeure assistante (EMSE, France)	Examinatrice
Tsampas, Michail (Mihalis)	Chercheur (DIFFER, Netherlands)	Examinateur
Vernoux, Philippe	Directeur de Recherche (IRCELYON, France)	Directeur de thèse
Caravaca, Angel	Chargé de Recherche (IRCELYON, France)	Co-directeur de thèse (Invité)
Passananti, Monica	Professeure Associée (UNITO, Italy)	Directrice de thèse
Sordello, Fabrizio	Professeur Assistant (UNITO, Italy)	Co-directeur de thèse (Invité)

Université Claude Bernard – LYON 1

Président de l'Université	M. Frédéric FLEURY
Président du Conseil Académique	M. Hamda BEN HADID
Vice-Président du Conseil d'Administration	M. Didier REVEL
Vice-Président du Conseil des Etudes et de la Vie Universitaire	M. Philippe CHEVALLIER
Vice-Président de la Commission de Recherche	M. Petru MIRONESCU
Directeur Général des Services	M. Pierre ROLLAND

COMPOSANTES SANTE

Département de Formation et Centre de Recherche en Biologie Humaine	Directrice : Mme. Anne-Marie SCHOTT
Faculté d'Odontologie	Doyenne : Mme. Dominique SEUX
Faculté de Médecine et Maïeutique Lyon Sud - Charles Mérieux	Doyenne : Mme. Carole BURILLON
Faculté de Médecine Lyon-Est	Doyen : M. Gilles RODE
Institut des Sciences et Techniques de la Réadaptation (ISTR)	Directeur : M. Xavier PERROT
Institut des Sciences Pharmaceutiques et Biologiques (ISBP)	Directrice : Mme. Christine VINCIGUERRA

COMPOSANTES & DEPARTEMENTS DE SCIENCES & TECHNOLOGIE

Département Génie Electrique et des Procédés (GEP)	Directrice : Mme. Rosaria FERRIGNO
Département Informatique	Directeur : M. Behzad SHARIAT
Département Mécanique	Directeur : M. Marc BUFFAT
Ecole Supérieure de Chimie, Physique, Electronique (CPE Lyon)	Directeur : M. Gérard PIGNAULT
Institut de Science Financière et d'Assurances (ISFA)	Directeur : M. Nicolas LEBOISNE
Institut National du Professorat et de l'Education	Administrateur Provisoire : M. Pierre CHAREYRON
Institut Universitaire de Technologie de Lyon 1	Directeur : M. Christophe VITON
Observatoire de Lyon	Directrice : Mme. Isabelle DANIEL
Polytechnique Lyon	Directeur : M. Emmanuel PERRIN
UFR Biosciences	Administratrice provisoire : Mme. Kathrin GIESELER
UFR des Sciences et Techniques des Activités Physiques et Sportives (STAPS)	Directeur : M. Yannick VANPOULLE
UFR Faculté des Sciences	Directeur : M. Bruno ANDRIOLETTI

Università degli Studi di Torino

Doctoral School of the University of Torino

PhD Programme in Chemical and Materials Sciences (35th Cycle)

Towards an efficient treatment and valorisation of plastic-wastes: Hydrogen production by electrolysis

Candidate:	**Nicolas Grimaldos Osorio**
Supervisors:	**Dr. Philippe Vernoux** Research Director (IRCELYON, France) **Dr. Monica Passananti** Associate Professor (UNITO, Italy)
Co-supervisors:	**Dr. Angel Caravaca** Researcher (IRCELYON, France) **Dr. Fabrizio Sordello** Assistant Professor (UNITO, Italy)
Jury Members:	**Dr. Elena Baranova** Professor (uOttawa, Canada) **Dr. Antonio De Lucas Consuegra** Professor (UCLM, Spain) **Dr. Sonia Gil Villarino** Associate Professor (UCBL, France) **Dr. Vincent Monteil** Research Director (CP2M, France) **Dr. Mathilde Rieu** Assistant Professor (EMSE, France) **Dr. Michail (Mihalis) Tsampas** Researcher (DIFFER, Netherlands)
Head of the Doctoral School:	Prof. Alberto Rizzuti
PhD Programme Coordinator:	Prof. Bartolomeo Civalleri

Torino, 2022

Acknowledgements

There is no work that is possible without the help of others. Thank you very much to all the people who supported me in diverse ways along this path.

First, I would like to express my gratitude to each of the members of the jury who accepted to judge and evaluate my thesis work. Special thanks to Elena Baranova and Antonio de Lucas Consuegra for their availability and diligence as rapporteurs. Likewise, my sincere gratitude to Sonia Gil Villarino, Vincent Monteil, Mathilde Rieu and Michail (Mihalis) Tsampas for agreeing to be the evaluators of this thesis.

I would like to acknowledge my supervisors at IRCELYON, without whom this work would have been much more difficult and who placed their trust and support in me at every stage of this process. First to Philippe Vernoux, who welcomed me into his team and followed my training and work during these three years. I acknowledge him for his kindness, patience and openness, as well as for the fruitful scientific discussions and cheerful talks on different topics. Thank you so much for all the invaluable advice and help. In the same way, I want to express my sincere gratitude and appreciation to Angel Caravaca, who was always present and taught me everything from day one. I thank him for always being available to discuss and analyse the results, for his ideas and unconditional help. Without his support and mentorship, this work would not have been possible.

Similarly, I want to express my appreciation to my supervisors at UniTo, who gave me the valuable opportunity to develop this thesis under co-supervision. Thanks to them, I could discover a new work mentality and be part of a laboratory that welcomed me in the best way since my arrival. To Monica Passananti for her help throughout this process, for her valuable advice and her good humour. And to Fabrizio Sordello for all his help during my research stay, for his availability to analyse the results and for the talks on various subjects. The experience in Turin, although short, was incredibly enriching.

This work would not have been possible without the funding and support of l'Ecole Urbaine de Lyon (EUL). Many thanks to each of the team members, especially Jérémy Cheval and Alice Sender, for their help during these three years and for the work they have done. Infinite thanks to EUL for showing me different ways of doing science and opening my thinking to areas that I would never have known otherwise. The world of science needs more projects like this.

I would like to thank the different analysis and characterisation services at IRCELYON. Sincere thanks to each person who was always ready and available to perform and help me analyse these measurements: Yoann Aizac, Pascal Mascunan, Nicolas Bonnet, Laurance Burel, Mimoun Aouinem, and Chantal Lorentz. Many thanks to Antoinette Boreave, Pierrick Peixoto and Laurence Retailleau-Mevel for their technical assistance during the different experiments and in the laboratory. Likewise, I would like to thank Fabrizio Caldera for his help with the viscosity measurements and Francesco Pellegrino for his collaboration with the synthesis setup. Special recognition to Jesús González Cobos, who was always available to discuss the results and help me when necessary.

A special thanks to all the members of the CARE (IRCELYON) team, for the valuable moments, for the excellent work environment and for the talks during the group meetings and the coffee. Sharing this time was very enriching. Thanks to all my colleagues and friends at IRCELYON: Brenda, Alice (Jie), Guillermo, Estela, Simon, Florent, Carole, Mathieu, Elizabeth, Eddy, Rulan. As well as my colleagues in the UniTo lab: Giulia, Angela, Fede, Robi, Davide, Bea, Erica, Marti, Marco. Thank you all for the good times, the laughs and the shared experiences.

Thanks to the people who have been present along this path. To my friends who have become family: Sasha, Mishu, Nato and Mafe. To those who have accompanied me since my arrival in Lyon and have made this time memorable: Dani, Carlos, Caro P., Andrés, Anita, Santiago, Sergio, and all those I may have forgotten to mention. Thanks to my inseparable and great music and tennis partners, Juan and Diego. To the beautiful people that Turin left me. Thanks to those who have been around from the distance for so many years, it is always nice to know that you are still there.

Many thanks to all the members of my family, who are always present in my memories and heart. Finally, infinite thanks to my mom, my dad, and my brother. There is no way in the world to show how valuable your support has been. Thank you for being my guide in life and for always being there both in happy and difficult times. Thank you for showing me the right path to follow and for being by my side every step of the way. Home will always be where you are. I love you. This thesis is dedicated to the three of you.

Thanks, grazie, merci, GRACIAS.

Abstract

Hydrogen is called to play an important role in the energy transition because of its ability to act as an energy carrier without emitting carbon dioxide. The production of carbon-free hydrogen is a major concern in order to make its use a sustainable solution. The electrolysis of water makes it possible to generate pure and carbon-free hydrogen from the various intermittent sources of renewable energy. Nonetheless, the energy demand for this process is elevated (>1.23 V at room temperature). The electro-oxidation of organic molecules was suggested as an answer to this problem because their thermodynamic oxidation potential is much lower than that of the oxygen evolution reaction, which takes place at the anode of the electrolysers. Organic waste could be a sustainable source of organic fuels if their electro-oxidation kinetics are sufficiently efficient.

Nowadays, several problems are threatening the stability of life on the planet and the survival of humanity is in question. We have reached the point of having to reconsider our models of consumption and production of energy and goods. For this reason, not only energy sustainability must be evaluated, but also the fate of the waste that we produce daily. One of the most important and environmentally harmful wastes is plastic, which can also be considered an important source of hydrogen because of its organic nature. Taking advantage of this type of waste for the production of H_2 seems to be an attractive option, as long as the multiple limitations that this application represents can be overcome. The aim of this work is to explore in depth, for the first time, the electrolysis of polymers at low temperature for the production of hydrogen.

This thesis work proposes a new approach to understand the electrolysis of plastic waste using two model polymers: polymethyl methacrylate (PMMA) and polyethylene glycol (PEG). The different composition of these polymers, as well as the use of different experimental strategies, allowed us to establish a series of significant discoveries on the feasibility of this type of process, as well as a series of improvements necessary to upturn their performance. The electro-oxidation of the lateral ester groups of PMMA has been approached according to three different strategies: *(i)* treatment of model molecules, *(ii)* solubilisation in a binary solvent, and *(iii)* direct attack by electrochemical methods. On the other hand, the electro-oxidation of aqueous solutions of PEG allowed us to deepen our understanding of the phe-

nomena involved in the breaking of C-O bonds characteristic of a wide range of polymeric materials.

For the electrochemical treatment of PMMA and PEG, the transport of macromolecules in the porosity of the electrodes strongly limits the kinetics of electro-oxidation. A series of characterisation techniques were used to determine the impact of the porosity and the nanostructure of the different implemented electrodes. A more porous morphology of the Pt/Carbon catalyst associated with a better dispersion of the Pt nanoparticles makes possible to considerably increase the electrochemical conversion performance of the PEG. Finally, it is proposed that the technology to be implemented to recover plastic waste depends on the nature of the most easily electro-oxidisable chemical bonds in the main polymer chain.

Keywords: Electro-oxidation of plastics, polymethyl methacrylate (PMMA), polyethylene glycol (PEG), electrolysis, proton exchange membrane (PEM) cell, polymer electro-reforming, decarbonised hydrogen production.

Résumé

L'hydrogène est appelé à jouer un rôle important dans la transition énergétique en raison de sa capacité à agir comme vecteur énergétique sans émission de dioxyde de carbone. La production d'hydrogène décarboné est une préoccupation majeure afin de faire de son utilisation une solution durable. L'électrolyse de l'eau permet de générer de l'hydrogène pur et décarboné à partir des différentes sources intermittentes d'énergie renouvelable. Néanmoins, la demande d'énergie pour ce processus est élevée (>1.23 V à température ambiante). L'électro-oxydation de molécules organiques pourrait pallier ce problème car leur potentiel thermodynamique d'oxydation est plus faible que celui de la réaction d'évolution de l'oxygène qui se déroule à l'anode des électrolyseurs. Les déchets organiques pourraient être une source durable de combustibles organiques si leur cinétique d'électro-oxydation est suffisamment performante.

Actuellement, plusieurs problèmes menacent la stabilité de la vie sur la planète et la survie de l'humanité est remise en question. Nous en sommes arrivés à devoir reconsidérer nos modèles de consommation et de production d'énergie et de biens. Pour cette raison, non seulement les sources durables d'énergie doivent être évaluées, mais aussi le devenir des déchets que nous produisons au quotidien. L'un des déchets les plus importants et nuisibles pour l'environnement est le plastique, qui peut également être considéré comme une source importante d'hydrogène en raison de sa nature organique. Tirer parti de ce type de déchets pour la production d'H_2 semble être une option intéressante, à condition de pouvoir surmonter les multiples limitations que représente cette application. L'objectif de ce travail est d'explorer en profondeur, pour la première fois, l'électrolyse de polymères à basse température pour la production d'hydrogène.

Ce travail de thèse propose une nouvelle approche pour comprendre l'électrolyse de déchets plastiques en utilisant deux polymères modèles : le polyméthacrylate de méthyle (PMMA) et le polyéthylène glycol (PEG). La composition différente de ces polymères, ainsi que l'utilisation de différentes stratégies expérimentales, nous ont permis d'établir une série de découvertes significatives sur la faisabilité de ce type de procédé ainsi que sur les verrous restant à lever. L'électro-oxydation des groupements esters latéraux du PMMA a été abordée selon trois stratégies différentes : *(i)* traitement de molécules modèles, *(ii)* solubilisation dans un solvant

binaire, et *(iii)* attaque directe par des méthodes électrochimiques. D'autre part, l'électro-oxydation de solutions aqueuses de PEG nous a permis d'approfondir notre compréhension des phénomènes impliqués dans la rupture des liaisons C-O caractéristiques d'une large gamme de matériaux polymères.

Pour le traitement électrochimique du PMMA et du PEG, le transport des macromolécules dans la porosité des électrodes limite fortement les cinétiques d'électro-oxydation. Une série de techniques de caractérisation ont été utilisées pour déterminer la porosité et la nanostructure des différentes couches catalytiques mise en œuvre. Une morphologie plus poreuse du catalyseur Pt/Carbone associée à une meilleure dispersion des nanoparticules de Pt permet d'augmenter considérablement les performances de conversion électrochimique du PEG. Enfin, il est proposé que la technologie à mettre en œuvre pour valoriser un déchet plastique dépende de la nature des liaisons chimiques les plus facilement électro-oxydables dans la chaîne principale des polymères.

Mots clés : Électro-oxydation des plastiques, polyméthacrylate de méthyle (PMMA), polyéthylène glycol (PEG), électrolyse, pile à membrane échangeuse de protons (PEM), électro-reformage de polymères, production d'hydrogène décarboné.

Sintesi

L'idrogeno svolgerà un ruolo importante nella transizione energetica per la sua capacità di agire come vettore energetico senza emettere biossido di carbonio. La produzione di idrogeno senza emissioni di CO_2 è una delle principali preoccupazioni al fine di rendere il suo utilizzo una soluzione sostenibile. L'elettrolisi dell'acqua permette di generare idrogeno puro e senza emissioni di CO_2 dalle varie fonti intermittenti di energia rinnovabile. Tuttavia, la richiesta di energia per questo processo è elevata ($>$1.23 V a temperatura ambiente). L'ossidazione di molecole organiche, mediante processi elettrochimici, è stato suggerita come una possible risposta a questo problema perché il potenziale di ossidazione termodinamico di alcune molecole organiche è inferiore a quello della reazione dell'ossigeno, che avviene all'anodo degli elettrolizzatori. I rifiuti organici potrebbero essere una fonte sostenibile di combustibili organici se la loro cinetica di elettroossidazione è sufficientemente efficiente.

Al giorno d'oggi, diversi problemi minacciano la stabilità della vita sul pianeta e la sopravvivenza dell'umanità è in discussione. Siamo arrivati al punto di dover riconsiderare i nostri modelli di consumo e produzione di energia e di beni. Per questo non va valutata solo la sostenibilità energetica, ma anche l'intero ciclo di vita dei servizi dei beni prodotti. Uno dei rifiuti più importanti e dannosi per l'ambiente è la plastica, che tuttavia può essere considerata un'importante fonte di idrogeno grazie alla sua componente organica. Lo sfruttamento di questo tipo di scarti per la produzione di H_2 sembra essere un'opzione allettante, a patto che si possano superare le molteplici limitazioni che questa applicazione presenta. L'obiettivo di questo lavoro è esplorare a fondo, per la prima volta, l'elettrolisi di polimeri a bassa temperatura per la produzione di idrogeno.

Questo lavoro di tesi propone un nuovo approccio per comprendere l'elettrolisi dei rifiuti di plastica, mediante l'uso di due polimeri modello: polimetilmetacrilato (PMMA) e polietilenglicole (PEG). La diversa composizione di questi polimeri, nonché l'utilizzo di diverse strategie sperimentali, ha permesso di raccogliere una serie di importanti dati sulla fattibilità di questo tipo di processo, nonché una serie di cambiamenti necessari per migliorarne le prestazioni. L'elettroossidazione dei gruppi esterei laterali del PMMA è stata valutata attraverso tre diverse strategie: *(i)* studio di molecole modello, *(ii)* solubilizzazione in un solvente binario e

(iii) attacco diretto con metodi elettrochimici. D'altra parte, l'elettroossidazione di soluzioni acquose di PEG ci ha permesso di approfondire la comprensione dei fenomeni coinvolti nella rottura dei legami C – O caratteristici di un'ampia gamma di materiali polimerici.

Per il trattamento elettrochimico sia del PMMA, sia del PEG, il trasporto di macromolecole nella porosità degli elettrodi limita fortemente la cinetica di elettroossidazione. Sono state utilizzate una serie di tecniche di caratterizzazione per determinare l'impatto della porosità e della nanostruttura dei diversi elettrodi implementati. Un aumento della porosità del catalizzatore Pt/Carbon associata ad una migliore dispersione delle nanoparticelle di Pt permette di aumentare considerevolmente le prestazioni di conversione elettrochimica del PEG. Infine, si propone che la tecnologia da implementare per recuperare i rifiuti di plastica dipenda dalla natura dei legami chimici più facilmente elettro-ossidabili nella catena polimerica principale.

Parole chiave: Elettroossidazione delle materie plastiche, polietilenglicole (PEG), polimetilmetacrilato (PMMA), elettrolisi, cella a membrana a scambio protonico (PEM), elettro-reforming di polimeri, produzione di idrogeno decarbonizzato.

Contents

List of Figures

List of Tables

General Introduction

General Introduction

Hydrogen is an essential industrial target area, not only because of its use as an energy carrier and practical employment in fuel cells but also for its role as a significant raw material for the chemical industry [1]. This energy dense fuel can be produced by different processes (CH_4 reforming being the most common), but the electrolysis of water is called to be an environmentally friendly solution. This process has taken force lately because it can be easily integrated into the electrical grid and use renewable energy sources (i.e. solar or wind) to produce pure decarbonated H_2 from water, producing only O_2 as a by-product [2]. However, the thermodynamic cell voltage to achieve the water electrolysis reaction is around 1.23 V at room temperature [3]. Consequently, different strategies have been proposed to electrolyse organic molecules instead of water at the anode of low-temperature electrolysers to reduce the energy demand. Plastic wastes contain an abundant source of hydrogen and can be a promising renewable feedstock for electrolysis. Research on this sense would help to the resolution of two simultaneous problems: the reduction of the energy needs of the electrolysis process and finding new ways to treat and valorise plastic wastes. This PhD work seeks to establish a series of initial findings on the electro-oxidation of polymeric materials at low temperature for the production of hydrogen. The conceptual and experimental development of the studies conforming the present manuscript was performed in co-supervision between the IRCELYON (Institut de Recherches sur la Catalyse et l'Environnement de Lyon, Unité Mixte de Recherche 5256 CNRS - Université de Lyon) and the Department of Chemistry of the University of Turin (Università degli Studi di Torino, UNITO). The PhD grant and the funding for the mobility were possible thanks to the support of the École Urbaine de Lyon (EUL), an « Institut Convergences » program in the frame of the Plan d'Investissement d'Avenir (PIA2).

This manuscript was divided into five main chapters, some of which have already been partially or completely issued in indexed publications. The first chapter, in its initial part, explores the environmental and energy context that gave rise to the conception of this work. The issues of waste production, and how the simultaneous production of hydrogen could be an answer to both, were addressed. Then, it delves into the production processes of H_2 by electrochemical means from organic waste at low and intermediate temperatures. In the final part, the handful of publications that have seen the light throughout this time are exposed. The choice of model polymeric materials (poly(methyl methacrylate) (PMMA) and polyethylene glycol (PEG)) to facilitate the understanding of the phenomena involved in the electro-oxidation of this type of materials is also justified. As it will be exposed later, the understanding of the electro-oxidation of these two kinds of polymers would allow

a first step into the comprehension of the reaction paths involved in the electro-oxidation of similar macromolecules.

Hence, a four-stage research work is proposed to explore different approaches regarding the treatment of plastics by electrochemical means. The second chapter of the present work deals with the study of a model molecule of PMMA (methyl pivalate, MP) that represents the most relevant chemical bonds of that polymer. For that matter, a proton-exchange membrane (PEM) reactor was used to find important information about the feasibility of the ester group breaking. This preliminary electrochemical study has confirmed the production of pure hydrogen at the appropriate conditions of concentration and temperature with an on-line mass spectrometer (MS). We have also determined the basic kinetic parameters involved in this type of process.

The third chapter of this thesis explores for the first time the electro-oxidation of PMMA molecules in solution. By employing a dissolution strategy with a binary solvent, it was possible to understand the main limitations of a typical commercial electrode material based on Pt/C. Similarly, a home-made anode was prepared to overcome the main problems of the system, such as the accumulation of PMMA and the poisoning by adsorption of different species. This work was performed in a two-electrode cell arrangement that facilitates the operation and favours the recognition of elemental electrochemical aspects.

The results of the previous study suggested that the electro-oxidation of PMMA macromolecules could be affected by the size of the chain or the particle diameter in the case of not solubilised polymers. Following this idea, the fourth chapter tried to explore the direct electro-oxidation of PMMA nanoparticles. In that regard, the synthesis of PMMA particles suspensions was performed in order to produce a wide range of molecular weights. These samples were further characterised and studied for the production of hydrogen in a three-electrode cell arrangement. Additionally, two pre-treatment methodologies were tested to facilitate the production of species prone to be electrolysed by basic and acid hydrolysis of the PMMA particles.

The final part of the work was devoted to the second selected polymer, PEG. With these water-soluble compounds, a PEM reactor was equally employed to facilitate the understanding of different features at the anodic level. First, a preliminary study with pure ethylene glycol was performed to get basic information about the system. Then, electro-oxidation tests on a series of PEG from 200 to 4000 g mol^{-1} allowed us to understand the limitations of the electrode material initially used. Subsequently, an optimisation study was performed to formulate an electrode with much better performance and further study the electro-oxidation of PEG. Different characterisations were performed to help the comprehension of the followed reac-

tion path, and the production of pure H_2 was confirmed by gas phase analysis.

References

[1] Ayers, K., Danilovic, N., Ouimet, R. et al. Perspectives on Low-Temperature Electrolysis and Potential for Renewable Hydrogen at Scale. *Annual Review of Chemical and Biomolecular Engineering*, 10:219–239, 2019. doi: 10.1146/annurev-chembioeng-060718-030241.

[2] Shiva Kumar, S. and Himabindu, V. Hydrogen production by PEM water electrolysis – A review. *Materials Science for Energy Technologies*, 2(3):442–454, 2019. doi: 10.1016/j.mset.2019.03.002.

[3] González-Cobos, J., Baranton, S. and Coutanceau, C. A Systematic in Situ Infrared Study of the Electrooxidation of C3 Alcohols on Carbon-Supported Pt and Pt-Bi Catalysts. *Journal of Physical Chemistry C*, 120(13):7155–7164, 2016. doi: 10.1021/acs.jpcc.6b00295.

CHAPTER 1

Context and state-of-the-art

Context and state-of-the-art

The initial part of this work has been devoted to the contextualisation of the problem addressed, as well as a bibliographic review that allows for a better understanding of the scientific principles that were used throughout the investigations performed during this project. Initially, the social and environmental background is briefly explored, with an emphasis on plastic waste generation over time and the current treatment strategies. Then, the energy context and problems are addressed, along with the role of hydrogen in the decarbonisation of economy and industry. Successively, I discuss a previous publication on the use of electrochemical treatment strategies of organic waste (including plastic materials) in parallel with the production of H_2. And finally, the state-of-the-art on the electrochemical reforming of plastics is introduced together with the position of this research regarding the previously discussed topics and the planned research line.

1.1 Societal and environmental context

After the beginning of the *First Industrial Revolution* by the late 18th century, our society embarked on a series of changes that allowed the transition from rural-based communities to the modern era [1, 2]. The agricultural uprising, the improvement of the textile industry, the expansion of the iron and steel industry, the large-scale production of several chemicals, and the evolution of transportation as we know it today, all started at that time [2]. However, even if the developments achieved during that period represented a milestone in the progress of humankind in multiple areas, it can also be considered as the breakthrough that led to the foundation of many new problems [3]. Today, our planet encounters several environmental issues directly related to the flourishing of industrial society and the enlarged human capacity of transforming nature: overexploitation of non-renewable resources (such as fossil fuels), considerable extinction of animal species, human population growth, climate and habitat degradation, increasing natural disasters, etc. [4–8]. All these things considered, the concept of "Anthropocene" was employed to describe the epochal time during which humankind activities became a dominant influence on Earth's stability and future, but its formalisation is still debated [9–14].

The trace of humanity on the planet can be followed and measured by studying the stratigraphic signatures of our activities, most of them driven by three preponderant factors: accelerated technological development, the rapid rise of the human population, and increased consumption of resources [15]. Recent anthropogenic deposits are mainly composed of products of mining, industrial, and construction activities, which mass production started during the *Great Acceleration*

after World War II (Figure 1.1) [15]. These include materials such as artificial radionuclides, metallic aluminum, black carbon, ash particles, persistent organic pollutants, a broad diversity of biological markers, and others [15, 16]. Similarly, organic polymers (also known as plastics) have been suggested as an environmental and anthropogenic geological indicator [15–19]. On account of its ubiquity and longevity, plastics materials could reach a wide variety of places all over the globe and they represent a special threat to the environment [20–22]. The distribution of plastic residues has been documented for almost any location, from large landfill sites to sedimentary debris in rocky surfaces, from the oceans to the Artic waters and remote lakes [23–32]. In this thesis, we explored the development of novel techniques, aiming for the efficient transformation and valorisation of plastic wastes into hydrogen.

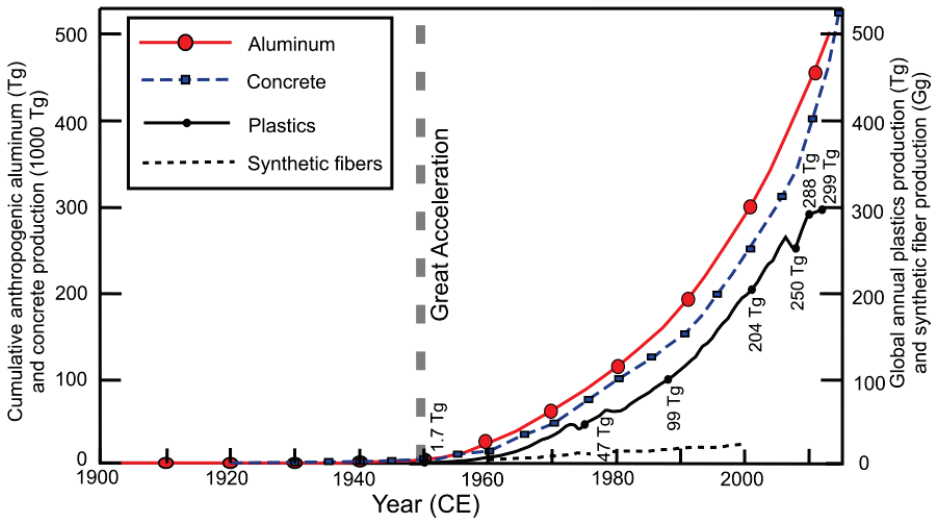

Figure 1.1: The production of selected new anthropogenic materials: cumulative growth of manufactured aluminum in the surface environment, cumulative growth of production of concrete, annual growth of plastics production, and synthetic fibres production. Adapted from [15].

On the other hand, the prosperity of the human population is related to different factors, such as the access to a regular food supply and the availability of natural resources and energy [33]. Energy, being the primary driving force of all economic activities, grew into a global necessity and it is now in the focus of the sustainable development targets of most of our societies [34, 35]. In this sense, nowadays we rely massively on the combustion of fossil fuels (coal, oil and natural gas). These resources are not only limited, but they are also responsible for most of worldwide emissions of CO_2 to the atmosphere, leading to the well-known global warming on account of the greenhouse effect. After the Kyoto protocol, most countries committed to decrease the CO_2 emissions [36, 37], since the cost for the planet is becoming unsustainable in the long run [38–40]. Hence, the adoption of non-conventional

and renewable energy sources is the only alternative to traditional energy production. Resources such as the sun, wind and tides can be exploited in an almost unlimited extend, but they are characterised by their irregular generation and high dependence on weather. Therefore, it supposes a fluctuating energy production and a consequent technological challenge regarding the storage of this renewable electricity [41].

Finding solutions to assure the sustainable development of energy systems is also of scientific concern. The following sections explain why this work is on the border between the treatment of plastic waste, energy recovery, and the storage of renewable energy, and how it responds to these necessities.

1.2 Plastics and waste valorisation processes

Polymers are organic macromolecules that include a large variety of materials formed by smaller units called monomers. They are both from natural or synthetic origin, in the latter case produced by a chemical reaction known as *polymerisation* [42–44]. Because of their wide range of characteristics, polymers can be classified depending on different criteria, for example: structure, synthesis mechanism, chain topology, origin, etc. [43, 44]. One of the most common classifications is the one that considers their use, which derives from the thermodynamic and mechanical properties of the materials. Among them, it is possible to find [44]:

- Plastics or thermoplastics: Polymers that behave as viscous liquids when heated to a specific temperature. These materials can be shaped with the help of a mould for several times, however, this repetitive process can degrade their properties.
- Thermosets: Polymers that are made by chemical reaction of precursors into the mould, forming a cross-linked network that cannot be reshaped under heating.
- Elastomers and rubbers: Flexible materials that exhibit a high impact resistance. These polymers are usually formed into a desired shape and then cross-linked to preserve shape and stability.
- Fibres: These are polymers with a high resistance to deformation and high moduli, but with a poor capacity of elongation.
- Paints and coatings: This group is based on the materials' capacity of forming a film, acting as a binder or carrier of pigments and other additives. The materials belonging to this category are usually used for surface treatment and protection.

The total production volume could be used as well to classify polymers: *commodity*, *engineering*, or *specialty/high performance* [44]. Some examples of the so-called *commodity polymers*, with the higher production volumes, are: polyethylene (LDPE and HDPE), polypropylene (PP), poly(vinyl chloride) (PVC), poly(ethylene terephthalate) (PET), polystyrene (PS), and derivatives [44, 45]. All the previously mentioned are also *thermoplastics*, or just *plastics*, coining the generic name for most of the generally used polymers [46].

The industrial fabrication of plastics from 1950 changed the world drastically. In fact, no other kind of man-made materials have been ever produced in the same proportions, perhaps just except for some construction materials [15]. Unfortunately, the exponential growth of the production and consumption of plastics is accompanied by an uncontrollable generation of waste that does not seem to stop as they are used in everyday life applications [47]. During the last years, just a small decrease in the plastics industry production was reported in the course of the first half of 2020 because of the COVID-19 pandemic [48, 49], but it was followed by a strong recovery thanks to the usage of these materials for many applications, from surgical gloves to home-delivered groceries [50]. Traditionally, plastic waste treatment processes are classified into four main categories, as pictured in Figure 1.2 [51]:

- Primary: This method uses semi-clean scrap, industrial or single-polymer debris to fabricate new products with similar characteristics that those of the original materials [47]. It is also known as re-extrusion and it represents the main recycling technique, despite of the requirement of high quality of plastic waste [52]. The most common example is the recycling of used PET to produce new bottles [53].
- Secondary: Mechanical treatment of plastic waste to produce less demanding merchandises. The quality of the final material strongly depends on the initial characteristics of the used plastic waste. Better known as mechanical recycling, it can be applied to single-polymers as PE, PP, PS, etc. This process needs several steps, including separation, cleaning, milling, agglutination and extrusion [47, 54].
- Tertiary: Equally known as chemical recycling, it groups the advanced strategies for converting polymeric materials into smaller molecules that can serve as feedstock for the production of new compounds [47]. These processes are based on the transformation of the chemical structure of the plastic waste and the methods are diverse, as shown in Figure 1.2 [51], making possible the retrieval of the original conforming monomers or the production of other chemicals. Large quantities of heterogeneous plastic waste can be treated by

chemical methods that can also be integrated into the already existent petrochemical industry, giving much more profit to than other recycling strategies [52, 54, 55].

— Quaternary: It is based on the idea of the energy recovery by incineration of plastic waste for the production of heating, steam and/or electricity [54]. It is usually the last option when no other recycling methods are suitable or to reduce the volume of landfilling waste disposal. Plastic waste usually posses a high calorific value as it derives from crude oil, with values even higher than some known fossil fuels [51, 55]. Although it is a simple method to treat plastic waste, the main disadvantage of the quaternary method is the pollution caused by the combustion process, notably by the quantities of CO_2, CO, halogenated compounds, particulate matter and VOCs emanated from incinerator effluents [56].

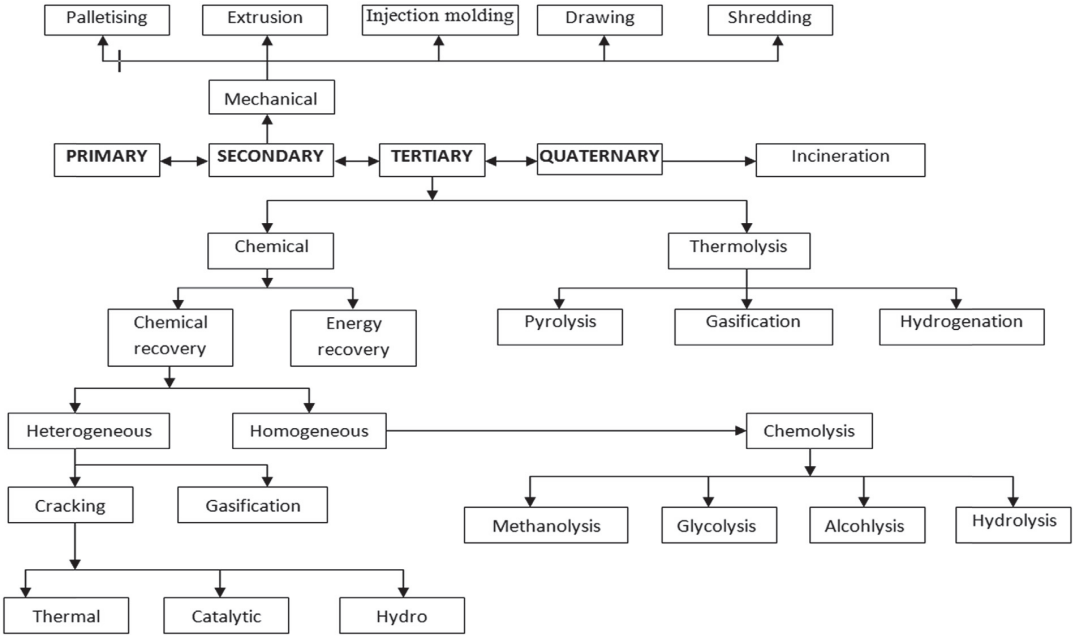

Figure 1.2: General overview of the plastic waste recycling approaches. Adapted from [51].

Even if there is a wide variety of possibilities for plastic waste valorisation, these recycling processes are insufficient to treat the growing quantities of plastic waste. In 2020, the total plastic post-consumer waste collected in the UE was around 29.5 Mt, from which ∼34% is being recycled (mainly by primary and secondary methods) and ∼42% of the total is sent to Energy Recovery (quaternary methods) [48]. An important part of the plastic wastes (6.9 Mt) finished in landfill facilities [48], an amount that shows a decreasing tendency over the last years, but still represents a hazard for the environment. A different trend can be observed in the USA, where over 80% of the total plastic waste is disposed in landfills, around 10% is

incinerated and the small remaining portion is recycled [57]. The environmental threats of landfilling are numerous, including the scarcity of land and groundwater pollution. But the major pollution is caused by the degradation of plastic waste upon the effect of ultraviolet (UV) radiation, leading to the production of micro and nanoplastics [57, 58]. These fragments are themselves of risk for aquatic ecosystems, but their toxicity becomes even more worrying if considered the release of additives and impurities as the degradation process takes place [58].

All in all, plastic waste is still a challenge both from the environmental and economic point of view. Taking under consideration that the production of 1 kg of plastic consumes around 2 kg of crude oil [57], one could estimate the quantity of this scarce resource that finishes in landfills and water sources. In fact, plastic waste is considered as a source of energy when it is treated in waste-to-energy plants, but with the subsequent environmental effects. Nowadays, optimise the transformation of plastics waste is a concern in several research fields and no singular solution is possible. A problematic of this magnitude should be approached from as much flanks as possible and that is the case, for example, of the research on biodegradation of plastics or its re-use for the construction industry [59]. Similarly, the production of bio-sourced plastics to lessen the utilisation of fossil resources and reduce the environmental impact is an alternative that is currently under development [60]. This problem has even been approached from the economic and societal point of view by presenting new ways to understand and evaluate plastic waste as a main actor of circular economy strategies [61–63].

The research that has been carried out during the present work deals with tertiary treatment (i.e., the chemical transformation) of plastics. Polymers are organic molecules mainly composed by C, H, and O, and in minor quantities by others like N and S. In our case, we consider plastic waste as a source of hydrogen. While H_2 can be obtained from plastic by several technologies, here we propose a new path. Before explaining our approach in detail, we will take a look at the role of H_2 in the future of sustainable development, energy and economy, and then, we will present the link between the treatment of plastic waste and the production of this important compound.

1.3 Energy outlook and the hydrogen economy

Energy is the primary driving force of all economic activities, and it is now in the focus of the global sustainable development targets [34, 35]. Economic growth exhibits a complex relation with factors such as the energy production and consumption, pollution and the efforts to achieve a sustainable development [64]. Govern-

ments are taking real decisions to commit to the clean energy transition without putting pressure on economy and citizens. However, even if we know that long-term climate targets need long-term efforts to be achieved, during the last years we have witnessed unforeseen circumstances that may change the curse of these resolutions, for example: the pandemic-induced recession, weather-related factors, and outages on the supply [65]. Only one thing is certain, to achieve the 2015 Paris Agreement objectives, CO_2 emissions related to energy production need to decline effectively [66, 67].

Figure 1.3 displays the projections of the global worldwide electricity mix in 2040 under different scenario types (including reference, evolving and ambitious climate policies), showing an overall growth of the total electricity generation. Fossil fuels (mainly natural gas, since it seems to be the cleanest of all fossil fuels) continue to have an important share in the cases of reference and evolving policies, but they show an important decrease in all ambitious climate scenarios. Hydro and nuclear resources are planned to increase in all cases, but the most important impact is the one from the non-hydro renewable energies that reveal a considerable portion progression [66]. To accomplish the Net Zero Emissions (NZE) by 2050 Scenario proposed by the International Energy Agency, an increase in clean energy technologies is necessary, and it has already become the first choice for consumers around the world [65].

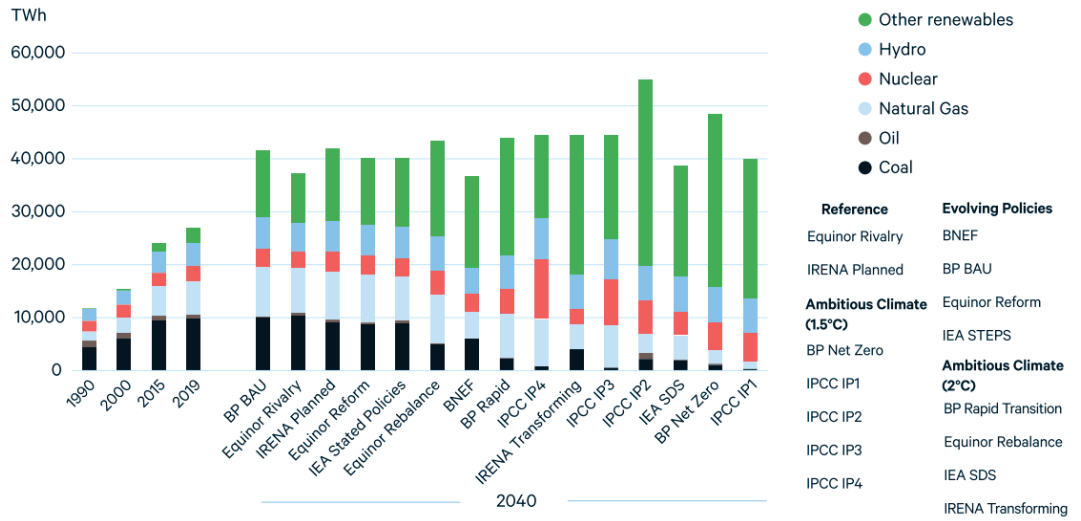

Figure 1.3: Global electricity mix in 2040 in different scenario types. Adapted from [66].

In Figure 1.4a, it is possible to see the estimated market sizes of clean technologies (2030 and 2050) on the NZE Scenario and the Stated Policies Scenario (STEPS). The Stated Policies Scenario (STEPS) represents a path based on the energy and climate measures that governments have put in place to date and specific policy initiatives under development. In both cases, there is an important growth

of the total market value for this economic sector, but there is still a breach to overcome between the ideal and the already proposed policies. Furthermore, this gap represents an important market opportunity for clean technologies such as wind turbines, solar panels, batteries, electrolysers and fuel cells to become a new area of investment and international competition with a potential explosive growth during the next decade [65].

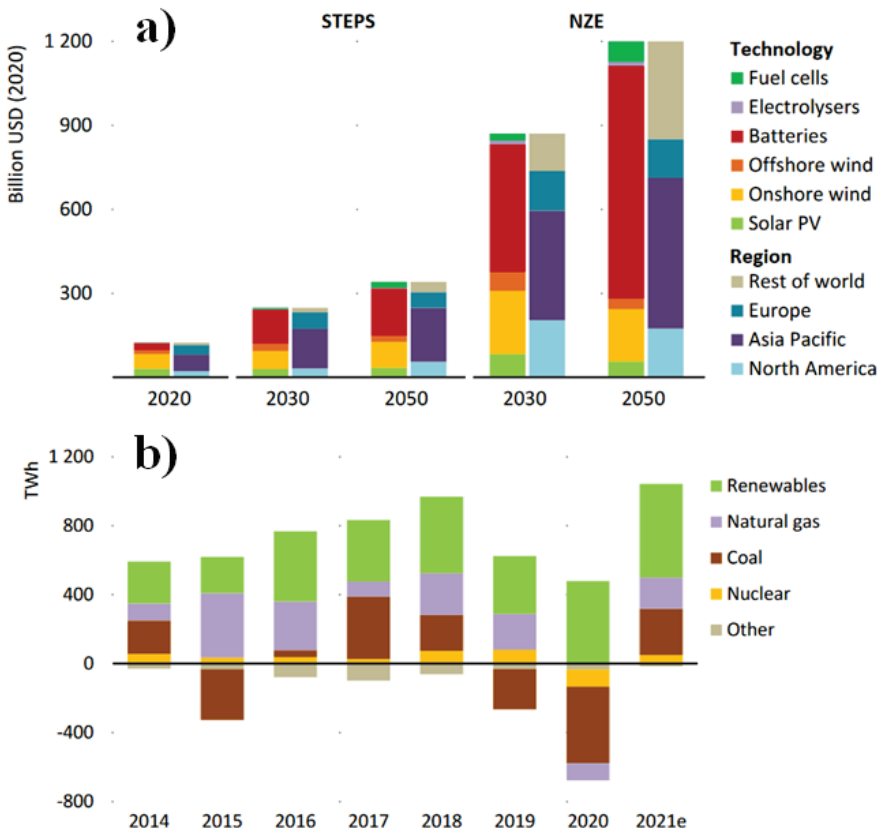

Figure 1.4: a) Estimated worldwide market size for selected energy technologies (2020-2050). b) Change in global electricity generation (2014-2021). Adapted from [65].

Another important point to note is the variability on the energy consumption by unexpected events (being the most recent the pandemic crisis caused by COVID-19). As Figure 1.4b shows, during the years 2019 and 2020, it was registered an important deceleration on the electricity demand that pushed the consumption to higher levels during 2021. Despite the higher production coming from renewables in 2021, it is not enough to overcome the rise in electricity demand, which had to be covered by fossil fuel-based electricity generation [65], which opposes to the environmental objectives to achieve the NZE Scenario [68]. This demonstrates the need for a resilient power system capable of covering contingencies and the variability of energy production/consumption, but also with enough flexibility to respond to the fluctuations in supply and demand coming from the increasing share of renewable energy sources [69, 70]. In this sense, a reliable power system should be stable un-

der continuous operation, but sources as wind and solar are intermittent and then have an influence on the stability of multiple grid parameters [71]. In fact, as the penetration of electricity from renewable resources becomes more important, the balance of the electrical grid will be more difficult to maintain, because the strategies used until now (e.g. regional cooperation, fossil fuels, pumped hydro power, batteries, compressed air storage, etc.) will not cover seasonal shortage [69]. To solve this problem and ensure the renewable energy escalation, a mix of different solutions is required: flexible power generation, grid expansion, final demand management, hybridisation of the heating systems, curtailment of surplus intermittent generation peaks, and energy storage [72].

Regarding the energy storage, chemical methods have aroused particular interest [73]. Even if several options have been considered until now (e.g. synthetic fuels, batteries, etc.)[74], hydrogen is one of the future energy carriers that has emerged thanks to its unique properties [72]. Energy can be stored by using it to dissociate water into hydrogen and oxygen. The first one is stored, transported and distributed and the latter could be released in the atmosphere. Then, H_2 can be further used in a thermal engine or a fuel cells to produce energy (electricity, work or heat) while realising water as only by-product [75]. This idea has been around for about two centuries [76], but it becomes real because of the investment and roadmaps defined by several governments, together with the research efforts dealing with the H_2 generation and the final utilisations [77]. As a product of the broad consensus about hydrogen as a key element for the energy transition, the term "hydrogen economy" and the related discussion begins to have a place at the national level, for example in Japan, the United States and the United Kingdom, and even at European level [77–79]. In the same way, different strategies are being deployed to develop national industrial sectors as part of the recovery schemes after the COVID-19 pandemic, but the "hydrogen economy" is an international project involving actors all over the globe [77, 80].

So far, natural molecular hydrogen has been poorly searched and exploited. Even if it is present in every type of environment on Earth, its role is still underestimated and misunderstood [81]. Nonetheless, further intentional exploration may increase the chances of finding geological hydrogen wells in the future, as it is already the case in different locations [81–83]. Nowadays, hydrogen is not considered as a primary energy source, it needs to be produced either from fossil or renewable energy resources; it represents a way to fuel independence (compared with fossil fuels, with limited and unequally distributed reserves) for many countries owing to its global availability [80]. H_2 is a colourless and odourless gas. However, its environmentally friendly reputation depends on the method of production [84]. This

molecule can be fabricated by different procedures that have been codified with diverse colours depending on the employed technology and energy source [76, 85], even if such a classification is not scientifically rigorous. In Figure 1.5, it is possible to find the four main kinds of hydrogen [86]. *Grey hydrogen* is the most currently used method to produce this compound, and it globally uses ∼6% of the natural gas and ∼2% of the coal total production, generating about 830 Mt of CO_2 and other related pollutants [85, 87]. *Blue hydrogen* highly depends on the further improving of carbon capture and storage (CCS) to achieve low greenhouse gases (GHG) emissions [76]. *Turquoise hydrogen* represents a different technological solution that is still under development. It produces solid carbon (or carbon black) as the only by-product (an important feedstock for other industrial processes) [76]. Other hydrogen colours are also under consideration, e.g. *yellow/purple hydrogen*, that relies on electrolysers to produce H_2 by using electricity from nuclear power plants [85].

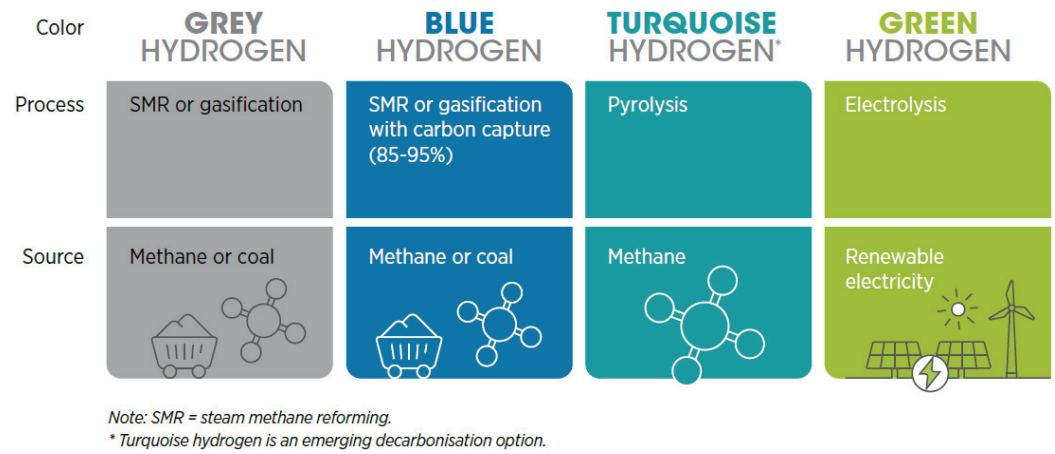

Figure 1.5: Hydrogen colour classification. Adapted from [86].

Among all the colours of hydrogen, the most appropriate one to support the sustainable energy transition is the *green hydrogen*, also known as renewable hydrogen. This latter is produced by electrolysers powered by renewable electricity (mainly wind and solar), but it also includes H_2 coming from bio-based sources such as bio-methane reforming or solid biomass gasification [76, 88]. The electrolysers technology will be further explained in the next section. In any case, the production and consumption of this hydrogen does not carry any generation of GHG as the carbon balance is near zero if it uses only renewable resources. As Figure 1.6 represents, the value chain of renewable hydrogen is wide and complex. It assures the transport and storage of energy, while playing an important role for the decarbonation of industrial sectors that have been traditionally difficult to convert (metal processing, fertilisers production, plastics manufacturing, transportation, buildings and heating, etc.) [72, 88–91]. The success of the green hydrogen penetration in

the industrial and energy systems depends on multiple factors that need to be effectively overcome to represent a real option for economy decarbonisation, such as its high production cost, the lack of dedicated infrastructure and recognition, the energy requirement and losses, and the need for society to ensure sustainability [80, 86].

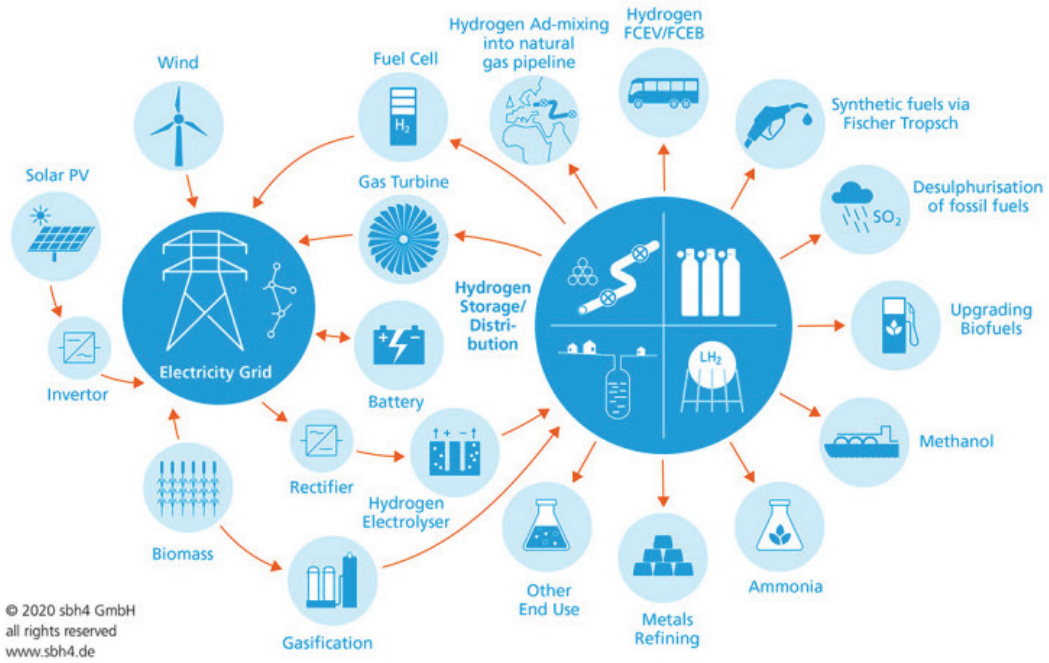

Figure 1.6: Renewable (or green) hydrogen value chain. Adapted from [89].

Water electrolysis and fuel cells are at the core of the hydrogen economy as they are the methods that allow directly linking the electricity grid with the production and consumption of H_2. As Figure 1.4a showed, it is expected an important growth of the market size for these appliances. The improvement of the existent technologies and the development of new ones will allow the exploitation of renewable energies in a much efficient way [92]. Similarly, further investigation on integrating multiple technologies is needed, for example, the valorisation of wastes with parallel production of H_2. The exchange between different areas of research and development could help to solve multiple problems simultaneously. Some methods to treat a variety of wastes have been already propose, but they are still under research, as the steam gasification, pyrolysis and fermentation [93]. Further efforts could strengthen this trend.

In the next section, we will explore the main available technologies for the electrolysis of water and their main advantages and drawbacks, as well as the state-of-the-art for the coupling of electrolysis with the treatment of non-plastic organic wastes (mainly biomass derivatives). Then, we will further discuss the possibility of using this kind of technology for producing hydrogen while treating the waste of our interest: plastics (Section 1.5).

1.4 Electrolysis for coupling the production of pure hydrogen and the valorisation of organic wastes

The main body of this section has been adapted from a book chapter published by Nicolas Grimaldos-Osorio, Kristina Beliaeva, Jesús González-Cobos, Angel Caravaca and Philippe Vernoux, as Chapter 9 (DOI: 10.1515/9783110596250-017) of the book Volume 1 Hydrogen Production and Energy Transition, part of the multi-volume work Energy, Environment and New Materials. Edited by Marcel Van de Voorde, Berlin, Boston: De Gruyter, 2021. The sections dealing with the electrolysis of plastics and polymeric materials are properly updated for the purpose of this thesis and are shown in Section 1.5.

1.4.1 Generalities

Green hydrogen will play a major role in the future decarbonised energy systems. Green hydrogen is an energy vector for grid balancing, power-to-liquid and power-to-gas technologies [77]. Hydrogen is the most abundant element but does not exist in the nature in its molecular formula. It is usually associated with different molecules, such as methane CH_4 or water H_2O. To this date, hydrogen is mainly produced by the steam reforming of natural gas, a fossil fuel, at high temperatures 500 – 800 °C on Ni-based catalysts [87]. However, further purification steps are necessary to obtain pure hydrogen with a concomitant emission of carbon dioxide. The most promising technology for the green hydrogen production is the water electrolysis, which consists to break water molecule into H_2 and O_2 using only renewable electricity [94] in an electrochemical cell with no carbon source. The intermittent primary renewable energy sources such as wind, solar, tidal can be ideally combined with electrolysers [95]. Green hydrogen can substitute fossil fuels for the industry, the transport or the electricity production without greenhouse gas emissions.

Electrolysers can operate below 100 °C [87, 94–96] when water is liquid or at high temperatures (500 – 1000 °C) [97] depending on the nature of the electrolyte. Alkaline water electrolysers (AWE), based on liquid alkaline electrolytes such as potassium hydroxide, are a mature technology with many advantages such as a low capital cost, non-noble metal-based electrodes and a long-term stability (30 – 40 year). A diaphragm permeable for OH^- separate the two electrode compartments and the product gases. It is commonly made of either glass reinforced polyphenylene sulfide (Ryton) or polysulfone-bonded zirconia (Zirfon). Hydrogen is produced at the cathode (HER, Hydrogen Evolution Reaction) while oxygen is released at the

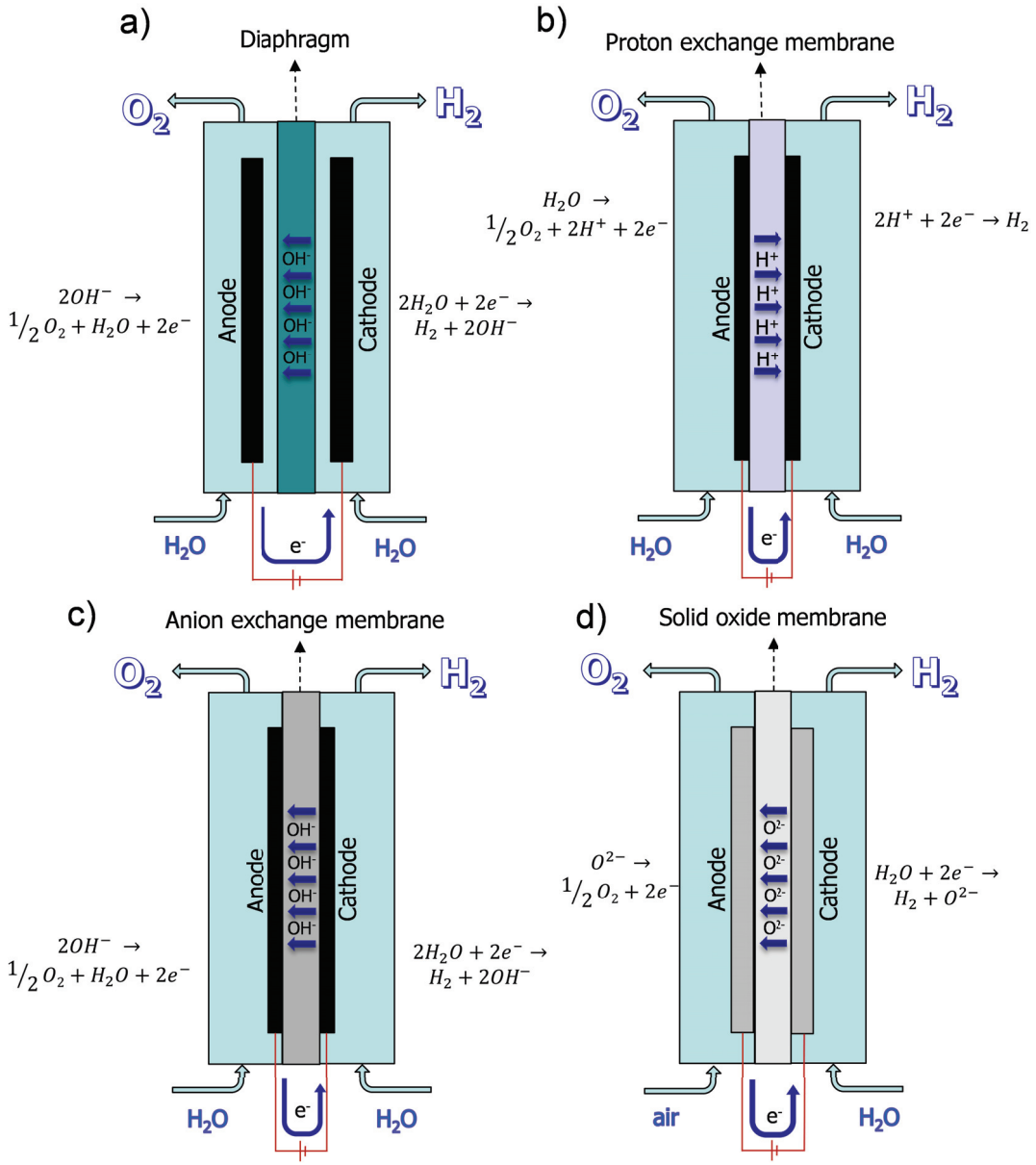

Figure 1.7: Schematic representation of different types of electrolysers: a) AWE, b) PEM electrolyser, c) AEM electrolyser and d) SOE.

anode (OER, Oxygen Evolution Reaction) (Figure 1.7a). The mean AWE drawback deals with their low achieved current densities [98] (in the range 250 – 450 mA cm^{-2}) due to the slow ionic conduction of the liquid electrolyte (high ohmic losses) and the formation of gas bubbles which can block the electrodes surface. Furthermore, AWEs exhibit a slow response upon the application of transient voltages because of the liquid electrolyte high volume, making this technology difficult to combine with the oscillating behaviours of renewable energy sources. In addition, AWEs cannot produce hydrogen at high pressure for safety reasons. Therefore, a compressor is required for hydrogen storage and transportation.

The other types of electrolysers are equipped with a solid electrolyte membrane

to separate the anodic and the cathodic compartments. Proton-exchange membrane (PEM, Figure 1.7b) and anion-exchange membrane (AEM, Figure 1.7c) electrolysers are both operated at low temperature (typically 20 – 100 °C) with a polymeric electrolyte membrane conducting H^+ cations and OH^- anions, respectively. On the other hand, solid oxide electrolytic membranes are implemented in Solid Oxide Electrolysers (SOE, Figure 1.7d) working at high temperatures (500 – 1000 °C) with $O_2{}^-$ anions.

PEM electrolysers based on protonic polymeric membranes capitalise the development of PEM fuel cells, including an optimised compact design (low thickness of the membrane of around 60 – 200 μm) and a very short start-up time. PEM electrolysers can achieve high current densities (>1 A cm^{-2}) and can operate at a higher pressure than AWE, which is more suitable for further hydrogen compression and storage. Even if they are already commercialised, they undergo the high cost of the polymeric membranes. In addition, water has to be pure (deeply deionised) to avoid any poisoning of the proton-conductive polyfluorosulfonic acid membranes. Furthermore, the very acidic media limits the choice of electrodes to expensive noble metals (platinum at the cathode, IrO_2 at the anode) since the OER and HER kinetics are lower by 2 – 3 orders of magnitude than in alkaline conditions. These harsh conditions also limit the lifetime between 5 and 20 years [96]. AEM electrolysers could overcome these problems, but it is a developing technology and actual AEMs show a poorer chemical and mechanical stability, as well as a lower conductivity than PEMs.

A major drawback of AWE, AEM and PEM electrolysers, which run at low temperatures with the system $H_2 - O_2 - H_2O$, is the high energy demand to split the water molecules under standard conditions considering liquid water ($\Delta G^o = 237.1$ kJ mol^{-1}). Consequently, the required cell voltage for water splitting is 1.23 V under standard conditions. Furthermore, electrode overpotentials, especially for the OER, are high on noble metals in acid media and on non-noble metals in alkaline media due to the low kinetics of the electrochemical reactions. This enhances the required cell voltage up to around 1.6 – 2 V for high current densities (1 A cm^{-2}), leading to low energy efficiencies of PEM and AEM electrolysers resulting in a minimum electrical energy demand of around 45 kWh kg^{-1} H_2. In addition, the anode product (O_2) has a little economic value. All these issues lead to a high cost of green hydrogen. To overcome this problem, two possibilities are currently explored.

The first is to develop high-temperature electrolysers such as SOEs as the electrical energy demand (ΔG) and the electrode overpotentials significantly decrease with the temperature, leading to a theoretical SOE cell voltage of around 1.3 V. However, the net efficiency of SOEs, considering the heating energy demand, is

in the range 40 – 60% compared to 59 – 70% and 65 – 82% for AWE and PEM electrolysers, respectively [99]. The second solution is to replace the OER in low-temperature electrolysers with a less-energy intensive reaction both from a thermodynamic and kinetic point of view. The electrochemical oxidation of much more oxidisable organic molecules such as biomass derived alcohols [100–103] is reported in the literature. Considering the total oxidation of alcohols into CO_2 (Eq. (1.1)), the theoretical standard cell potential is 0.016 V for methanol, 0.084 V for ethanol and 0.0029 V for glycerol compared to 1.23 V needed for water electrolysis [104]. In practice, cell voltages to achieve significant hydrogen production rates are higher mainly due to the slow kinetic of the alcohol electro-oxidation at the anode, but still significantly lower than 1.23 V. Methanol was the most studied alcohol in PEM electrolyser but this compound is toxic and mainly produced from natural gas [104]. Except for methanol, the electro-oxidation is never complete, as the C–C bond breaking is quite difficult at low temperature, leading to the formation of by-products that limits the production of hydrogen. For this specific case of alcohols, the concomitant production of chemicals at the anode and hydrogen at the cathode is denoted as electrochemical reforming in the literature. The by-products hinder the production of hydrogen, but valuable chemicals can be generated at the anode such as acetic acid (from ethanol), glycolate and oxalate (from ethylene glycol), dihydroxyacetone, glycerate and tartronate (from glycerol) [105, 106].

$$C_nH_{2n+1}OH + (2\,n\text{-}1)\,H_2O \rightarrow nCO_2 + 3\,nH_2 \tag{1.1}$$

The electro-oxidation of bio-sourced ethanol and glycerol (a surplus by-product of biodiesel fabrication) at the anode of PEM electrolysers could be promising but only low current densities (few hundred mA cm^{-2}) are reported on expensive Pt-based anodes, making this approach economically unattractive. Recently, F.M. Sapountzi et al. [107] have suggested that higher performances could be achieved in alkaline media because anodic and ohmic overpotentials are lower. For instance, electrochemical reforming of various alcohols (ethanol, ethylene glycol, glycerol and 1,2-propanediol) was investigated in an AEM electrolyser between 25 and 80 °C in NaOH [108]. The anode was based on Pd nanoparticles supported on 3D titania nanotubes (1.7 mg Pd cm^{-2}). Current densities larger than 1 A cm^{-2} were obtained at 80 °C, corresponding to an energy consumption in the range 18 – 20 kWh kg^{-1} H_2 instead of 47 kWh kg^{-1} H_2 if the electrolyser is only alimented with water.

The recent advances in electrochemical reforming of alcohols have been reviewed by Linares et al. [109] and Coutanceau and Baranton [104], while other reviews deal with the use of such technology for the specific case of glycerol electrolysis

[106]. This idea of replacing the OER with a less-energy intensive oxidation reaction in order to depolarise electrolysers can also be combined with the treatment and valorisation of wastes without emissions of harmful products. Indeed, organic wastes containing H atoms can be fully or partially oxidised at the anode of electrolysers to produce simultaneously pure hydrogen and valuable compounds. Recent developments on the valorisation of biomass in low-temperature electrolysers will be first described.

1.4.2 Low and middle temperature electrolysers for the valorisation of biomass organic wastes

Among the biomass wastes, lignin is a major component of woody wastes and is the second most abundant natural polymer. Therefore, lignin is a good potential anodic fuel. Lignin is a tridimensional bio-polymer, which is a waste of the Kraft paper-making industry with an annual production of over 50 million tons. Lignin is usually incinerated to produce heat. The incineration is accompanied by the generation of toxic emissions [110–113]. Only a small part of lignin waste is valorised into valuable chemicals by pyrolysis, gasification, catalytic oxidation and reduction [106–108]. Depending on the technique, temperature and catalytic materials, lignin could be valorised into phenols, aldehydes or syngas. Production of valuable chemicals such as vanillin and vanillic acid from lignin was also mentioned in literature [113–115].

Lignin electrolysis is still in an early state exploratory technology, but two main families of studies can be identified in the literature. The first solely focused on its electrochemical depolymerisation, leading to the production of high-value products, namely vanillin and vanillic acid, without considering the simultaneous production of hydrogen. These studies have been recently summarised in some review articles by Zirbes and Waldvogel [116] and Du et al. [117]. Most of those works were performed in a high range of electrical potentials (sometimes as high as 12 V [118] and 15 V [119]) where the electro-oxidation of lignin (lignin + OH^- $\rightarrow$ $lignin_{ox}$ + e^-) competes with the oxygen evolution reaction. The main reason to work in such drastic energy-demanding conditions is most likely attributed to the challenge to cleave the C–C bonds of organic molecules at low electrochemical potentials and temperatures below 90 °C, as it was observed in some studies dealing with the electro-oxidation of ethanol [120–122] and glycerol solutions [106, 123]. Nevertheless, several studies focused on H_2 as the main product of interest [110, 124–131]. This process is potentially less energy-intensive, considering that the depolarising effect of lignin allows producing H_2 from electrical cell

potentials as low as 0.2 V. However, the valorisation of the lignin electro-oxidation products and the yield of H_2 might be limiting, considering that the depolymerisation (i.e. the cleavage of C–C bonds) of lignin under such conditions is unlikely.

The recent research efforts on lignin electrolysis can be classified according to the temperature. Below 100 °C, experiments can operate in PEM electrolysers using the actual mature technology (membrane, electrodes, design, etc.) or in AEM electrolysers exploiting the recent developments on OH^- conducting membranes. However, as previously mentioned, the kinetics for the electrochemical oxidation reactions below 100 °C are slow and the depolymerisation of lignin is tricky [119]. Another route is to perform electro-oxidation of lignin at temperatures higher than 100 °C, typically between 100 and 200 °C (intermediate temperature range) to boost the kinetics and the lignin depolymerisation even if new alternative materials such as polymer membranes have to be developed.

— Low temperature electro-oxidation (<100 °C)

Several studies describe the electro-oxidation of pure lignin or black liquor (lignocellulosic effluent with a concentration of lignin about 40%) on noble metal-based anodes [110, 124, 125, 127, 131, 132]. Some of those studies were performed in standard batch 3-electrode cells using liquid electrolytes, where lignin was electrolysed at low temperatures (30 – 90 °C) and at lower potentials compared to water electrolysis. The hydrogen production increased with the temperature and the lignin concentration. IRCELYON was the first to prove that lignin oxidation can be performed in an AEM cell with a continuous flow at 90 °C using a bimetallic PtRu anode supported on carbon cloth [110]. As in the batch 3-electrode cell, lignin electrolysis in a PEM cell appeared at lower potentials (∼0.45 V) compared to water (∼1.23 V). It was also found that the optimal temperature for lignin electrolysis in a PEM cell was 80 °C. Even though its performance was demonstrated for a wide range of reaction temperatures (up to 90 °C) upon the application of electrical cell potentials <1.2 V, the current densities obtained (and therefore the H_2 production) were still rather low (Figure 1.8a). It suggests that the kinetics for the lignin electro-oxidation reaction under these conditions were hindered importantly.

In order to get further insights into the oxidation mechanism on the PtRu anode, and therefore on the main limitations of this electrode, 2-phexyethanol (2-PE) was recently used as a model molecule, to represent the majoritarian β-O-4 quintessential linkage present in lignin [133]. The study of Belieava et al. confirmed that the rate-determining step of the electrolysis process even at 90 °C in alkaline media is the lignin anodic oxidation. The main electro-oxidation route involves the production of carboxylic acid, which seems to be the final product. In addition,

thermodynamic DFT calculations suggest an electro-oxidation path where the 2-PE model molecule would be oxidised to the aldehyde, followed by its further oxidation into the carboxylic acid. It was also observed a deactivation of the PtRu anode, most likely due to strong adsorption of reaction intermediates. Another publication on the electro-oxidation of lignin and 2-PE on an alkaline medium was published by Belieava et al. [132], employing Ni-based electrodes both on 3-electrodes batch cell and AEM cell configuration. It was demonstrated that the model molecule oxidation is favoured by the formation of NiOOH species produced at applied potentials >1.3 V, following a two-step electro-oxidation process. Anyway, it was also found that the promising Ni/C electrocatalyst suffered an important deactivation because of the adsorption of intermediate species, probably phenolic and aldehyde-type compounds [132].

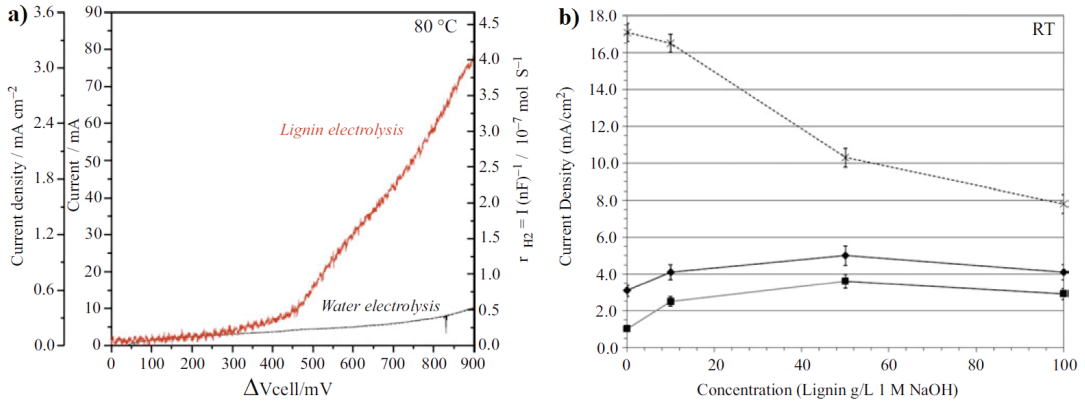

Figure 1.8: a) Linear sweep voltammetry from 0 to 0.9 V at 80 °C; sweep rate : 0.5 mV s^{-1}, PtRu/C anode: 10 g L^{-1} lignin in 1 M NaOH (lignin electrolysis in red) or 1 M NaOH (water electrolysis in black). Adapted from [110]. b) Current density at room temperature as a function of lignin concentration at 1.4 V (■, bottom solid line), 1.5 V (♦, middle solid line) and 1.6 V (×, top dotted line). Adapted from [131].

The group of J.A. Staser at the Ohio University [131] has also reported interesting results on the lignin electrochemical oxidation in an AEM electrolyser aiming the production of hydrogen at low temperatures using a non-noble metal, i.e. a $NiCo/TiO_2$ catalyst. Experiments were done between room temperature and 60 °C and between 1.4 V and 1.6 V. Figure 1.8b displays that, at room temperature, the presence of lignin dissolved in NaOH (1 M) at the anode enhances the current density up to a cell voltage of 1.5 V and a concentration of 50 g L^{-1}. Above 1.5 V, OER dominates and lignin reduces the reaction rate. Above 50 g L^{-1}, lignin may partially block the active anodic sites. The same group has also tested different environmental friendly Ni based catalysts for the effective lignin electro-oxidation [134, 135]. Ni-based anodes are efficient in alkaline media and Ni exhibits a high corrosion stability. First, different ratios of Ni and Co were investigated [135]. It

was found that, by increasing the ratio of Co catalyst, the current and the formation of aromatic compounds were enlarged. Secondly, NiSn catalyst was studied in a conventional three-electrode cell, as well as in an AEM electrolyser. The composition NiSn (containing 20 at.%) was found to be the most effective to oxidise electrochemically lignin at room temperature upon 1.2 and 1.4 V. The authors have shown a production of vanillin, which is maximised at 1.4 V on NiSn20 anode at room temperature [134].

Another route is to first chemically decompose the raw biomass and then to electrolyse the obtained solution in a PEM electrolyser. This solution was explored by the group of Prof. Deng at the Georgia Institute of Technology. Before the electrolysis, biomass such as lignin, cellulose, wood powder, or starch was mixed with a solution of polyoxometalates (POMs), water-soluble molecular metal-oxide clusters [136] or with a solution of $FeCl_3$ [111]. These two catalysts can degrade under heating (typically at 100 °C for few hours) or irradiation (UV for a few hours) biomass into small oxidised products, while POM and Fe^{3+} are reduced. This solution is then introduced in the anode of the PEM electrolyser. Under the polarisation, the reduced POM form and Fe^{2+} are re-oxidised (and then regenerated), acting as electron-proton carriers that can trap the electrons from biomass and protons coming from water. Therefore, a noble metal free anode can be used, such as pure graphite felt material. Successive oxidation/discharge (electrolysis) cycles can be performed to convert fully the raw biomass into hydrogen and CO. For instance, after three oxidation/discharge cycles at 100 °C (total 18 h), it has been found that around 18% of the lignin was oxidised to small aromatic molecules [111]. However, small current densities are reported for this chemical-electrolysis process, lower than 0.5 A cm^{-2} for electrolysis temperatures in the range 80 – 100 °C. Nevertheless, low electric energy consumption is reported as low as 0.69 kWh Nm^{-3} H_2 at 0.2 A cm^{-2}.

— Intermediate temperature electro-oxidation (100 – 200 °C)

Operating an electrolyser at temperatures above 100 °C provides some advantages, such as better kinetics of the electrode reactions, more favourable thermodynamic conditions (1.14 V at 200 °C vs. 1.23 V at room temperature) and higher degradation rates of the biomass wastes. The group of Hibino [129] at the Nagoya University in Japan was the first to explore the lignin electrolysis between 100 and 200 °C in a PEM electrolyser by using a $Sn_{0.9}In_{0.1}P_2O_7$-polytetrafluoroethylene (PTFE) protonic membrane (stable up to 200 °C with a high proton conductivity) and state-of-the-art Pt/C electrodes. A lignin powder mixed with H_3PO_4 (85%) was deposited on the anode surface. Thus, the study was made in a batch mode, meaning that

when the total amount of impregnated lignin was oxidised, a new sample of lignin had to be impregnated on the catalytic surface. Nevertheless, interesting results have been reported, showing an onset potential of the lignin electro-oxidation at around 0.25 V. Current densities increased with the temperature to reach 0.2 A cm^{-2} at 200 °C on Pt/C. Analysis has shown that lignin can be depolymerized in the phosphoric acid into C4-C7 aromatics and aliphatic molecules at 200 °C.

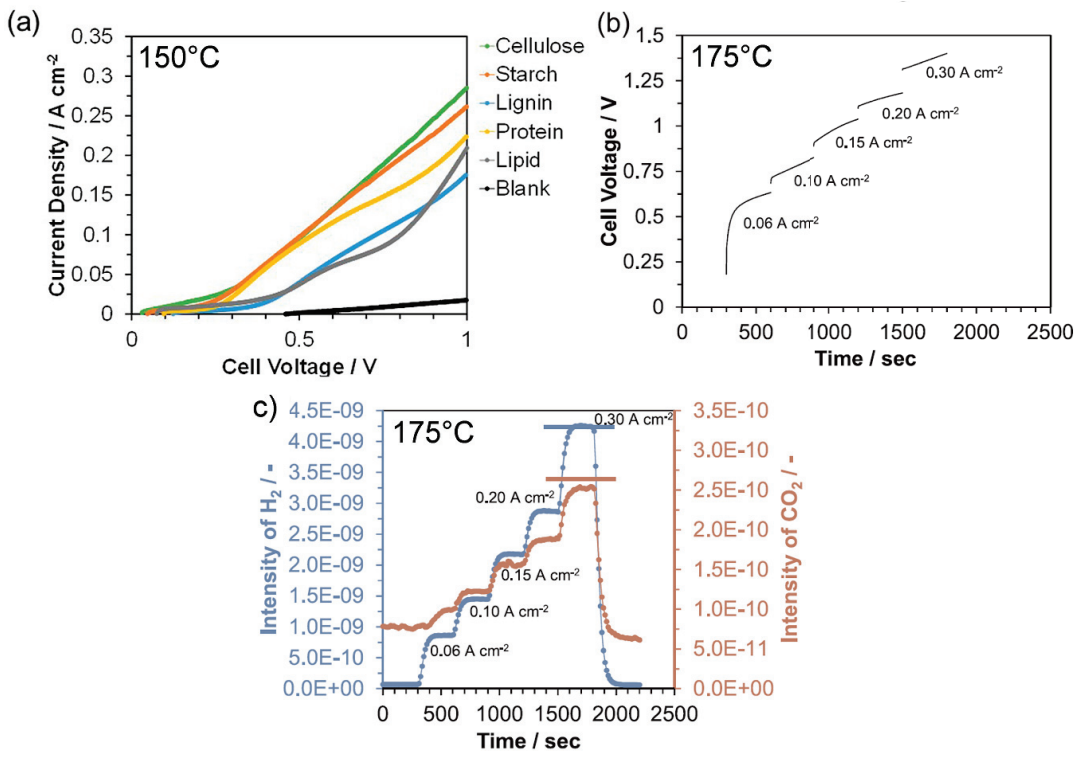

Figure 1.9: a) *IV* curves at 150 °C of the electrolysis of various model biomass components (mixed in H_3PO_4 with a weight ratio of fuel to 85% H_3PO_4 of 1:15) in a batch cell. Adapted from [137]. b) and c) Electrolysis of newspapers at 175 °C in a batch cell (cell voltage evolution with time during continuous electrolysis (b) and production of H_2 and CO_2 recorded with a mass spectrometer (c)). Adapted from [129].

More recently, the same group [137] has investigated the electrochemical oxidation at 150 °C of raw biomass dissolved in H_3PO_4 (85%) using an anode based on a carbonyl-group functionalised mesoporous carbon and the same Pt/C cathode and membrane than in reference [129]. This study has compared the electro-oxidation at 150 °C of model biomass molecules (Figure 1.9a). These latter can be electro-oxidised at cell voltages less than 0.5 V with current densities lower than 0.3 A cm^{-2}. Differences between components were explained based on the main functional groups (carbonyl groups in cellulose and starch more reactive than carboxyl groups in proteins) and on the acid-solubility (lignin and lipid less soluble). Electrolysis was also operated with the same materials in the temperature range 150 – 175 °C with real biomass wastes of bread, cypress sawdust, rice chaff and newspa-

pers [138] (a real lignocellulosic waste with a more complex structure and higher molecular weights than pure cellulose and lignin) in a batch and flow cell. They have reported similar performances than for model biomass wastes (current densities in the range. 0.15 – 0.4 A cm^{-2}). Regarding newspapers which are mainly containing cellulose (69.2%) and lignin (11.8%), the onset voltage was around 0.2 V. Stable current densities in the range 0.15 – 0.25 A cm^{-2} were achieved in a flow cell during continuous voltages (Figure 1.9b). In addition, the main oxidation product was CO_2 with a current efficiency near 90% (Figure 1.9c). Let us note that, in H_3PO_4 at 150 °C, newspapers are decomposed to mono and disaccharide derivatives and an aliphatic keto acid. More recently, the same group has substituted the expensive Pt/C cathode by an optimal mesoporous carbon, which can catalyse the hydrogen evolution at 150 °C. The electrolysis of cellulose was performed in a metal-free PEM electrolyser at 150 °C, showing similar electrochemical performances (0.3 A cm^{-2} at 1 V). These studies demonstrate that the electrolysis of real biomass wastes is possible with no noble metal from 150 °C. Nevertheless, the low obtained current densities combined with the energy require to heat the electrolyser make this solution unattractive up to now. This situation can be improved if high added-value products are generated by the electro-oxidation of the biomass, such as vanillin.

1.5 Electrochemical processes for the valorisation of plastic waste and proposed research line

1.5.1 State-of-the-art electrochemical processes for plastic waste treatment

Until here, we have seen the complete context regarding the production and treatment of plastic waste, the energy and ecological outlook to achieve carbon neutrality, as well as the role of hydrogen in this transformation. Similarly, we explore the different techniques for coupling electrochemical H_2 production methods with the valorisation of organic wastes. As the intention of the work is depicted, it is important to have in mind the research interest that both H_2 and plastic waste treatment represent for the future of our planet. Finding new ways to pair these two processes is of major importance as the potential is broad. Usually, the processes involving the chemical transformation of polymers into valuable products are based on thermochemical strategies with specific conditions depending on the treated waste and the desired products [139, 140]. Several studies have showed the feasibility of the decomposition of plastics to produce H_2-rich gases by thermal methods [141–144],

solar-driven [145, 146] and microwave-assisted [147] reactions. Nevertheless, new treatment techniques capable of providing high-quality and high-impurity H_2 are still needed. As plastic wastes represent an important source of hydrogen, their valorisation in electrolysers is a promising approach and a challenge for the scientific community. This electrolytic process involves the common hydrogen evolution reaction (HER) at the cathode while the oxygen evolution reaction (OER) is replaced at the anode by the electro-oxidation of plastic wastes. A handful of publications have been issued, and this subsection briefly explores the state-of-the-art on this subject.

The group of Prof. Hibino was the first in 2020 to electrolyse plastic wastes at low/intermediate temperatures in a PEM electrolyser [148]. The implemented strategy was to in situ dissolve plastic wastes into H_3PO_4 in the anodic compartment of the PEM electrolyser. Real plastics were used, such as sponges (mainly composed of polyurethane), cable ties and stockings (mainly nylon-6,6) and ropes (mainly vinylon). All these plastics were found to be fully soluble in H_3PO_4 at 200 °C, except for the ropes indicating that vinylon seems to be less soluble than polyurethane and nylon-6,6. In addition, FTIR characterisations have shown that dissolved plastics were still in the form of macromolecules, suggesting a minimal decomposition during the dissolution. First series of electrochemical results were obtained in a batch configuration where the plastic samples (after grounded to millimetric fragments) were mixed at room temperature with a solution of 85% H_3PO_4/15% H_2O (plastic mass/acid solution ratio: 1/15) to form a gel-like paste which was deposited onto the Pt/C anode. The protonic membrane was the same as the one used for the intermediate temperature electrolysis of biomass wastes [129, 137]. The comparison of IV curves between sponges and pure polyurethane shows similar results, suggesting that plasticiser components and additives in the real sponges did not affect the electrochemical oxidation process. However, this could be also due to the fact that electrochemical performances are transport limited. Indeed, the porosity of the anodic carbon support plays a major role in hindering these transport limitations. Thus, this is also why low concentrations of plastic wastes, i.e. 1.42 wt.%, in H_3PO_4 were used in the flow cell experiments, in order to avoid any clogging problems and the deposition of plastic residues on the anode.

The highest current densities were achieved at 200 °C on mesoporous carbon supports with pore volumes larger than 2 $m^3\ g^{-1}$ (pore size of around 10 nm). Figure 1.10a displays IV curves at 200 °C in the flow mode for the different plastic wastes, as well as for a highly acid resistant polyethylene terephthalate (PET) bottle. Onset voltages are quite low (<0.2 V), confirming the thermodynamic gain compared to the OER. It is important to note that the cell voltage was stopped

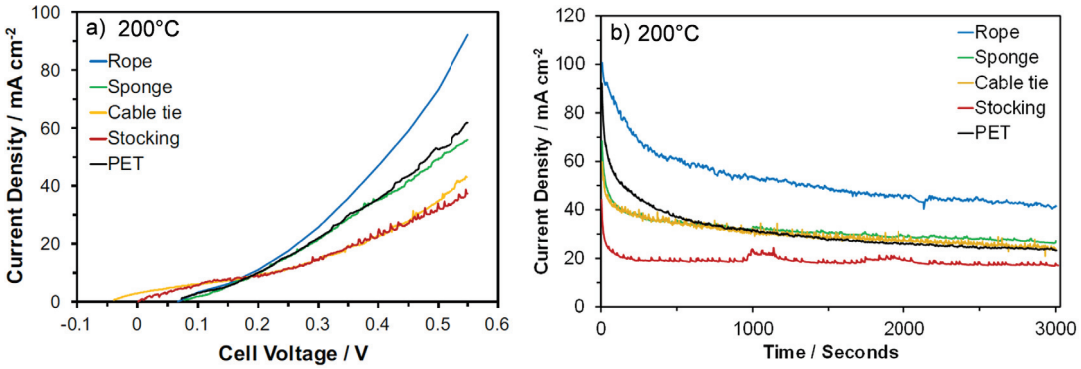

Figure 1.10: a) *IV* curves in a flow mode at 200 °C at a scan rate of 2.5 mv s^{-2} (plastic waste: 1.42 wt.% in 85% H_3PO_4, anodic flow rate = 0.13 mL min^{-1}, anode: Pt (1.7 mg cm^{-2}) on mesoporous carbon. b) Current-time curves obtained from the electrolyser with different plastic fuels at 200 °C and a cell voltage of 0.55 V. Adapted from [148].

at 0.55 V to avoid the oxidation of Pt, limiting the current densities below 100 mA cm^{-2}. The nature of the raw polymer affects the electrolysis activity in the following order: vinylon > polyurethane = PET > nylon-6,6 even if the acid solubility should probably also impact. Current-time curves recorded at 200 °C upon 0.55 V exhibit a significant drop of the current density over the initial 1000 s (Figure 1.10b), which is attributed to the mass transport limitation (low plastic concentrations). In the case of the PET bottles, plastic residues were accumulated on the electrode. This underlines that the anode microstructure has to be tuned to handle plastic macromolecules to avoid any problem of diffusion and transport. Similarly, meso/macro porous carbon supports have to be developed to manage high concentrations of plastic macromolecules. Finally, the authors have identified the formation of OH· radicals from water upon anodic polarisation as the active oxygen species.

Up to now, just one work has been published at low temperatures. Shi et al. proposed a process for electro-oxidation of poly(ethylene terephthalate) (PET) at room temperature by using a pre-treatment of the plastic material with a 10 M KOH solution at 60 °C for 4 h [149]. This study takes advantage of the hydrolysable nature of PET to produce smaller molecules that can be electrolysed at low temperature, a strategy that will also be considered in the present work. During this initial step, the PET composing units are formed (ethylene glycol (EG) and terephthalate), then the EG is electro-oxidised on a Pd/Ni foam anode to produce carbonate and glyoxal. Simultaneously, the HER takes place at the cathode with a faradaic efficiency of H_2 of 98%. This system demonstrates a novel approach to achieve successfully the upcycling of PET into high value-added chemicals and H_2. Another study reported by Jiang et al. [150] showed the electrochemical depolymerisation of polypropylene and H_2 generation at intermediate temperature (350 – 400 °C) employing a Solar Thermal Electrochemical Process (STEP). This is a fully solar driven process that

couples thermochemical and electrochemical strategies using a molten salt media. The process achieves better total conversion than traditional pyrolysis process and allows the enhanced production of H_2 and light hydrocarbons [150]. Besides, the electro-oxidation of organic wastes in Solid Oxide Electrolysers (SOE) is scarcely reported in the literature because other high-temperature processes such as pyrolysis and gasification are economically more attractive. Only two studies, published by Pati et al. at the University of Boston [151, 152], describe the direct electrochemical oxidation of polyethylene at the anode at 1000 °C. Liquid anodes based on Sn and Fe – Sn alloy were used while other SOE materials were conventional, such as yttria-stabilised zirconia (YSZ) as the oxide membrane and a Ni-YSZ cermet for the cathode. A lab prototype was built from a YSZ tube. A current density of around 0.3 A cm^{-2} was achieved at 1000 °C for a cell voltage of 1.5 V. No gas analysis at the anode outlet was performed, but the authors assume that polyethylene was converted into CO and CO_2. They have evaluated the hydrogen energy cost in the range of 8 – 10 kWh kg^{-1} of H_2.

As formerly exposed, the main advantage of using intermediate and high temperature electrochemical devices is the enhanced reaction kinetics. Higher temperatures also act as a promoter of thermochemical reactions that facilitate the production of easier electrolysable species. But, from the thermodynamic point of view, the use of co-electrolysis of organic waste and water is interesting because of the reduction of the energy needs for the production of pure hydrogen. In this sense, the use of low temperature electrochemical strategies seems to be more adequate, because of the low heat requirements that finally translate to a reduced global energy input to the system. Unfortunately, so far, very few valorisation methods for plastic waste of these characteristics have been proposed. This sets a research niche with potential growth in the upcoming years, as the interest in both H_2 production and plastic waste valorisation become a matter of economical and environmental importance.

1.5.2 Position of the project and proposed research line

During this chapter, we have seen the general context and the interest in proposing new hydrogen production technologies by the valorisation of organic wastes via electrolysis. In consequence, the research that has been performed during this thesis is centred on the idea of producing H_2 from plastic wastes. The first decision we had to overcome was to choose the source of plastic waste. As explained before, one key problem in the treatment of plastics is the heterogeneity of the waste, that is usually composed of several kinds of polymeric materials, impurities and additives that could make more difficult the understanding of the process. From this perspec-

tive, we decided to use pure compounds as a first approach to establish a starting point for this barely explored research area. Another issue was the large number of polymers to study. In this sense, the choice was made by taking an approach from the chemical point of view. Polymers are mainly composed of C, H, O, N and S atoms and the same type of bonds between them. Hence, for this reason, two different polymers with diverse structural and chemical conformation were selected and studied, in order to understand the main features for their electro-oxidation. The following chapters attend to understand the main phenomena involved in the co-electrolysis of water with poly(methyl methacrylate) (PMMA) and polyethylene glycol (PEG). In Figure 1.11 is possible to see the structural formulas of the two selected polymers.

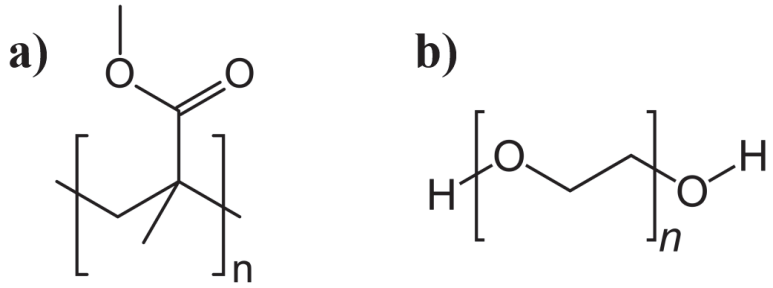

Figure 1.11: Structure of the selected polymers: a) PMMA and b) PEG.

Both structures represent different features that are further analysed in the subsequent chapters. Neither of these compounds are part of the polymers known as *commodity*, but they shall offer valuable information about the reaction paths that this kind of macromolecules can follow under low temperature electrolytic conditions. PMMA (Figure 1.11a) is an amorphous thermoplastic synthesised by various methods from the methyl methacrylate monomer. It posses a glass transition temperature (T_g) between 100 – 130 °C, as well as good mechanical properties, outstanding weatherability and UV tolerance [153, 154]. PMMA could present the three different tacticities (isotactic, atactic, and syndiotactic) depending on the synthesis method, a feature that could change its mechanical properties [153, 155]. PMMA is used in a wide range of applications, from construction to pharmaceutical. The presence of an adjacent CH_3 group prevents the close packing and the free rotation around the C–C bonds [153]. Regarding the electrochemical expected behaviour, PMMA is composed by a main chain composed by C–C bonds, that are known for being difficult to break under soft electrolytic conditions [122], but the lateral ester group could follow another trend as C–O bonds are present. On the other hand, PEG (Figure 1.11b) is a linear polymer that can be synthesised by anionic polymerisation of ethylene oxide with any hydroxyl initiator [156]. This water soluble polymer is available in a large range of molecular weights and it has gained

fame because of its structure flexibility, biocompatibility and high hydration capacity [156, 157]. It presents low T_g and boiling point values (<-35 °C and <68 °C, for PEG20000, respectively) [156]. The uses of this polymer have been explored in different applications, such as separation and purification aid, as anti-freeze, as lubricants for medical devices, food additives, and mainly for dermatological and pharmaceutical applications [156, 158]. In the electrochemical context, PEG is composed by a main chain with presence of C–C and C–O bonds, a characteristic that is shared by a large number of other polymers, making possible a different reaction path than in the PMMA case. The reason for the selection of PMMA and PEG is more strategical than practical, as they represent the main characteristics (e.g., chemical bonds) of a large variety of polymers. As it will be exposed later, the understanding of the electro-oxidation of these two kinds of polymers will allow a first step into the comprehension of the reaction paths of other macromolecules.

As explained in the General Introduction, a four-stage research work is proposed to explore different approaches to the treatment of plastics by electrochemical means. The first three chapters were consecrated to the study of the electro-oxidation of the lateral ester groups of PMMA following to three different strategies: *(i)* treatment of model molecules, *(ii)* solubilisation in a binary solvent, and *(iii)* direct attack by electrochemical methods. These studies allowed us to understand the main advantages and drawbacks of the application of electrochemical methods to the treatment of macromolecules. The fourth chapter of this manuscript present the results on the electro-oxidation of aqueous solutions of PEG, with which we could deepen our understanding of the phenomena involved in the breaking of C–O bonds characteristic of a wide range of polymeric materials. Finally, the most important results and the general conclusions are presented, as well as the future perspective for the research on this topic and the constraints to be overcome to think of an application for the treatment of real plastic wastes.

References

[1] Warde, P. The environmental history of pre-industrial agriculture in Europe. In Sörlin, S. and Warde, P., editors, *Nature's End: History and the Environment*, chapter 3, pages 70–92. Palgrave Macmillan, London, 1 edition, 2009. doi: 10.1057/9780230245099.

[2] Mohajan, H.K. The First Industrial Revolution: Creation of a New Global Human Era. *Journal of Social Sciences and Humanities*, 5(4):377–387, 2019.

[3] Albritton Jonsson, F. The Industrial Revolution in the Anthropocene. *Journal of Modern History*, 84(September):679–696, 2012. doi: 10.1086/666049.

[4] Kasa, S. Industrial Revolutions and Environmental Problems. In Østreng, W., editor, *Confluence. Interdisciplinary Communications 2007/2008*, pages 70–74. Centre for Advanced Study, Oslo, 2008.

[5] Shivanna, K.R. The Sixth Mass Extinction Crisis and its Impact on Biodiversity and Human Welfare. *Resonance*, 25(1):93–109, 2020. doi: 10.1007/s12045-019-0924-z.

[6] Beyer, R.M. and Manica, A. Historical and projected future range sizes of the world's mammals, birds, and amphibians. *Nature Communications*, 11 (5633):1–8, 2020. doi: 10.1038/s41467-020-19455-9.

[7] Mussgnug, F. Species at war? The animal and the Anthropocene. *Paragraph*, 42(1):116–130, 2019. doi: 10.3366/para.2019.0291.

[8] Chure, G., Banks, R.A., Flamholz, A.I. et al. The Anthropocene by the Numbers : A Quantitative Snapshot of Humanity's Influence on the Planet. Technical report, 2021.

[9] Sklair, L. and Murphy, M.W. Introduction to the Special Issue on World-Systems Analysis and the Anthropocene. *Journal of World-Systems Research*, 26(2):175–183, 2020. doi: 10.5195/JWSR.1.

[10] Arias-Maldonado, M. Sustainability in the Anthropocene: Between Extinction and Populism. *Sustainability*, 12(2538):1–13, 2020. doi: 10.3390/su12062538.

[11] Nadal-Romero, E. and Cammeraat, E. Geo-ecology in the Anthropocene. *Geographical Research Letters*, 45(1):5–18, 2019. doi: 10.18172/cig.3876.

[12] Hope, W. The Anthropocene, global capitalism and the crisis of futurity. *New Zealand Sociology*, 35(2):121–142, 2020.

[13] Crutzen, P.J. Geology of mankind. *Nature*, 415(January):2002, 2002. doi: 10.1038/415023a.

[14] Otto, I.M., Wiedermann, M., Cremades, R. et al. Human agency in the An-

thropocene. *Ecological Economics*, 167(October 2019):106463, 2020. doi: 10.1016/j.ecolecon.2019.106463.

[15] Waters, C.N., Zalasiewicz, J., Summerhayes, C. et al. The Anthropocene is functionally and stratigraphically distinct from the Holocene. *Science*, 351 (6269), 2016. doi: 10.1126/science.aad2622.

[16] Zalasiewicz, J., Waters, C.N., Ivar do Sul, J.A. et al. The geological cycle of plastics and their use as a stratigraphic indicator of the Anthropocene. *Anthropocene*, 13:4–17, 2016. doi: 10.1016/j.ancene.2016.01.002.

[17] Zalasiewicz, J., Gabbott, S. and Waters, C.N. *Plastic Waste: How Plastics Have Become Part of the Earth's Geological Cycle*. Elsevier Inc., 2 edition, 2019. doi: 10.1016/b978-0-12-815060-3.00023-2.

[18] Geyer, R., Jambeck, J.R. and Law, K.L. Production, use, and fate of all plastics ever made. *Science Advances*, 3(e1700782):1–5, 2017.

[19] Bakkes, J., van den Born, G., Helder, J. et al. An overview of environmental indicators: state of the art and perspectives. Technical report, UNEP/RIVM, Nairobi, 1994.

[20] Veidis, E.M., LaBeaud, A.D., Phillips, A.A. et al. Tackling the Ubiquity of Plastic Waste for Human and Planetary Health. *The American Journal of Tropical Medicine and Hygiene*, 106(1):12–14, 2022. doi: 10.4269/ajtmh.21-0968.

[21] Browne, M.A. and Rochman, C.M. Classify Plastic Waste as hazardous. *Nature*, 494:169–171, 2013.

[22] Gabbott, S., Key, S., Russell, C. et al. *The geography and geology of plastics*. Elsevier Inc., 2020. doi: 10.1016/b978-0-12-817880-5.00003-7.

[23] Jambeck, J.R., Geyer, R., Wilcox, C. et al. Plastic waste inputs from land into the ocean. *Science*, 347(6223):768–771, 2015. doi: 10.1126/science.1260879.

[24] Campanale, C., Massarelli, C., Savino, I. et al. A detailed review study on potential effects of microplastics and additives of concern on human health. *International Journal of Environmental Research and Public Health*, 17(1212):1–26, 2020. doi: 10.3390/ijerph17041212.

[25] Gestoso, I., Cacabelos, E., Ramalhosa, P. et al. Plasticrusts: A new potential threat in the Anthropocene's rocky shores. *Science of the Total Environment*, 687:413–415, 2019. doi: 10.1016/j.scitotenv.2019.06.123.

[26] Schwarz, A.E., Ligthart, T.N., Boukris, E. et al. Sources, transport, and accumulation of different types of plastic litter in aquatic environments: A review study. *Marine Pollution Bulletin*, 143(March):92–100, 2019. doi: 10.1016/j.marpolbul.2019.04.029.

[27] Eriksen, M., Lebreton, L.C., Carson, H.S. et al. Plastic Pollution in the World's Oceans: More than 5 Trillion Plastic Pieces Weighing over 250,000 Tons Afloat at Sea. *PLoS ONE*, 9(12):1–15, 2014. doi: 10.1371/journal.pone.0111913.

[28] Lusher, A.L., Tirelli, V., O'Connor, I. et al. Microplastics in Arctic polar waters: The first reported values of particles in surface and sub-surface samples. *Scientific Reports*, 5(September):1–9, 2015. doi: 10.1038/srep14947.

[29] Free, C.M., Jensen, O.P., Mason, S.A. et al. High-levels of microplastic pollution in a large, remote, mountain lake. *Marine Pollution Bulletin*, 85(1):156–163, 2014. doi: 10.1016/j.marpolbul.2014.06.001.

[30] Napper, I.E. and Thompson, R.C. *Marine Plastic Pollution: Other Than Microplastic*. Elsevier Inc., 2 edition, 2019. doi: 10.1016/b978-0-12-815060-3.00022-0.

[31] Stubbins, A., Law, K.L., Muñoz, S.E. et al. Plastics in the Earth system. *Science*, 373:51–55, 2021. doi: 10.1126/science.abb0354.

[32] De-la Torre, G.E., Dioses-Salinas, D.C., Pizarro-Ortega, C.I. et al. New plastic formations in the Anthropocene. *Science of the Total Environment*, 754:14221–6, 2021. doi: 10.1016/j.scitotenv.2020.142216.

[33] Eisenbud, M. Population Growth, Food, Energy, and Raw Materials. In *Environment, Technology, and Health*, pages 79–115. Palgrave, London, 1978. doi: 10.1007/978-1-349-04752-9_5.

[34] M. Shahid, A. Economic Growth with Energy. *Munich Personal RePEc Archive*, (1260):1–25, 2006.

[35] Rosen, M.A. Energy sustainability: A pragmatic approach and illustrations. *Sustainability*, 1:55–80, 2009. doi: 10.3390/su1010055.

[36] United Nations Framework Convention on Climate Change. *Kyoto Protocol Reference Manual on Accounting of Emissions and Assigned Amount*. 2008. doi: 10.5213/jkcs.1998.2.2.62.

[37] Kim, Y., Tanaka, K. and Matsuoka, S. Environmental and economic effectiveness of the Kyoto Protocol. *PLoS ONE*, 15(7):1–15, 2020. doi: 10.1371/journal.pone.0236299.

[38] Røpke, I. Econ 101—In need of a sustainability transition. *Ecological Economics*, 169(October 2019):106515, 2020. doi: 10.1016/j.ecolecon.2019.106515.

[39] Schor, J.B. Prices and quantities: Unsustainable consumption and the global economy. *Ecological Economics*, 55:309–320, 2005. doi: 10.1016/j.ecolecon.2005.07.030.

[40] Mahmood, N., Wang, Z. and Hassan, S.T. Renewable energy, economic growth, human capital, and CO2 emission: an empirical analysis. *En-*

vironmental Science and Pollution Research, 26:20619–20630, 2019. doi: 10.1007/s11356-019-05387-5.

[41] Hadjadj, R., Deák, C., Palotás, Á.B. et al. Renewable energy and raw materials – The thermodynamic support. *Journal of Cleaner Production*, 241, 2019. doi: 10.1016/j.jclepro.2019.118221.

[42] Macromolecule (Polymer Molecule). In *The IUPAC Compendium of Chemical Terminology*, page 1. IUPAC, 2014. doi: 10.1351/goldbook.m03667.

[43] Ravve, A. *Principles of Polymer Chemistry*. Springer Science+Business Media, Niles, IL, USA, 1954. doi: 10.1007/978-1-4614-2212-9.

[44] Saldívar-Guerra, E. and Vivaldo-Lima, E., editors. *Handbook of Polymer Synthesis, Characterization and Processing*. John Wiley & Sons, Inc., Hoboken, NJ, USA, 2019.

[45] Olabisi, O. and Adewale, K., editors. *Handbook of Thermoplastics*. CRC Press, Boca Raton, FL, USA, feb 2016.

[46] Rasmussen, S.C. Revisiting the early history of synthetic polymers: Critiques and new insights. *Ambix*, pages 356–372, 2018. doi: 10.1080/00026980.2018.1512775.

[47] Al-Salem, S.M., Lettieri, P. and Baeyens, J. Recycling and recovery routes of plastic solid waste (PSW): A review. *Waste Management*, 29(10):2625–2643, 2009. doi: 10.1016/j.wasman.2009.06.004.

[48] PlasticsEurope and EPRO. Plastics – the Facts 2021: An analysis of European plastics production, demand and waste data. Technical report, Brussels, 2021.

[49] Benson, N.U., Bassey, D.E. and Palanisami, T. COVID pollution: impact of COVID-19 pandemic on global plastic waste footprint. *Heliyon*, 7(2):e06343, 2021. doi: 10.1016/j.heliyon.2021.e06343.

[50] Sills, J. and Adyel, T.M. Accumulation of plastic waste during COVID-19. *Science*, 369(6509):1314, 2020. doi: 10.1126/science.abd9925.

[51] Singh, N., Hui, D., Singh, R. et al. Recycling of plastic solid waste: A state of art review and future applications. *Composites Part B: Engineering*, 115:409–422, 2017. doi: 10.1016/j.compositesb.2016.09.013.

[52] Zhang, F., Zhao, Y., Wang, D. et al. Current technologies for plastic waste treatment: A review. *Journal of Cleaner Production*, 282(124523), 2021. doi: 10.1016/j.jclepro.2020.124523.

[53] Garcia, J.M. and Robertson, M.L. The future of plastics recycling. *Science*, 358(6365):870–872, 2017. doi: 10.1126/science.aaq0324.

[54] Al-Salem, S., Lettieri, P. and Baeyens, J. The valorization of plastic solid waste (PSW) by primary to quaternary routes: From re-use to energy and

chemicals. *Progress in Energy and Combustion Science*, 36:103–129, 2010. doi: 10.1016/j.pecs.2009.09.001.

[55] Plastic Waste Management Institute. An Introduction to Plastic Recycling. Technical report, Tokyo, 2019.

[56] Jiang, B., Yu, J. and Liu, Y. The Environmental Impact of Plastic Waste. *Journal of Environmental and Earth Sciences*, 2(2):26–35, 2020. doi: 10.30564/jees.v2i2.2340.

[57] Rudolph, N., Kiesel, R. and Aumnate, C. *Understanding Plastics Recycling - Economic, Ecological, and Technical Aspects of Plastic Waste Handling*. Carl Hanser Verlag, Munich, 2017. doi: 10.3139/9781569908471.fm.

[58] Rillig, M.C., Kim, S.W., Kim, T.Y. et al. The global plastic toxicity debt. *Environmental Science and Technology*, 55(5):2717–2719, 2021. doi: 10.1021/acs.est.0c07781.

[59] Chandra Singh, J.S. and Gupta, S.A. A Review on Waste Plastic Utilization and Biodegradation. *Journal of Scientific Research*, 65(2):13–16, 2021. doi: 10.37398/jsr.2021.650203.

[60] Rawat, N.K., Stoica, I. and Haghi, A., editors. *Green Polymer Chemistry and Composites: Pollution Prevention and Waste Reduction*. Apple Academic Press Inc./CRC Press, Palm Bay, FL, USA, 2021.

[61] Huysman, S., De Schaepmeester, J., Ragaert, K. et al. Performance indicators for a circular economy: A case study on post-industrial plastic waste. *Resources, Conservation and Recycling*, 120:46–54, 2017. doi: 10.1016/j.resconrec.2017.01.013.

[62] Kaur, G., Uisan, K., Ong, K.L. et al. Recent Trends in Green and Sustainable Chemistry & Waste Valorisation: Rethinking Plastics in a circular economy. *Current Opinion in Green and Sustainable Chemistry*, 9:30–39, 2018. doi: 10.1016/j.cogsc.2017.11.003.

[63] Paletta, A., Leal Filho, W., Balogun, A.L. et al. Barriers and challenges to plastics valorisation in the context of a circular economy: Case studies from Italy. *Journal of Cleaner Production*, 241:118149, 2019. doi: 10.1016/j.jclepro.2019.118149.

[64] Androniceanu, A.M., Caplescu, R.D., Tvaronaviciene, M. et al. The Interdependencies between Economic Growth, Energy Consumption and Pollution in Europe. *Energies*, 14(2577):1–23, 2021. doi: 10.3390/en14092577.

[65] International Energy Agency. World Energy Outlook 2021. Technical report, 2021.

[66] Newell, R., Raimi, D., Villanueva, S. et al. Global Energy Outlook 2021: Pathways from Paris. Technical Report June, Resources for the Future, 2021.

[67] Gielen, D., Boshell, F., Saygin, D. et al. The role of renewable energy in the global energy transformation. *Energy Strategy Reviews*, 24:38–50, 2019. doi: 10.1016/j.esr.2019.01.006.

[68] Züttel, A., Remhof, A., Borgschulte, A. et al. Hydrogen: The future energy carrier. *Philosophical Transactions of the Royal Society A: Mathematical, Physical and Engineering Sciences*, 368(1923):3329–3342, 2010. doi: 10.1098/rsta.2010.0113.

[69] Jasiunas, J., Lund, P.D. and Mikkola, J. Energy system resilience – A review. *Renewable and Sustainable Energy Reviews*, 150(111476):1–18, 2021. doi: 10.1016/j.rser.2021.111476.

[70] Wang, D., Muratori, M., Eichman, J. et al. Quantifying the Flexibility of Hydrogen Production Systems to Support Large-Scale Renewable Energy Integration. *Journal of Power Sources*, 399:383–391, 2018. doi: 10.1016/j.jpowsour.2018.07.101.

[71] Impram, S., Nese, S.V. and Oral, B. Challenges of renewable energy penetration on power system flexibility: A survey. *Energy Strategy Reviews*, 31 (100539):1–12, 2020. doi: 10.1016/j.esr.2020.100539.

[72] Ball, M., Basile, A. and Veziroglu, T.N., editors. *Compendium of Hydrogen Energy - Volume 4 - Hydrogen Use, Safety and the Hydrogen Economy*. Elsevier, 2016. doi: 10.1016/c2014-0-02671-8.

[73] Schlögl, R. Chemical energy storage enables the transformation of fossil energy systems to sustainability. *Green Chemistry*, 23:1584–1593, 2021. doi: 10.1039/d0gc03171b.

[74] Mahlia, T., Saktisahdan, T., Jannifar, A. et al. A review of available methods and development on energy storage: technology update. *Renewable and Sustainable Energy Reviews*, 33:532–545, 2014. doi: 10.1016/j.rser.2014.01.068.

[75] Abe, J., Popoola, A., Ajenifuja, E. et al. Hydrogen energy, economy and storage: Review and recommendation. *International Journal of Hydrogen Energy*, 44:15072–15086, 2019. doi: 10.1016/j.ijhydene.2019.04.068.

[76] Noussan, M., Raimondi, P.P., Scita, R. et al. The Role of Green and Blue Hydrogen in the Energy Transition — A Technological and Geopolitical Perspective. *Sustainability*, 13(298):1–26, 2021. doi: 10.3390/su13010298.

[77] Chapman, A., Itaoka, K., Hirose, K. et al. A review of four case studies assessing the potential for hydrogen penetration of the future energy system. *International Journal of Hydrogen Energy*, 44:6371–6382, 2019. doi: 10.1016/j.ijhydene.2019.01.168.

[78] Yue, M., Lambert, H., Pahon, E. et al. Hydrogen energy systems: A critical review of technologies, applications, trends and challenges. *Renewable and*

Sustainable Energy Reviews, 146(111180):1–21, 2021. doi: 10.1016/j.rser.2021.111180.

[79] van Renssen, S. The hydrogen solution? *Nature Climate Change*, 10:799–801, 2020. doi: 10.1038/s41558-020-0891-0.

[80] Demirbas, A. Future hydrogen economy and policy. *Energy Sources, Part B: Economics, Planning and Policy*, 12(2):172–181, 2017. doi: 10.1080/15567249.2014.950394.

[81] Zgonnik, V. The occurrence and geoscience of natural hydrogen: A comprehensive review. *Earth-Science Reviews*, 203(103140):1–51, 2020. doi: 10.1016/j.earscirev.2020.103140.

[82] Frery, E., Langhi, L., Maison, M. et al. Natural hydrogen seeps identified in the North Perth Basin, Western Australia. *International Journal of Hydrogen Energy*, 46:31158–31173, 2021. doi: 10.1016/j.ijhydene.2021.07.023.

[83] Prinzhofer, A., Tahara Cissé, C.S. and Diallo, A.B. Discovery of a large accumulation of natural hydrogen in Bourakebougou (Mali). *International Journal of Hydrogen Energy*, 43:19315–19326, 2018. doi: 10.1016/j.ijhydene.2018.08.193.

[84] Siegel, R. What Color is Your Hydrogen? *Mechanical Engineering*, (October/November):38–43, 2021.

[85] Newborough, M. and Cooley, G. Developments in the global hydrogen market: The spectrum of hydrogen colours. *Fuel Cells Bulletin*, 2020(11):16–22, 2020. doi: 10.1016/S1464-2859(20)30546-0.

[86] IRENA. Green Hydrogen: A guide to policy making. Technical report, International Renewable Energy Agency, Abu Dhabi, 2020.

[87] Nikolaidis, P. and Poullikkas, A. A comparative overview of hydrogen production processes. *Renewable and Sustainable Energy Reviews*, 67:597–611, 2017. doi: 10.1016/j.rser.2016.09.044.

[88] Staffell, I., Scamman, D., Velazquez Abad, A. et al. The role of hydrogen and fuel cells in the global energy system. *Energy & Environmental Science*, 12:463–491, 2019. doi: 10.1039/c8ee01157e.

[89] Harrison, S.B. Giga-scale green hydrogen projects. Available online: https://www.pollutionsolutions-online.com/news/green-energy/42/sbh4-gmbh/giga-scale-green-hydrogen-projects/54578, 2021.

[90] Oliveira, A.M., Beswick, R.R. and Yan, Y. A green hydrogen economy for a renewable energy society. *Current Opinion in Chemical Engineering*, 33 (100701):1–7, 2021. doi: 10.1016/j.coche.2021.100701.

[91] Balali, Y. and Stegen, S. Review of energy storage systems for vehicles based on technology, environmental impacts, and costs. *Renewable and Sustain-*

able Energy Reviews, 135(110185):1–15, 2021. doi: 10.1016/j.rser.2020.110185.

[92] Chi, J. and Yu, H. Water electrolysis based on renewable energy for hydrogen production. *Chinese Journal of Catalysis*, 39:390–394, 2018. doi: 10.1016/S1872-2067(17)62949-8.

[93] Lui, J., Chen, W.H., Tsang, D.C. et al. A critical review on the principles, applications, and challenges of waste-to-hydrogen technologies. *Renewable and Sustainable Energy Reviews*, 134(110365):1–14, 2020. doi: 10.1016/j.rser.2020.110365.

[94] Zeng, K. and Zhang, D. Recent progress in alkaline water electrolysis for hydrogen production and applications. *Progress in Energy and Combustion Science*, 36:307–326, 2010. doi: 10.1016/j.pecs.2009.11.002.

[95] Rashid, M.M., Al Mesfer, M.K., Naseem, H. et al. Hydrogen production by water electrolysis: a review of alkaline water electrolysis, PEM water electrolysis and high temperature water electrolysis. *International Journal of Engineering and Advanced Technology*, 4(3):80–93, 2015.

[96] Carmo, M., Fritz, D.L., Mergel, J. et al. A comprehensive review on PEM water electrolysis. *International Journal of Hydrogen Energy*, 38:4901–4934, apr 2013. doi: 10.1016/j.ijhydene.2013.01.151.

[97] Ni, M., Leung, M.K. and Leung, D.Y. Technological development of hydrogen production by solid oxide electrolyzer cell (SOEC). *International Journal of Hydrogen Energy*, 33:2337–2354, 2008. doi: 10.1016/j.ijhydene.2008.02.048.

[98] Abbasi, R., Setzler, B.P., Lin, S. et al. A Roadmap to Low-Cost Hydrogen with Hydroxide Exchange Membrane Electrolyzers. *Advanced Materials*, 31 (1805876):1–14, 2019. doi: 10.1002/adma.201805876.

[99] Sapountzi, F.M., Gracia, J.M., Weststrate, C.J.K.J. et al. Electrocatalysts for the generation of hydrogen, oxygen and synthesis gas. *Progress in Energy and Combustion Science*, 58:1–35, 2017. doi: 10.1016/j.pecs.2016.09.001.

[100] Tuomi, S., Santasalo-Aarnio, A., Kanninen, P. et al. Hydrogen production by methanol–water solution electrolysis with an alkaline membrane cell. *Journal of Power Sources*, 229:32–35, 2013. doi: 10.1016/j.jpowsour.2012.11.131.

[101] Caravaca, A., Sapountzi, F.M., De Lucas-Consuegra, A. et al. Electrochemical reforming of ethanol-water solutions for pure H2 production in a PEM electrolysis cell. *International Journal of Hydrogen Energy*, 37(12):9504–9513, 2012. doi: 10.1016/j.ijhydene.2012.03.062.

[102] Caravaca, A., De Lucas-Consuegra, A., Calcerrada, A.B. et al. From biomass to pure hydrogen: Electrochemical reforming of bio-ethanol in a PEM elec-

trolyser. *Applied Catalysis B: Environmental*, 134-135:302–309, 2013. doi: 10.1016/j.apcatb.2013.01.033.

[103] Marshall, A.T. and Haverkamp, R.G. Production of hydrogen by the electrochemical reforming of glycerol–water solutions in a PEM electrolysis cell. *International Journal of Hydrogen Energy*, 33:4649–4654, 2008. doi: 10.1016/j.ijhydene.2008.05.029.

[104] Coutanceau, C. and Baranton, S. Electrochemical conversion of alcohols for hydrogen production: a short overview. *Wiley Interdisciplinary Reviews: Energy and Environment*, 5(4):388–400, 2016. doi: 10.1002/wene.193.

[105] Kwon, Y., Birdja, Y., Spanos, I. et al. Highly selective electro-oxidation of glycerol to dihydroxyacetone on platinum in the presence of bismuth. *ACS Catalysis*, 2(5):759–764, 2012. doi: 10.1021/cs200599g.

[106] Simões, M., Baranton, S. and Coutanceau, C. Electrochemical valorisation of glycerol. *ChemSusChem*, 5(11):2106–2124, 2012. doi: 10.1002/cssc.201200335.

[107] Sapountzi, F.M., Di Palma, V., Zafeiropoulos, G. et al. Overpotential analysis of alkaline and acidic alcohol electrolysers and optimized membrane-electrode assemblies. *International Journal of Hydrogen Energy*, 44:10163–10173, 2019. doi: 10.1016/j.ijhydene.2019.02.205.

[108] Chen, Y.X., Lavacchi, A., Miller, H.A. et al. Nanotechnology makes biomass electrolysis more energy efficient than water electrolysis. *Nature Communications*, 5(May):1–6, 2014. doi: 10.1038/ncomms5036.

[109] Linares, J.J., Vieira, C.C., Costa Santos, J.B. et al. Chapter 4 Electrochemical Reforming of Alcohols. In *Electrochemical Methods for Hydrogen Production*, pages 94–135. The Royal Society of Chemistry, 2020. doi: 10.1039/9781788016049-00094.

[110] Caravaca, A., Garcia-Lorefice, W.E., Gil, S. et al. Towards a sustainable technology for H2 production: Direct lignin electrolysis in a continuous-flow Polymer Electrolyte Membrane reactor. *Electrochemistry Communications*, 100(January):43–47, 2019. doi: 10.1016/j.elecom.2019.01.016.

[111] Du, X., Liu, W., Zhang, Z. et al. Low energy catalytic electrolysis for simultaneous hydrogen evolution and lignin depolymerization. *ChemSusChem*, 10: 847–854, mar 2017. doi: 10.1002/cssc.201601685.

[112] Liu, Z.H., Le, R.K., Kosa, M. et al. Identifying and creating pathways to improve biological lignin valorization. *Renewable and Sustainable Energy Reviews*, 105:349–362, 2019. doi: 10.1016/j.rser.2019.02.009.

[113] Wang, H., Pu, Y., Ragauskas, A. et al. From lignin to valuable products–strategies, challenges, and prospects. *Bioresource Technology*, 271:449–461, 2018. doi: 10.1016/j.biortech.2018.09.072.

[114] Cao, L., Iris, K.M., Liu, Y. et al. Lignin valorization for the production of renewable chemicals: State-of-the-art review and future prospects. *Bioresource Technology*, 269:465–475, 2018.

[115] Zakzeski, J., Jongerius, A.L., Bruijnincx, P.C.A. et al. Catalytic lignin valorization process for the production of aromatic chemicals and hydrogen. *ChemSusChem*, 5:1602–1609, 2012.

[116] Zirbes, M. and Waldvogel, S.R. Electro-conversion as sustainable method for the fine chemical production from the biopolymer lignin. *Current Opinion in Green and Sustainable Chemistry*, 14:19–25, 2018. doi: 10.1016/j.cogsc.2018.05.001.

[117] Du, X., Zhang, H., Sullivan, K.P. et al. Electrochemical Lignin Conversion. *ChemSusChem*, 13:4318–4343, 2020. doi: 10.1002/cssc.202001187.

[118] Parpot, P., Bettencourt, A.P., Carvalho, A.M. et al. Biomass conversion: attempted electrooxidation of lignin for vanillin production. *Journal of Applied Electrochemistry*, 30(6):727–731, 2000. doi: 10.1023/A:1004003613883.

[119] Stiefel, S., Lölsberg, J., Kipshagen, L. et al. Controlled depolymerization of lignin in an electrochemical membrane reactor. *Electrochemistry Communications*, 61:49–52, 2015.

[120] Wang, H., Jusys, Z. and Behm, R. Ethanol Electrooxidation on a Carbon-Supported Pt Catalyst: Reaction Kinetics and Product Yields. *The Journal of Physical Chemistry B*, 108(50):19413–19424, 2004. doi: 10.1021/jp046561k.

[121] Monyoncho, E.A., Steinmann, S.N., Michel, C. et al. Ethanol electrooxidation on palladium revisited using Polarization Modulation Infrared Reflection Absorption Spectroscopy (PM-IRRAS) and Density Functional Theory (DFT): Why Is It Difficult To Break the C–C Bond? *ACS Catalysis*, 6(8):4894–4906, 2016. doi: 10.1021/acscatal.6b00289.

[122] Monyoncho, E.A., Steinmann, S.N., Sautet, P. et al. Computational screening for selective catalysts: Cleaving the CC bond during ethanol electrooxidation reaction. *Electrochimica Acta*, 274:274–278, 2018. doi: 10.1016/j.electacta.2018.04.102.

[123] Coutanceau, C., Baranton, S. and Kouamé, R.S.B. Selective Electrooxidation of Glycerol Into Value-Added Chemicals: A Short Overview. *Frontiers in Chemistry*, 7:100, 2019. doi: 10.3389/fchem.2019.00100.

[124] Lalvani, S.B. and Rajagopal, P. Lignin-augmented water electrolysis. *Journal of The Electrochemical Society*, 139(1):L1–L2, jan 1992. doi: 10.1149/1.2069212.

[125] Lalvani, S.B. and Rajagopal, P. Hydrogen production from lignin-water solution by electrolysis:. *Holzforschung-International Journal of the Biology,*

Chemistry, Physics and Technology of Wood, 47(4):283–286, 1993. doi: 10.1515/hfsg.1993.47.4.283.

[126] Roy Ghatak, H. Electrolysis of black liquor for hydrogen production: Some initial findings. *International Journal of Hydrogen Energy*, 31(7):934–938, 2006. doi: 10.1016/j.ijhydene.2005.07.013.

[127] Ghatak, H.R., Kumar, S. and Kundu, P. Electrode processes in black liquor electrolysis and their significance for hydrogen production. *International Journal of Hydrogen Energy*, 33(12):2904–2911, 2008. doi: 10.1016/j.ijhydene.2008.03.051. 2nd World Congress of Young Scientists on Hydrogen Energy Systems.

[128] Movil, O., Garlock, M. and Staser, J.A. Non-precious metal nanoparticle electrocatalysts for electrochemical modification of lignin for and cost-effective production of hydrogen. *International Journal of Hydrogen Energy*, 40(13): 4519–4530, 2015. doi: 10.1016/j.ijhydene.2015.02.023.

[129] Hibino, T., Kobayashi, K., Nagao, M. et al. Hydrogen Production by Direct Lignin Electrolysis at Intermediate Temperatures. *ChemElectroChem*, 4(12): 3032–3036, 2017. doi: 10.1002/celc.201700917.

[130] Bateni, F., NaderiNasrabadi, M., Ghahremani, R. et al. Low-Cost Nanostructured Electrocatalysts for Hydrogen Evolution in an Anion Exchange Membrane Lignin Electrolysis Cell. *Journal of The Electrochemical Society*, 166 (14):F1037–F1046, 2019. doi: 10.1149/2.0221914jes.

[131] NaderiNasrabadi, M., Bateni, F., Chen, Z. et al. Biomass-Depolarized Electrolysis. *Journal of The Electrochemical Society*, 166(10):E317–E322, 2019. doi: 10.1149/2.1471910jes.

[132] Beliaeva, K., Grimaldos-Osorio, N., Ruiz-López, E. et al. New insights into lignin electrolysis on nickel-based electrocatalysts: Electrochemical performances before and after oxygen evolution. *International Journal of Hydrogen Energy*, pages 1–13, 2021. doi: 10.1016/j.ijhydene.2021.01.224.

[133] Beliaeva, K., Elsheref, M., Walden, D. et al. Towards Understanding Lignin Electrolysis: Electro-Oxidation of a β-O-4 Linkage Model on PtRu Electrodes. *Journal of The Electrochemical Society*, 167(134511):1–8, 2020. doi: 10.1149/1945-7111/abb8b5.

[134] Ghahremani, R., Farales, F., Bateni, F. et al. Simultaneous Hydrogen Evolution and Lignin Depolymerization using NiSn Electrocatalysts in a Biomass-Depolarized Electrolyzer. *Journal of The Electrochemical Society*, 167(043502), 2020. doi: 10.1149/1945-7111/ab7179.

[135] Ghahremani, R. and Staser, J.A. Electrochemical oxidation of lignin for the production of value-added chemicals on Ni-Co bimetallic electrocatalysts. *Holzforschung*, 72:1–10, 2018.

[136] Liu, W., Cui, Y., Du, X. et al. High efficiency hydrogen evolution from native biomass electrolysis. *Energy and Environmental Science*, 9(2):467–472, 2016. doi: 10.1039/c5ee03019f.

[137] Hibino, T., Kobayashi, K., Ito, M. et al. Efficient Hydrogen Production by Direct Electrolysis of Waste Biomass at Intermediate Temperatures. *ACS Sustainable Chemistry and Engineering*, 6(7):9360–9368, 2018. doi: 10.1021/acssuschemeng.8b01701.

[138] Hibino, T., Kobayashi, K., Ito, M. et al. Direct electrolysis of waste newspaper for sustainable hydrogen production: an oxygen-functionalized porous carbon anode. *Applied Catalysis B: Environmental*, 231:191–199, 2018. doi: 10.1016/j.apcatb.2018.03.021.

[139] Al-Salem, S.M., Antelava, A., Constantinou, A. et al. A review on thermal and catalytic pyrolysis of plastic solid waste (PSW). *Journal of Environmental Management*, 197(1408):177–198, 2017. doi: 10.1016/j.jenvman.2017.03.084.

[140] Aguado, J., Serrano, D.P. and Escola, J.M. Fuels from waste plastics by thermal and catalytic processes: A review. *Industrial and Engineering Chemistry Research*, 47(21):7982–7992, 2008. doi: 10.1021/ie800393w.

[141] Wu, C., Nahil, M.A., Miskolczi, N. et al. Production and application of carbon nanotubes, as a co-product of hydrogen from the pyrolysis-catalytic reforming of waste plastic. *Process Safety and Environmental Protection*, 103:107–114, 2016. doi: 10.1016/j.psep.2016.07.001.

[142] Wu, C., Nahil, M.A., Miskolczi, N. et al. Processing real-world waste plastics by pyrolysis-reforming for hydrogen and high-value carbon nanotubes. *Environmental Science and Technology*, 48:819–826, 2014. doi: 10.1021/es402488b.

[143] Czernik, S. and French, R.J. Production of hydrogen from plastics by pyrolysis and catalytic steam reform. *Energy and Fuels*, 20:754–758, 2006. doi: 10.1021/ef050354h.

[144] Dharmaraj, S., Ashokkumar, V., Chew, K.W. et al. Novel strategy in biohydrogen energy production from COVID - 19 plastic waste: A critical review. *International Journal of Hydrogen Energy*, 2021. doi: 10.1016/j.ijhydene.2021.08.236.

[145] Uekert, T., Kuehnel, M.F., Wakerley, D.W. et al. Plastic waste as a feedstock for solar-driven H2 generation. *Energy and Environmental Science*, 11(10):2853–2857, 2018. doi: 10.1039/c8ee01408f.

[146] Kawai, T. and Sakata, T. Photocatalytic Hydrogen Production From Water By the Decomposition of Poly-Vinylchloride, Protein, Algae, Dead Insects, and Excrement. *Chemistry Letters*, pages 81–84, 1981. doi: 10.1246/cl.1981.81.

[147] Jie, X., Li, W., Slocombe, D. et al. Microwave-initiated catalytic deconstruction of plastic waste into hydrogen and high-value carbons. *Nature Catalysis*, 3(11):902–912, 2020. doi: 10.1038/s41929-020-00518-5.

[148] Hori, T., Ma, Q., Kobayashi, K. et al. Electrolysis of humidified methane to hydrogen and carbon dioxide at low temperatures and voltages. *International Journal of Hydrogen Energy*, 44(5):2454–2460, 2019. doi: 10.1016/j.ijhydene.2018.12.044.

[149] Shi, R., Liu, K.S., Liu, F. et al. Electrocatalytic reforming of waste plastics into high value-added chemicals and hydrogen fuel. *Chem. Commun.*, 57: 12595–12598, 2021. doi: 10.1039/D1CC05032J.

[150] Jiang, T., Zhao, X., Gu, D. et al. STEP polymer degradation: Solar thermo-coupled electrochemical depolymerization of plastics to generate useful fuel plus abundant hydrogen. *Solar Energy Materials and Solar Cells*, 204 (September 2019):110208, jan 2020. doi: 10.1016/j.solmat.2019.110208.

[151] Pati, S., Gopalan, S. and Pal, U.B. A solid oxide membrane electrolyzer for production of hydrogen and syn-gas from steam and hydrocarbon waste in a single step. *International Journal of Hydrogen Energy*, 36(1):152–159, 2011. doi: 10.1016/j.ijhydene.2010.10.013.

[152] Pal, U.B., Pati, S., Yoong, K.J. et al. (Invited) Electrolyzer for Waste to Energy Conversion. *ECS Transactions*, 41(12):93–101, 2012. doi: 10.1149/1.3697432.

[153] Ali, U., Karim, K.J.B.A. and Buang, N.A. A Review of the Properties and Applications of Poly (Methyl Methacrylate) (PMMA). *Polymer Reviews*, 55: 678–705, 2015. doi: 10.1080/15583724.2015.1031377.

[154] Gayathri, A., Naveena Sajja, J., Vidhyashree Daswani, M. et al. An extensive review of shape memory polymers for biomedical applications. *IOP Conference Series: Materials Science and Engineering*, 993(012161):1–10, 2020. doi: 10.1088/1757-899X/993/1/012161.

[155] Soleymani Eil Bakhtiari, S., Bakhsheshi-Rad, H.R., Karbasi, S. et al. Poly(methyl methacrylate) bone cement, its rise, growth, downfall and future. *Polymer International*, 70:1182–1201, 2021. doi: 10.1002/pi.6136.

[156] D'souza, A.A. and Shegokar, R. Polyethylene glycol (PEG): a versatile polymer for pharmaceutical applications. *Expert Opinion on Drug Delivery*, 13 (9):1257–1275, 2016. doi: 10.1080/17425247.2016.1182485.

[157] Chen, J., Spear, S.K., Huddleston, J.G. et al. Polyethylene glycol and solutions of polyethylene glycol as green reaction media. *Green Chemistry*, 7: 64–82, 2005. doi: 10.1039/b413546f.

[158] Wu, Y., Wang, Q. and Libera, M. PEG-based microgels to modify biomaterials

surfaces. *Macromolecular Symposia*, 329:35–40, 2013. doi: 10.1002/masy.201200106.

CHAPTER 2

From plastic-waste to H_2: Electrolysis of a Poly(methyl methacrylate) model molecule on polymer electrolyte membrane reactors

From plastic-waste to H_2: Electrolysis of a Poly(methyl methacrylate) model molecule on polymer electrolyte membrane reactors

N. Grimaldos-Osorio[1,2], F. Sordello[2], M. Passananti[2]
P. Vernoux[1], A. Caravaca[1]

[1] *Université de Lyon, Institut de Recherches sur la Catalyse et l'Environnement de Lyon, UMR 5256, CNRS, Université Claude Bernard Lyon 1, 2 avenue A. Einstein, 69626 Villeurbanne, France.*
[2] *Dipartimento di Chimica, Università di Torino, Via Pietro Giuria 5, 10125 Turin, Italy.*

Journal of Power Sources 480 (2020) 228800
DOI: 10.1016/j.jpowsour.2020.228800
Received 8 May 2020; Received in revised form 17 July 2020
Accepted 12 August 2020; Available online 7 September 2020

Keywords: Hydrogen production, PEM electrolysis cell, plastic-waste valorisation, PMMA valorisation, methyl pivalate model molecule

Abstract: Hydrogen production by the electrolysis of plastic-waste was recently suggested as an alternative approach to water electrolysis, owing to its favoured thermodynamics. However, the fundamental aspects of such electro-catalytic process were not studied in detail. Here we propose a new approach to understand the electrolysis of polymers, by the use of model molecules. Our target is to develop a technology for the electrolysis of poly(methyl methacrylate), PMMA, plastic waste. We used methyl pivalate (MP) as a model molecule, since it contains similar functional groups than PMMA. We performed electrolysis experiments in a Polymer Electrolyte Membrane reactor with Nafion® protonic membranes and Pt/C electrodes at low temperatures (<90 °C). The results obtained demonstrated that the electro-oxidation of MP allows to produce H_2 in a range of electrical potentials where water electrolysis is not thermodynamically possible (<1.2 V). The kinetics of this process were studied and a preliminary global mechanism was proposed to explain the electro-oxidative cleavage of this model molecule. We have clearly demonstrated that the electrolysis of a plastic-like model monomer leads to the production of hydrogen. These results could be further extrapolated in view of the practical implementation of this technology for the valorisation of PMMA waste.

2.1 Introduction

The incursion of renewable energy sources in the electrical grid is an on-going process that will accelerate in the coming years. Renewable energy production (e.g. wind, hydraulic and solar) is increasing, but still fluctuating, making it challenging for their integration into the energy system [1]. To store these oscillating sources of energy and facilitate their transport, an energy carrier is required, hydrogen being the most promising one [2]. In this context, water electrolysis is one of the most popular electrochemical technologies that would allow transforming the renewable energies into pure H_2, with O_2 as the only by-product [3]. However, this process is not sustainable from energetic and economic points of view, since a minimum thermodynamic cell potential of 1.23 V is necessary to electrochemically cleave the H_2O molecule [4, 5]. Consequently, different researchers have proposed to electrolyse organic molecules (e.g. methanol [6–9] and ethanol [10–15], instead of water, to reduce the energy demand, since the thermodynamic potential for the electro-oxidation of these organic compounds is significantly lower than that for water. This opens the possibility for the use of organic wastes as a H_2 resource. Different organic wastes/by-products have already been studied in electrolysers such as wastewaters [16], biomass-based wastes [17–19], pyrolysis oil derivates [20], lignin [21–29] and glycerol [30, 31].

In this frame, plastic-wastes are organic polymers and must also be contemplated as a massive source of hydrogen. Nowadays, less than 10 % and ∼30 % of the plastics are recycled in USA and Europe, respectively [32, 33]. In 2017, a considerable fraction of the plastic waste produced within the EU went to Energy Recovery (∼39.5 %) [34] usually by direct combustion/incineration. However, this process often causes a significant environmental impact owing to hazardous emissions (NO_x, SO_x, Volatile Organic Compounds, etc.). The same year, the remaining vast amount of plastic waste was directly sent to landfill (∼30.8 %) [34], which is not a viable option in the long run. In addition, plastic wastes are becoming a major environmental issue in aquatic systems as a result of a permissible waste management and plastic fragmentation processes in the environment [35–38].

Among the different plastics, poly(methyl methacrylate) (PMMA) is a widely used polymer in automotive, construction and electrical industries, and is also crucial for the production of Plexiglass® and Perspex® [39]. The global market for this plastic is estimated to reach a value of about USD 11 billion for 2022 [40]. Even if different thermal and chemical methods are used today for recycling PMMA with a worthy recuperation rate of its monomer methyl methacrylate (MMA), no processes for direct Energy Recovery different than incineration are known. In the present

study we propose, for the very first time, a novel potential route to valorise PMMA waste by producing H_2 via low temperature electrolysis.

The direct electrolysis of synthetic polymers for H_2 production has been scarcely studied. To the best of our knowledge, only two studies [41, 42] reported the electrolysis of plastics (polypropylene) in high temperature Solid Oxide Electrolysers (>800 °C). One study reported a solar thermo-coupled electrochemical depolymerization of polypropylene at intermediate temperatures (350 – 400 °C) [43], and one study was recently carried out in low temperature (<200 °C) electrolysers [44]. Low temperature electrolysers are advantageous in terms of simplicity and energy-demand. In ref. [44], a wide variety of industrial common plastics (sponges, cable ties, stocking and rope) and pure polymers (polyvinyl alcohol (PVA) and polyurethane) were electrolyzed in acid media (∼85 % H_3PO_4) on Pt-based electrodes. Even though this study demonstrated the proof-of-concept to electrolyze plastic-waste resources in low temperature electrolysers, the electrochemical processes involved and mechanistic routes are not described. A deep comprehension of the processes involved will allow assessing the feasibility of the electrochemical cleavage of plastic polymer and the optimization of procedures to produce H_2 from plastic-waste. In addition, we believe that the strong acid media could transform the polymer into smaller molecules easy to electrolyse, and therefore the process would not be purely electro-catalytic.

In the present study, we report a different approach to understand the mechanism for the electro-oxidation of PMMA. Due to the complexity and the heterogeneity of real PMMA-based plastics, a model molecule representative of the main chemical bonds present in the polymer repeating unit was used: methyl trimethylacetate (methyl pivalate, MP). This molecule exhibits identical ester units, together with the C=O, C–C and C–H bonds than in PMMA, as opposed to the monomer methyl methacrylate (MMA), which exhibits a double C=C bond absent in the polymer (Figure A.1). The MP model molecule is slightly soluble in water, allowing performing electrochemical experiments in aqueous phase as opposed to PMMA, which is a water-insoluble solid. The idea of this work is to study, for the first time, the electro-oxidation of the MP model molecule. To do that, we performed electrolysis experiments in a Polymer Electrolyte Membrane-based (PEM) reactor with acidic-based membranes which serve as electrolyte (Nafion®). This configuration allows working in aqueous media in the absence of a liquid electrolyte (e.g. H_3PO_4), then preserving the MP molecules in the anodic compartment. This study represents a starting point towards understanding the electrochemical cleavage of the main bonds present in the PMMA plastic, and the results could be further extrapolated for real plastic-wastes.

2.2 Experimental

The experiments were performed in a commercial Polymer Electrolyte Membrane (PEM) electrolysis cell (Dioxide Materials®) using commercial electrodes and membranes (FuelCellStore®). Both electrodes (5.3 cm^2) were composed of a Pt/C catalyst impregnated on a carbon cloth with a carbon gas diffusion layer (0.2 mg cm^{-2} of 20 % wt. Pt supported on C_{Vulcan}). A Nafion™ 117 membrane was used as proton-conducting membrane (183 μm thickness). Before use, the membrane was pretreated by immersion at 100 °C for 2 h in 3 different solutions: 150 mL of 3 % wt. H_2O_2, then 150 mL of 0.5 M H_2SO_4 and finally 150 mL of deionized water. The membrane electrode assembly (MEA, anode/membrane/cathode) was prepared by hot-pressing under 1 metric ton at 120 °C for 3 min. Then, the MEA was introduced between two Teflon gaskets to ensure correct sealing of the cell and the PEM cell assembly was mounted. A temperature control system and reactants/products flasks for anodic and cathodic compartments were put in place as well. Figure 2.1 shows the scheme of the PEM experimental set-up.

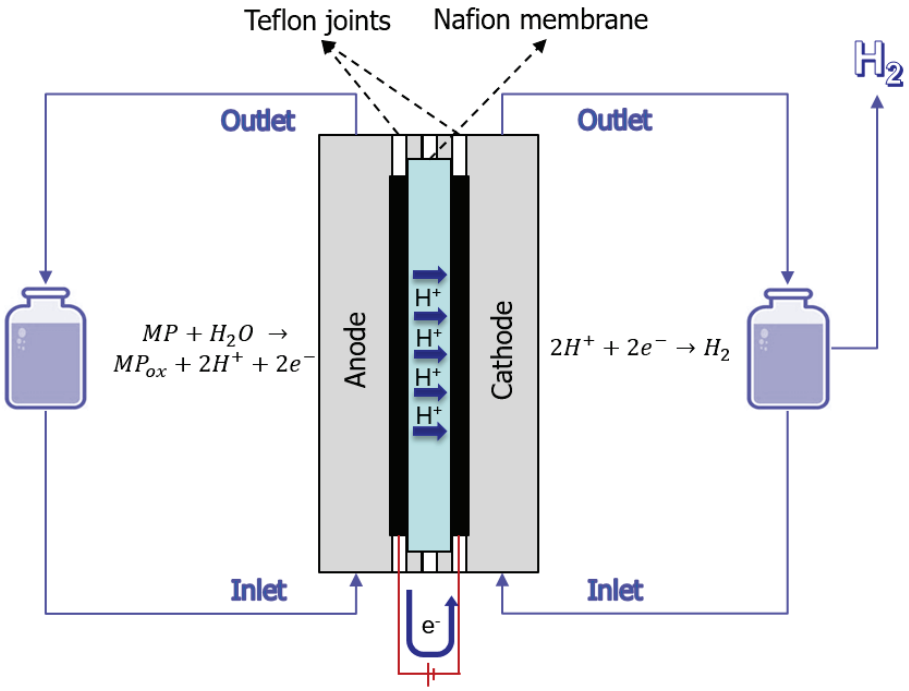

Figure 2.1: General scheme of the Polymer Electrolyte Membrane-based (PEM) experimental set-up used in this study, together with the global electrode reactions.

Methyl trimethylacetate (methyl pivalate, MP, 99 % purity, boiling point 110 °C, <15 g L^{-1} solubility in water), trimethylacetic acid (pivalic acid, PA, 99 % purity) and methanol (MeOH, ≥99.9 % purity) were purchased from Sigma-Aldrich. During the electrolysis experiments, an aqueous solution of the model molecule (30 mL, 10 g L^{-1} methyl pivalate, 1000 rpm stirring, 1.8 mL min^{-1}) and deionized water

(30 mL, 1.8 mL min^{-1}) were fed to the anode and cathode compartments, respectively. For comparison purposes, every experiment was first performed under the same conditions by feeding deionized water to both, anode and cathode. All solutions were fed in recirculation mode starting 30 min before applying polarization (for stabilization purposes). A peristaltic pump assured constant liquid flow rates. For the polarization of the PEM cell, a potentiostat-galvanostat equipped with a 10 A booster (Origalys®) was used.

In addition, the hydrogen purity and production was verified online with a quadrupole mass spectrometer (Portable Quadrupole MS, Aspec). The QMS operates with high vacuum of around $1.3x10^{-6}$ mbar, evacuated by a 70 L/s turbo molecular drag pump combined with a backing pump. The relative molecular concentrations of different compounds such as H_2 (m/z = 2 amu), H_2O (18 amu), N_2 (28 amu), O_2 (32 amu), and CO_2 (44 amu) were online monitored. The gas out-stream in the cathodic vessel (see Figure 2.1) was mixed with a constant flow of inert gas (He, 33 mL min^{-1}) and further introduced into the QMS device. The H_2 trend was analysed and expressed in arbitrary units.

2.3 Results and discussion

The first tests were performed to demonstrate the possibility to electrolyse the organic model molecule (MP) in a range of electrical potentials where water electrolysis is thermodynamically impossible, i.e., V_{cell} <1.23 V. Figure 2.2a shows the 10^{th} cycle of cyclic voltammetry experiments (V_{cell} = 0 – 1100 mV, scanning rate of 10 mV s^{-1}) by feeding deionized water or the MP solution to the anode, always in the absence of any liquid electrolyte, at 80 °C. With regards to water electrolysis, a trend observed in previous studies for Pt-based materials [27] was obtained, with a weak forward onset oxidation potential at ~0.9 V attributed to a partial passivation of Pt (formation of oxygen layer), which would be reduced during the backward scan.

The introduction of the organic model molecule leads to a completely different trend. First of all, much higher electrical currents (i.e. higher electrolysis efficiency) were obtained during both, forward and backward scans. As previously shown in Figure 2.1 (PEM scheme), since acid H^+ membranes were used, MP solutions fed to the anode are electro-oxidized ($MP + H_2O \rightarrow MP_{ox} + 2H^+ + 2e^-$), with the subsequent production of oxidized products and H^+. The protons migrate through the membrane, leading to the corresponding H_2 evolution cathodic reaction ($2H^+ + 2e^- \rightarrow H_2$). Therefore, the enhanced performance of the electrolyser in the presence of MP can be clearly attributed to the electro-oxidation of the organic

model molecule. In addition, during the forward scan, with an onset potential of ~400 mV, a significant oxidation peak was observed at ~700 mV. After that, the current decreased, and a new oxidation trend seemed to start around the maximum potential applied (1100 mV). During the backward scan, after an electrical current decrease, a new oxidation peak was obtained at a very similar potential than the forward peak (~750 mV). As a matter of fact, similar trends were obtained for the electro-oxidation of simple alcohols (e.g. methanol [45], ethanol [46, 47]) in Pt-based electrodes. The results obtained could be explained according to two different mechanisms:

(i) the forward peak is usually due to the electro-oxidation of the organic molecule to some reaction intermediate, while the backward oxidation peak could be attributed to the oxidation of such reaction intermediate still adsorbed on the catalyst surface, as suggested for methanol in ref. [48].
(ii) the backward oxidation peak could be just attributed to the adsorption of new molecules of the organic feedstock [45].

In the case of the present study, the second option seems more likely, considering that the oxidation peak for both, forward and backward scans, takes place at very similar cell potentials. If this is the case, it is worth mentioning that the backward peak is much smaller than the forward peak, which indicates that the catalyst surface might change upon the application of higher potentials, or some of the reaction intermediates produced during the forward scan remained chemisorbed on the catalyst, leading to a partial poisoning of the anodic Pt active sites.

The purity and production of hydrogen at the cathode was verified by mass-spectrometry (MS) measurements of the gas species produced. Figure 2.2c shows the whole voltammetry experiment previously described (10 cycles) for the MP model molecule in dynamic mode, i.e., current vs. time, together with the variation of the MS signal for H_2 (in arbitrary units). As expected, considering the pure H^+ conductivity of Nafion membranes, no other gas product was detected at the cathode. In addition, it can be clearly observed that the hydrogen measured followed exactly the same trend than that for the current obtained in the cyclic voltammetry experiment. It points out that this powerful technique allows to correlate in-operando the obtained current with the production of pure hydrogen in this electrolysis technology.

To get more insights into the electrochemical behaviour of the MP electrolysis, chrono-amperometry experiments were performed under the same reaction conditions (Figure 2.2b). Different potentials were applied in a range from 0 to 1100 mV (forward and backward) for 10 min each with a step change of 100 mV. During the forward experiments, a very similar trend than that observed for the cyclic

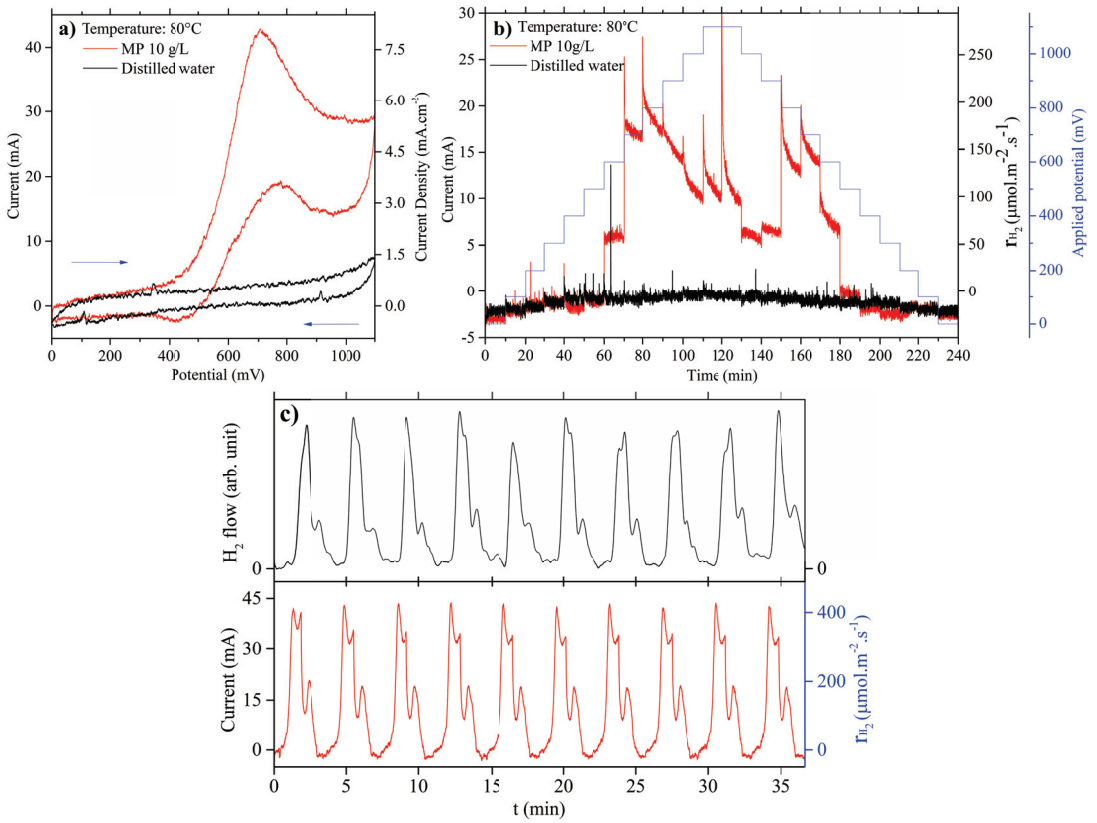

Figure 2.2: Comparison between MP and water electrolysis in a PEM cell: a) Cyclic voltammetry (scan rate 10 mV s^{-1}) from 0 to 1100 mV (only 10^{th} cycle), b) Chrono-amperometry from 0 to 1100 mV (forward and backward) under a step change of 100 mV (10 min at each potential), c) In-situ H_2 measuring by mass spectrometry (He dilution flow of 33 mL min^{-1}) during a cyclic voltammetry (scan rate 10 mV s^{-1}) from 0 to 1100 mV. Anode: MP 10 g L^{-1} in distillate water (MP electrolysis) or distillate water (water electrolysis), 30 mL solution, 1.8 mL min^{-1}. Cathode: distillate water, 30 mL, 1.8 mL min^{-1}. Temperature = 80 °C.

voltammetry was obtained, with maximum currents at 700 – 800 mV. The cathodic H_2 production was calculated according to the Faraday's law ($r_{H_2} = j_p/nF$), where j_p is the current density obtained under polarization, n is the number of transferred electrons, 2 in this case, and F is the Faraday's constant). At every applied potential higher than 600 mV, the current suffered a strong decay with time. In addition, during the backward experiments (from 1100 to 0 mV), a similar trend was observed, but the obtained currents were slightly lower in general.

The obtained results suggest an enhanced performance for the electro-oxidation of the MP organic model molecule in a range of potentials were water electrolysis is simply not possible, i.e., ~700 – 800 mV. The following conclusions could be deduced from these figures: i) the trend observed could be rationalized as in a previous study by Wang et al. with ethanol on Pt electrodes [46], where they suggested that at high potentials the electro-oxidation of the organic could be hindered by

the passivation/oxidation of Pt to PtO, in good agreement with the trend observed when water was fed to the system (Figure 2.2a). During the backward scan, the electro-oxidation competes with PtO reduction, first leading to a current decrease, followed by the formation of a second oxidation peak. ii) together with the likely oxidation of Pt, the system seems to suffer a significant deactivation even in short periods of time, suggesting that the anodic Pt catalyst could be partially poisoned by some reaction intermediates or products produced at the optimum potentials. To support this hypothesis, long-run chrono-amperometric experiments were also carried out with a fresh MEA at different fixed potentials (500, 750 and 1000 mV) for 45 min. As shown in Figure A.2, the currents obtained at 750 and 1000 mV were lower than in the above described experiment, which could be attributed to degradation of the catalyst during the long-run experiment at 500 mV. Nevertheless, these experiments show that the performance of the system decreased with the time at all the studied potentials, with a higher registered current when the PEM cell works at 750 mV, in good agreement with the experiments shown in Figure 2.2b. A similar deactivation phenomenon was observed in previous studies for ethanol electrolysis on Pt-based electrodes [49, 50]. In those studies, the catalyst was further regenerated by a cyclic strategy, by applying steady polarizations between 0 and 1 V forward and backwards until the activity was recovered. We demonstrated that the application of such potentials led to the further electro-oxidation of the poisonous species. Therefore, a similar cyclic strategy will be proposed in future studies aiming for the regeneration of the Pt catalyst used in this study.

Aiming for a study of the overall kinetics for the electro-oxidation of the MP model molecule, the influence of the MP concentration in the starting solution was studied. Figure 2.3a shows a series of cyclic voltammetry experiments (V_{cell} = 0 - 1100 mV, scanning rate of 10 mV s^{-1}) at a constant temperature of 80 °C for the different MP concentrations. The maximum MP concentration tested was 10 g L^{-1} due to the limited solubility of MP in water. Even if a similar trend was observed for all the experiments, the electrochemical performance towards MP electro-oxidation clearly increased with its concentration in the initial solution. After each voltammetry experiment, a chrono-amperometry test was performed at each concentration upon the application of 750 mV for 30 min (Figure 2.3b), where a growing current (and therefore H_2 production) was also obtained as the MP concentration increased.

Since the PEM device works in recirculation mode, it can be considered as a batch system, where the overall rate law can be simplified as [51]:

$$r_{H_2} = kC_{H_2O}^{a} C_b^{n} = k_{obs} C_b^{n} \tag{2.1}$$

where k is the rate constant, C_{H_2O} and C_b are the initial H_2O and MP concentra-

tions, and a and n are the reaction orders with respect to H_2O and MP, respectively. Assuming an almost constant water concentration due to the water excess in the initial solution, k_{obs} comprises the rate constant, together with the concentration of water. According to Eq. (2.1), the representation $ln(r_{H_2})$ vs. $ln(C_b)$ leads to a linear fit, and its slope corresponds to the reaction order n. Figure 2.3c depicts the average r_{H_2} (obtained by integrating the curves shown in Figure 2.3b, divided by the duration of the experiment) vs. the initial MP concentration, while the inset in such figure displays the logarithm fit. The reaction order observed was $n \approx 1$. These results clearly demonstrate that the system is not governed by diffusional limitations, and that the production of hydrogen is strongly dependent on the concentration of the model molecule. In this sense, and considering the limited solubility of MP in water, an initial concentration of 10 g L^{-1} was chosen for the rest of the experiments of this study.

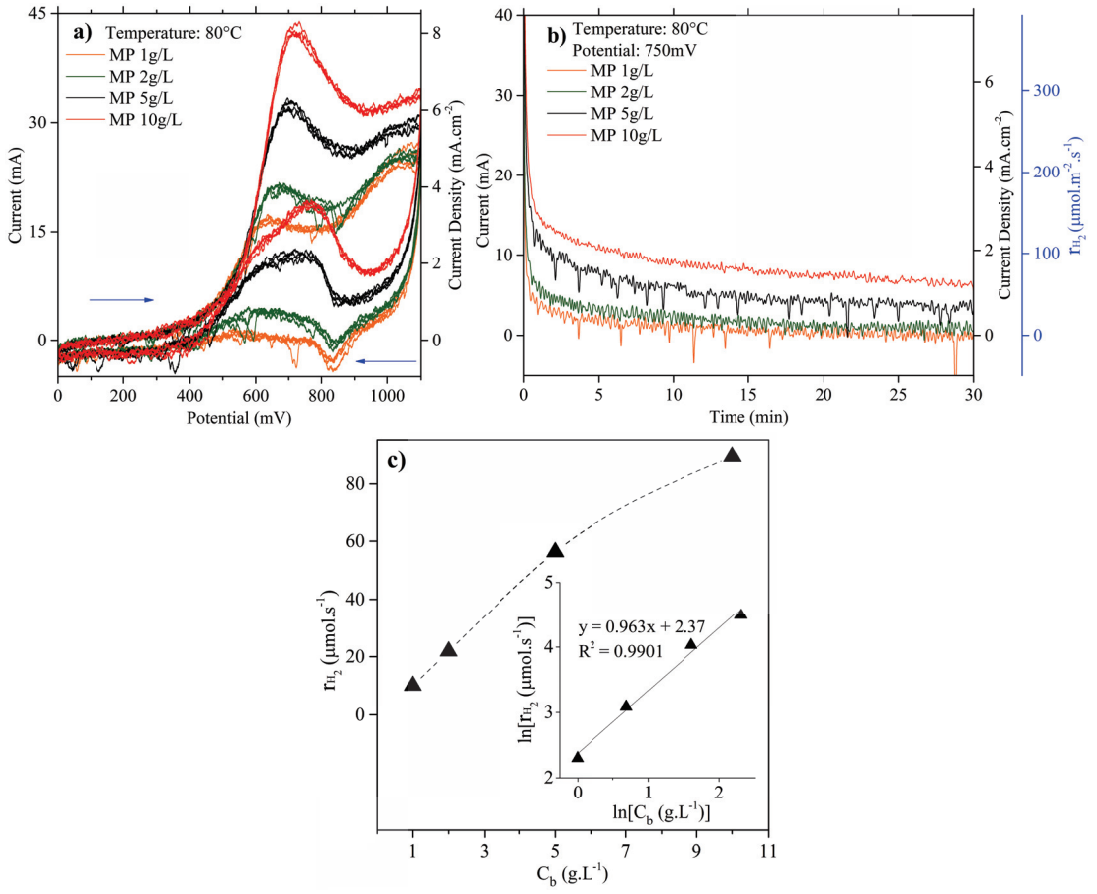

Figure 2.3: Effect of the concentration (C_b) on the MP electrolysis in a PEM cell: a) Cyclic voltammetry (scan rate 10 mV s^{-1}) from 0 to 1100 mV (only 4^{th}, 6^{th}, 8^{th} and 10^{th} cycles), b) Chrono-amperometry at 750 mV during 30 min, c) Influence of the initial MP concentration on the H_2 production and reaction order calculated from CA experiences (inset). Anode: MP 10 g L^{-1} in distillate water, 30 mL solution, 1.8 mL min^{-1}. Cathode: distillate water, 30 mL, 1.8 mL min^{-1}. Temperature = 80 °C.

In the next series of experiments, the influence of the reaction temperature was studied for the electrolysis of the MP model molecule. Figures 2.4a and 2.4b show, respectively, cyclic voltammetry (Vcell = 0 – 1100 mV, scanning rate of 10 mV s^{-1}) and chrono-amperometry experiments (0 to 1100 mV, step change of 100 mV, 10 min at each potential) at 50, 70 and 80 °C. Experiments at higher temperatures were not performed in order to avoid the partial evaporation of the anodic solution. Similar trends were observed in both figures for all the reaction temperatures. However, the activity of the system seems to be almost negligible at 50 °C. As expected, higher temperatures improved the overall performance. It can be attributed to two factors: the enhanced ionic conductivity of the polymer electrolyte membrane and the acceleration of electro-oxidation kinetics. A similar phenomenon was observed in a previous study for lignin electrolysis [27] (a complex organic bio-polymer), where a temperature of at least 50 °C was required to activate the

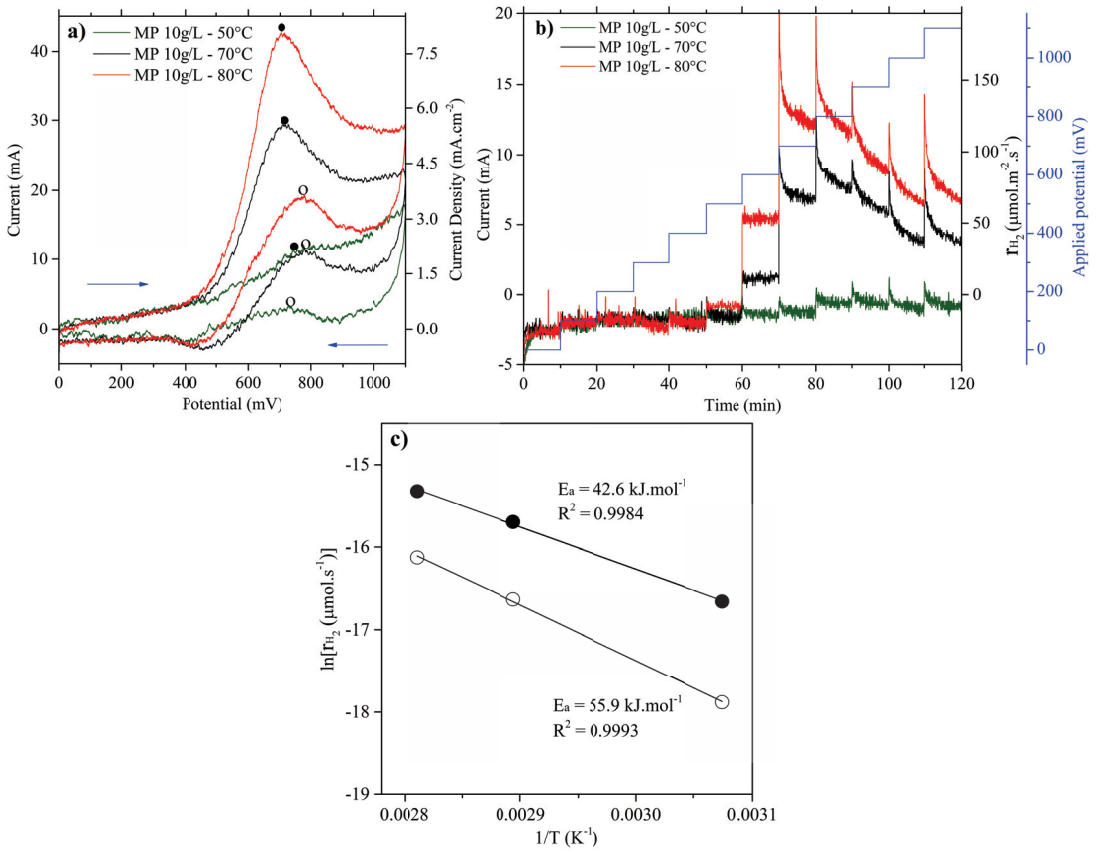

Figure 2.4: Effect of the reaction temperature on MP electrolysis in a PEM cell: a) Cyclic voltammetry (scan rate 10 mV s^{-1}) from 0 to 1100 mV (only 10th cycle), b) Chrono-amperometry from 0 to 1100 mV under a step change of 100 mV (10 min at each potential), c) Arrhenius plots: $ln(r_{H_2})$ vs. $1/T$ (• forward peaks, ∘ backward peaks). The calculations were made by using the data from Figure 2.4a and the slope of the fit corresponds to $-E_a/R$ (where $R = 8.314$ J mol^{-1} K^{-1}). Anode: MP 10 g L^{-1} in distillate water, 30 mL solution, 1.8 mL min^{-1}. Cathode: distillate water, 30 mL, 1.8 mL min^{-1}. Temperature = 50 – 80 °C.

electro-oxidation of the organic molecule. However, the electrolysis of simple organic alcohols (e.g. methanol, ethanol and glycerol) is known to take place even at room temperature. It seems to indicate that the electro-oxidation of complex organic molecules, such as MP, needs to overcome significant kinetic barriers. In this context, the activation energies for the oxidation processes were calculated by the Arrhenius equation (Figure 2.4c):

$$k = Ae^{(-E_a/RT)} \tag{2.2}$$

where k is the rate constant, A is a pre-exponential factor, E_a is the activation energy, T is the temperature and R is the gas constant. The Arrhenius plots ($ln(r_{H_2})$ vs. $1/T$) were obtained by using the hydrogen production (calculated from the current values by the Faraday's law) at the maximum values of the forward and backward electro-oxidation peaks previously discussed (Figure 2.4a). E_a values of 42.6 kJ mol^{-1} (forward scan, V_{cell} ~700 mV) and 55.9 kJ mol^{-1} (backward scan, V_{cell} ~750 mV) were calculated, respectively. Several factors affect the activation energy calculation, including the applied potential. For instance, values between 10 and 25 kJ mol^{-1} [52, 53] have been reported for methanol electro-oxidation on Pt/C electrodes at 0.5 – 0.7 V. These results suggest that the electro-oxidation observed during the backward scan needs to overcome a more energetic barrier than the forward electro-oxidation. It could be due to the fact that the electro-oxidation of MP takes places in several consecutive steps, and therefore those peaks could be attributed to different reactions. Nevertheless, as previously explained, it could also be attributed to the partial passivation/oxidation of Pt at high potentials during the forward scan, which would hinder the MP electro-oxidation during the backward scan. In any case, it seems that the electro-oxidation of the model organic molecule is limited at low reaction temperatures, and higher activation energies than those previously reported for methanol on similar anode materials are required.

During the electro-oxidation of alcohols more complex than methanol on Pt-based materials, such as ethanol, the cleavage of the molecule generally leads to its partial oxidation towards aldehyde and carboxylic acids at similar temperatures and upon the application of low electrical potentials (<1.23 V). That indicates that the activity of the system is limited to the oxidation of the alcohol (−OH) terminal functional groups. However, the MP molecule does not have −OH terminal bonds in its structure (nor the PMMA polymer, see Figure A.1). Therefore, considering that C−C cleavage seems very unlikely under such conditions [46, 54, 55], we propose that the electro-oxidation activity observed in Figures 2.2- 2.5 is linked to the electro-oxidative cleavage of the ester C−O bonds, as we will explain later in the manuscript. All in all, these experiments prove that, potentially, the electrolysis of the PMMA plastic polymer is possible in a range of potentials lower than

that for pure water electrolysis. Further analysis of the charge transfer kinetics for MP electro-oxidation was performed by varying the scanning rates during cyclic voltammetry experiments. Figure 2.5a shows the voltammograms (10^{th} cycle) at scanning rates between 10 and 50 mV/s, by feeding solutions of MP to the anode (10 g L^{-1}) at 80 °C. The full voltammetry experiments are shown in Figure A.3.

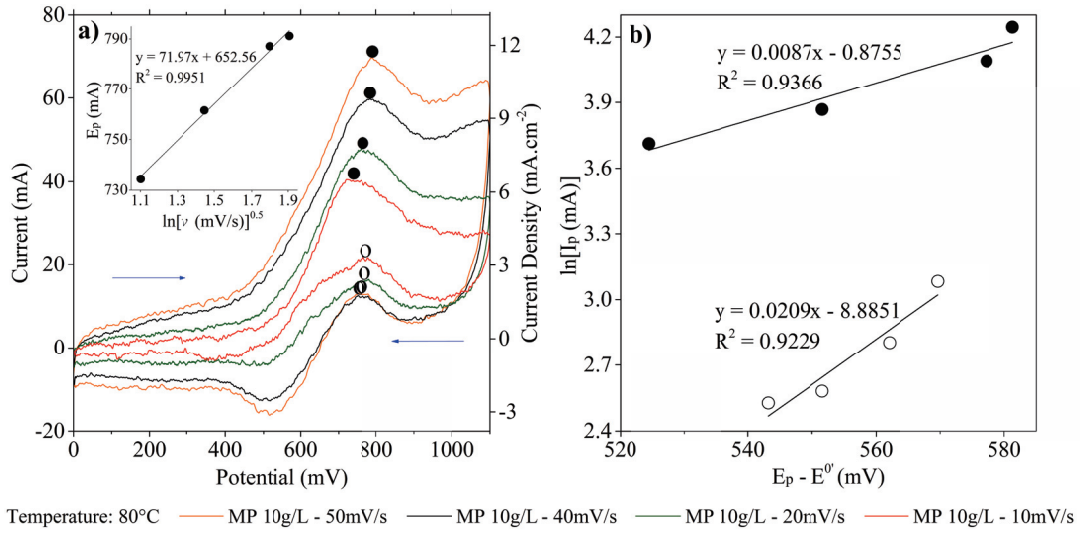

Figure 2.5: Effect of the scanning rate on MP electrolysis in a PEM cell: a) Cyclic voltammetry (scan rate 10 – 50 mV s^{-1}) from 0 to 1100 mV (only the 10^{th} cycle). Inset figure: E_p vs. $ln(\nu^{1/2})$ plot, where E_p is the potential of the forward peaks, and ν is the scan rate: a linear trend indicates the irreversibility of the electro-oxidation process. b) $ln(I_p)$ vs. $(E_p - E^{0'})$ plot, where I_p and E_p are the current and potential at the forward (•) and backward peaks (∘) (Figure 2.5a). The intercept allows for k^0 calculations. Anode: MP 10 g L^{-1} in distillate water, 30 mL solution, 1.8 mL min^{-1}. Cathode: distillate water, 30 mL, 1.8 mL min^{-1}. Temperature = 80 °C.

As expected, faster scan rates lead to higher electrical currents during the forward scan (and slightly lower currents during the backward scan) due to a decrease of the diffusion layer size. As previously reported for the electrolysis of other organic molecules (e.g. ethanol [56] and lignin [57]), the electro-oxidation of MP is most likely an irreversible process. As discussed by Han et al. [56], the peak potential exhibits a linear dependence upon the logarithm of the square root of the scanning rate if the reaction is irreversible, as is the case in this study (see inset in Figure 2.5a). Therefore, following a similar approach than Movil et al. [57] for totally irreversible one-step/one-electron reactions (described in detail in ref. [58]), we calculated the standard charge transfer rate constant (k^0) for the two main electro-oxidation processes observed during the forward (k_1^0) and the backward (k_2^0) scans by using equation (2.3):

$$I_p = nAFk^0C_b e^{\frac{-\alpha F}{RT}(E_p - E^{0'})} \tag{2.3}$$

where I_p is the current obtained at the peak, A is the area of the electrode, α is

the transfer coefficient, C_b is the reactant concentration, E_p is the peak potential and $E^{0'}$ is the formal potential (standard electrode potential under specific reaction conditions). Considering a low degree of consumption of MP compared to its high initial concentration (10 g L^{-1}), C_b was assumed to be constant. In addition, since no values of $E^{0'}$ could be found in literature for the MP model molecule, we will keep the same assumption of Movil et al. [57], considering the formal electrode potential for MP is the same than that for carbon (0.21 V vs. SHE). Taking the I_p and E_p data for both oxidation peaks at different scanning rates, a linearization of Eq. (2.3) can be done in the form of $ln(I_p)$ vs. $(E_p - E^{0'})$. The plots are shown in Figure 2.5b, where the intercept of each line is equal to $ln(nAFk^0C_b)$. It allows calculating the following k^0 values: k_1^0=4.74x10^{-3} cm s^{-1} and k_2^0=1.58x10^{-6} cm s^{-1} for the forward and backward peaks, respectively. The physical interpretation of these values is associated with the kinetic facility of the redox couple. In other words, high k^0 values indicate that the system will rapidly achieve the equilibrium. Both values of k^0 fall in the intermediate range, considering common k^0 values between 1 and 10 (for fast processes) and 10^{-9} (for slow processes) [58]. The standard charge transfer rate constant range of our investigated electrochemical system is typical of irreversible reactions. Hence, the results obtained suggest that the forward peak is related to an electro-oxidation process with simpler and faster transfer of electrons than the backward peak. Two assumptions can be proposed: i) the competition between the reduction of oxidized Pt and the MP electro-oxidation reaction during the backward scan, or ii) the formation of strongly adsorbed species during the forward scan, which would hinder the kinetics of the electro-oxidation process during the backward scan.

Having in mind the irreversible nature of the MP electro-oxidation process, a preliminary global reaction mechanism can be proposed. From previous studies on electrolysis of other small organic molecules (e.g. ethanol [46, 54, 55] and glycerol [59, 60]), we can assume that cleaving C–C bonds is very unlikely at low temperatures and applied potentials <1.2 V. In addition, it is well-known that acid hydrolysis of esters is simply the reverse of the esterification process, leading to the formation of a carboxylic acid and an alcohol [61] (R–C=O–O–R′ + H_2O → R–C=O–OH + R′–OH). As the MP electrolysis is carried out in a PEM cell with an acid membrane in the absence of any liquid electrolyte, the cleavage of the MP model molecule is purely (or mainly) electrochemical, as opposed to the reference study recently published for plastic electrolysis [44], where the plastic could be potentially transformed into smaller molecules in the H_3PO_4 liquid electrolyte. Hence, we believe that the electro-oxidation of MP is most likely due to the cleavage of the ester group, leading to the production of a carboxylic acid (pivalic acid, PA) and intermediate methoxy-type species (CH_3O^-), in a similar way than the esters acid hydrolysis pre-

viously described. The methoxy intermediate species would be further oxidized into CO_2, with the subsequent production of H^+ and e^-, which would further migrate to the cathode to produce hydrogen, as represented by the following equations:

$$Anode : (CH_3)_3CCOOCH_3 + 2\,H_2O \rightarrow (CH_3)_3CCOOH + CO_2 + 6\,H^+ + 6\,e^- \quad (2.4)$$

$$Cathode : 6\,H^+ + 6\,e^- \rightarrow 3\,H_2 \quad (2.5)$$

In order to support this overall reaction mechanism, cyclic voltammetry experiences (10^{th} cycle) with aqueous solutions of methanol and pivalic acid (in the absence of liquid electrolyte) were performed at 80 °C, using the stoichiometric concentrations corresponding to a total conversion of a MP 10 g L^{-1} solution, i.e. 0.086 mol L^{-1} (Figure 2.6). Regarding the methanol curve, it is worth noting its similar trend compared to the MP electro-oxidation, with forward and backward peaks appearing at similar potentials, even though the obtained current was higher for methanol. This could be attributed to the higher activation energy (i.e., the higher kinetic barrier) observed for the electrolysis of the MP model molecule, compared to that previously reported for direct methanol electrolysis. On the other hand, no activity was obtained for the electrolysis of pivalic acid under the proposed working conditions. This is expected, considering that the further oxidation of carboxylic acid at low potentials and reaction temperatures is very unlikely, as previously observed for the electrolysis of ethanol on Pt-based catalyst-electrodes. Therefore, these experiments agree with the global mechanism proposed by Eqs. (2.4) and (2.5). Considering this initial theory, MP seems to be the right model molecule

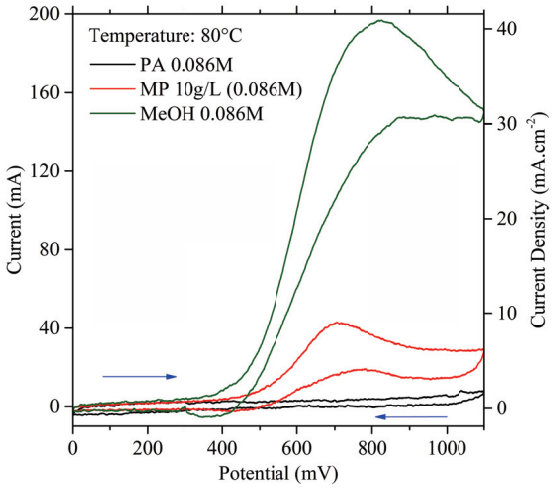

Figure 2.6: Comparison of electrolysis in a PEM cell of MP, methanol and pivalic acid (PA). Cyclic voltammetry (scan rate 10 mV s^{-1}) from 0 to 1100 mV (only 10^{th} cycle). Anode: MP 10 g L^{-1} in distillate water (MP electrolysis), PA 0.086 mol L^{-1} (PA electrolysis), or methanol 0.086 mol L^{-1} (MeOH electrolysis), 30 mL solution, 1.8 mL min^{-1}. Cathode: distillate water, 30 mL, 1.8 mL min^{-1}. Temperature = 80 °C.

as a representative of PMMA. Taking into account the unlikely C – C cleavage, the electrochemical depolymerization of PMMA can be disregarded under the studied reaction conditions with the Pt/C catalyst. The above-suggested electrochemical cleavage of the ester functional group, leading to the production of methoxy groups (which would be further electro-oxidized leading to the production of H_2, could potentially happen in an important extent with the PMMA with similar energy requirements, without breaking the polymer backbone chain. Despite, other issues should be taking into consideration, including the fact that PMMA is not soluble in water and therefore such material should be pretreated or introduced in form of nano-dispersions to minimize the very likely diffusional limitations. In any case, further experiments will be performed in future studies coupled with products analysis by liquid chromatography and spectroscopic techniques to corroborate the fundamental aspects of this original system.

2.4 Conclusions

This study reports the electrochemical behaviour for the electro-oxidation of MP, an organic model molecule with similar bonds than the PMMA polymer, on Pt-based electrodes. First of all, we clearly demonstrated that the electro-oxidation of this molecule leads to an enhanced performance compared to water electrolysis at low temperatures (50 – 80 °C) and in a low range of electrical potentials (<1.2 V). The highest electrochemical performances for MP electro-oxidation were achieved at intermediate reaction potentials (700 – 800 mV), where the partial oxidation of Pt did not occur. However the system suffered a significant deactivation with time, likely owing to the strong chemisorption of reaction intermediates or products. All in all, this study establishes a starting point towards understanding the electrocatalytic transformation of MP, allowing for the production of H_2 (most likely) from the cleavage of the ester groups. These results could be extrapolated to PMMA, in view of the further valorisation of the massive amounts of this kind of plastic waste to produce pure green hydrogen.

CRediT authorship contribution statement

N. Grimaldos-Osorio: Conceptualization, Methodology, Writing - review & editing. F. Sordello: Methodology, Validation. M. Passananti: Conceptualization, Supervision, Writing - review & editing. P. Vernoux: Conceptualization, Methodology, Validation, Supervision, Writing - review & editing. A. Caravaca: Conceptualization, Methodology, Validation, Supervision, Writing - review & editing.

Declaration of competing interest

The authors declare that they have no known competing financial interests or personal relationships that could have appeared to influence the work reported in this paper.

Acknowledgments

The authors gratefully acknowledge the French institution “Ecole Urbaine de Lyon” (EUL - Institut de Convergences) for funding a PhD grant offered to the leading author of this study, Mr. Grimaldos-Osorio.

Supplementary Information

Figure A.1

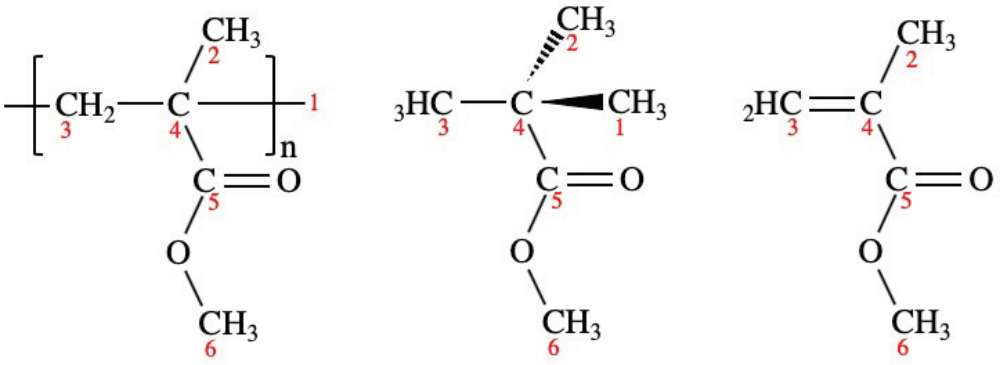

Figure A.1: Chemical structures of a) polymethyl methacrylate (PMMA, target plastic polymer), b) methyl pivalate (MP, model molecule) and c) methyl methacrylate (MMA).

Figure A.2

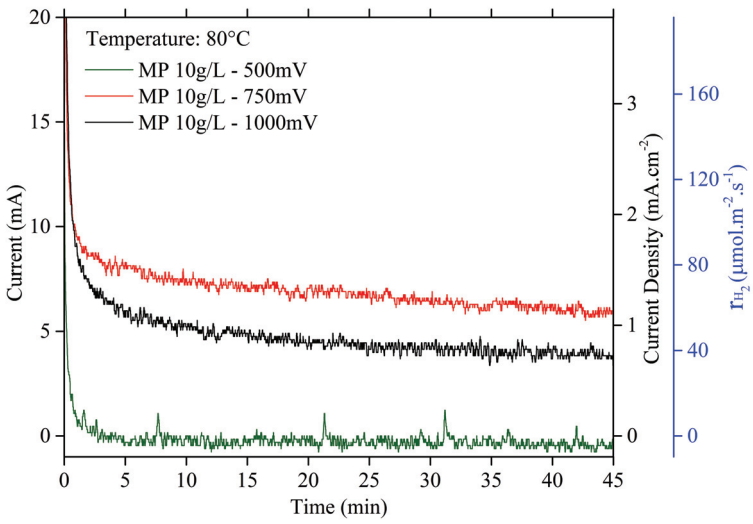

Figure A.2: Long-run chrono-amperometry for MP electrolysis in a PEM cell at three different fixed potentials (V_{cell} = 500, 750 and 1000 mV). Anode: MP 10 g L^{-1} in distillate water, 30 mL solution, 1.8 mL min^{-1}. Cathode: distillate water, 30 mL, 1.8 mL min^{-1}. Temperature = 80 °C.

Figure A.3

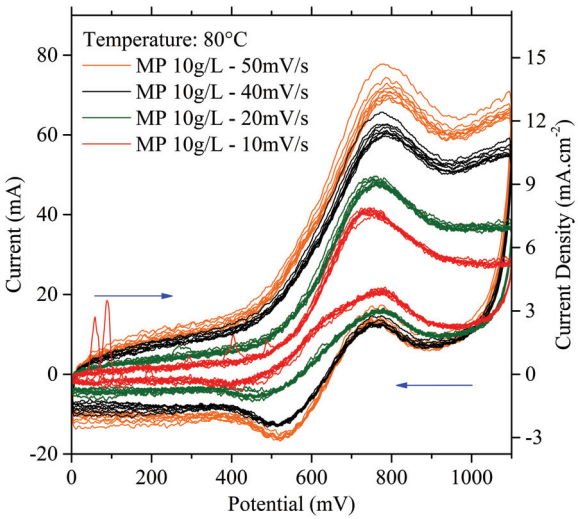

Figure A.3: Cyclic voltammetry experiments for MP electrolysis in a PEM cell at different scan rates (10-50 mV s-1) from 0 to 1100 mV. Overall experiment showing all cycles. Anode: MP 10 g L^{-1} in distillate water, 30 mL solution, 1.8 mL min^{-1}. Cathode: distillate water, 30 mL, 1.8 mL min^{-1}. Temperature = 80 °C.

References

[1] Bareiß, K., de la Rua, C., Möckl, M. et al. Life cycle assessment of hydrogen from proton exchange membrane water electrolysis in future energy systems. *Applied Energy*, 237(July 2018):862–872, 2019. doi: 10.1016/j.apenergy.2019.01.001.

[2] Züttel, A., Remhof, A., Borgschulte, A. et al. Hydrogen: The future energy carrier. *Philosophical Transactions of the Royal Society A: Mathematical, Physical and Engineering Sciences*, 368(1923):3329–3342, 2010. doi: 10.1098/rsta.2010.0113.

[3] Shiva Kumar, S. and Himabindu, V. Hydrogen production by PEM water electrolysis – A review. *Materials Science for Energy Technologies*, 2(3):442–454, 2019. doi: 10.1016/j.mset.2019.03.002.

[4] Buttler, A. and Spliethoff, H. Current status of water electrolysis for energy storage, grid balancing and sector coupling via power-to-gas and power-to-liquids: A review. *Renewable and Sustainable Energy Reviews*, 82(September):2440–2454, 2018. doi: 10.1016/j.rser.2017.09.003.

[5] Coutanceau, C. and Baranton, S. Electrochemical conversion of alcohols for hydrogen production: a short overview. *Wiley Interdisciplinary Reviews: Energy and Environment*, 5(4):388–400, 2016. doi: 10.1002/wene.193.

[6] Guenot, B., Cretin, M. and Lamy, C. Clean hydrogen generation from the electrocatalytic oxidation of methanol inside a proton exchange membrane electrolysis cell (PEMEC): effect of methanol concentration and working temperature. *Journal of Applied Electrochemistry*, 45(9):973–981, 2015. doi: 10.1007/s10800-015-0867-3.

[7] Lamy, C., Guenot, B., Cretin, M. et al. (Invited) A Kinetics Analysis of Methanol Oxidation under Electrolysis/Fuel Cell Working Conditions. *ECS Transactions*, 66(29):1–12, 2015. doi: 10.1149/06629.0001ecst.

[8] Pham, A.T., Baba, T., Sugiyama, T. et al. Efficient hydrogen production from aqueous methanol in a PEM electrolyzer with porous metal flow field: Influence of PTFE treatment of the anode gas diffusion layer. *International Journal of Hydrogen Energy*, 38(1):73–81, 2013. doi: 10.1016/j.ijhydene.2012.10.036.

[9] Uhm, S., Jeon, H., Kim, T.J. et al. Clean hydrogen production from methanol-water solutions via power-saved electrolytic reforming process. *Journal of Power Sources*, 198:218–222, 2012. doi: 10.1016/j.jpowsour.2011.09.083.

[10] Caravaca, A., Sapountzi, F.M., De Lucas-Consuegra, A. et al. Electrochemical reforming of ethanol-water solutions for pure H2 production in a PEM elec-

trolysis cell. *International Journal of Hydrogen Energy*, 37(12):9504–9513, 2012. doi: 10.1016/j.ijhydene.2012.03.062.

[11] Gutiérrez-Guerra, N., Jiménez-Vázquez, M., Serrano-Ruiz, J.C. et al. Electrochemical reforming vs. catalytic reforming of ethanol: A process energy analysis for hydrogen production. *Chemical Engineering and Processing: Process Intensification*, 95:9–16, 2015. doi: 10.1016/j.cep.2015.05.008.

[12] Gutiérrez-Martín, F., Calcerrada, A.B., de Lucas-Consuegra, A. et al. Hydrogen storage for off-grid power supply based on solar PV and electrochemical reforming of ethanol-water solutions. *Renewable Energy*, 147:639–649, 2020. doi: 10.1016/j.renene.2019.09.034.

[13] Ruiz-López, E., Amores, E., Raquel de la Osa, A. et al. Electrochemical reforming of ethanol in a membrane-less reactor configuration. *Chemical Engineering Journal*, 379(March 2019):122289, 2020. doi: 10.1016/j.cej.2019.122289.

[14] Lamy, C., Jaubert, T., Baranton, S. et al. Clean hydrogen generation through the electrocatalytic oxidation of ethanol in a Proton Exchange Membrane Electrolysis Cell (PEMEC): Effect of the nature and structure of the catalytic anode. *Journal of Power Sources*, 245:927–936, 2014. doi: 10.1016/j.jpowsour.2013.07.028.

[15] Caravaca, A., De Lucas-Consuegra, A., Calcerrada, A.B. et al. From biomass to pure hydrogen: Electrochemical reforming of bio-ethanol in a PEM electrolyser. *Applied Catalysis B: Environmental*, 134-135:302–309, 2013. doi: 10.1016/j.apcatb.2013.01.033.

[16] Cheng, W., Singh, N., Maciá-Agulló, J.A. et al. Optimal experimental conditions for hydrogen production using low voltage electrooxidation of organic wastewater feedstock. *International Journal of Hydrogen Energy*, 37(18):13304–13313, 2012. doi: 10.1016/j.ijhydene.2012.06.073.

[17] Chen, Y.X., Lavacchi, A., Miller, H.A. et al. Nanotechnology makes biomass electrolysis more energy efficient than water electrolysis. *Nature Communications*, 5(May):1–6, 2014. doi: 10.1038/ncomms5036.

[18] Hibino, T., Kobayashi, K., Ito, M. et al. Efficient Hydrogen Production by Direct Electrolysis of Waste Biomass at Intermediate Temperatures. *ACS Sustainable Chemistry and Engineering*, 6(7):9360–9368, 2018. doi: 10.1021/acssuschemeng.8b01701.

[19] Crisafulli, R., de Lino Amorim, F.M., de Oliveira Marcionilio, S.M. et al. Electrochemistry for biofuels waste valorization: Vinasse as a reducing agent for Pt/C and its application to the electrolysis of glycerin and vinasse. *Electrochemistry Communications*, 102(March):25–30, 2019. doi: 10.1016/j.elecom.2019.03.012.

[20] Brueckner, T.M., Hawboldt, K.A. and Pickup, P.G. Electrolysis of pyrolysis oil

distillates and permeates in a multi-anode proton exchange membrane cell. *Applied Catalysis B: Environmental*, 256(June):117892, 2019. doi: 10.1016/j.apcatb.2019.117892.

[21] Lalvani, S.B. and Rajagopal, P. Lignin-augmented water electrolysis. *Journal of The Electrochemical Society*, 139(1):L1–L2, jan 1992. doi: 10.1149/1.2069212.

[22] Lalvani, S.B. and Rajagopal, P. Hydrogen production from lignin-water solution by electrolysis:. *Holzforschung-International Journal of the Biology, Chemistry, Physics and Technology of Wood*, 47(4):283–286, 1993. doi: 10.1515/hfsg.1993.47.4.283.

[23] Roy Ghatak, H. Electrolysis of black liquor for hydrogen production: Some initial findings. *International Journal of Hydrogen Energy*, 31(7):934–938, 2006. doi: 10.1016/j.ijhydene.2005.07.013.

[24] Ghatak, H.R., Kumar, S. and Kundu, P. Electrode processes in black liquor electrolysis and their significance for hydrogen production. *International Journal of Hydrogen Energy*, 33(12):2904–2911, 2008. doi: 10.1016/j.ijhydene.2008.03.051. 2nd World Congress of Young Scientists on Hydrogen Energy Systems.

[25] Movil, O., Garlock, M. and Staser, J.A. Non-precious metal nanoparticle electrocatalysts for electrochemical modification of lignin for and cost-effective production of hydrogen. *International Journal of Hydrogen Energy*, 40(13):4519–4530, 2015. doi: 10.1016/j.ijhydene.2015.02.023.

[26] Hibino, T., Kobayashi, K., Nagao, M. et al. Hydrogen Production by Direct Lignin Electrolysis at Intermediate Temperatures. *ChemElectroChem*, 4(12):3032–3036, 2017. doi: 10.1002/celc.201700917.

[27] Caravaca, A., Garcia-Lorefice, W.E., Gil, S. et al. Towards a sustainable technology for H2 production: Direct lignin electrolysis in a continuous-flow Polymer Electrolyte Membrane reactor. *Electrochemistry Communications*, 100 (January):43–47, 2019. doi: 10.1016/j.elecom.2019.01.016.

[28] Bateni, F., NaderiNasrabadi, M., Ghahremani, R. et al. Low-Cost Nanostructured Electrocatalysts for Hydrogen Evolution in an Anion Exchange Membrane Lignin Electrolysis Cell. *Journal of The Electrochemical Society*, 166(14):F1037–F1046, 2019. doi: 10.1149/2.0221914jes.

[29] NaderiNasrabadi, M., Bateni, F., Chen, Z. et al. Biomass-Depolarized Electrolysis. *Journal of The Electrochemical Society*, 166(10):E317–E322, 2019. doi: 10.1149/2.1471910jes.

[30] Simões, M., Baranton, S. and Coutanceau, C. Electrochemical valorisation of glycerol. *ChemSusChem*, 5(11):2106–2124, 2012. doi: 10.1002/cssc.201200335.

[31] Kongjao, S., Damronglerd, S. and Hunsom, M. Electrochemical reforming of an acidic aqueous glycerol solution on Pt electrodes. *Journal of Applied Electrochemistry*, 41(2):215–222, 2011. doi: 10.1007/s10800-010-0226-3.

[32] Kunwar, B., Cheng, H.N., Chandrashekaran, S.R. et al. Plastics to fuel: a review. *Renewable and Sustainable Energy Reviews*, 54:421–428, 2016. doi: 10.1016/j.rser.2015.10.015.

[33] Rahimi, A. and García, J.M. Chemical recycling of waste plastics for new materials production. *Nature Reviews Chemistry*, 1:1–11, 2017. doi: 10.1038/s41570-017-0046.

[34] Lopez, G., Artetxe, M., Amutio, M. et al. Thermochemical routes for the valorization of waste polyolefinic plastics to produce fuels and chemicals. A review. *Renewable and Sustainable Energy Reviews*, 73(January 2017):346–368, 2017. doi: 10.1016/j.rser.2017.01.142.

[35] Al-Salem, S.M., Lettieri, P. and Baeyens, J. Recycling and recovery routes of plastic solid waste (PSW): A review. *Waste Management*, 29(10):2625–2643, 2009. doi: 10.1016/j.wasman.2009.06.004.

[36] Singh, N., Hui, D., Singh, R. et al. Recycling of plastic solid waste: A state of art review and future applications. *Composites Part B: Engineering*, 115: 409–422, 2017. doi: 10.1016/j.compositesb.2016.09.013.

[37] Schwarz, A.E., Ligthart, T.N., Boukris, E. et al. Sources, transport, and accumulation of different types of plastic litter in aquatic environments: A review study. *Marine Pollution Bulletin*, 143(March):92–100, 2019. doi: 10.1016/j.marpolbul.2019.04.029.

[38] Moura, M.R., Falcão, S.M., da Silva, A.C. et al. Developing a plastic waste management program: From river basins to urban beaches (case study). *Journal of Engineering and Technological Sciences*, 52(1):108–120, 2020. doi: 10.5614/j.eng.technol.sci.2020.52.1.8.

[39] Achilias, D.S. Chemical Recycling of Polymers. The Case of Poly(methyl methacrylate). *Internation conference on Energy and Environmental systems*, 2006(January 2006):271–276, 2006.

[40] Godiya, C.B., Gabrielli, S., Materazzi, S. et al. Depolymerization of waste poly(methyl methacrylate) scraps and purification of depolymerized products. *Journal of Environmental Management*, 231(November 2018):1012–1020, 2019. doi: 10.1016/j.jenvman.2018.10.116.

[41] Pati, S., Gopalan, S. and Pal, U.B. A solid oxide membrane electrolyzer for production of hydrogen and syn-gas from steam and hydrocarbon waste in a single step. *International Journal of Hydrogen Energy*, 36(1):152–159, 2011. doi: 10.1016/j.ijhydene.2010.10.013.

[42] Pal, U.B., Pati, S., Yoong, K.J. et al. (Invited) Electrolyzer for Waste to Energy Conversion. *ECS Transactions*, 41(12):93–101, 2012. doi: 10.1149/1.3697432.

[43] Jiang, T., Zhao, X., Gu, D. et al. STEP polymer degradation: Solar thermo-coupled electrochemical depolymerization of plastics to generate useful fuel plus abundant hydrogen. *Solar Energy Materials and Solar Cells*, 204 (September 2019):110208, jan 2020. doi: 10.1016/j.solmat.2019.110208.

[44] Hori, T., Kobayashi, K., Teranishi, S. et al. Fuel cell and electrolyzer using plastic waste directly as fuel. *Waste Management*, 102:30–39, 2020. doi: 10.1016/j.wasman.2019.10.019.

[45] Chung, D.Y., Lee, K.J. and Sung, Y.E. Methanol Electro-Oxidation on the Pt Surface: Revisiting the Cyclic Voltammetry Interpretation. *The Journal of Physical Chemistry C*, 120(17):9028–9035, 2016. doi: 10.1021/acs.jpcc.5b12303.

[46] Wang, H., Jusys, Z. and Behm, R. Ethanol Electrooxidation on a Carbon-Supported Pt Catalyst: Reaction Kinetics and Product Yields. *The Journal of Physical Chemistry B*, 108(50):19413–19424, 2004. doi: 10.1021/jp046561k.

[47] Pushkarev, A.S., Pushkareva, I.V., Ivanova, N.A. et al. Pt/C and Pt/SnOx/C Catalysts for Ethanol Electrooxidation: Rotating Disk Electrode Study. *Catalysts*, 9(3), 2019. doi: 10.3390/catal9030271.

[48] Mancharan, R. and Goodenough, J.B. Methanol oxidation in acid on ordered NiTi. *Journal of Materials Chemistry*, 2:875–887, 1992. doi: 10.1039/JM9920200875.

[49] Caravaca, A., De Lucas-Consuegra, A., Calcerrada, A.B. et al. From biomass to pure hydrogen: Electrochemical reforming of bio-ethanol in a PEM electrolyser. *Applied Catalysis B: Environmental*, 134-135:302–309, 2013. doi: 10.1016/j.apcatb.2013.01.033.

[50] Caravaca, A., Sapountzi, F.M., De Lucas-Consuegra, A. et al. Electrochemical reforming of ethanol-water solutions for pure H2 production in a PEM electrolysis cell. *International Journal of Hydrogen Energy*, 37(12):9504–9513, 2012. doi: 10.1016/j.ijhydene.2012.03.062.

[51] Caravaca, A., Jones, W., Hardacre, C. et al. H2 production by the photocatalytic reforming of cellulose and raw biomass using Ni, Pd, Pt and Au on titania. *Proceedings of the Royal Society A: Mathematical, Physical and Engineering Sciences*, 472(2191), 2016. doi: 10.1098/rspa.2016.0054.

[52] Jing, M., Jiang, L., Yi, B. et al. Comparative study of methanol adsorption and electro-oxidation on carbon-supported platinum in acidic and alkaline electrolytes. *Journal of Electroanalytical Chemistry*, 688:172–179, 2013.

doi: 10.1016/j.jelechem.2012.10.028. Special Issue in Honor of Professors Chuansin Cha and Zhaowu Tian.

[53] Wakabayashi, N., Uchida, H. and Watanabe, M. Temperature-Dependence of Methanol Oxidation Rates at PtRu and Pt Electrodes. *Electrochemical and Solid-State Letters*, 5(11):E62, 2002. doi: 10.1149/1.1513021.

[54] Monyoncho, E.A., Steinmann, S.N., Michel, C. et al. Ethanol electro-oxidation on palladium revisited using Polarization Modulation Infrared Reflection Absorption Spectroscopy (PM-IRRAS) and Density Functional Theory (DFT): Why Is It Difficult To Break the C–C Bond? *ACS Catalysis*, 6(8):4894–4906, 2016. doi: 10.1021/acscatal.6b00289.

[55] Monyoncho, E.A., Steinmann, S.N., Sautet, P. et al. Computational screening for selective catalysts: Cleaving the CC bond during ethanol electro-oxidation reaction. *Electrochimica Acta*, 274:274–278, 2018. doi: 10.1016/j.electacta.2018.04.102.

[56] Han, L., Ju, H. and Xu, Y. Ethanol electro-oxidation: Cyclic voltammetry, electrochemical impedance spectroscopy and galvanostatic oscillation. *International Journal of Hydrogen Energy*, 37(20):15156–15163, 2012. doi: 10.1016/j.ijhydene.2012.08.034. The 2011 Asian Bio-Hydrogen and Biorefinery Symposium (2011ABBS).

[57] Movil, O., Garlock, M. and Staser, J.A. Non-precious metal nanoparticle electrocatalysts for electrochemical modification of lignin for low-energy and cost-effective production of hydrogen. *International Journal of Hydrogen Energy*, 40(13):4519–4530, 2015. doi: 10.1016/j.ijhydene.2015.02.023.

[58] Bard, A.J. and Faulkner, L.R. *Electrochemical methods: Fundamentals and Applications*. John Wiley & Sons, Inc., 2nd edition, 2001.

[59] Coutanceau, C., Baranton, S. and Kouamé, R.S.B. Selective Electrooxidation of Glycerol Into Value-Added Chemicals: A Short Overview. *Frontiers in Chemistry*, 7:100, 2019. doi: 10.3389/fchem.2019.00100.

[60] Simões, M., Baranton, S. and Coutanceau, C. Electrochemical valorisation of glycerol. *ChemSusChem*, 5(11):2106–2124, 2012. doi: 10.1002/cssc.201200335.

[61] Anantakrishnan, S.V. and Krishnamurti, S. Kinetic studies in ester hydrolysis. *Proceedings of the Indian Academy of Sciences - Section A*, 14(3):270–278, 1941. doi: 10.1007/BF03046068.

CHAPTER 3

From plastic-waste to H_2: A first approach to the electrochemical reforming of dissolved Poly(methyl methacrylate) particles

From plastic-waste to H_2: A first approach to the electrochemical reforming of dissolved Poly(methyl methacrylate) particles

N. Grimaldos-Osorio[1,2], F. Sordello[2], M. Passananti[2,3], J. González-Cobos[1], A. Bonhommé[1], P. Vernoux[1], A. Caravaca[1]

[1] *Université de Lyon, Institut de Recherches sur la Catalyse et l'Environnement de Lyon, UMR 5256, CNRS, Université Claude Bernard Lyon 1, 2 avenue A. Einstein, 69626 Villeurbanne, France.*

[2] *Dipartimento di Chimica, Università di Torino, Via Pietro Giuria 5, 10125 Turin, Italy.*

[3] *Institute for Atmospheric and Earth System Research/Physics, Faculty of Science, University of Helsinki, FI-00014, Finland.*

International Journal of Hydrogen Energy (2022)
DOI: 10.1016/j.ijhydene.2022.02.229
Received 21 December 2021; Received in revised form 22 February 2022
Accepted 26 February 2022; Available online 26 March 2022

Keywords: Hydrogen production, electrochemical cell, plastic-waste valorisation, poly(methyl methacrylate) (PMMA) valorisation, electrooxidation of plastics.

Abstract: The development of sustainable processes for the recycling of plastic is a major environmental issue to reduce the pollution by this kind of waste. The electro-oxidation of plastic wastes in electrolysers powered by renewable energies is a promising option to produce hydrogen at low temperature while diminishing the energy demand compared to Oxygen Evolution Reaction (OER). Poly(methyl-methacrylate) (PMMA) particles, a widely used polymer, were dissolved (0.1-2% wt.) in an isopropanol(IPA)/H_2O binary solvent and electro-oxidised on Pt/C-based electrodes in a liquid batch electrochemical cell at 70 °C in acidic media. Despite the dissolution strategy, polymer macromolecules partially block the accessibility of the active sites of a commercial electrode and strongly degrades its electrochemical performances mainly linked to IPA electro-oxidation. The preparation of a more porous electrode supported on carbon paper was found to strongly hinder this deactivation. Furthermore, the electrooxidation of PMMA or PMMA-derived molecules can be performed during cyclic voltammetries up to 1.4 V and chrono-amperometries at 1.4 V.

3.1 Introduction

Earth is facing serious environmental issues today, most of which are caused by the impact of human actions. The rapid growth of the global population, climate deterioration, extinction of many living species, increasing natural catastrophes, and overexploitation of natural resources are only some of the many issues concerning our planet [1]. In this context, the term "anthropocene" has been introduced to describe the present era, in which humankind's activities are challenging Earth's boundaries and threatening the future of humanity [2]. Plastics are one of the main residues related to our lifestyle, even to the point of being considered as an anthropogenic geological indicator [3, 4].

Since the industrialisation of polymers' production, their consumption and consequent waste generation have never stopped rising, as they are used in a large variety of daily life applications [5]. The rise and abuse of plastic packaging, residues mismanagement, unauthorised dumping, and uncontrolled landfilling have important consequences for the environment and especially for terrestrial and marine ecosystems [6, 7]. Plastic pollution has been reported for over 40 years and it has become an economic and societal question [8]. When plastics undergo erosion and degradation, they can be transformed into micro and nanoplastics, a problem indeed harder to control because of their capacity to escape traditional water cleaning treatments and react with chemical species in the environment [9].

Nowadays, manufactured polymers recycling accounts for only ∼30% of the total production in Europe and less than 10% in the USA [10, 11]. Energy recovery is the most common end-use for polymeric waste, with a fraction near 43% [12]. This is a relatively effective management method and an alternative way to generate energy and heat [13]. However, this technology releases CO_2 into the atmosphere [14], together with the generation of CO and other hazardous pollutants. When polymers recycling or energy recovery are not possible, disposal of plastic waste in landfills is the last likely option, with the consequent contamination of the Earth's surface and serious environmental-related issues [15].

In this frame, looking for new options for the treatment and valorisation of plastic waste is a research field with increasing interest. Typically, the processes involving the chemical transformation of polymers into valuable products (also known as tertiary treatments) have been classified into four major categories: pyrolysis, gasification, cracking, and pyrolysis-reforming [16, 17]. All of them are based on thermochemical reactions with specific conditions depending on the treated waste and the desired products [18, 19]. Considering the composition of polymeric materials, they can be considered as a rich hydrogen source. This is a very interest-

ing point since H_2 is regarded nowadays as the most efficient energy carrier for a wide variety of upcoming stationary and dynamic technologies [20]. However, these thermochemical techniques provide low-quality/high-impurity H_2-rich gases. Various studies have shown that it is possible to decompose plastics to produce H2-rich gases by thermal methods [21–24], solar-driven [25, 26] and microwave-assisted [27] reactions. Plastic wastes can be also electrochemically valorized in low-temperature electrolysers [28, 29] to produce pure and green H_2. This electrolytic process involves the common hydrogen evolution reaction (HER) at the cathode while the oxygen evolution reaction (OER) is replaced at the anode by the electro-oxidation of plastic wastes.

From a thermodynamic point of view, the electrooxidation of organic molecules can take place at lower potentials than the OER, then reducing the energy demand. This has been demonstrated for small organic molecules as methane [30] and formic acid [31], as well as for simple alcohols such as methanol [32–38] and ethanol [39–45] and for more complex organic molecules, including wastes and by-products such as biomass-based waste/effluents [46–49], glycerol [50–52], pyrolysis derivates [53], and the lignin biopolymer [54–60]. Until now, the low-temperature electrolysis of synthetic polymers has been only reported in two recent studies. Hori et al. used low-temperature (200 °C) electrolysers to produce hydrogen on Pt-based electrodes in acid media (85% H_3PO_4) using several kinds of commercial plastics (sponges, cable ties, stockings, and ropes) and pure polymers (polyvinyl alcohol and polyurethane) as anodic feedstock [28]. Our group published a first work on the electro-oxidation of a water-soluble model molecule (methyl pivalate, MP) of poly(methyl methacrylate) (PMMA) [29] on Pt-based electrodes in a Polymer Electrolyte Membrane (PEM) electrolyser at 80 °C. And finally, Shi et al. proposed a process for electro-oxidation of poly(ethylene terephthalate) (PET) at room temperature by using a pre-treatment of the plastic material with a 10 M KOH solution at 60 °C for 4 h [61].

The present study aims at advancing one step forward, studying for the first time the electrolysis of real commercial PMMA for the production of hydrogen at 70 °C on Pt/C based electrodes in a liquid batch electrochemical cell. As PMMA is a solid material, we propose to a dissolution approach in a binary solvent to overcome mass transport limitations. One of the most important contributions of using a binary solvent was the possibility of developing an electrode-regeneration strategy. Attenuated Total Reflection-Fourier-Transform Infrared Spectroscopy (ATR-FTIR) coupled with electrochemical characterisations were used to investigate the electro-oxidation of PMMA-based solutions on two different Pt/C electrodes.

3.2 Experimental

A two-electrode batch cell was employed (Figure B.1) with a double-wall construction that allowed heating by an external liquid carrier regulated at 70 °C with a thermostat. All experiments were performed at atmospheric pressure without purging with an inert gas flow and under continuous stirring by magnetic agitation. The anode (9 cm^2) was a commercial material, composed of a Pt/C catalyst impregnated on a carbon cloth with a carbon gas diffusion layer plus a Nafion® coating to assure proton conductivity (0.2 mg cm^{-2} of 20% wt. Pt supported on C_{Vulcan}, FuelCellStore®). A Pt-wire coil was employed as a counter electrode, and no reference electrode was used, since the purpose of this study was to directly evaluate the overall cell voltage in view to its further practical implementation. For the polarisation of the two-electrode cell, a potentiostat-galvanostat equipment (Origalys®) was used. A variety of electrochemical experiences was performed, mainly cyclic voltammetries (CV) (0-1400 mV, scan rates: 50 mV s^{-1}, 50-100 cycles) and chronoamperometries (CA) (fixed potentials: 800, 1000, or 1400 mV, for 1-4 h).

A homemade Pt/C (20% wt.) anodic electrocatalyst was prepared by using the well-known polyol method, similarly as described in a previous study [60]. $Pt(NH_3)_4(NO_3)_2$ (Sigma Aldrich) was used as metal precursor, ethylene glycol (Carl-ROTH) served as a reducing agent, NaOH (NORMAPUR) was used to adjust the pH while carbon Vulcan XC-72 (FuelCellStore®) was the catalytic support. The Pt precursor was mixed and stirred with ethylene glycol in a beaker until complete dissolution. The pH was adjusted to a value of 9 by adding NaOH 0.2 M, and then the mixture was heated until 190 °C under continuous stirring for 2 h. The carbon support was then introduced and further stirred at room temperature for 48 h. The synthesis product was filtered and washed with distilled water, and was finally dried at 80 °C in a static air furnace. This catalyst was dispersed in 2-propanol (4 mg mL^{-1}, 2 h sonication) and then impregnated by drop-casting on a carbon paper (AvCarb MGL280, FuelCellStore®) to produce our home-made Pt/C electrode (4 cm^2) with a higher catalyst loading of 1 mg cm^{-2}.

Poly(methyl methacrylate) (PMMA) powder average M_w ~15000 g mol^{-1}) was purchased from Sigma-Aldrich. Sulfuric acid (H_2SO_4, 95 – 97 % purity for analysis) was bought from Merck KGaA and 2-propanol (isopropanol, IPA) (HPLC-isocratic grade) was got from Carlo Erba Reagents. A binary solvent strategy was followed to dissolve the PMMA polymer. Therefore, for the experiments, a solvent/electrolyte solution was prepared in advance: 1 M H_2SO_4 in 80% v/v IPA/water. This mixture will be referred to as “solvent/electrolyte”. PMMA at different concentrations (0.1-

2% wt. in 50 mL of solvent/electrolyte) was dissolved by stirring and heating at 50 °C for 30 min prior to the electro-chemical tests. All solutions were fed to the electrochemical cell with continuous stirring 30 min before polarisation and the temperature stability was controlled to keep reproducible conditions.

Fourier-Transform Infrared Spectroscopy (FTIR) spectra were collected on a Perkin Elmer "Spectrum Two FT-IR spectrophotometer" equipped with a Perkin Elmer UATR-TWO diamond ATR cell. Each spectrum is the average of 64 scans, with a resolution of 4 cm^{-1} recorded from 2000 to 800 cm^{-1}. The applied pressure to the electrode was equal in all measurements to evade any potential difference brought by the pressure and penetrating depth. XRD patterns were collected using a Philips PW 3830 diffractometer equipped with a PW 3020 goniometer, a PW 3710 MPD control X-ray diffraction system, and a PW 1140 Cu Kα radiation source generator operated at 40 kV and 30 mA. High-resolution transmission electron microscopy (TEM) was performed in a JEOL 2010 LaB6 instrument with 200 kV acceleration voltage, and scanning electron microscopy (SEM) images were taken through a Phenom-World Phenom Pro Desktop. The Pt-based anodes morphology was analysed by Atomic Force Microscopy (AFM) with a Park System XE–100 microscope in contact mode (using Nanosensors PPP-CONTSCR cantilever) and non-contact mode (using AppNano ACTA 10M cantilever); the tridimensional topographic analysis was performed by analysis software (XEI - Image-Processing and Analysis, Park Systems).

3.3 Results and discussion

3.3.1 Ex-situ characterisations of the commercial anode

According to the manufacturer, the commercial electrode is composed of several layers of different materials: a carbon cloth support, a mesoporous carbon film, a Nafion® coating, and finally the Pt/C catalyst itself. Scanning Electron Microscopy (SEM) allowed analysing the global surface of the electrode (Figure 3.1a-b), mainly the catalyst surface, which exhibits some cracks and several areas with a high concentration of Pt agglomerates (bright spots in the SEM images), highlighting a poor distribution of Pt/C on the carbon cloth support. To get more insights onto the catalyst morphology with higher magnification images, Transmission Electron Microscopy (TEM) was performed. Few grains of the most superficial layer were taken by scratching the electrode surface, where the 20% wt. Pt/C_{Vulcan} catalyst is supposed to be placed. Two micrographs at different magnifications (Figure 3.1c-d) display the amorphous nature of the mesoporous carbon support containing particles of ca. 30 – 50 nm diameter [62–64]. Pt nanoparticles (dark spots) are ho-

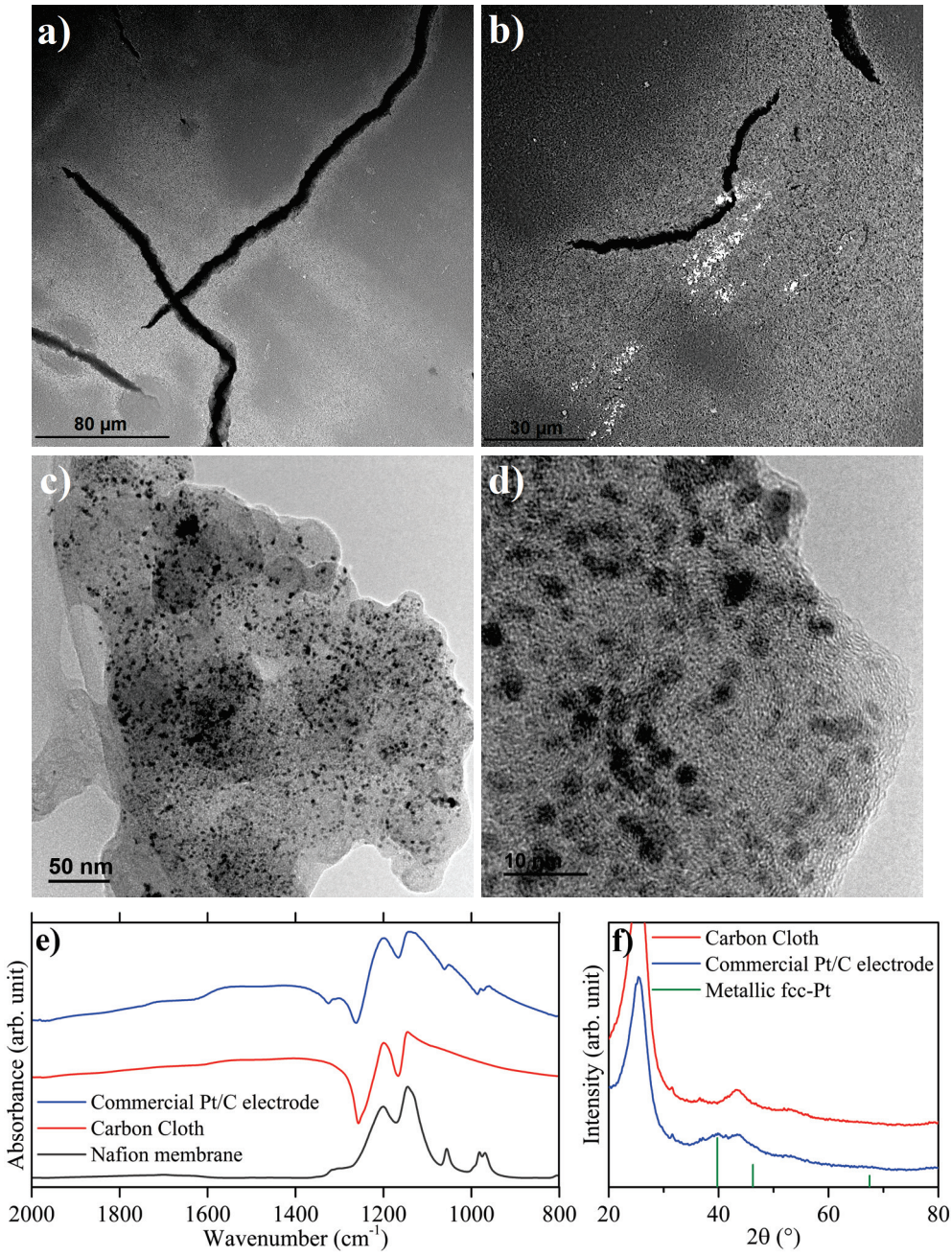

Figure 3.1: Characterization of the commercial electrode material used for the present study: SEM images of the surface at low magnification (a-b), TEM images of the catalyst particles extracted from the surface (c-d), FTIR-ATR spectra (e) and XRD diffractogram (together with FCC-Pt patterns, JCPDS No. 01-070-2057) (f).

mogeneously dispersed on the carbon support with a mean particle size of 2.8 ± 0.7 nm, from a statistical sample of over 50 nanoparticles. Regardless of the high metallic loading, the Pt dispersion is high with an almost negligible agglomeration. However, the irregular overall distribution of the catalyst over the electrode surface observed at the micrometric level could be an issue for the electrolysis of macromolecules.

ATR-FTIR spectroscopy was performed to further analyse the composition of the

commercial electrode surface. Figure 3.1e shows the spectra for the electrode itself, as well as samples of a typical C_{cloth} support (similar to the one used for the commercial electrode) and a commercial Nafion™ 117 membrane for comparison. The Nafion membrane presents typical vibrational bands in the region from 950 to 1300 cm^{-1} associated with C–O–C, CF, SO and CF_2 stretchings [65]. These bands are also present in the C_{cloth} support, owed to a Nafion coating usually applied to improve the proton conductivity of the material. The FTIR-ATR spectrum of the electrode clearly contains those Nafion bands, confirming the significant loading of the ionomer in the electrode. X-Ray Diffraction (XRD) confirms the metallic form of Pt by comparing it with the characteristic peaks of Pt^0 in its fcc crystalline structure (Figure 3.1f). The intensity of these characteristic peaks is very low, which could be attributed to the high dispersion of the Pt nanoparticles on the carbon support (as observed by TEM), together with the small amount of Pt metal in the whole electrode (composed of carbon cloth, mesoporous layer, and catalyst). In addition, most of the background signal (peaks around 25, 31, 37, 41, and 46°) could be attributed to the carbon-based materials present in the C_{cloth} support (Figure 3.1f) as similarly reported for other electrodes prepared likewise [60].

Besides, AFM was used to better characterise the topography of the commercial electrode (Figure 3.2). Figure 3.2a shows a regular area without cracks. The existence of a low roughness is confirmed by maximum level variations of ±200 nm. To quantify this roughness, the root-mean-square average (R_q) of height deviations extracted from the mean image data plane was estimated. For that, it was taken for calculation only the 20 μm x 20 μm area shown in Figure 3.2a, giving an ultimate value of $R_q = 89.9$ nm. As observed by TEM, we assume that the areas with higher elevations correspond to zones with a high concentration of catalyst grains. In addition, as observed by SEM, this sample exhibits low porosity, which could eventually cause mass transport limitations. The zone registered in Figure 3.2b exhibits a completely different profile. The image corresponds to a slit-containing zone, with a significant change regarding the scale on the y-axis. Compared to the image in Figure 3.2a, the unevenness caused by the fissure is in the order of ±5 μm, which generates a high variation of the roughness in regions of this type ($R_q = 2.58$ μm, for the 20 μm x 20 μm area). These cracks are present throughout the commercial electrode, and looking at their depth, they could eventually act as a deposit/trap of the polymer.

All things considered, the characterisation techniques performed in this section allowed us to observe the principal features of the anodic commercial Pt/C electrode. The catalyst itself (Pt/C) exhibits nanometric metallic Pt particles very well and homogeneously dispersed on the amorphous carbon mesoporous support. ATR-

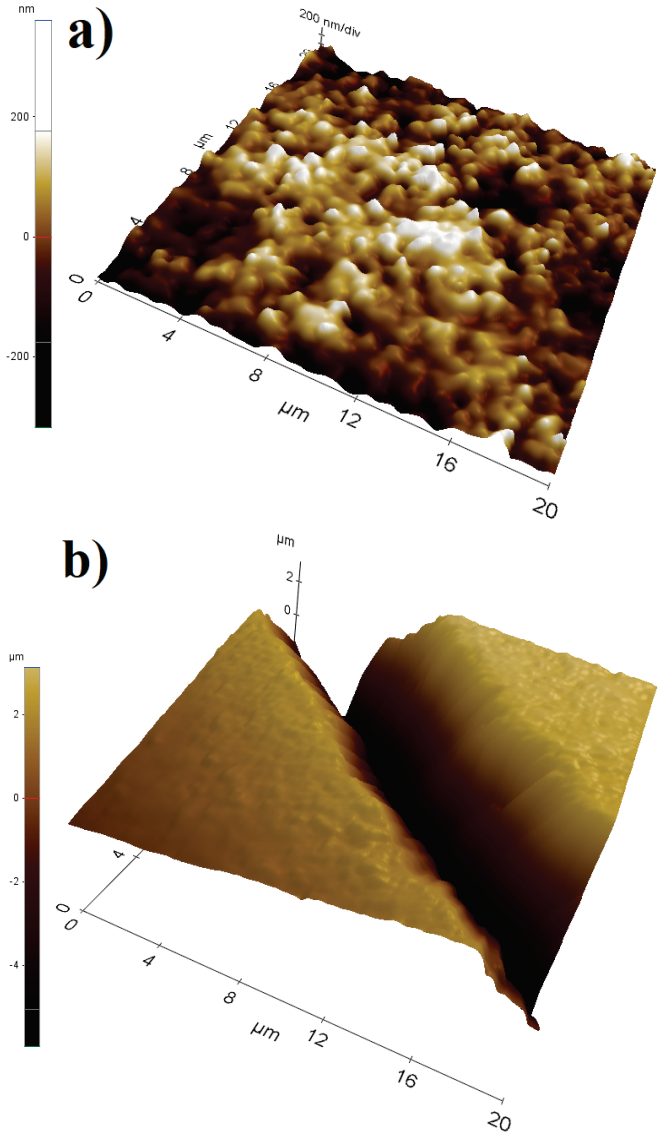

Figure 3.2: Topographic characterization of the commercial electrode surface by Atomic Force Microscopy (AFM): a) On a flat/regular zone, and b) on a slit containing zone.

FTIR confirms the existence of Nafion in the catalyst's proximity. However, the electrode showed an overall low porosity and high roughness, as well as many micrometric size cracks. At a large scale, SEM micrographs have shown a heterogeneous distribution of the catalyst on the surface.

3.3.2 Solubility of PMMA in a binary solvent

The electrolysis of a wide variety of organic molecules for the production of H_2 has been extensively reported in previous studies (i.e. methanol [32–37], ethanol [39–45], glycerol [50–52], and others [30, 31, 46–49, 53–60]. Most of these molecules are electrolysed in an aqueous medium, as they are water-soluble liquids at room temperature (such as methanol and ethanol) or soluble solids (such as lignin, which

dissolves in soft alkaline solutions). In our previous work [29], we studied methyl pivalate as a molecule that can be dissolved at low concentrations in water. However, PMMA is not soluble in water nor in soft acid/alkaline electrolytic solutions, but it can be dissolved in a binary water/alcohol solvent by taking advantage of the polarity of polymer and water [66, 67].

As previously explained, the main interest of the electro-reforming of organic molecules at the anode of electrolysis cells is to reduce the energy demand for water electrolysis. Therefore, both water and an additional organic compound are essential. Having these facts into account, we have selected a solvent solution of 80% v/v IPA in deionised water. This binary solvent composition dissolves PMMA by hydrating the polymer chains via the formation of hydrogen bonds between the water molecules and the polymer ester groups, leaving the hydrophobic side chains exposed to IPA molecules. This results in isolated PMMA chains in solution avoiding the formation of clusters. This binary solvent dissolution approach uses cheap and non-toxic compounds and it is simple to implement, only requiring a heating step at 50 °C. After cooling down at room temperature, the dissolution remains stable, and no precipitation was noted, neither in the presence nor in the absence of sulfuric acid.

3.3.3 Electrochemical oxidation of PMMA-based solutions on a commercial Pt/C anode

To understand the process of electro-oxidation of PMMA in solution, a series of electrochemical experiments were performed at 70 °C. Higher operation temperatures were not applied to avoid reaching the boiling point of the IPA/water mixture ($\sim$ 81 °C) [68]. First, CVs were carried out to understand the effect of the PMMA concentration (from 0 up to 2% wt.) in the solvent/electrolyte on the electrochemical performances in acidic conditions (1 M H_2SO_4). Figure 3.3a shows the whole CV experiments (100 cycles each), while Figure 3.3b shows the 100^{th} cycle for better clarity. Without PMMA, the generated current (with an onset cell potential below 100 mV) is related to the IPA electro-oxidation. The electro-oxidation of this alcohol has been widely reported on Pt-based electrodes [69–75] in acidic media. It is mostly assumed that the main reaction pathway leads to the production of acetone as the primary product of IPA dehydrogenation (Eq. (3.1)). Total IPA oxidation to CO_2 through some reaction intermediate, likely adsorbed acetone, may also take place in the potential region where OH is formed on the Pt surface, i.e., above 0.4 V vs. RHE (Eq. (3.2)) [71]. Still, acetone is usually the main product obtained up to 1-1.5 V vs. RHE, as confirmed by either in-situ mass spectroscopy [74, 75] or in-situ

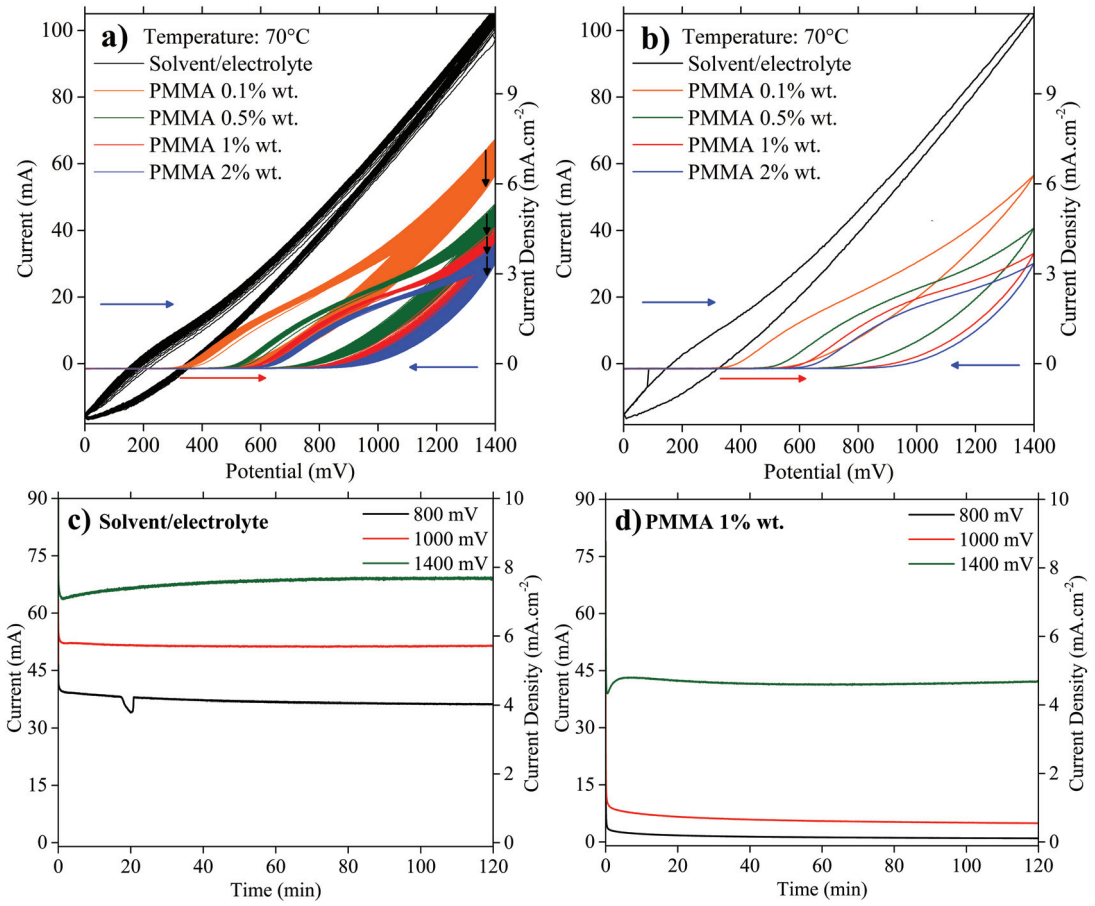

Figure 3.3: Influence of the PMMA content on the overall electrocatalytic performance: a) Complete cyclic voltammetries (scan rate 50 mV s^{-1}, 100 cycles, 70 °C) from 0 to 1400 mV, b) 100th cycle of each experience, c) Chrono-amperometries at fixed applied potentials (800, 1000, 1400 mV) for 2 h at 70 °C for the pure solvent (1 M H_2SO_4 in 80% v/v IPA/water), and d) PMMA 1 % wt. in solvent.

infrared spectroscopy [72–74]. Indeed, adsorbed acetone is the main cause of the deactivation of Pt-based isopropanol oxidation catalysts. In any case, the anodic semi-reaction is accompanied by the cathodic production of hydrogen (verified by the production of bubbles at the cathode), represented in Eq. (3.3), regardless of possible side reactions due to membrane-less configuration.

Anode:

$$CH_3CHOHCH_3 \rightarrow CH_3COCH_3 + 2\,H^+ + 2\,e^- \tag{3.1}$$

$$CH_3CHOHCH_3 \rightarrow \textit{(intermediate)} + n_1H^+ + n_1e^- \xrightarrow{+n_3H_2O} CO_2 + n_2H^+ + n_2e^- \tag{3.2}$$

Cathode:

$$2\,nH^+ + 2\,ne^- \rightarrow nH_2 \tag{3.3}$$

In the present study, a "shoulder" at ~200 – 250 mV was observed during the forward scan, likely associated with isopropanol dehydrogenation reaction (Eq. (3.1)). Then a continuous increase of current took place upon increasing the cell voltage up

to 1.4 V, with a possible contribution from both Eq. (3.1) and (3.2), although acetone is still probably the main product obtained even at high potential. According to the visible absence of bubbles evolving from the anode during the experiments, and to the literature mentioned above on isopropanol electro-oxidation in this potential range [72–75], one can assume that the CO_2 production, if any, is not significant. Then, during the backward scan, slightly lower currents were obtained, essentially below 700 mV. The obtained cyclic voltammetry curve is in good agreement with that reported by Sapountzi et al. with a similar Pt/C electrode [70]. As the main different feature, therein the authors observed some oxidation peaks during the reverse scan, with enhanced current density values as compared to the forward scan. However, they used a reactor with an MEA configuration, operated with 5.5 M IPA at room temperature (vs. 10.46 M IPA at 70°C in the membrane-less cell of the present work).

By adding PMMA to the solution (Figure 3.3a-b), the onset potential increased with the polymer concentration, whereas the current densities follow an opposite trend and decreased along with the cycles. PMMA macromolecules inhibit the IPA electro-oxidation by partially blocking the electrode porosity and the catalyst active sites. However, we cannot exclude a small contribution of the PMMA electro-oxidation in the generated currents as, according to our previous work dealing with the electro-oxidation of a PMMA model molecule (methyl pivalate, MP) [29], it should take place starting from ∼400 mV with a maximal oxidation peak at ∼700 mV. In addition, the current measured during the backward scan in the presence of PMMA was significantly lower than that during the forward scan. This seems to confirm that polymer macromolecules are strongly adsorbed to the anodic surface, leaving no available active sites for the adsorption of new molecules of PMMA.

To get more insights into the steady performance of this system, CA experiments were performed (Figure 3.3c-d) upon the application of different polarizations on a commercial electrode not previously exposed to PMMA. At low potentials (800 and 1000 mV) and without PMMA in the solution (Figure 3.3c), a slight decrease over time in the dynamic electrocatalytic performance was noted, which could be attributed to a poisoning of the anodic catalyst due to strong adsorption of produced acetone [76, 77]. In contrast, a significant increase of the current (steady state at ∼68 mA after 1 h) was noticed when a potential of 1400 mV was applied, a feature that could be explained by the formation of OH_{ad} on the Pt catalyst surface at high applied potentials where the OER can take place. Indeed, the application of high potentials is usually reported as an efficient regeneration strategy for the removal of the poisonous species from the surface of the electrode [71, 74]. In the presence of PMMA (1% wt.), the observed performance considerably changed at the same

applied potentials. For the case of 800 and 1000 mV, the activity quickly decreased and stabilised at low current values of ∼1 and ∼4 mA, respectively. As previously mentioned in the CV experiments (Figure 3.3a-b), the electrode clogging due to the accumulation of polymer species inhibited the IPA electrooxidation. Nevertheless, as observed with the pure solvent/electrolyte, an applied potential of 1400 mV produces, after ∼30 min polarisation, a drastically higher value of ∼42 mA. This behaviour confirms the cleansing role of OH_{ad} species produced from water to continuously regenerate the active sites of the anodic catalyst. Nevertheless, this regeneration is only partial as the current value (42 mA) remains lower than that recorded (68 mA) without PMMA.

Consecutive CAs have been performed with the same electrode with and without PMMA (Figure 3.4) at a constant applied potential of 1000 mV, where the OER cannot occur as confirmed by CVs recorded without IPA in a solution of 1 M H_2SO_4 (Figure B.2a). Moreover, a suitable electrochemical stability of the carbon support under these reaction conditions can be also assumed from the latter CVs as negligible currents were obtained at potentials below 1000 mV. The first CA in Figure 3.4 was performed in the presence of the solvent/electrolyte, where lower initial currents to those registered in Figure 3.3c were observed and followed a significant activity reduction. This indicates that the commercial electrode could undergo aging because of the harsh conditions and the accumulation of species on the surface during preceding experiments. Prior to the second CA, the cell was washed with the solvent/electrolyte solution and the electrode was rinsed with deionised water to remove traces of accumulated compounds. Immediately after, a solution containing 1% wt. PMMA was fed to the cell and the potential of 1000 mV was applied (as in Figure 3.3d). The system exhibited poor electrochemical performances and

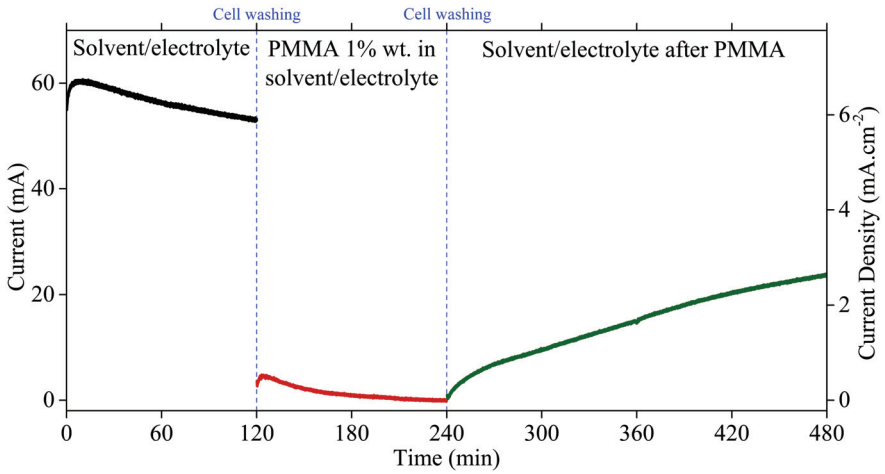

Figure 3.4: Effect of the presence of PMMA on the electrocatalytic performance, performed under three different subsequent solutions. Chrono-amperometries with fixed applied potential (1000 mV) at 70 °C.

a gradual deactivation in which the activity went to current values below 1 mA. At that point, the electrode was removed from the electrochemical cell and rinsed once more with deionised water. In addition, a new solvent/electrolyte solution was fed (without polymer) in the cell, previously washed with the same mixture. Then, the same potential of 1000 mV was applied for 4 h. The initially generated current was very low (1-2 mA) compared to the first CA (∼60 mA), demonstrating that PMMA macromolecules were not fully removed by the cleaning step and were still blocking the active sites. This was confirmed by SEM observations (Figure B.3), where a moving organic phase under the electron beam, probably PMMA, was found at the surface of an electrode that was previously immersed in a 1% wt. PMMA solvent/electrolyte solution for 30 min, subsequently washed with deionised water and dried. However, a constant and progressive reactivation of the electrode took place upon 1000 mV to reach a current of ∼23 mA after 4 h. We consider that the release of the active sites could be explained by the slow electro-oxidation of PMMA and derived species strongly adsorbed. A similar regeneration effect was observed in previous studies dealing with the electrolysis of ethanol solutions on Pt-based electrodes [40, 44], where the application of potentials higher than 0.8 V vs. RHE allowed the electro-oxidation of adsorbed intermediates species that were blocking the catalyst active sites.

In order to illustrate the electrode deactivation issues, together with a possible regeneration strategy, a new experimental approach was proposed (Figure 3.5). The first two steps (Figure 3.5a-b) comprise CV experiments similar to those already shown (Figure 3.3) in the absence (a) and in the presence (b) of the PMMA polymer. The performance was similar to that previously discussed, where PMMA strongly hindered the overall electrocatalytic activity. After that, both the electrode and the cell were washed with the solvent/electrolyte solution. The cell was fed with pure solvent/electrolyte once again (i.e. no PMMA was added to the solution) and a new CV experiment was performed (Figure 3.5c). The curve remained almost unchanged compared to step (b), even if the solution did not contain any plastic, confirming that PMMA was not fully removed by the washing step. Nevertheless, current densities slightly increase along with the 50 cycles, in agreement with a slow electrode regeneration process. Right after, a CA was performed (Figure 3.5d) at a potential of 1400 mV for 2 h, where OER can take place and lead to the formation of abundant OH_{ad} species (Figure B.2a). As previously reported for other organic molecules, OH_{ad} species can effectively oxidise strongly adsorbed species [71, 78]. Only ∼100 min were sufficient to reach a steady-state at ∼61 mA, a similar current value than that recorded on a fresh electrode (∼68 mA) (Figure 3.3c). Subsequent CVs in the presence of solvent/electrolyte confirm the efficient regeneration of the electrode during the CA at 1400 mV, as they show similar performances

as in step (a). A slight difference can be observed, including the onset potential, probably due to electrode aging or to an incomplete regeneration process. Based on these experiments, one could propose a dynamic strategy for the electro-oxidation of polymers dissolved in binary solvents, combining the polymer electro-oxidation with the regeneration steps, preferably in a PEM-like cell configuration. Of course, some modifications can be applied to this novel approach to enhance the overall performance of the system and optimise the cost, by adjusting, for instance, the charge of PMMA in solution, the exposition time or the applied potential.

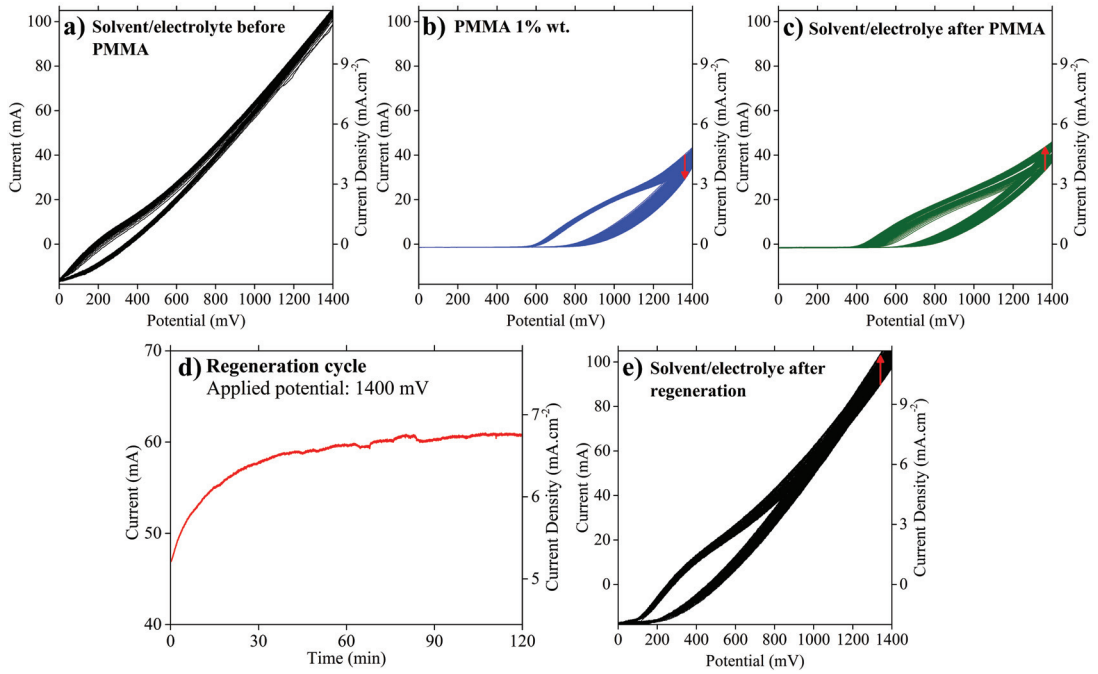

Figure 3.5: Proposed electrode regeneration strategy for the commercial Pt/C electrode: a) CVs in the presence of pure solvent/electrolyte, b) CVs in the presence of PMMA 1% wt. in solvent/electrolyte, c) CV curves in solvent/electrolyte after contact with PMMA, d) Regeneration cycle in solvent/electrolyte (70 °C, chrono-amperometry: 2h at 1400 mV), e) CV experiences in solvent/electrolyte after the regeneration cycle. (The electrode washed with deionised water between each step and all the cyclic voltammetries were performed under the same conditions: 70 °C, 0-1400 mV, 50 cycles, scan rate: 50 mV s^{-1}).

These series of experiments strongly suggest the electrochemical nature of the electrode regeneration step during CA, as it is much more efficient at 1.4 V than at 1 V. In the same way, we have realised that a more adapted anode material is necessary to overcome major problems as poisoning, species accumulation and clogging. Because of this, the next section explores an alternative homemade electrode using a higher loading of a Pt/C self-prepared catalyst (1 instead of 0.2 mg cm^{-2}) on a macroporous C_{paper} support.

3.3.4 Electrochemical oxidation of PMMA-based solutions on a macroporous homemade Pt/C electrode

The macroporous Pt/C electrode was characterised by the same techniques as the commercial one. Figure 3.6 shows the SEM and TEM micrographs, as well as the FTIR and XRD results. In the SEM micrographs (Figure 3.6a-b), the nature of the carbon paper support composed of carbon fibers impregnated with the Pt/C_{Vulcan}

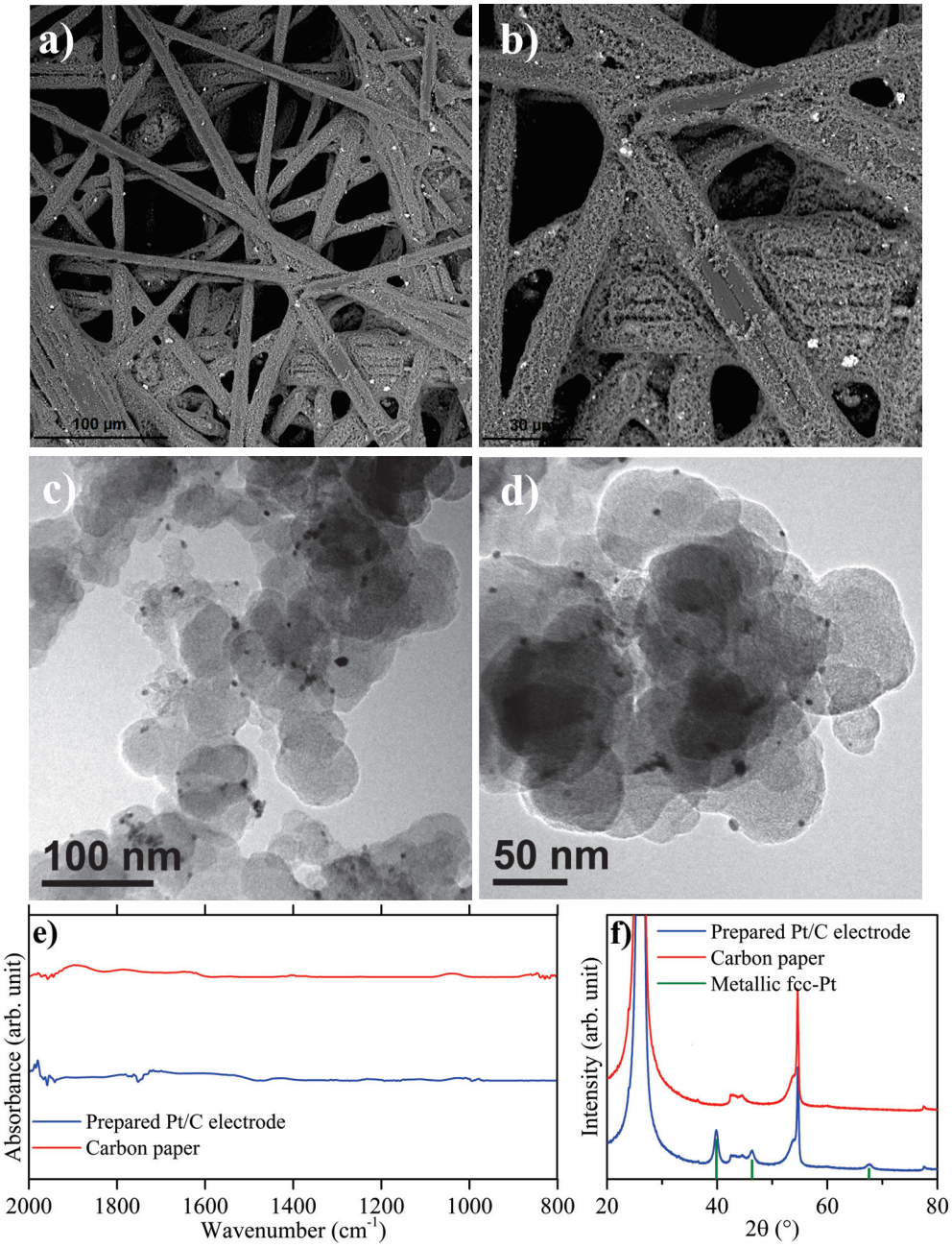

Figure 3.6: Characterisation of the homemade electrode materials: SEM micrographs of the surface at low magnification (a-b), TEM micrographs of a 20% Pt/C catalyst particle (c-d), FTIR-ATR spectra (e) and XRD diffractograms (together with fcc-Pt patterns, JCPDS No. 01-070-2057) (f).

catalyst can be easily identified. Compared to the commercial electrode, the homemade anode presents a macroporous structure (10-20 μm size cavities), a characteristic granted by the C_{paper} support with a 78% of porosity (reported by the fabricant). An elevated concentration of agglomerated metal nanoparticles was spotted this time, which reflected the higher catalyst loading. Figure 3.6c-d shows the TEM images of the synthesised catalyst. In this case, slightly bigger Pt nanoparticles are spotted, with a mean particle size of 5.1 ± 1.5 nm, but with an overall homogeneous distribution of the Pt/C catalyst on the C_{paper}. In addition, and opposed to the commercial material, FTIR spectra (Figure 3.6e) showed that the homemade electrode does not present any important vibrational bands as no Nafion coating was used. Finally, XRD (Figure 3.6f) allowed us to verify the cubic phase of the metallic Pt with a more significant intensity of the peaks compared with the commercial electrode, in agreement with the higher loading of the catalyst over the carbon paper support.

To compare the performance of the new electrode with the commercial one, the same experimental approach was used as with the commercial material (Figure 3.5). As it can be seen in Figure 3.7, the behaviour of the latter electrode is significantly different. The deactivation of the homemade electrode is rather limited compared to the commercial electrode. Even if there is a loss of activity after introducing the PMMA solution, it can be partially regenerated by applying a CV without PMMA (Figure 3.7c). A quantitative approach was used to rationalize differences between both electrodes. We calculated the activity loss (*AL*) and the regeneration factor (*RF*) of the commercial and homemade electrodes from cyclic voltammetries of Figure 3.5 and 3.7 according to Eq. 4 and 5, as follows:

$$AL(\%) = 100 - \left(\frac{Q_t(step\ b)}{Q_t(step\ a)}\right) \times 100 \tag{3.4}$$

$$RF(\%) = \left(\frac{Q_t(step\ c\ or\ e)}{Q_t(step\ a)}\right) \times 100 \tag{3.5}$$

where Q_t is the overall electric charge calculated from the integration of the 50^{th} cycle of each recorded CV (see Figure B.4 for more clarity) at a given step (a, b, c or e on Figure 3.5 and 3.7).

As evidenced in Table 3.1, the commercial Pt/C catalyst shows a larger *AL* (∼80%) after being in contact with PMMA instead of ∼51% for the home-made electrode, demonstrating that the macroporosity can hinder the catalyst deactivation by promoting active sites accessibility. Furthermore, our homemade electrode exhibits a faster reactivation as the *RF* value is already ∼91% just after a cyclic voltammetry (step c), showing a near-complete regeneration. This result highlights that the

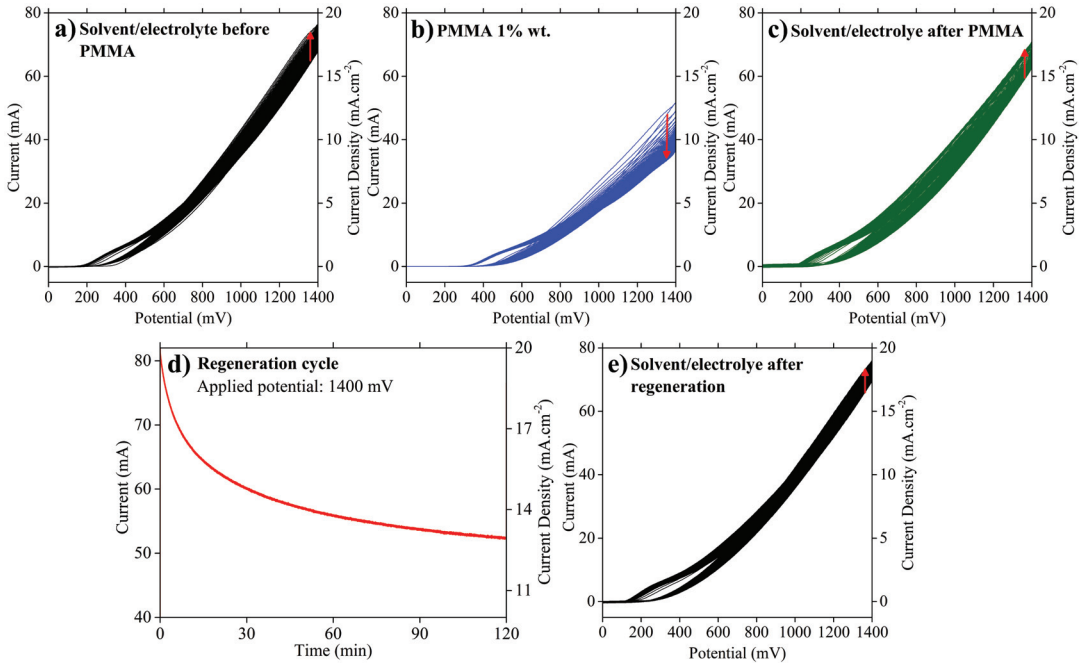

Figure 3.7: Regeneration strategy applied to the homemade macroporous Pt/C_{paper} electrode: a) CV experience in the presence of pure solvent/electrolyte, b) CV experience in the presence of PMMA 1% wt. in solvent/electrolyte, c) CV curves in solvent/electrolyte after contact with PMMA, d) Regeneration cycle in solvent/electrolyte (70 °C, chrono-amperometry: 2h at 1400 mV), e) CV experience in solvent/electrolyte after the regeneration cycle. (The electrode was washed with deionised water between each step and all the cyclic voltammetries were performed under the same conditions: 70 °C, 0-1400 mV, 50 cycles, scan rate: 50 mV s^{-1}).

Table 3.1: Total charge and regeneration factor values calculated from the 50th cycle of CV experiments (Figure B.4).

	Q_t at the 50th cycle				AL(%)	RF(%)	
	Step a	Step b	Step c	Step e	1-(b/a)	c/a	e/a
Commercial Pt/C electrode	2.28	0.45	0.73	1.98	80 ± 4	32 ± 2	87 ± 4
Home-made Pt/C electrode	1.26	0.61	1.14	1.31	51 ± 3	91 ± 5	104 ± 5

PMMA electro-oxidation is taking place during CVs up to 1.4 V. This is confirmed by the chrono-amperometry (CA) experiment at 1.4 V (Figure 3.7d) as the initial current density of ∼20 mA cm^{-2} is much higher than that observed on the fresh commercial electrode (Figure 3.5d, 7 mA cm^{-2}). CA also shows a rapid drop of the current to reach 12.5 mA cm^{-2} after 2 h, possibly attributed to Pt oxidation at this high cell voltage and/or to acetone poisoning. The better electrocatalytic performance of the home-made catalyst, with respect to the commercial one, could be also favoured by the bigger Pt nanoparticles in the former case, which are less

prone to oxidation [79]. Small Pt nanoparticles supported on carbon usually undergo severe deactivation due to the stronger interaction of the adsorbates (e.g. H, OH and CO) with the metallic surface, as demonstrated in previous studies for the electro-oxidation of low molecular weight alcohols and CO [80, 81]. These results demonstrate that an increase both of the porosity and of the catalyst loading strongly promote the electrochemical properties in presence of PMMA. Therefore, the electrooxidation of PMMA or PMMA-derived molecules seems to occur at high potentials at 70 °C in acidic media on a Pt/C electrode. However, the generated current is, to a large extend, linked to the solvent (IPA) electrooxidation, making impossible to quantify the kinetic of the dissolved PMMA electrooxidation.

To clarify the species adsorbed on the electrode, ATR-FTIR spectroscopy was used to analyse the surface of the electrodes (Figure 3.8). Unfortunately, the commercial electrode contains a Nafion® layer that affects the FTIR analysis due to vibrational bands between 950 and 1300 cm^{-1} (as clearly observed in Figure 3.1e), the same region where PMMA shows important characteristic bands (Figure 3.8a). For this reason, the FTIR characterisation study was only performed for the homemade Pt/C electrode without Nafion®. First, the homemade electrode was initially impregnated with PMMA by immersion in a solvent/electrolyte solution containing 1% wt. PMMA at room conditions, and then, dried at 80 °C overnight to ensure that all traces of binary solvent were removed. Figure 3.8b) and d) show the FTIR spectra of the Pt/C homemade electrode before (step 1 in Figure 3.8) and after the impregnation with PMMA (step 2 in Figure 3.8). The presence of PMMA on the elecrode is confirmed by its characteritic vibrational bands. The PMMA-impregnated electrode was immersed for 1 h in 1 M H_2SO_4 at 70 °C under stirring and then the electrochemical performance was carried out without IPA in 1 M H_2SO_4 at 70 °C during a 50 cycles CV from 0 to 1400 mV. A FTIR spectrum was recorded before (step 3 in Figure 3.8b) and after CVs (step 4 in Figure 3.8b). Before ATR-FTIR analysis, the electrode was rinsed with water and dried at 80 °C overnight. As it can be seen in Figure 3.8b, no significant change was found on FTIR spectra neither after the immersion in sulfuric acid nor after polarisation. In fact, Figure 3.8c is comparable to a CV recorded before impregnation with PMMA (Figure B.2b), showing the negligible electro-oxidation of PMMA without IPA in the solution. This indicates that only dissolved PMMA macromolecules can be electro-oxidized.

A second set of experiments was carried out in the presence of the solvent/electrolyte (Figure 3.8d-e). When the impregnated electrode was immersed into the solvent/electrolyte for 1 h at 70 °C under stirring (step 3 in Figure 3.8d), a significant part of the polymer was removed from the surface as FTIR spectrum showed a drastic reduction in the vibrational PMMA bands. We believe that this immersion step

in the solvent leads to the dissolution of the polymer weakly attached to the surface of the electrode. However, small PMMA bands were still present while an unidentified small broad band appeared at ~860 cm^{-1}. After CV (50 cycles from 0 to 1400 mV at 70 °C, step 4 in Figure 3.8d), residual PMMA bands have disappeared and the electrochemical oxidation of the remaining polymer was confirmed by the activity recovery during the successive CVs (Figure 3.8e), where the onset potential progressively decreased while the maximum current increased along cycles. The unidentified band was also removed after CVs. These results strongly suggest that the removal of the polymer from the surface of the electrode can be attributed to the combined effect of the dissolution strategy in the binary solvent and the electrocatalytic oxidation. We consider that the former can dissolve the polymer weakly

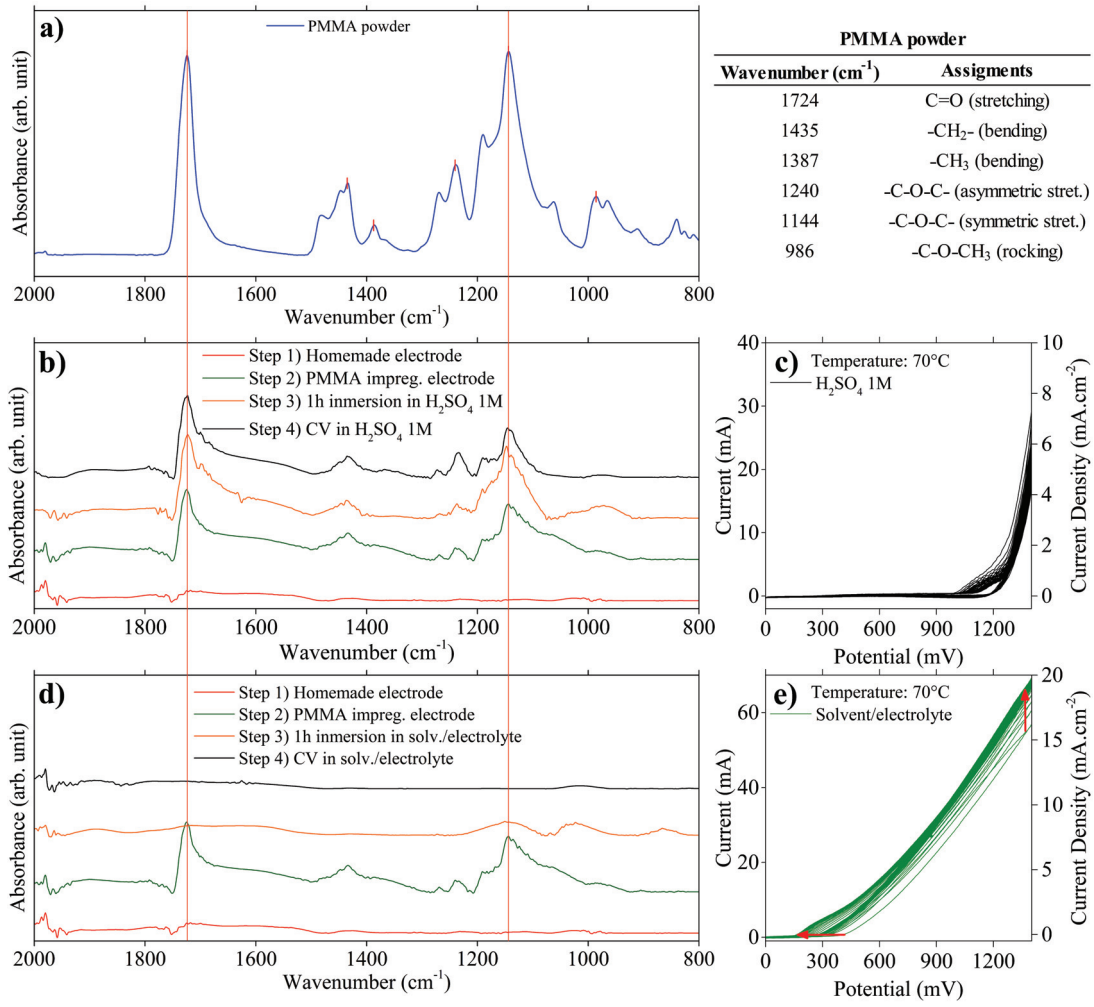

Figure 3.8: Evaluation of the solvent effect on the electro-oxidation of PMMA by FTIR-ATR: a) Spectrum and band assignments of pure PMMA (M_W = 15000 g mol^{-1}), b) Spectra of an electrode after impregnation and different treatments under a 1 M H_2SO_4 solution, c) Cyclic voltammetry applied during the last step of b), d) Spectra of an electrode after impregnation and different treatments under solvent/electrolyte (1 M H_2SO_4 in 80% v/v IPA/water), and e) Cyclic voltammetry applied during the last step of d).

attached to the surface of the electrode, while the latter can electro-oxidise the strongly adsorbed polymer or polymer-derived particles at the catalyst active sites. Although both phenomena led to the regeneration of the catalyst, the electrochemical process is the one that led to the production of H_2 at the cathode which is also boosted by the IPA electro-oxidation from our dissolution strategy.

3.4 Conclusions

The electro-oxidation of dissolved real PMMA particles in an IPA-H_2O binary solution was investigated at 70 °C in acidic media on two different Pt/C based electrodes, aiming to recycle PMMA wastes into H_2 in an electrolyser. The IPA electro-oxidation was found to be the predominant electrochemical reaction below 1.4 V. However, this reaction, implemented on the commercial mesoporous electrode, is strongly hindered by PMMA. Despite the dissolution strategy, polymer macromolecules, in a concentration range 0.1 – 2 wt%, partially block the accessibility of the active sites. Therefore, we prepared a macroporous electrode material with a higher catalyst loading (1 mg cm^{-2}) which can, on one hand, strongly limit the deactivation of the IPA electro-oxidation and, on the other hand, electro-oxidize dissolved polymer macromolecules during cyclic voltammetries up to 1.4 V and chrono-amperometries at 1.4 V. These results open the route to a new recycling two-step process of PMMA wastes including the PMMA dissolution at 50 °C in an IPA/H_2O binary solution following by its electro-oxidation at the anode of electrolysers at 70 °C at potentials from 1.4 V where OER and IPA electro-oxidation both occur. To go further, the design of more porous and active anode materials, such as metallic foams, are absolutely required.

Declaration of competing interest

The authors declare that they have no known competing financial interests or personal relationships that could have appeared to influence the work reported in this paper.

Acknowledgments

The authors gratefully acknowledge the French institution “Ecole Urbaine de Lyon” (EUL - Institut de Convergences) for funding a PhD grant offered to the leading author of this study, Mr. Grimaldos-Osorio.

Supplementary Information

Figure B.1

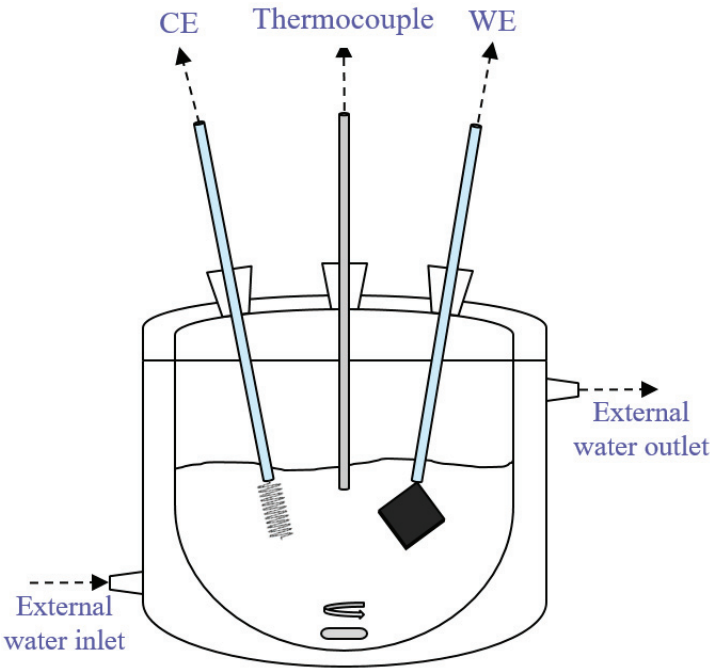

Figure B.1: General scheme of the 2-electrode electrochemical set-up.

Figure B.2

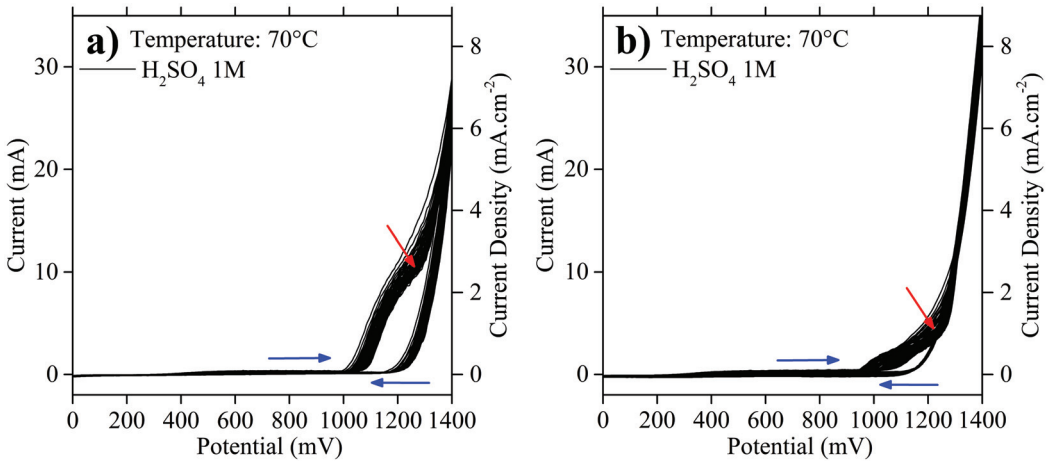

Figure B.2: Performance of the commercial anode (a) and the homemade macroporous Pt/C_{paper} anode (b) during a CV experience in the presence of 1 M H_2SO_4 (70 °C, 0-1400 mV, 50 cycles, scan rate: 50 mV s^{-1}).

Figure B.3

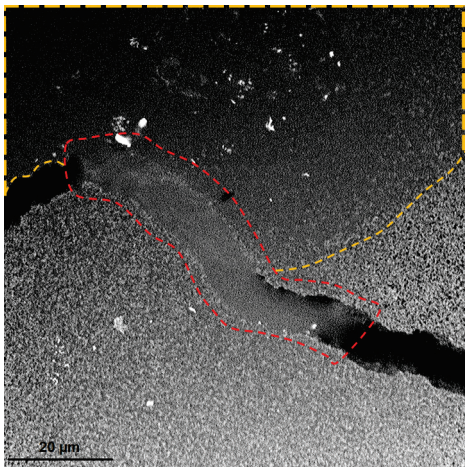

Figure B.3: SEM image of surface of a commercial electrode immersed in a 1% wt. PMMA solvent/electrolyte solution for 30 min, subsequently washed with deionised water and dried (red dotted area: slit partially filled with an organic phase, yellow dotted area: flat zone covered by an organic phase).

Figure B.4

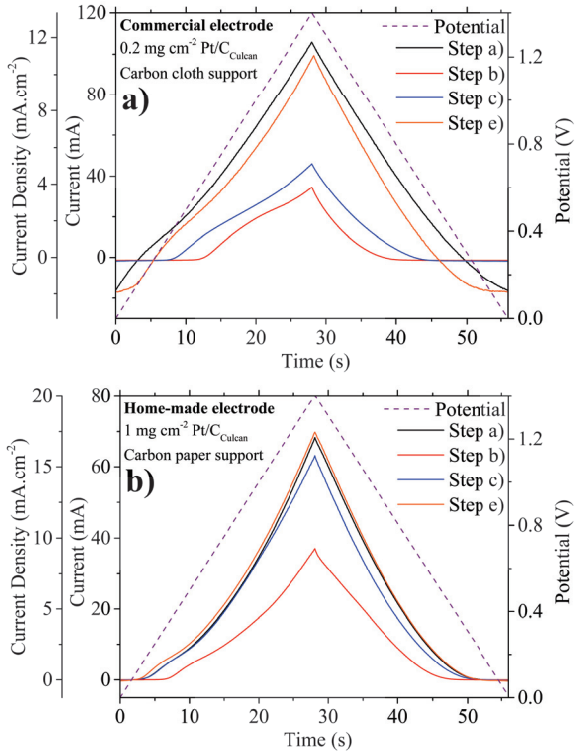

Figure B.4: Dynamic mode plot of the 50th cycles of the CV experiments of the regeneration strategy applied to the commercial and home-made Pt/C electrodes (Figure 3.5 and Figure 3.7).

References

[1] Shivanna, K.R. The Sixth Mass Extinction Crisis and its Impact on Biodiversity and Human Welfare. *Resonance*, 25(1):93–109, 2020. doi: 10.1007/s12045-019-0924-z.

[2] Sklair, L. and Murphy, M.W. Introduction to the Special Issue on World-Systems Analysis and the Anthropocene. *Journal of World-Systems Research*, 26(2):175–183, 2020. doi: 10.5195/JWSR.1.

[3] Geyer, R., Jambeck, J.R. and Law, K.L. Production, use, and fate of all plastics ever made. *Science Advances*, 3(e1700782):1–5, 2017.

[4] Zalasiewicz, J., Waters, C.N., Ivar do Sul, J.A. et al. The geological cycle of plastics and their use as a stratigraphic indicator of the Anthropocene. *Anthropocene*, 13:4–17, 2016. doi: 10.1016/j.ancene.2016.01.002.

[5] Al-Salem, S.M., Lettieri, P. and Baeyens, J. Recycling and recovery routes of plastic solid waste (PSW): A review. *Waste Management*, 29(10):2625–2643, 2009. doi: 10.1016/j.wasman.2009.06.004.

[6] Kedzierski, M., Frère, D., Le Maguer, G. et al. Why is there plastic packaging in the natural environment? Understanding the roots of our individual plastic waste management behaviours. *Science of the Total Environment*, 740:139985, 2020. doi: 10.1016/j.scitotenv.2020.139985.

[7] Li, W.C., Tse, H.F. and Fok, L. Plastic waste in the marine environment: A review of sources, occurrence and effects. *Science of the Total Environment*, 566-567:333–349, 2016. doi: 10.1016/j.scitotenv.2016.05.084.

[8] Bianco, A. and Passananti, M. Atmospheric micro and nanoplastics: An enormous microscopic problem. *Sustainability (Switzerland)*, 12(18), 2020. doi: 10.3390/SU12187327.

[9] Bianco, A., Sordello, F., Ehn, M. et al. Degradation of nanoplastics in the environment: Reactivity and impact on atmospheric and surface waters. *Science of the Total Environment*, 742:140413, 2020. doi: 10.1016/j.scitotenv.2020.140413.

[10] Rahimi, A. and García, J.M. Chemical recycling of waste plastics for new materials production. *Nature Reviews Chemistry*, 1:1–11, 2017. doi: 10.1038/s41570-017-0046.

[11] Kunwar, B., Cheng, H.N., Chandrashekaran, S.R. et al. Plastics to fuel: a review. *Renewable and Sustainable Energy Reviews*, 54:421–428, 2016. doi: 10.1016/j.rser.2015.10.015.

[12] PlasticsEurope and EPRO. Plastics – the Facts 2020: An analysis of European plastics production, demand and waste data. Technical report, Brussels, 2020.

[13] Yassin, L., Lettieri, P., Simons, S. et al. Energy recovery from thermal processing of waste: A review. *Proceedings of the Institution of Civil Engineers: Engineering Sustainability*, 158(2):97–103, 2005. doi: 10.1680/ensu.2005.158.2.97.

[14] Thunman, H., Berdugo Vilches, T., Seemann, M. et al. Circular use of plastics-transformation of existing petrochemical clusters into thermochemical recycling plants with 100 *Sustainable Materials and Technologies*, 22:e00124, 2019. doi: 10.1016/j.susmat.2019.e00124.

[15] Singh, N., Hui, D., Singh, R. et al. Recycling of plastic solid waste: A state of art review and future applications. *Composites Part B: Engineering*, 115:409–422, 2017. doi: 10.1016/j.compositesb.2016.09.013.

[16] Lopez, G., Artetxe, M., Amutio, M. et al. Thermochemical routes for the valorization of waste polyolefinic plastics to produce fuels and chemicals. A review. *Renewable and Sustainable Energy Reviews*, 73(January 2017):346–368, 2017. doi: 10.1016/j.rser.2017.01.142.

[17] Lopez, G., Artetxe, M., Amutio, M. et al. Recent advances in the gasification of waste plastics. A critical overview. *Renewable and Sustainable Energy Reviews*, 82:576–596, 2018. doi: 10.1016/j.rser.2017.09.032.

[18] Al-Salem, S.M., Antelava, A., Constantinou, A. et al. A review on thermal and catalytic pyrolysis of plastic solid waste (PSW). *Journal of Environmental Management*, 197(1408):177–198, 2017. doi: 10.1016/j.jenvman.2017.03.084.

[19] Aguado, J., Serrano, D.P. and Escola, J.M. Fuels from waste plastics by thermal and catalytic processes: A review. *Industrial and Engineering Chemistry Research*, 47(21):7982–7992, 2008. doi: 10.1021/ie800393w.

[20] Ishaq, H., Dincer, I. and Crawford, C. A review on hydrogen production and utilization: Challenges and opportunities. *International Journal of Hydrogen Energy*, 2021. doi: 10.1016/j.ijhydene.2021.11.149.

[21] Wu, C., Nahil, M.A., Miskolczi, N. et al. Production and application of carbon nanotubes, as a co-product of hydrogen from the pyrolysis-catalytic reforming of waste plastic. *Process Safety and Environmental Protection*, 103:107–114, 2016. doi: 10.1016/j.psep.2016.07.001.

[22] Wu, C., Nahil, M.A., Miskolczi, N. et al. Processing real-world waste plastics by pyrolysis-reforming for hydrogen and high-value carbon nanotubes. *Environmental Science and Technology*, 48:819–826, 2014. doi: 10.1021/es402488b.

[23] Czernik, S. and French, R.J. Production of hydrogen from plastics by pyrolysis and catalytic steam reform. *Energy and Fuels*, 20:754–758, 2006. doi: 10.1021/ef050354h.

[24] Dharmaraj, S., Ashokkumar, V., Chew, K.W. et al. Novel strategy in biohydrogen energy production from COVID - 19 plastic waste: A critical review. *International Journal of Hydrogen Energy*, 2021. doi: 10.1016/j.ijhydene.2021.08.236.

[25] Uekert, T., Kuehnel, M.F., Wakerley, D.W. et al. Plastic waste as a feedstock for solar-driven H2 generation. *Energy and Environmental Science*, 11(10): 2853–2857, 2018. doi: 10.1039/c8ee01408f.

[26] Kawai, T. and Sakata, T. Photocatalytic Hydrogen Production From Water By the Decomposition of Poly-Vinylchloride, Protein, Algae, Dead Insects, and Excrement. *Chemistry Letters*, pages 81–84, 1981. doi: 10.1246/cl.1981.81.

[27] Jie, X., Li, W., Slocombe, D. et al. Microwave-initiated catalytic deconstruction of plastic waste into hydrogen and high-value carbons. *Nature Catalysis*, 3 (11):902–912, 2020. doi: 10.1038/s41929-020-00518-5.

[28] Hori, T., Kobayashi, K., Teranishi, S. et al. Fuel cell and electrolyzer using plastic waste directly as fuel. *Waste Management*, 102:30–39, 2020. doi: 10.1016/j.wasman.2019.10.019.

[29] Grimaldos-Osorio, N., Sordello, F., Passananti, M. et al. From plastic-waste to H2: Electrolysis of a Poly(methyl methacrylate) model molecule on polymer electrolyte membrane reactors. *Journal of Power Sources*, 480:228800, 2020. doi: 10.1016/j.jpowsour.2020.228800.

[30] Hori, T., Ma, Q., Kobayashi, K. et al. Electrolysis of humidified methane to hydrogen and carbon dioxide at low temperatures and voltages. *International Journal of Hydrogen Energy*, 44(5):2454–2460, 2019. doi: 10.1016/j.ijhydene.2018.12.044.

[31] Guo, W.L., Li, L., Li, L.L. et al. Hydrogen production via electrolysis of aqueous formic acid solutions. *International Journal of Hydrogen Energy*, 36(16):9415–9419, 2011. doi: 10.1016/j.ijhydene.2011.04.127.

[32] Guenot, B., Cretin, M. and Lamy, C. Clean hydrogen generation from the electrocatalytic oxidation of methanol inside a proton exchange membrane electrolysis cell (PEMEC): effect of methanol concentration and working temperature. *Journal of Applied Electrochemistry*, 45(9):973–981, 2015. doi: 10.1007/s10800-015-0867-3.

[33] Lamy, C., Guenot, B., Cretin, M. et al. (Invited) A Kinetics Analysis of Methanol Oxidation under Electrolysis/Fuel Cell Working Conditions. *ECS Transactions*, 66(29):1–12, 2015. doi: 10.1149/06629.0001ecst.

[34] Uhm, S., Jeon, H., Kim, T.J. et al. Clean hydrogen production from methanol-water solutions via power-saved electrolytic reforming process. *Journal of Power Sources*, 198:218–222, 2012. doi: 10.1016/j.jpowsour.2011.09.083.

[35] Pham, A.T., Baba, T., Sugiyama, T. et al. Efficient hydrogen production from aqueous methanol in a PEM electrolyzer with porous metal flow field: Influence of PTFE treatment of the anode gas diffusion layer. *International Journal of Hydrogen Energy*, 38(1):73–81, 2013. doi: 10.1016/j.ijhydene.2012.10.036.

[36] Wojcieszak, R., Ghazzal, M.N., Gaigneaux, E.M. et al. Low temperature oxidation of methanol to methyl formate over Pd nanoparticles supported on γ-Fe2O3. *Catalysis Science and Technology*, 4(3):738–745, 2014. doi: 10.1039/c3cy00859b.

[37] Ruiz-López, E., Caravaca, A., Vernoux, P. et al. Over-faradaic hydrogen production in methanol electrolysis cells. *Chemical Engineering Journal*, 396 (125217), 2020. doi: 10.1016/j.cej.2020.125217.

[38] Pham, A.T., Baba, T. and Shudo, T. Efficient hydrogen production from aqueous methanol in a PEM electrolyzer with porous metal flow field: Influence of change in grain diameter and material of porous metal flow field. *International Journal of Hydrogen Energy*, 38(24):9945–9953, 2013. doi: 10.1016/j.ijhydene.2013.05.171.

[39] Gutiérrez-Guerra, N., Jiménez-Vázquez, M., Serrano-Ruiz, J.C. et al. Electrochemical reforming vs. catalytic reforming of ethanol: A process energy analysis for hydrogen production. *Chemical Engineering and Processing: Process Intensification*, 95:9–16, 2015. doi: 10.1016/j.cep.2015.05.008.

[40] Caravaca, A., Sapountzi, F.M., De Lucas-Consuegra, A. et al. Electrochemical reforming of ethanol-water solutions for pure H2 production in a PEM electrolysis cell. *International Journal of Hydrogen Energy*, 37(12):9504–9513, 2012. doi: 10.1016/j.ijhydene.2012.03.062.

[41] Gutiérrez-Martín, F., Calcerrada, A.B., de Lucas-Consuegra, A. et al. Hydrogen storage for off-grid power supply based on solar PV and electrochemical reforming of ethanol-water solutions. *Renewable Energy*, 147:639–649, 2020. doi: 10.1016/j.renene.2019.09.034.

[42] Ruiz-López, E., Amores, E., Raquel de la Osa, A. et al. Electrochemical reforming of ethanol in a membrane-less reactor configuration. *Chemical Engineering Journal*, 379(March 2019):122289, 2020. doi: 10.1016/j.cej.2019.122289.

[43] Lamy, C., Jaubert, T., Baranton, S. et al. Clean hydrogen generation through the electrocatalytic oxidation of ethanol in a Proton Exchange Membrane Electrolysis Cell (PEMEC): Effect of the nature and structure of the catalytic anode. *Journal of Power Sources*, 245:927–936, 2014. doi: 10.1016/j.jpowsour.2013.07.028.

[44] Caravaca, A., De Lucas-Consuegra, A., Calcerrada, A.B. et al. From biomass to pure hydrogen: Electrochemical reforming of bio-ethanol in a PEM elec-

trolyser. *Applied Catalysis B: Environmental*, 134-135:302–309, 2013. doi: 10.1016/j.apcatb.2013.01.033.

[45] Miller, H.A., Lavacchi, A. and Vizza, F. Storage of renewable energy in fuels and chemicals through electrochemical reforming of bioalcohols. *Current Opinion in Electrochemistry*, 21:140–145, 2020. doi: 10.1016/j.coelec.2020.02.001.

[46] Cheng, W., Singh, N., Maciá-Agulló, J.A. et al. Optimal experimental conditions for hydrogen production using low voltage electrooxidation of organic wastewater feedstock. *International Journal of Hydrogen Energy*, 37 (18):13304–13313, 2012. doi: 10.1016/j.ijhydene.2012.06.073.

[47] Chen, Y.X., Lavacchi, A., Miller, H.A. et al. Nanotechnology makes biomass electrolysis more energy efficient than water electrolysis. *Nature Communications*, 5(May):1–6, 2014. doi: 10.1038/ncomms5036.

[48] Hibino, T., Kobayashi, K., Ito, M. et al. Efficient Hydrogen Production by Direct Electrolysis of Waste Biomass at Intermediate Temperatures. *ACS Sustainable Chemistry and Engineering*, 6(7):9360–9368, 2018. doi: 10.1021/acssuschemeng.8b01701.

[49] Crisafulli, R., de Lino Amorim, F.M., de Oliveira Marcionilio, S.M. et al. Electrochemistry for biofuels waste valorization: Vinasse as a reducing agent for Pt/C and its application to the electrolysis of glycerin and vinasse. *Electrochemistry Communications*, 102(March):25–30, 2019. doi: 10.1016/j.elecom.2019.03.012.

[50] Simões, M., Baranton, S. and Coutanceau, C. Electrochemical valorisation of glycerol. *ChemSusChem*, 5(11):2106–2124, 2012. doi: 10.1002/cssc.201200335.

[51] Kongjao, S., Damronglerd, S. and Hunsom, M. Electrochemical reforming of an acidic aqueous glycerol solution on Pt electrodes. *Journal of Applied Electrochemistry*, 41(2):215–222, 2011. doi: 10.1007/s10800-010-0226-3.

[52] González-Cobos, J., Baranton, S. and Coutanceau, C. A Systematic in Situ Infrared Study of the Electrooxidation of C3 Alcohols on Carbon-Supported Pt and Pt-Bi Catalysts. *Journal of Physical Chemistry C*, 120(13):7155–7164, 2016. doi: 10.1021/acs.jpcc.6b00295.

[53] Brueckner, T.M., Hawboldt, K.A. and Pickup, P.G. Electrolysis of pyrolysis oil distillates and permeates in a multi-anode proton exchange membrane cell. *Applied Catalysis B: Environmental*, 256(June):117892, 2019. doi: 10.1016/j.apcatb.2019.117892.

[54] Lalvani, S.B. and Rajagopal, P. Lignin-augmented water electrolysis. *Journal of The Electrochemical Society*, 139(1):L1–L2, jan 1992. doi: 10.1149/1.2069212.

[55] Lalvani, S.B. and Rajagopal, P. Hydrogen production from lignin-water solution by electrolysis:. *Holzforschung-International Journal of the Biology, Chemistry, Physics and Technology of Wood*, 47(4):283–286, 1993. doi: 10.1515/hfsg.1993.47.4.283.

[56] Movil, O., Garlock, M. and Staser, J.A. Non-precious metal nanoparticle electrocatalysts for electrochemical modification of lignin for and cost-effective production of hydrogen. *International Journal of Hydrogen Energy*, 40(13): 4519–4530, 2015. doi: 10.1016/j.ijhydene.2015.02.023.

[57] Caravaca, A., Garcia-Lorefice, W.E., Gil, S. et al. Towards a sustainable technology for H2 production: Direct lignin electrolysis in a continuous-flow Polymer Electrolyte Membrane reactor. *Electrochemistry Communications*, 100 (January):43–47, 2019. doi: 10.1016/j.elecom.2019.01.016.

[58] Hibino, T., Kobayashi, K., Nagao, M. et al. Hydrogen Production by Direct Lignin Electrolysis at Intermediate Temperatures. *ChemElectroChem*, 4(12): 3032–3036, 2017. doi: 10.1002/celc.201700917.

[59] Bateni, F., NaderiNasrabadi, M., Ghahremani, R. et al. Low-Cost Nanostructured Electrocatalysts for Hydrogen Evolution in an Anion Exchange Membrane Lignin Electrolysis Cell. *Journal of The Electrochemical Society*, 166(14): F1037–F1046, 2019. doi: 10.1149/2.0221914jes.

[60] Beliaeva, K., Grimaldos-Osorio, N., Ruiz-López, E. et al. New insights into lignin electrolysis on nickel-based electrocatalysts: Electrochemical performances before and after oxygen evolution. *International Journal of Hydrogen Energy*, pages 1–13, 2021. doi: 10.1016/j.ijhydene.2021.01.224.

[61] Shi, R., Liu, K.S., Liu, F. et al. Electrocatalytic reforming of waste plastics into high value-added chemicals and hydrogen fuel. *Chem. Commun.*, 57: 12595–12598, 2021. doi: 10.1039/D1CC05032J.

[62] Nguyen, T.G.H., Pham Van Anh, T., Phuong, T.X. et al. Nano-Pt/C electrocatalysts: Synthesis and activity for alcohol oxidation. *Advances in Natural Sciences: Nanoscience and Nanotechnology*, 4(3):2–10, 2013. doi: 10.1088/2043-6262/4/3/035008.

[63] Santasalo-Aarnio, A., Borghei, M., Anoshkin, I.V. et al. Durability of different carbon nanomaterial supports with PtRu catalyst in a direct methanol fuel cell. *International Journal of Hydrogen Energy*, 37(4):3415–3424, 2012. doi: 10.1016/j.ijhydene.2011.11.009.

[64] Ye, J., Liu, J., Zhou, Y. et al. High catalytic performance and stability of Pt/C using acetic acid functionalized carbon. *Journal of Power Sources*, 194(2): 683–689, 2009. doi: 10.1016/j.jpowsour.2009.06.032.

[65] Liang, Z., Chen, W., Liu, J. et al. FT-IR study of the microstructure of Nafion®

membrane. *Journal of Membrane Science*, 233(1-2):39–44, 2004. doi: 10.1016/j.memsci.2003.12.008.

[66] Hoogenboom, R., Becer, C.R., Guerrero-Sanchez, C. et al. Solubility and thermoresponsiveness of PMMA in alcohol-water solvent mixtures. *Australian Journal of Chemistry*, 63:1173–1178, 2010. doi: 10.1071/CH10083.

[67] Cowie, J.M., Mohsin, M.A. and McEwen, I.J. Alcohol-water cosolvent systems for poly(methyl methacrylate). *Polymer*, 28:1569–1572, 1987. doi: 10.1016/0032-3861(87)90360-0.

[68] Lebo, R.B. Properties of mixtures of isopropyl alcohol and water. *Journal of the American Chemical Society*, 43(5):1005–1011, 1921. doi: 10.1021/ja01438a004.

[69] Wang, B., Tao, L., Cheng, Y. et al. Electrocatalytic Oxidation of Small Molecule Alcohols over Pt, Pd, and Au Catalysts: The Effect of Alcohol's Hydrogen Bond Donation Ability and Molecular Structure Properties. *Catalysts*, 9(4):387, 2019. doi: 10.3390/catal9040387.

[70] Sapountzi, F.M., Tsampas, M.N., Fredriksson, H.O. et al. Hydrogen from electrochemical reforming of C1–C3 alcohols using proton conducting membranes. *International Journal of Hydrogen Energy*, 42(16):10762–10774, 2017. doi: 10.1016/j.ijhydene.2017.02.195.

[71] Habibi, B. and Dadashpour, E. Electrooxidation of 2-propanol and 2-butanol on the Pt-Ni alloy nanoparticles in acidic media. *Electrochimica Acta*, 88:157–164, 2013. doi: 10.1016/j.electacta.2012.10.020.

[72] Sun, S.G. and Lin, Y. Kinetic aspects of oxidation of isopropanol on Pt electrodes investigated by in situ time-resolved FTIR spectroscopy. *Journal of Electroanalytical Chemistry*, 375(1-2):401–404, 1994. doi: 10.1016/0022-0728(94)03536-9.

[73] Sun, S.G., Yang, D.F. and Tian, Z.W. In situ FTIR studies on the adsorption and oxidation of n-propanol and isopropanol at a platinum electrode in sulphuric acid solutions. *Journal of Electroanalytical Chemistry*, 289(1-2):177–187, 1990. doi: 10.1016/0022-0728(90)87215-6.

[74] Waidhas, F., Haschke, S., Khanipour, P. et al. Secondary Alcohols as Rechargeable Electrofuels: Electrooxidation of Isopropyl Alcohol at Pt Electrodes. *ACS Catalysis*, 10(12):6831–6842, 2020. doi: 10.1021/acscatal.0c00818.

[75] Khanipour, P., Speck, F.D., Mangoufis-Giasin, I. et al. Electrochemical Oxidation of Isopropanol on Platinum-Ruthenium Nanoparticles Studied with Real-Time Product and Dissolution Analytics. *ACS Applied Materials and Interfaces*, 12(30):33670–33678, 2020. doi: 10.1021/acsami.0c07190.

[76] Burke, L.D., O'Leary, W.A., Nakamoto, T. et al. A Study of Isopropanol Oxidation at Platinised Platinum Electrodes in Acid Solution. *Proceedings of the*

Royal Irish Academy. Section B: Biological, Geological, and Chemical Science, 89B:389–398, 1989.

[77] Liu, Y., Zeng, Y., Liu, R. et al. Poisoning of acetone to Pt and Au electrodes for electrooxidation of 2-propanol in alkaline medium. *Electrochimica Acta*, 76: 174–178, 2012. doi: 10.1016/j.electacta.2012.04.130.

[78] Podlovchenko, B.I., Petry, O.A., Frumkin, A.N. et al. The behaviour of a platinized-platinum electrode in solutions of alcohols containing more than one carbon atom, aldehydes and formic acid. *Journal of Electroanalytical Chemistry*, 11(1):12–25, 1966. doi: 10.1016/0022-0728(66)80053-0.

[79] Yang, T., Kastenmeier, M., Ronovský, M. et al. Selective electrooxidation of 2-propanol on Pt nanoparticles supported on Co3O4: An in-situ study on atomically defined model systems. *Journal of Physics D: Applied Physics*, 54 (164002):1–14, 2021. doi: 10.1088/1361-6463/abd9ea.

[80] Mukerjee, S. and McBreen, J. Effect of particle size on the electrocatalysis by carbon-supported Pt electrocatalysts: An in situ XAS investigation. *Journal of Electroanalytical Chemistry*, 448:163–171, 1998. doi: 10.1016/S0022-0728(97)00018-1.

[81] Li, X., Qiu, X., Yuan, H. et al. Size-effect on the activity of anodic catalysts in alcohol and CO electrooxidation. *Journal of Power Sources*, 184:353–360, 2008. doi: 10.1016/j.jpowsour.2008.03.058.

CHAPTER 4

Preliminary findings on the direct electro-oxidation of Poly(methyl methacrylate) nanoparticles

Preliminary findings on the direct electro-oxidation of Poly(methyl methacrylate) nanoparticles

4.1 Introduction

The electro-oxidation of Poly(methyl methacrylate) (PMMA) has been approached from two different perspectives until this point. The previous chapters showed the possibility of treating a model molecule (methyl pivalate, MP) and dissolved low molecular weight macromolecules of PMMA while producing hydrogen. Here, we explored different possibilities for the electro-oxidation of PMMA nanoparticles. The reason to carry out these experiences was to get closer to the real case, in which the polymer of interest should be processed into small particles after a selection, cleaning and grinding process, as for several of the secondary and tertiary processes explained in the first chapter of this thesis. In this sense, the present chapter briefly explains the experimental methods and preliminary results on the preparation of such nanoparticles and their treatment to produce hydrogen. The first attempt on the electrochemical reforming of PMMA was performed by employing direct electrolysis using a three-electrode cell arrangement. The second path included a pre-treatment step (acid or alkaline hydrolysis) followed by an electrochemical stage in a similar arrangement. The results here presented are just a set of initial experiences seeking to explore the different possibilities for the electro-reforming of PMMA nanoparticles and to show the prospects and drawbacks of these methods.

4.2 Experimental

For the PMMA nanoparticle colloids synthesis, methyl methacrylate (MMA, 99% purity, Aldrich Chemistry) and 2,2'-azobis(2-methylpropionamidine) dihydrochloride (97% purity, Aldrich Chemistry) were used without further pre-treatment as monomer and reaction initiator, respectively. The preparation was carried out through an emulsifier-free emulsion polymerisation method, as described in two different previous studies [1, 2]. For this purpose, a batch experimental setup, as the one depicted in Figure 4.1 was used. First, 500 mL of Milli Q water were added to the three-necked flask and heated until 80 °C with vigorous mechanical stirring (1000 rpm) while a mild nitrogen flow ($\approx$ 500 mL min^{-1}) was bubbled into the aqueous phase. The monomer was added to the flask, followed by the initiator only when the temperature was stable. Different proportions of monomer/initiator were used, as it will be further explained, to produce PMMA samples with differ-

ent molecular weights. The conditions remained stable for 5 h. Then, the heating was turned off while the N_2 flow continued until the system reached room temperature. The resulting colloids were stored, and samples were collected for further characterisations.

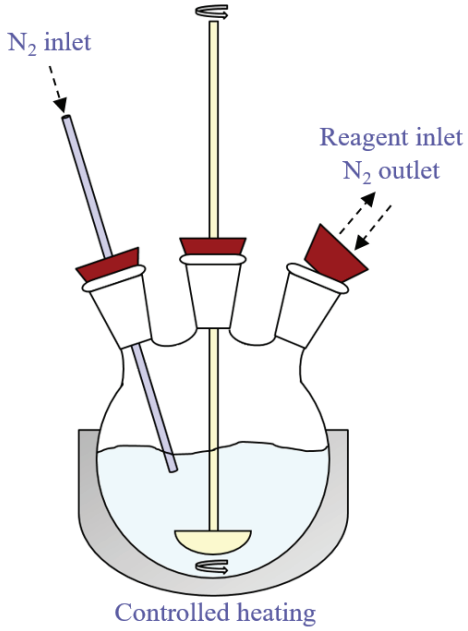

Figure 4.1: Experimental setup for the synthesis of PMMA suspensions.

PMMA colloid samples (45 mL) were dried at 80 °C overnight to determine the final product concentration. Preliminary molecular weights were measured by the viscometric method using tetrahydrofuran (THF, Sigma Aldrich) as solvent. The viscosity-average molecular weight ($\bar{M}_v$) was calculated following the Mark-Houwink equation (Eq. (4.1)), where α and K are parameters depending on the specific polymer-solvent system ($K = 1.22 \times 10^{-2}$ mL g^{-1} and $\alpha = 0.69$, for the PMMA/THF system at 35 °C [3]). The intrinsic viscosity (η_{int}) is calculated from the Huggins equation (Eq. (4.2)), where *k'* is the Huggins coefficient and *c* is the concentration of the solution (g mL^{-1}) [3, 4]. The term of reduced viscosity (η_{red}) is determined by measurements made with an Ubbelohde capillary viscometer at 35 °C, the complete procedure to determine this value is presented in the supplementary section together with Figure C.1.

$$\eta_{int} = K\bar{M}_v^{\alpha} \tag{4.1}$$

$$\eta_{red} = \eta_{int} + k'\eta_{int}^2 c \tag{4.2}$$

The PMMA particle size was determined by Dynamic Light Scattering (DLS) on a CILAS Nano DS instrument (Orleans, France) with a scattering angle of 90°. The samples were directly taken from the synthesised colloids and further dispersed in

Milli Q water and analysed after sonication for 30 min to assure good quality measurements. The reported particle dimensions were obtained through the fit of the (decay time) distribution function to the integral equation, relating the field correlation function and the said distribution function by means of a constrained regularisation method (CONTIN algorithm) developed by Provencher [5]. The intensity distribution function was obtained averaging 10 measurements for each sample.

PMMA powder samples were also analysed by Fourier-Transform Infrared Spectroscopy (FTIR), the spectra were collected on a Perkin Elmer "Spectrum Two FT-IR spectrophotometer" equipped with a Perkin Elmer UATR-TWO diamond ATR cell. Each spectrum is the average of 64 scans, with a resolution of 4 cm^{-1} recorded from 4000 to 400 cm^{-1}. The applied pressure to the sample was equal in all measurements to evade any potential difference brought by the pressure and penetrating depth.

Concerning the electrochemical reforming of PMMA nanoparticles, different strategies were employed to study the general behaviour of the system. Regardless of the approach, an electrochemical batch cell was used, similar to the one represented on Figure 4.2, and with analogous characteristics as the one employed for Chapter 3. Different electrodes were employed as reference electrode (RE) depending on the electrolyte (Ag/AgCl - 3 M KCl with saturated AgCl for acid medium or Hg/HgO - 0.1 M KOH for alkaline medium). Their specific use will be declared when presenting the respective results. As a working electrode (WE), two different materials were utilised, as in the previous chapter. For the first part of the study, we employed a commercial material composed of a Pt/C catalyst dispersed on a carbon cloth with a carbon gas diffusion layer plus a Nafion® coating to assure proton conductivity (0.2 mg cm^{-2} of 20% wt. Pt supported on C_{Vulcan}, FuelCellStore®). The

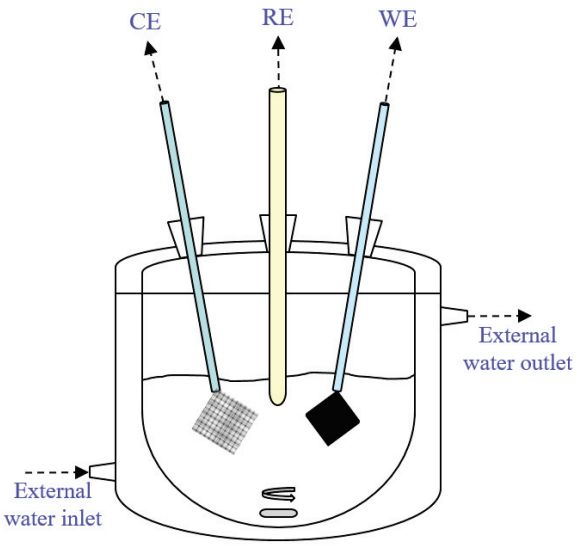

Figure 4.2: General scheme of the 3-electrode electrochemical set-up.

second set of experiments was performed with a home-made Pt/C (20% wt.) electrocatalyst prepared by using the well-known polyol method, similarly as described in Section 3.2 [6]. $Pt(NH_3)_4(NO_3)_2$ (Sigma Aldrich) was used as metal precursor, ethylene glycol (CarlROTH) served as a reducing agent, NaOH (NORMAPUR) was used to adjust the pH while carbon Vulcan XC-72 (Fuel Cell Store®) was the catalytic support. The Pt precursor was mixed and stirred with ethylene glycol in a beaker until complete dissolution. The pH was adjusted to a value of 9 by adding NaOH 0.2 M, and then the mixture was heated until 190 °C under continuous stirring for 2 h. The carbon support was then introduced and further stirred at room temperature for 48 h. The synthesis product was filtered and washed with distilled water, and was finally dried at 80 °C in a static air furnace. The Pt/C catalyst was dispersed in 2-propanol (4 mg mL^{-1}, 2 h sonication) and then impregnated by spray-coating (using nitrogen as a dispersion medium) on a carbon paper (AvCarb MGL280, FuelCellStore®) under heating at 80 °C to produce the home-made Pt/C electrode (4 cm^2) with a catalyst loading of 1 mg cm^{-2}. In all cases, the counter electrode (CE) was a Pt mesh.

The first set of electrochemical experiments was performed by directly using the synthesised colloid suspensions, adjusting the concentration of PMMA with Milli Q water to 2-20 g L^{-1} and adding sulfuric acid (H_2SO_4, 95-97% purity for analysis, Merck KGaA) as electrolyte. The experiences were performed starting by the low PMMA concentrations, followed by the more charged samples. Between experiments, the cell was washed with distilled water and then dried. The second part of the study was conceived to study the influence of different pre-treatment methods on the electrochemical behaviour of the system. For this, dried samples of PMMA nanoparticles were pre-treated following two strategies: acid and alkaline hydrolysis. The employed procedures were adjusted from similar protocols reported in literature, which are presented with the respective results section. The acid pre-treatment was made directly in the electrochemical cell by mixing 180 mg of PMMA powder with 5.4 mL of pure H_2SO_4, under heating (45 °C) and stirring (1000 rpm) for 24h. A constant mild N_2 flow was equally applied to work in an inert atmosphere. Then, the volume was adjusted with distilled water to achieve a concentration of 1 M H_2SO_4. For the alkaline pre-treatment, 1.25 g of PMMA powder was mixed with 50 mL of 10 M NaOH (Chimie-Plus Laboratoires) at 40 °C under stirring (1000 rpm) directly in the electrochemical cell or under sonication during 4 h. The solution was then adjusted to a concentration of 5 M NaOH. For the polarisation of the three-electrode cell, a potentiostat-galvanostat equipment (Origalys®) was used. A variety of electrochemical experiences was performed, mainly cyclic voltammetries (CV) (different applied potential ranges, scan rate: 10 mV s^{-1}, 10 cycles).

4.3 Results and discussion

4.3.1 Synthesis and characterisation of PMMA nanoparticle suspensions

As previously pointed out, the initial idea of this investigation was to analyse the electro-oxidation of PMMA nanoparticles to establish a starting point for direct treatment of solid polymeric materials. In fact, analysing the impact of the molecular weight on the electrochemical behaviour seemed to be of major concern. Consequently, the synthesis of PMMA of a large variety of molecular weights was the first aim of the present study. A set of PMMA colloids were prepared to find an empirical relation between the reactants proportion and the average molecular weight measured by the viscometric method. As Figure 4.3 shows, the ratio between the initial quantities of reactants (R = volume of monomer / mass of initiator) influences the final value of $\bar{M}_v$ following a logarithmic tendency, as revealed by the calculated regression. The values plotted in this figure correspond to the samples that were further used during this study.

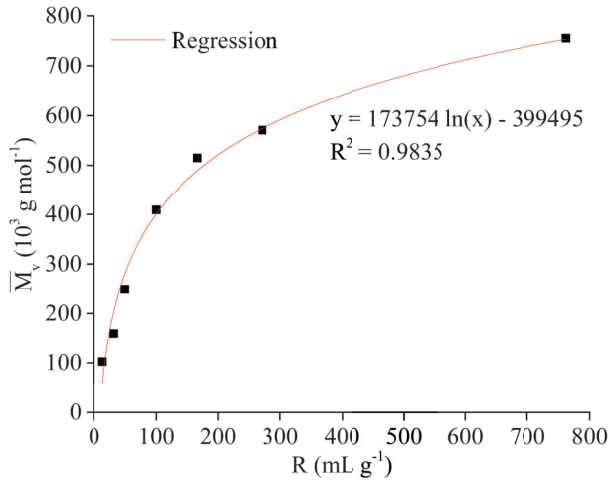

Figure 4.3: Relation between the molecular weight of PMMA samples and the volume/mass ratio monomer/initiator (R).

We could not pursue the synthesis of lower molecular weight samples, because of the impossibility of properly measuring the viscosity for samples with R < 10 (or $\bar{M}_v$ < 100 kg mol^{-1}), but the set of prepared samples was considered sufficient for preliminary studies. In Table 4.1, we report the data of the initial quantities of reactants, the value of R, the measured $\bar{M}_v$ value and the sample name (based on the measured molecular weight) for all the synthesises. Similarly, the PMMA concentration was calculated in order to work later at the same initial concentrations by adding more water when necessary. In any case, the differences in the

concentration values let us know that either the reaction was not complete in some of the synthesis, or some monomer/product was lost during the process due to monomer volatilisation losses. The reaction system could be further improved to avoid these problems by lengthening the reaction time and adding a coolant at the N_2 outlet to prevent the evaporation of monomer, correspondingly. Similarly, on a few occasions, the nitrogen flow was altered by accumulation of PMMA in the inlet tube, impacting the regularity of all the synthesis. Other factor to have in mind is the impossibility of rapidly controlling the temperature during the first minutes of the reaction (very exothermic) that could promote local higher temperatures and finally affect the result of PMMA concentration.

Table 4.1: Details summary of the synthesised PMMA suspensions

Batch	Initiator (g)	Monomer (mL)	R (mL g^{-1})	$\bar{M}_v$ (kg mol^{-1})	PMMA concentration (g L^{-1})	Sample Name
1	3.750	50	14.0	102.5	72.4	PMMA100-k
2	1.552	50	32.2	159.1	53.9	PMMA160-k
3	1.000	50	50.0	249.3	68.0	PMMA250-k
4	0.500	50	100.0	409.0	56.9	PMMA410-k
5	0.300	50	166.7	515.0	75.8	PMMA515-k
6	0.184	50	271.6	570.9	82.0	PMMA570-k
7	0.066	50	762.2	755.3	73.2	PMMA755-k

To check if the synthesised PMMA nanoparticles are in fact pure samples of this polymer, FTIR-ATR was performed and compared to a commercial sample. The spectra of all dried synthesised PMMA samples can be found in Figure 4.4, as well as that of the reference material. It is possible to check that all the important peaks corresponding to PMMA are present for the complete set of prepared polymer: the $-C-O-CH_3$ rocking (986 cm^{-1}), the symmetric and asymmetric $-C-O-C-$ stretching (1144 and 1240 cm^{-1}, respectively), the $-CH_3$ and $-CH_2-$ bending (1387 and 1435 cm^{-1}, respectively), the C=O stretching (1724 cm^{-1}), and the $-CH_3$ and $-CH_2-$ stretching (2951 and 2996 cm^{-1}, respectively). This technique could be of help in case that the electrochemical reforming of PMMA is achieved, due to the likely loss of the methoxy group related vibrational bands, as the previous chapters have suggested.

The last characterisation performed for the PMMA nanoparticle colloids was the determination of the particle diameter by DLS. For this, a sample of each suspension was further dispersed in water and sonicated to avoid agglomeration of particles and distortion of the measurements. As it can be seen in Figure 4.5, all the suspensions are composed of particles with a mean diameter < 80 nm with a low standard deviation, suggesting that monodisperse colloids were obtained as reported for sim-

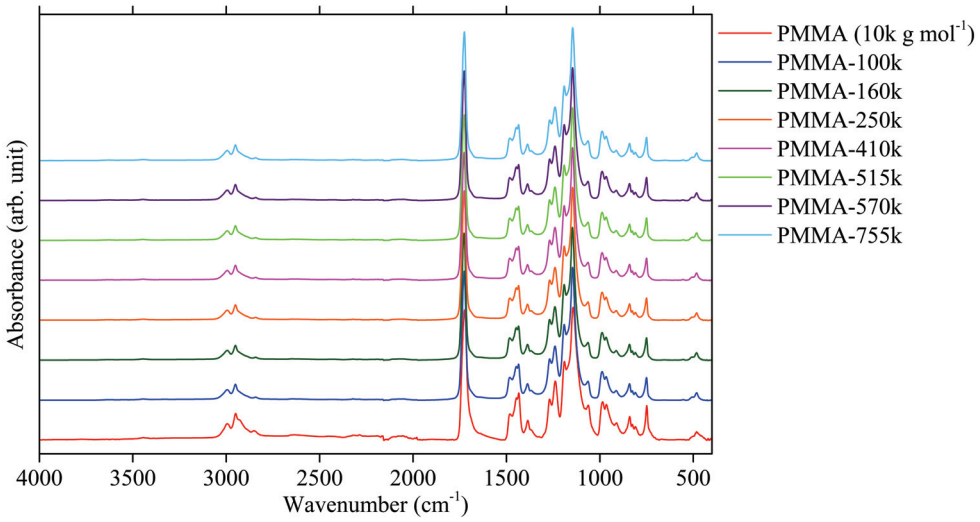

Figure 4.4: FTIR-ATR spectrum of the synthesised PMMA nanoparticles compared to a commercial PMMA sample (M_w ~10000 g mol^{-1}, red line).

ilar synthesis with mechanical stirring [1, 2]. The main variables controlling the particle size are related to the fluid dynamics: laminar or turbulent flow, presence of multiple phases and their interactions, etc. In all cases, the particles were in the range of desired sizes as similar conditions were used for all the synthesis (mechanical stirring, constant N_2 flow, total volume). The variability of the particle size could be explained by small differences in these parameters that were not strictly controlled.

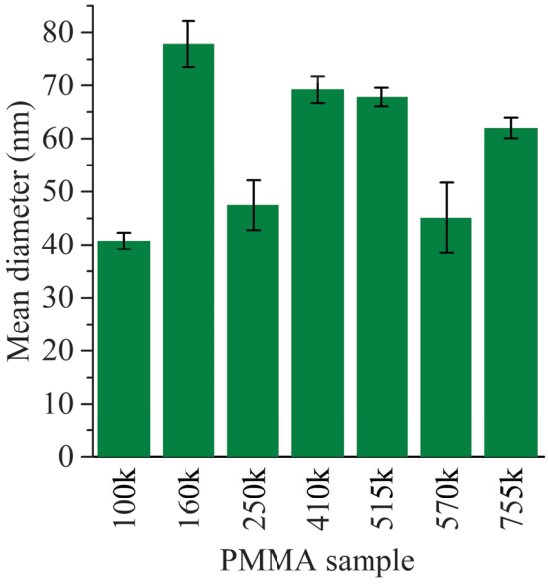

Figure 4.5: Mean diameter of the synthesised PMMA nanoparticles measured by Dynamic Light Scattering (DLS) (calculated from 10 successive measurements).

4.3.2 Electro-oxidation of PMMA suspensions in a three-electrode cell arrangement

In this section, a first approach to the direct electrolysis of PMMA nanoparticles is proposed. As shown in Figure 4.2, using a three-electrode cell arrangement implies the presence of a liquid electrolyte in the reaction media to assure the transfer of charge. Here, we employed sulfuric acid, as in the previous chapter. Figure 4.6a shows the cyclic voltammetry (CV) curves for different H_2SO_4 concentrations in the solution. The main features of the curves could be attributed to the oxidation/reduction of H_{ads} (applied potential < 200 mV vs. Ag/AgCl) and O_{ads} (applied potential > 400 mV vs. Ag/AgCl) at the electro-catalyst surface [7]. No important differences were noticed in the oxygen region, but the current of the peaks in the hydrogen region increases with the H_2SO_4 concentration, and it could be problematic if any reaction involving PMMA occurred in that range of potentials. For this reason, a concentration of 0.1 M H_2SO_4 was chosen for the following experiences. Concerning the employed temperature, the operation was carried out at 80 °C, since as we observed in Chapter 2, high temperatures promote the electro-oxidation of methyl pivalate (MP), and the same behaviour is expected for PMMA.

The next set of experiments aimed for a first approach on the electro-oxidation of PMMA nanoparticles. To define a starting point, the PMMA colloids with the lowest and highest values of average molecular weights were first treated (PMMA-100k and PMMA-755k). A series of CV experiments were carried out to study the influence of the PMMA concentration on the electrochemical behaviour of the system, as it can be seen in Figure 4.6. With PMMA-100k (Figure 4.6b), a reduction of the overall activity compared with the case of the water/H_2SO_4 system was noticed. This behaviour could be attributed to the clogging of the electrode, similar to the case of the diluted PMMA in the previous chapter. Differently, PMMA-755k (Figure 4.6c) showed a slight improvement for applied potentials over 350 mV vs. Ag/AgCl. This value is in the same range than the onset value previously observed for the electro-oxidation of MP (Figure C.2). One may think that such activity could be due to the presence of unreacted monomer (MMA), which could be electro-oxidised similarly to MP by attacking the ester group and producing methoxy species. However, considering that the colloid suspensions were directly used in the reaction environment, an increase in the polymer concentration would increase the concentration of such MMA species, potentially increasing therefore the observed electrochemical activity. Thus, the electrochemical performance did not follow a clear trend with the PMMA concentration, which allows to rule out that theory.

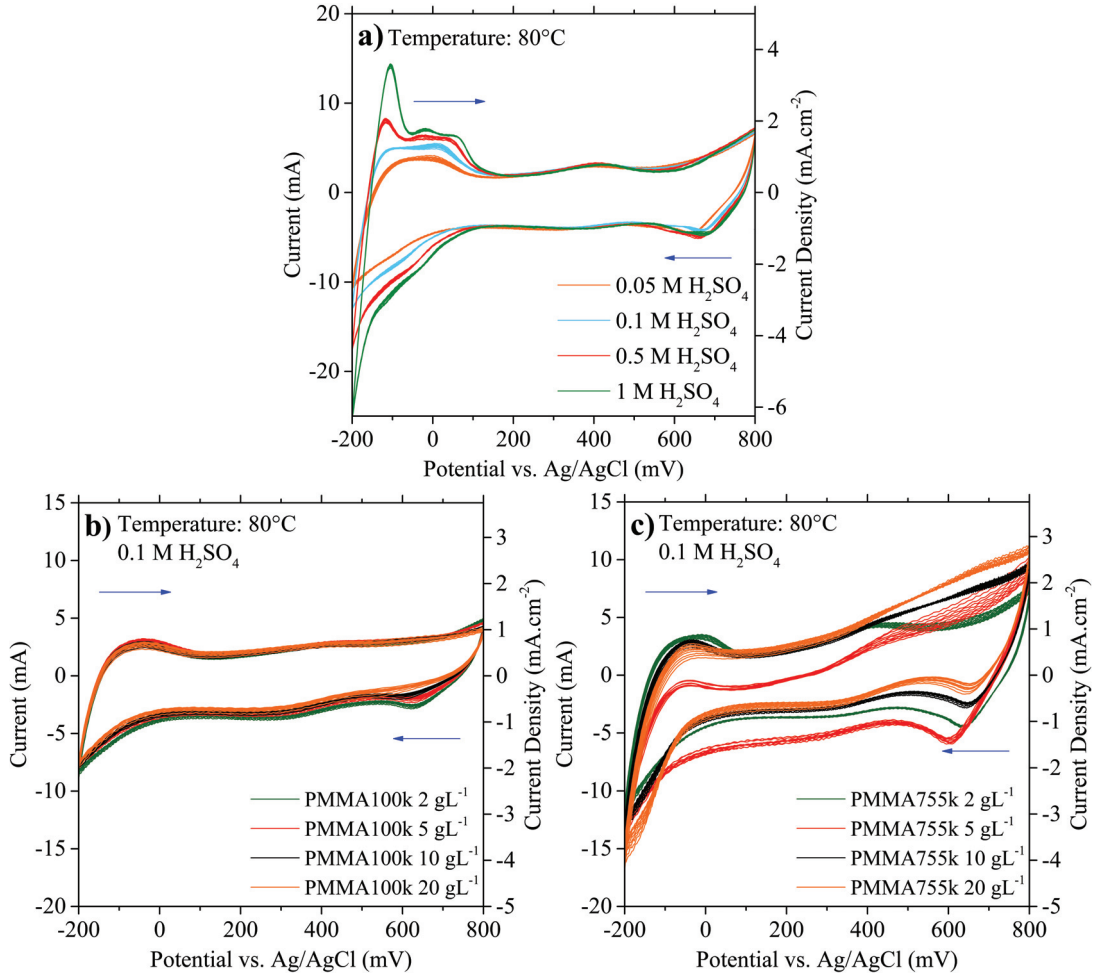

Figure 4.6: Influence of the temperature on the overall electrocatalytic performance: a) complete CV for the pure electrolyte, b) complete CV for pre-treated PMMA-100k, and c) complete CV for pre-treated PMMA-755k. (1 M H_2SO_4, CV: from -200 to 1200mV, scan rate 10 mV s^{-1}, 10 cycles).

The results presented in Figure 4.6 were totally unexpected, as more reactivity was foreseen for lower molecular weights, owing to the higher concentration of chain terminals, which are expected to be more reactive. Moreover, chain terminals are likely constituted by initiator moieties, which would likely behave differently compared with MP and PMMA chains. Therefore, the highest possible activity was expected to be near to the one registered for the electro-oxidation of methyl pivalate (MP) in a three-electrode cell arrangement (Figure C.2), with similar features to the behaviour already discussed in Chapter 2 [8]. Knowing this, it is possible to say that the higher achieved current for the performed experiments is near 2.8 mA cm^{-2} (for PMMA755k 20 g L^{-1} at 800 mV vs. Ag/AgCl), around 55% of the activity registered at similar conditions for MP. All in all, these preliminary experiments suggest that the observed activity could be mainly influenced by the size of the nanoparticles, rather than the total concentration of macromolecules.

While performing the previous experiments, we observed that the more concen-

trated colloids were unstable under stirring and occasionally the solid and aqueous phases got separated. To verify whether the presence of H_2SO_4 was the reason for the suspensions to collapse, a stability test was performed. Samples of PMMA-755k were dispersed in water and then sulfuric acid was added to change the pH of the initial colloids; finally, the nanoparticle size was measured by DLS. The results showed that bigger particles of PMMA were formed when the pH diminished, and a higher standard deviation was also registered (Figure 4.7). This can be explained by the modification of the colloid equilibrium by changing the balance of charges that maintained the nanoparticles in suspension [9–11]. Agglomeration of nanoparticles into bigger clusters could be the reason for the variability of the CV curves when increasing the polymer concentration. It is also important to have in mind that the electrode material used here was previously characterised (Figure 3.1 and 3.2), and we know that big PMMA agglomerates will be not able to travel through the material (due to the very low porosity) limiting the reaction to happen at the available active sites at the more superficial part of the electrode. Furthermore, another limiting point is the size of the electrocatalyst particles compared with the PMMA agglomerates, the latter are considerably bigger making the contact with the active site less likely.

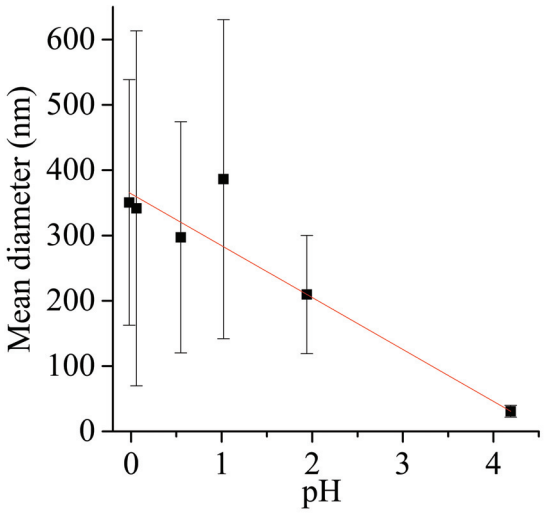

Figure 4.7: Stability of the PMMA nanoparticle size under different acid pH, measured by Dynamic Light Scattering (DLS) (calculated from 10 successive measurements).

The results presented on the direct electrolysis of PMMA colloids gave us valuable information about all the factors that may affect this kind of application, e.g. the impact of the pH on the stability of the suspension, the agglomeration of particles and the impossibility of defining a clear trend of the electrochemical activity with the concentration or the molecular weight of the macromolecules. Here we witness a clear fact, similarly as the study presented in Chapter 3 [6]: the need for an electrode material with tailored characteristics is a major concern. Aspects such

as the macroporosity and a catalyst specifically conceived for the electro-oxidation of macromolecules could improve the results presented in this part of the work. Unfortunately, considering the wide variety of aspects that eventually could impact the behaviour of the electrochemical system, no further experimentation was performed in this sense. Nevertheless, the outcomes of this research path could be used to establish a starting point for further research with this kind of approach.

4.3.3 Electro-oxidation of pre-treated PMMA nanoparticles

To ease the highly hindered electro-oxidation of PMMA, we decided to act on two factors simultaneously: *(i)* the morphology of the anode material, and *(ii)* a pre-treatment process to enhance the concentration of smaller molecules easier to electrolyse. Following the results from Chapter 3 [6], a formulation of a highly porous anode decorated with a better dispersed home-made Pt/C catalyst seemed the most promising path. The results presented for that electrode material suggested that the problems of accumulation of species at the surface were diminished. Also, higher activity and lower deactivation were observed for the electro-oxidation of PMMA dissolved in a binary solvent. Therefore, we employed an equivalent electrode formulation for the next series of experiments. The second factor is related to the poor electrochemical activity previously observed for the PMMA colloids in acid medium.

In fact, two publications suggested a more aggressive path by chemically attacking polymeric samples to facilitate the H_2 production from this type of feedstock. The studies published by different groups sought for the use of plastic waste (PET) to produce H_2 by electrochemical processes [12, 13]. The common key point between those works was the utilisation of a pre-treatment strategy, aiming to ease the processing of the polymeric materials. Both works used a hydrolysis step to reduce the size of the macromolecules to produce lighter species that could eventually be more easily transformed into H_2. Analogous pre-treatments were carried out with NaOH (2 or 10 M) at 60 °C for different reaction times. The results were remarkable in both cases, as PET could be hydrolysed to produce ethylene glycol and added value by-products. A different result could be expected for PMMA, as the only possibility is the hydrolysis of the lateral ester groups.

Having this in mind, we considered the application of a similar approach by testing both alkaline and acid hydrolysing agents. The following sets of experiences are based on previously reported methods for the production of poly(methacrylic acid) (PMAA) through acid and alkaline hydrolysis [14–17]. In theory, this would lead to the production of methanol that could be promptly electrolysed, as described in the study presented in Chapter 2 [8]. This would follow the general reaction for

the hydrolysis of esters, as described in Eq. (4.3), with certain variations depending on the acid or alkaline mechanism [18].

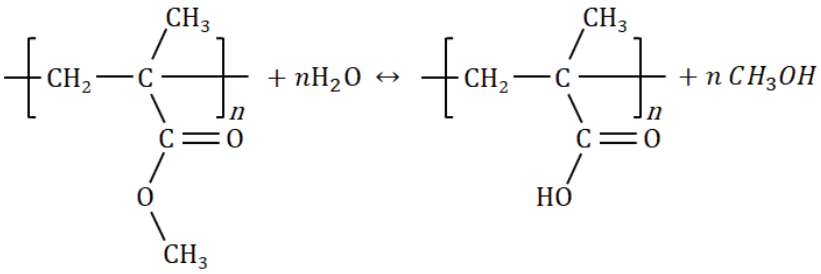

(4.3)

— Sulfuric acid pre-treatment

The acid hydrolysis step was performed as explained in the experimental section of the present chapter, and it was inspired on the procedure proposed by Smets et al. [14, 15] and Ali et al. [16]. Few modifications were made in order to enhance this process. First, the ratio PMMA/H_2SO_4 was increased to assure the existence of enough methoxy species that could be further electro-oxidised. Second, the temperature was fixed at 45 °C to avoid reaching the boiling point of methanol (65 °C), which should be produced from the hydrolysis step. Higher temperatures would affect the final content of these species because of the loss by evaporation. And finally, the pre-treatment time was increased to accumulate the hydrolysis products. Following the mixing of PMMA with H_2SO_4, the two phases that were initially separated became homogenous after ∼1 h mixing. Once the pre-treatment was finished (24 h in total), the resulting gel-like product was cooled down to 20 °C, and water was added to achieve the same volume as in previous experiments and the desired H_2SO_4 concentration. All this was done in the electrochemical cell arrangement to benefit of the controlled temperature system. The literature suggests that the pre-treatment conditions are sufficiently strong to hydrolyse the PMMA nanoparticles - at least partially - to form a copolymer with poly(methacrylic acid) (PMAA) blocks, together with methanol [16].

Figure 4.8 presents the results of the cyclic voltammetries performed at different temperatures for the pure electrolyte and the pre-treated PMMA samples after 24h pre-treatment. With the 1 M H_2SO_4 solution, a similar behaviour to the one presented in Figure 4.6a was verified. In this later case, the range of potential was larger, going over the theoretical applied potential needed for the oxygen evolution reaction (OER) to start. Low current values were registered because of the temperature used here. When compared with both pre-treated polymers (Figure 4.8b and c), it can be observed that no important improvement is attained. Actually, a reduction of the current at higher potentials in the case of PMMA-100k is registered. In fact, the tacticity of the polymer may strongly influence the hydrolysis step

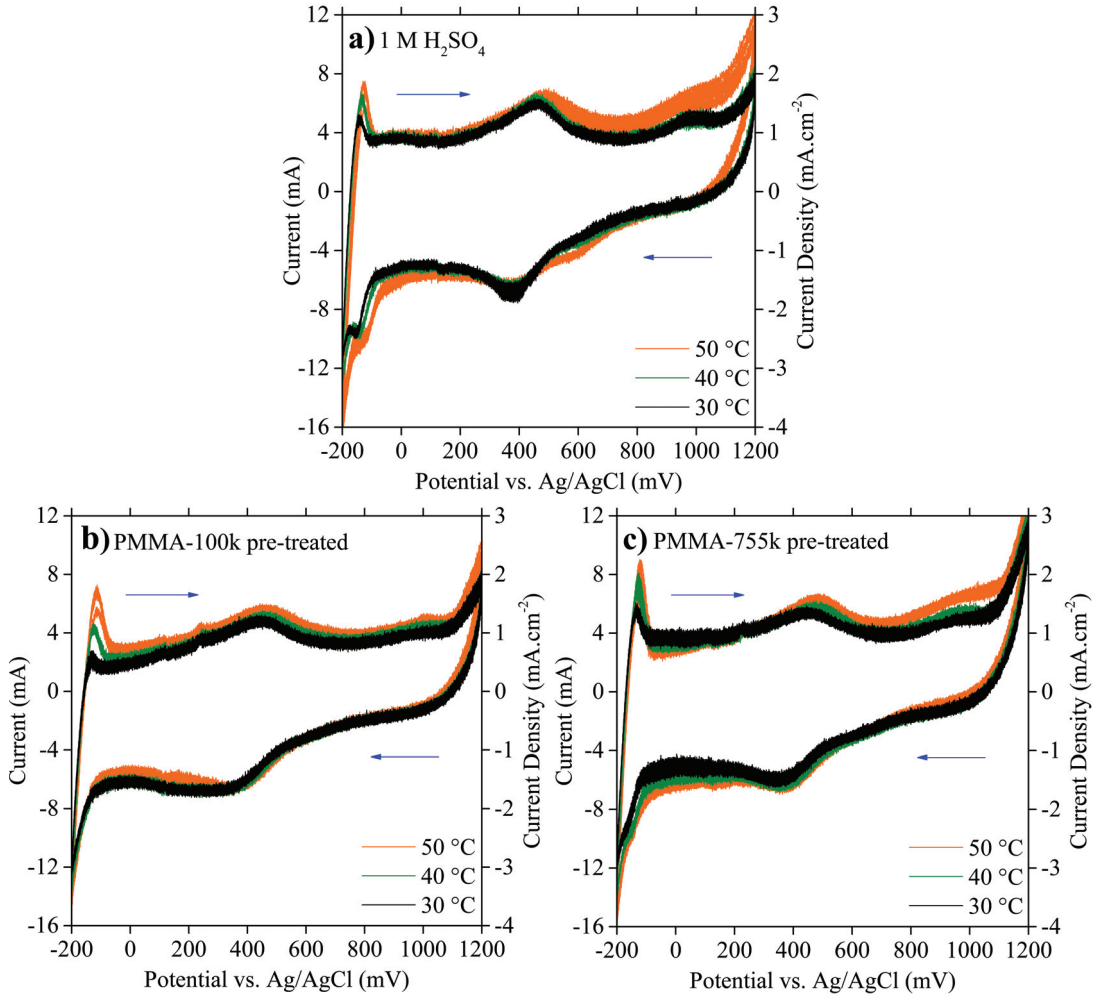

Figure 4.8: Influence of the temperature on the overall electrocatalytic performance: a) complete CV for the pure electrolyte, b) complete CV for pre-treated PMMA-100k, and c) complete CV for pre-treated PMMA-755k. (1 M H_2SO_4, CV: from -200 to 1200mV, scan rate 10 mV s^{-1}, 10 cycles).

[15, 16, 19], a variable that was not explored in this work. We have no evidence of whether the desired methoxy species were produced upon such pre-treatment. Nevertheless, even if such species were formed, the aforementioned problem of clogging and accumulation of macromolecules on the electrodes surface could not be disregarded. This phenomenon could eventually happen even in the case of full hydrolysis (Eq. (4.3)), as the electrode clogging could happen in the presence of PMAA or of the co-polymer PMMA/PMAA.

Seen as such approach did not provide good results, a potential alternative for future studies could be to electrolyse the gel-like mixture recovered from the acid pre-treatment, avoiding therefore the mass transport issues. For example, the middle temperature systems used by Hori et al.[20] took advantage of a similar approach to treat electrochemically gel-like samples of different polymeric materials treated with H_3PO_4. Additionally, they separated the electrodes by using a PTFE

membrane, which helps to assure the production of pure hydrogen at the cathodic side. In the same way, temperatures over 100 °C in a gas-tight system would decisively improve the general performance.

— Sodium hydroxide pre-treatment

Pre-treatment in an alkaline medium was also tested to produce species easier to electrolyse from PMMA nanoparticles. Here, the proposed method was based on the procedures suggested for the hydrolysis of PMAA/PMMA copolymers by Smets et al. [17] and the studies about the electrolysis of plastic materials already discussed [12, 13]. Similarly, the process was optimised to avoid the losses of methoxy species by decreasing the temperature to 40 °C with a pre-treatment time of 4 h for both the in situ (in the electrochemical cell under magnetic stirring) and under sonication pre-treatments. A rather different behaviour was noticed for the solution when the mixing method was changed. With the in situ pre-treatment, the phases were separated during the whole duration of the experiment. But under sonication, a better integration of the solid and liquid phases was observed. It could be explained by an enhanced interaction of the hydroxyl ions with the macromolecules, a phenomenon that can be affected by the electrostatic repulsion generated by the charges along the polymer chains [17]. One could think that the result of the pre-treatment under sonication could produce a higher concentration of methoxy groups in the solution. To avoid the problem of accumulation of non-reactive (mainly polymer) species at the anode's surface, as previously suggested, most of the remaining solids after pre-treatment were extracted by centrifugation before adjusting the final concentration of NaOH for the electrochemical tests. The easy-to- electrolyse compounds are expected to stay in the liquid phase.

At the electrochemical level, the result was not different from the case of the acid pre-treatment, as it can be seen in Figure 4.9. To relate these results with the reported in Figure 4.9, one should take into account that the Oxygen Evolution Reaction (OER) takes place at different potentials for both systems: 1.03 V vs. Ag/AgCl in very acid medium or 0.17 V vs. Hg/HgO in very alkaline medium. In fact, when compared the overall behaviour of both acid and basic electrolytes without PMMA, the latter shows a slightly higher current density at high applied potentials just because the polarisation covered a larger range in the positive sense. Regarding the results of the alkaline pre-treated PMMA, no change can be easily distinguished between the magnetic stirring and sonication cases, as Figure 4.9b-c show. Then, even if the sonication helped the integration of the solid and liquid phases, there is not a direct reflection on the electrochemical performance. Identical pre-treatments were applied for the lower molecular weight polymer sample (PMMA-100k), obtaining

similar results for the CV curves presented here for PMMA-755k.

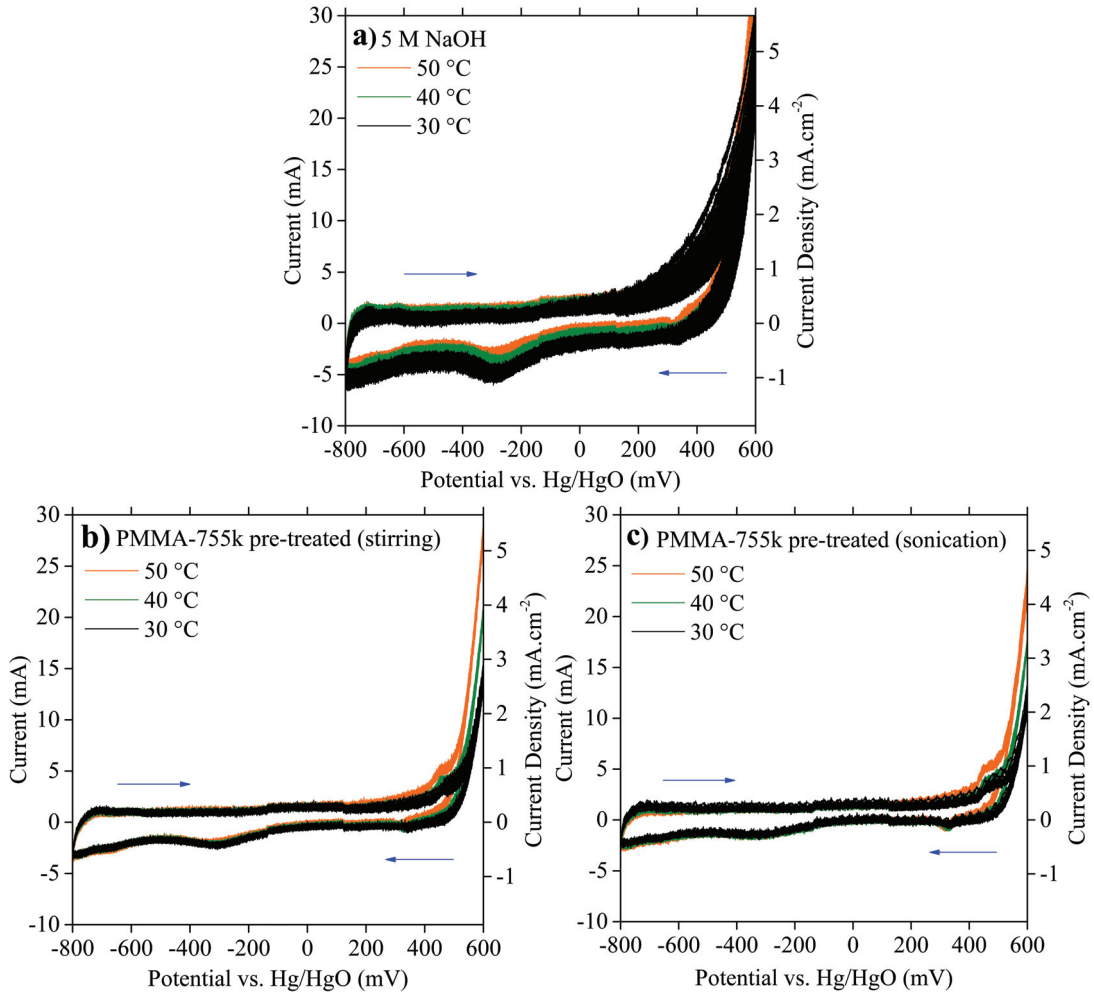

Figure 4.9: Influence of the temperature on the overall electrocatalytic performance: a) complete CV for the pure electrolyte, b) complete CV for pre-treated PMMA-755k under stirring, and c) complete CV for pre-treated PMMA-755k under sonication. (5 M NaOH, CV: from -800 to 600mV, scan rate 10 mV s^{-1}, 10 cycles).

The outcomes presented here were surprising, as slight improvements in the electro-oxidation of PMMA were expected, compared with the results of the direct electrolysis of PMMA colloids. Multiple possibilities could explain the failure of the strategy. First, the employed temperatures were maybe not high enough to promote the hydrolysis of the lateral ester groups of PMMA, with slow and incomplete generation of methoxy species to be oxidised. Second, the scarcely produced electrolysable species were lost by evaporation, but this option is unlikely because low temperatures were employed and, in the case of the alkaline pre-treatment, no N_2 flow was applied (sealed electrochemical cell). The third option is the one previously discussed for the acid pre-treatment about the clogging of the electrodes due to the presence of the polymeric by-products. Knowing these limitations, the system could be improved by different strategies. For example, to perform an ex-situ

pre-treatment at higher temperature to produce smaller molecules by depolymerisation, with a separation step to extract all the intrusive polymeric species, followed by the electrochemical step.

4.4 Conclusions

The results presented in this chapter dealt with preliminary investigations of the electro-oxidation of PMMA nanoparticles, and a first approach to the electrochemical valorisation of real colloidal PMMA samples. The synthesis of PMMA nanoparticles of different molecular weights was achieved through an emulsifier-free emulsion polymerisation method, and a preliminary characterisation was performed. More techniques could be used to have more information about the chain morphology and molecular weight distribution, and this would contribute to the understanding of the overall performance. Several limitations were found at the electrochemical level. It is likely that the dominant factors for the electro-oxidation are of mass-transport nature, whereas the molecular weight seemed to have a limited effect so far.

Moreover, PMMA has only C–C bond in the main chain, making considerably complex the electro-oxidation process. The chances of a contact between the ester groups and the electrocatalyst active sites are significantly low if we take into account the nature of the polymer nanoparticles (initial diameter > 40 nm, but much higher if the pH is modified), and their difficulty to reach the metallic nanoparticles because of the pore size of the mesoporous carbon support that is usually in the order of $5 - 20$ nm [21, 22]. Equally, we believe that further studies on the morphology of the anode materials are mandatory to avoid the mass transport issues. Even if for the second part of this chapter, a home-made electrode with higher porosity was used, further improvements could be conceived for the electro-oxidation of high molecular weight (and big particle size) compounds. There are multiple, and possibly interacting, factors affecting the electrochemical performance. Nonetheless the simplest strategy one can imagine would involve the use of macroporous support materials with a more active catalyst for this process. In order to achieve higher currents that could lead to the subsequent production of H_2, it is also advisable to further explore the pre-treatment conditions to successfully produce species easy to electrolyse. Using more chemically aggressive and controlled conditions, as well as a system that prevents the loss of the produced species, could help to achieve a better performance.

The results shown in this chapter provide valuable information about the limitations of this system and the possible paths to follow in the future. Indeed, the main

problems found throughout this chapter inspired the conception of the final study of this thesis work. As it will be discussed in Chapter 5, the study of polymeric materials that present C–O bonds in their main chain seems to be more appropriate for their treatment in electrochemical systems. Likewise, it will be shown that the need to develop electrodes with special characteristics is of paramount importance to increase the activity, and strategies to customise the anode configuration will be explored to propose an electrode optimised for the valorisation of low molecular weight polyethylene glycol (PEG).

Supplementary Information

Viscosity average molecular weight ($\bar{M}_v$) calculations

The methodology used here follows the procedures already reported in the literature [3, 4, 23]. In order to calculate the viscosity-average molecular weight, it was first necessary to establish the specific (η_{sp}) and reduced (η_{red}) viscosity of PMMA/THF solutions at different diluted concentrations. η_{sp} can be determined from Eq. (C.1) by assuming that the relative viscosity (η_r) is determined by the time t (and t_0) that the solution (and solvent) takes to flow between two points of an Ubbelohde capillary viscometer, and the density of the PMMA solutions is comparable to density of the pure solvent due to the low polymer concentrations, making possible the simplification to Eq. (C.2).

$$\eta_{sp} = \eta_r - 1 = \frac{t.\rho}{t_0.\rho_0} - 1 \tag{C.1}$$

$$\eta_{sp} \approx \frac{t - t_0}{t_0} \tag{C.2}$$

Then, η_{red} is calculated from Eq. (C.3), where c is the solution concentration in g mL^{-1}.

$$\eta_{red} = \frac{\eta_{sp}}{c} \tag{C.3}$$

Table C.1 shows an example of reduced viscosity calculations. Each t was measured three times and data out of the tendency was eliminated to have a more accurate average value.

Table C.1: Viscosity calculations from experimental data taken with an Ubbelohde capillary viscometer at 35 °C (PMMA-755k).

Sample	Solution volume (mL)	PMMA concent. (g L^{-1})	Time (s)				η_{sp}	η_{red} (mL g^{-1})
			t_1	t_2	t_3	$\bar{t}$		
THF	15	0.0000	124.49	124.40	126.62	125.17	0.0000	-
1	15	0.0075	269.66	278.32	272.41	273.46	1.1847	157.96
2	20	0.0056	237.39	231.45	231.25	233.36	0.8644	153.67
3	25	0.0045	207.49	210.53	211.74	209.92	0.6771	150.46
4	30	0.0038	195.03	193.23	-	194.13	0.5509	146.91
5	35	0.0032	-	184.74	-	184.74	0.4759	148.06

The resulting values of η_{red} were plotted against c, and the data was linearised to follow the form of the Huggins equation (Eq. (4.2)). Figure C.1 shows an example for the data of Table C.1. The intercept of the line corresponds to the value of the intrinsic viscosity (η_{int}) that correlates with the viscosity average molecular weight ($\bar{M}_v$), according to the Mark-Houwink equation (Eq. (4.1)).

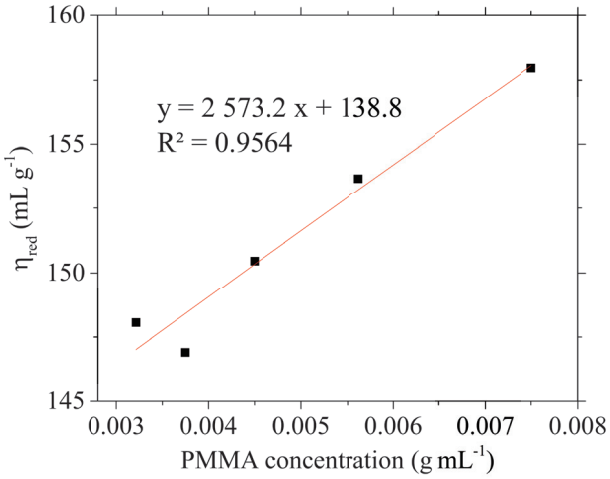

Figure C.1: Calculation of the intrinsic viscosity from experimental data by linearisation of the Huggins equation.

Figure C.2

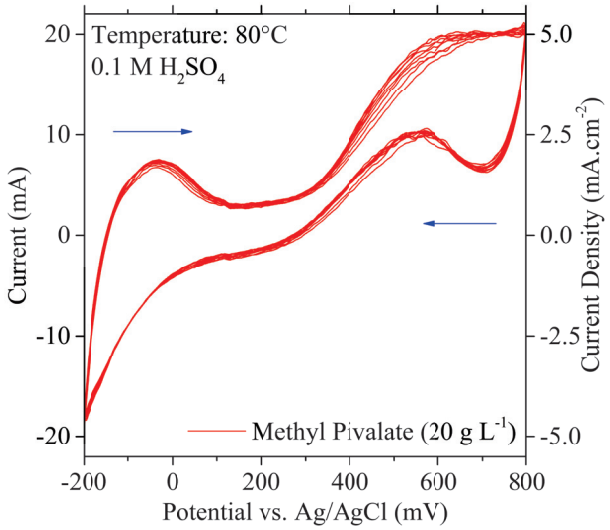

Figure C.2: Electro-oxidation of methyl pivalate (MP, 20 g L^{-1}) in a three-electrode cell arrangement: Complete cyclic voltammetry (0.1 M H_2SO_4, from -200 to 800 mV, scan rate 10 mV s^{-1}, 10 cycles, 80 °C).

References

[1] Waterhouse, G.I. and Waterland, M.R. Opal and inverse opal photonic crystals: Fabrication and characterization. *Polyhedron*, 26:356–368, 2007. doi: 10.1016/j.poly.2006.06.024.

[2] Sordello, F., Duca, C., Maurino, V. et al. Photocatalytic metamaterials: TiO2 inverse opals. *Chemical Communications*, 47:6147–6149, 2011. doi: 10.1039/c1cc11243k.

[3] Mori, S. and Barth, H.G. *Size exclusion chromatographie*. Springer-Verlag GmbH, Berlin, Heidelberg, 1 edition, 1999. doi: 10.1007/978-3-662-03910-6.

[4] Flory, P.J. *Principles of Polymer Chemistry*. Cornell University Press, Ithaca, New York, 1953.

[5] Provencher, S.W. Contin: A general purpose constrainded regularization program for inverting noisy linear algebraic and integral equations. *Computer Physics Communications*, 27:229–242, 1982. doi: 10.1016/s0010-4655(84)82935-5.

[6] Grimaldos-Osorio, N., Sordello, F., Passananti, M. et al. From plastic-waste to H2: A first approach to the electrochemical reforming of dissolved Poly(methyl methacrylate) particles. *International Journal of Hydrogen Energy*, pages 1–15, mar 2022. doi: 10.1016/j.ijhydene.2022.02.229.

[7] Bard, A.J. and Faulkner, L.R. *Electrochemical methods: Fundamentals and Applications*. John Wiley & Sons, Inc., 2nd edition, 2001.

[8] Grimaldos-Osorio, N., Sordello, F., Passananti, M. et al. From plastic-waste to H2: Electrolysis of a Poly(methyl methacrylate) model molecule on polymer electrolyte membrane reactors. *Journal of Power Sources*, 480:228800, 2020. doi: 10.1016/j.jpowsour.2020.228800.

[9] Fitch, R.M. *Polymer Colloids: A Comprehensive Introduction*. Elsevier Ltd., 2014. doi: 10.1016/B978-0-12-257745-1.X5000-7.

[10] Tielemans, M., Roose, P., De Groote, P. et al. Colloidal stability of surfactant-free radiation curable polyurethane dispersions. *Progress in Organic Coatings*, 55(2):128–136, 2006. doi: 10.1016/j.porgcoat.2005.08.010.

[11] Ottewill, R. Stability of Polymer Colloids. In Asua, J., editor, *Polymeric Dispersions: Principles and Applications*, pages 31–48. Springer, Dordrecht, 1997. doi: 10.1007/978-94-011-5512-0_3.

[12] Shi, R., Liu, K.S., Liu, F. et al. Electrocatalytic reforming of waste plastics into high value-added chemicals and hydrogen fuel. *Chem. Commun.*, 57:12595–12598, 2021. doi: 10.1039/D1CC05032J.

[13] Zhou, H., Ren, Y., Li, Z. et al. Electrocatalytic upcycling of polyethylene terephthalate to commodity chemicals and H2 fuel. *Nature Communications*, 12(4679):1–9, 2021. doi: 10.1038/s41467-021-25048-x.

[14] Smets, G. and De Loecker, W. Reaction kinetics and tacticity of macromolecules. I. Methacrylic acid—ester copolymers. *Journal of Polymer Science*, 45:461–467, 1960. doi: 10.1002/pol.1960.1204514615.

[15] Smets, G. and Van Humbeeck, W. Reaction Kinetics and Tacticity of Macromolecules. II. Acrylic Acid Copolymers. *Journal of Polymer Science*, 1:1227–1238, 1963.

[16] Ali, U., Karim, K.J.B.A. and Buang, N.A. A Review of the Properties and Applications of Poly (Methyl Methacrylate) (PMMA). *Polymer Reviews*, 55:678–705, 2015. doi: 10.1080/15583724.2015.1031377.

[17] Smets, G. and de Loecker, W. Alkaline hydrolysis of methacrylic acid–ester copolymers. *Journal of Polymer Science*, 41:375–380, 1959. doi: 10.1002/pol.1959.1204113831.

[18] Anantakrishnan, S.V. and Krishnamurti, S. Kinetic studies in ester hydrolysis. *Proceedings of the Indian Academy of Sciences - Section A*, 14(3):270–278, 1941. doi: 10.1007/BF03046068.

[19] Semen, J. and Lando, J. The Acid Hydrolysis of Isotactic and Syndiotactic Poly (methyl methacrylate). *Macromolecules*, 2(6):570–575, 1969. doi: 10.1021/ma60012a003.

[20] Hori, T., Kobayashi, K., Teranishi, S. et al. Fuel cell and electrolyzer using plastic waste directly as fuel. *Waste Management*, 102:30–39, 2020. doi: 10.1016/j.wasman.2019.10.019.

[21] Pérez-Rodríguez, S., Pastor, E. and Lázaro, M. Electrochemical behavior of the carbon black Vulcan XC-72R: Influence of the surface chemistry. *International Journal of Hydrogen Energy*, 43:7911–7922, 2018. doi: 10.1016/j.ijhydene.2018.03.040.

[22] Raghuveer, V. and Manthiram, A. Mesoporous Carbons with Controlled Porosity as an Electrocatalytic Support for Methanol Oxidation. *Journal of The Electrochemical Society*, 152(8):A1504–A1540, 2005. doi: 10.1149/1.1940767.

[23] Czechowska-Biskup, R., Wach, R.A., Rosiak, J.M. et al. Procedure for determination of molecular weight of chitosan by viscometry. *Progress on Chemistry and Application of Chitin and its Derivatives*, XXIII:45–54, 2018. doi: 10.15259/PCACD.23.04.

CHAPTER 5

From plastic-waste to H_2: Study of the electro-reforming of Poly(ethylene glycol) solutions

From plastic-waste to H_2: Study of the electro-reforming of Poly(ethylene glycol) solutions

5.1 Introduction

The first chapters of this work were devoted to the study of the electro-oxidation of PMMA from various approaches. As explained in the introduction section, the investigation of other polymeric materials with different chemical structures will allow to deepen and expand the use of the electrochemical technologies for hydrogen production. This chapter deals with the electro-oxidation (electro-reforming) of ethylene glycol (EG) and polyethylene glycol (PEG) of different molecular masses. As discussed in the state-of-the-art chapter, PEG (H—(O—CH_2—CH_2)$_n$—OH) is a linear polymer usually produced by polymerisation of ethylene oxide with a hydroxyl initiator [1]. PEG is water soluble and has a large range of applications going from anti-freezing/ lubricant agent to the extraction of heavy metals, as well as in the medical and pharmaceutical industry [2–4]. The physicochemical properties of PEG evolve with its molecular weight (Mw), a value that can go from the few hundreds to millions of Da (1 Da = 1 g mol^{-1}) [1]. The global annual production of PEG is in the order of hundreds of thousands of tons, with an increasing tendency during the last years [5, 6]. Due to its wide variety of applications, PEG is commonly found in urban and industrial water effluents, and concern has been raised about the true fate of these polymers in the environment. Therefore, the studies dealing with their biodegradability have increased in recent years [6–9].

The electro-oxidation of EG has been explored in several previous studies [10–18], mainly because of its possible use in direct alcohol fuel cells (DAFC), with many advantages as a high boiling point and energy density, as well as a lower toxicity and well established supply chain (compared to methanol) [19]. Another important advantage is that EG can be produced from biomass by a variety of processes [20–22], representing a potential bio-sourced hydrogen carrier. On the other hand, just a few studies have been published on the electrochemical behaviour of PEG, mainly regarding the use of this type of macromolecules as an additive in metal electrodeposition processes [23–26]. Using EG and PEG in the present chapter is a strategic choice. The idea is to benefit from their structural and chemical properties in order to further understand the electro-oxidation mechanisms that C–O bond-containing polymers could undergo at low temperature. One of the most significant advantages of the molecules proposed in this chapter compared to previous chapters is that both EG and PEG are soluble in water, on account of their high polarity that increases the hydrophilicity [1]. This would allow us to avoid

potentially the issues related to the accumulation and mass transport noticed for the previously reported studies with PMMA. For this purpose, aqueous solutions of these compounds will be studied by using an experimental setup similar to the one used in Chapter 2 (methyl pivalate electrolysis in a Polymer Electrolyte Membrane reactor). Briefly, a proton exchange membrane (PEM) reactor has been utilised for the electro-reforming of PEG. As previously discussed, this type of systems allows the separation of the anodic and cathodic semi-reactions, leading to the separation of the reaction products and hence facilitating the analysis of such products.

In this chapter, two electrodes have been investigated, both based on Pt/C catalysts but with different nanoparticles dispersion and size. Additionally, products of the anodic compartment were analysed by Size-Exclusion Chromatography (SEC). In parallel, it was possible to online monitor the production of pure hydrogen in the cathodic compartment through mass spectroscopy (MS). Consequently, it has been possible to determine that PEG chains can undertake its electro-oxidation either by the terminal groups of the polymeric chains or at random sites thereof. This phenomenon may be especially influenced by how the compound reaches the active site of the catalyst. Finally, despite an important improvement in the general activity of the anode and weak contribution of transport limitations, the electro-oxidation of polymers can be affected by strong adsorption of species on the Pt active sites. Even if this final work is still an approach in a very early stage of development for the treatment of plastic waste by electrochemical means, our results could be considered as an important step-forward to clarify the type of polymers that could be valorised by this technology. As it has been confirmed by other previously published researches [27–29], the nature of the polymer is the key. The existence of chemical bonds easy to oxidise in the main chain could be the key factor to treat plastic-wastes in low temperature electrochemical devices.

5.2 Experimental

A Polymer Exchange Membrane (PEM) electrolysis cell (Dioxide Materials®) was used, like the one depicted in Figure 2.1. The cathode was a commercial electrode material in all cases, composed of a Pt/C catalyst impregnated on a carbon cloth gas diffusion layer with a Nafion® coating to assure proton conductivity (5.3 cm^2, 0.2 mg cm^{-2} of 20% wt. Pt supported on C_{vulcan}, FuelCellStore®). Two different anodic catalysts were employed: a home-made material (20% wt. Pt supported on C_{vulcan}), and a commercial one (20% wt. Pt supported on C_{black}, HiSPEC® 3000, Alfa Aesar). The homemade Pt/C catalyst was prepared by using the well-known polyol method, similarly as described in Section 3.2 [29]. $Pt(NH_3)_4(NO_3)_2$ (Sigma Aldrich) was

used as metal precursor, ethylene glycol (CarlROTH) served as a reducing agent, NaOH (NORMAPUR) was used to adjust the pH while carbon Vulcan XC-72 (Fuel Cell Store®) was the catalytic support. The Pt precursor (389.9 mg) was mixed and stirred with ethylene glycol (50 mL) in a beaker until complete dissolution. The pH was adjusted to a value of 9 by adding NaOH 0.2 M drop by drop, and then the mixture was heated until 190 °C under continuous stirring for 2 h. After cooling to room temperature, the mesoporous carbon support (800 mg) was introduced and further stirred at room temperature for 48 h. The synthesis product was filtered and washed with 1 L of distilled water, and was finally dried at 80 °C in a static air furnace.

To deposit the catalysts onto the carbon paper Gas Diffusion Layer (GDL), we have prepared inks which were obtained from the dispersion of the correct amount of the powdered material for 2 h under sonication (Bandelin - Sonorex Digitec, DT 255 H, Ultrasonic nominal power: 160 W) in 10 mL of 2-propanol (HPLC-isocratic grade, Carlo Erba Reagents) together with the right proportion of Nafion® perfluorinated resin solution (5% wt. in lower aliphatic alcohols and water, Sigma-Aldrich). The Nafion®/catalyst mass proportion was optimised in this study. To produce the anode material, the Nafion®/catalyst ink was deposited by spray-coating (using nitrogen as a dispersion medium) on carbon paper GDL of different thickness (AvCarb MGL190/280/370, FuelCellStore®, see Table 5.1 for details and Figure D.1 for the microscopy characterisation) under heating at 80 °C to produce the home-made Pt/C electrodes (5.3 cm^2) with a final catalyst loading of 1 mg cm^{-2}. Carbon papers are composed of overlapped carbon fibres with large pores of few μm between the fibres. Both the home-made and commercial catalyst inks were deposited using the same protocol, and it is expected to have a higher concentration of ionomer and catalyst at the anode's surface than in the bulk (as represented in Figure 5.1) as the ink did not fully penetrate into the whole volume of the GDL. A Nafion™ 117 membrane was used as a proton-conducting membrane (183 μm thickness, FuelCellStore®). Before use, the membrane was pre-treated by immersion at 100 °C for 2 h in 3 different solutions: 150 mL of 3% wt. H_2O_2, then 150 mL of 0.5 M H_2SO_4, and finally 150 mL of deionized water. The Membrane Electrode Assembly (MEA, anode/membrane/cathode) was prepared without prior pressing directly in the PEM cell with the help of two Teflon gaskets (thickness: 0.01 in, FuelCellStore®), which also ensure the correct sealing of the cell. The anode's face where the Nafion®/catalyst ink was deposited was in direct contact with the ionomeric membrane, as shown in Figure 5.1. A temperature control system and reactants/products flasks for anodic and cathodic compartments were put in place.

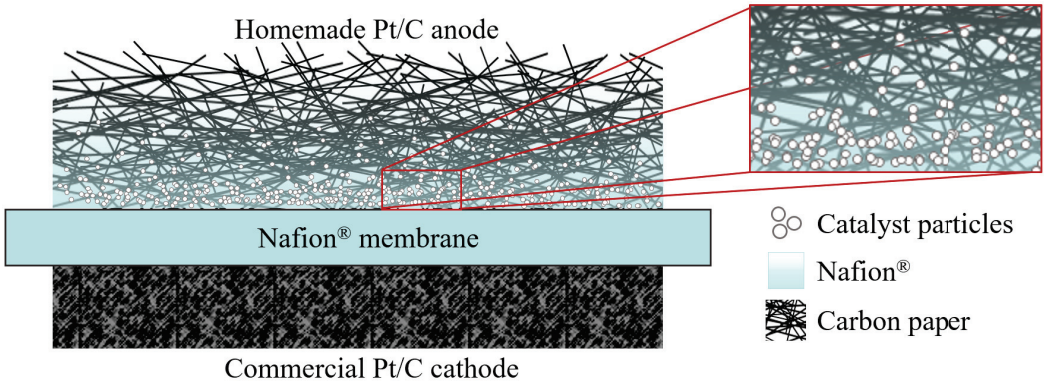

Figure 5.1: Schema of the Membrane Electrode Assembly (MEA) conformation (zoom on the anode zone near the Nafion® membrane).

Table 5.1: Carbon paper Gas Diffusion Layer (GDL) characteristics (reported by the supplier, FuelCellStore®).

Carbon paper GDL	Thickness (μm)	Bulk density (g cm^{-3})	Porosity (%)
MGL190	190	0.44	78
MGL280	280	0.44	78
MGL370	370	0.46	78

Ethylene glycol (EG, Reagent Plus®, ≥99% purity) and polyethylene glycol of different molecular weights (PEG, for synthesis, 200/400/1000/4000 g mol^{-1}) were purchased from Sigma-Aldrich. For the electro-oxidation experiments, aqueous solutions of EG or PEG (50 mL, 1-20 g L^{-1}, continuous stirring at 1000 rpm, liquid flow of 1.7 mL min^{-1}) and deionised water (50 mL, liquid flow of 1.7 mL min^{-1}) were fed in recirculation to the anodic and cathodic compartments, respectively. A peristaltic pump assured the constant liquid flow rates. The system was stabilised for 30 min before each electrochemical experiment to guarantee reproducible temperature conditions. The polarisation of the PEM cell assembly was performed with a potentiostat-galvanostat equipment (Origalys®). A variety of electrochemical experiences was performed at different temperatures, mainly cyclic voltammetries (CV, 0 – 1100 mV, scan rate: 10 mV s^{-1}, 10 cycles) and chrono-amperometries (CA, fixed potentials: 700, 800, 900, or 1000 mV, for 1 – 5 h).

The characterisation of the home-made electrode materials was performed by different techniques. The nanostructure of the catalyst was observed by high-resolution transmission electron microscopy (TEM) with a JEOL 2010 LaB6 instrument with 200 kV acceleration voltage, while its morphology was obtained by scanning electron microscopy (SEM) images with a Hitachi TM-1000 Tabletop Microscope. Optical microscope imagery was performed with a Keyence VHX-6000. The platinum metal loading was analysed twice for every sample, after chemical

attacking the catalyst samples with sulfuric acid and nitric acid at 350 °C, by optical emission spectrometry in an ICP-OES 5800 Agilent equipment.

The analysis of the products in the anodic liquid flow was made by Size-Exclusion Chromatography (SEC), carried out on a triple detection set from Viscotek - Malvern Instrument. The system is equipped with a refractometric detector, static light scattering RALS (90°) and LALS (7°) and a viscometer detector. The whole equipment is thermostated at 35 °C. A PC controls the assembly and reprocesses the results using the OmniSEC v4.7 software from Malvern Instrument. The set of employed columns comprises a pre-column (PLgel Olexis Guard 7.5x50mm) followed by three columns mounted in series (PLgel Olexis Guard 7.5x300mm) whose mass range covers from 500 to 2,000,000 (PS). The mobile phase is tetrahydrofuran (THF) at a flow rate of 1 mL min^{-1}. The samples are injected through a 100 μL loop and filtered online before separation on the columns. The calibration used here is a conventional calibration in PEG equivalent.

Additionally, the hydrogen purity and production at the cathode was online monitored with a quadrupole mass spectrometer (Portable Quadrupole MS, Aspec). The QMS operates with a high vacuum of around $1.7x10^{-6}$ mbar, evacuated by a 70 L s^{-1} turbo molecular drag pump combined with a backing pump. The relative molecular concentrations of different compounds, such as H_2 (m/z = 2 amu), H_2O (18 amu), N_2 (28 amu), O_2 (32 amu), and CO_2 (44 amu) were monitored. The gas out-stream in the cathodic vessel was mixed with a constant flow of inert gas (N_2, 70.6 mL min^{-1}) and further introduced into the QMS device. The H_2 trend was analysed and expressed in volumetric flow with the help of a calibration curve from an external H_2 source of known composition (2 and 5% v/v in N_2).

5.3 Results and discussion

5.3.1 Anode materials preparation

A series of anode materials were prepared for the present work. In order to make easier the comprehension of the electrochemical experiments, a table with the coded name and the characteristics of each one of the electrodes is presented here (Table 5.2). As it will be further explained, different factors were studied, as the proportion of Nafion®/catalyst in the ink, the thickness of the electrode, and the employed catalyst. The reasons for the different modifications, as well as the characterisations performed on each of the anode formulations, will be presented and further discussed along with the electrochemical experiences. Table 5.2 is presented as a guide for the reader.

Table 5.2: Formulation of the different anode materials used through the present study.

Anode code	Employed catalyst	Nafion charge (mg cm^{-2})	Nafion : Catalyst proportion (mg : mg)	Carbon paper GDL
PtCv-1-10	Pt/C_{vulcan} (HM)	1	1 : 1	MGL280
PtCv-1-05	Pt/C_{vulcan} (HM)	0.5	0.5 : 1	MGL280
PtCv-1-01	Pt/C_{vulcan} (HM)	0.1	0.1 : 1	MGL280
PtCv-1-00	Pt/C_{vulcan} (HM)	0	0 : 1	MGL280
PtCv-2-01	Pt/C_{vulcan} (HM)	0.1	0.1 : 1	MGL190
PtCv-3-01	Pt/C_{vulcan} (HM)	0.1	0.1 : 1	MGL370
PtCcom-2-01	Pt/C_{black} (COM)	0.1	0.1 : 1	MGL190

HM: Home-made, COM: Commercial

5.3.2 Electro-oxidation of EG in PEM reactor and preliminary experiences with PEG

Initially, we investigated the electro-oxidation of ethylene glycol (EG), a molecule that presents the same chemical units and bonds as polyethylene glycol (PEG), on a home-made anode prepared similarly as described in Chapter 3 [29] (PtCv-1-00, see Table 5.2). Some initial experiments were performed in order to establish a departure point for this study (cyclic voltammetries from 0 – 1100 mV, 10 cycles, 10 mV s^{-1}), during which we observed a delamination of the catalytic coating. Therefore, the Nafion® solution was added to the ink formulation to act as a binder, which indeed is also expected to enhance the proton conductivity at the three-phase boundaries [30, 31]. The above mentioned catalyst detaching from the GDL was first detected at high temperatures (T >60 °C) and high concentrations of EG/PEG (>10 g L^{-1}), probably as a consequence of the mechanical constraints suffered by the electrodes in a PEM cell configuration. To improve the adhesion of the catalytic layer, the ink was prepared with the same loading of catalyst and Nafion® (1 mg cm^{-2}), as previously reported in literature [32, 33]. The ink was then dispersed on a carbon paper GDL of 280 μm, to produce the anode that will be studied in the following experiments (PtCv-1-10, see Table 5.2). The applied cell potentials used though this work were always below the thermodynamic potential required for the Oxygen Evolution Reaction (OER, Vcell = 1.23 V vs NHE), as shown in Figure 5.2 for a cyclic voltammetry (CV) blank experiment in presence of distilled water. The main features of this CV could be attributed to the oxidation/reduction of H_{ads} (applied potential <0.4 V vs. NHE) and O_{ads} (applied potential >0.6 V vs. NHE) at the electro-catalyst surface [34]. Considering that most organic molecules can be (in theory) electro-oxidised at lower thermodynamic potentials than OER, the energy requirements of this technology should be lower than that of the electrolysis of water [35].

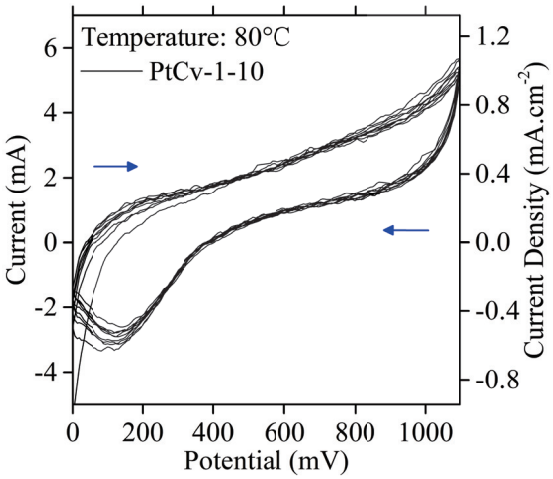

Figure 5.2: Electrochemical performance of the PtCv-1-10 anode in presence of distilled water in a PEM cell. (Temperature = 80 °C, cyclic voltammetry from 0 to 1100 mV, scan rate 10 mV s^{-1}, 10 cycles).

Firstly, we studied the effect of the EG concentration (C_b) and temperature on the overall electrochemical performances of the PEM cell, as shown in Figure 5.3. The effect of the EG concentration was studied through CV experiments (Figure 5.3a). Even though all the experiments followed the same trend, the obtained currents are importantly affected by the EG concentration. The onset potential in all cases was ∼500 mV. Remarkably, the current was higher during the backward scan than during the forward scan. This seems to indicate that the first electro-oxidation step during the forward scan is kinetically limited at this scan rate and continues during the backward scan, generating therefore higher currents. Similar phenomena were observed during the electro-oxidation of several alcohols, including ethanol and glycerol [14, 36–39]. It is also important to note that even for the lowest EG concentration, higher currents are registered compared to that of the blank experiment with distilled water (Figure 5.2), confirming that the electro-oxidation of EG is thermodynamically favoured in this range of electrical potentials.

As the obtained current increased with the applied potential, it can be assumed that the overall oxidation process is favoured by applying the highest possible potential. In that case, one could go further into the analysis of the system by performing some calculations. By taking the current at 1100 mV, it is possible to calculate the theoretical hydrogen production rate from the Faraday's Law (Eq. (5.1)), where j_p is the current density reached upon polarisation, n is the number of transferred electrons (2 in this case), and F is the Faraday's constant.

$$r_{H_2} = \frac{j_p}{nF} \tag{5.1}$$

Considering that the PEM cell works in recirculation mode, it can be approximated

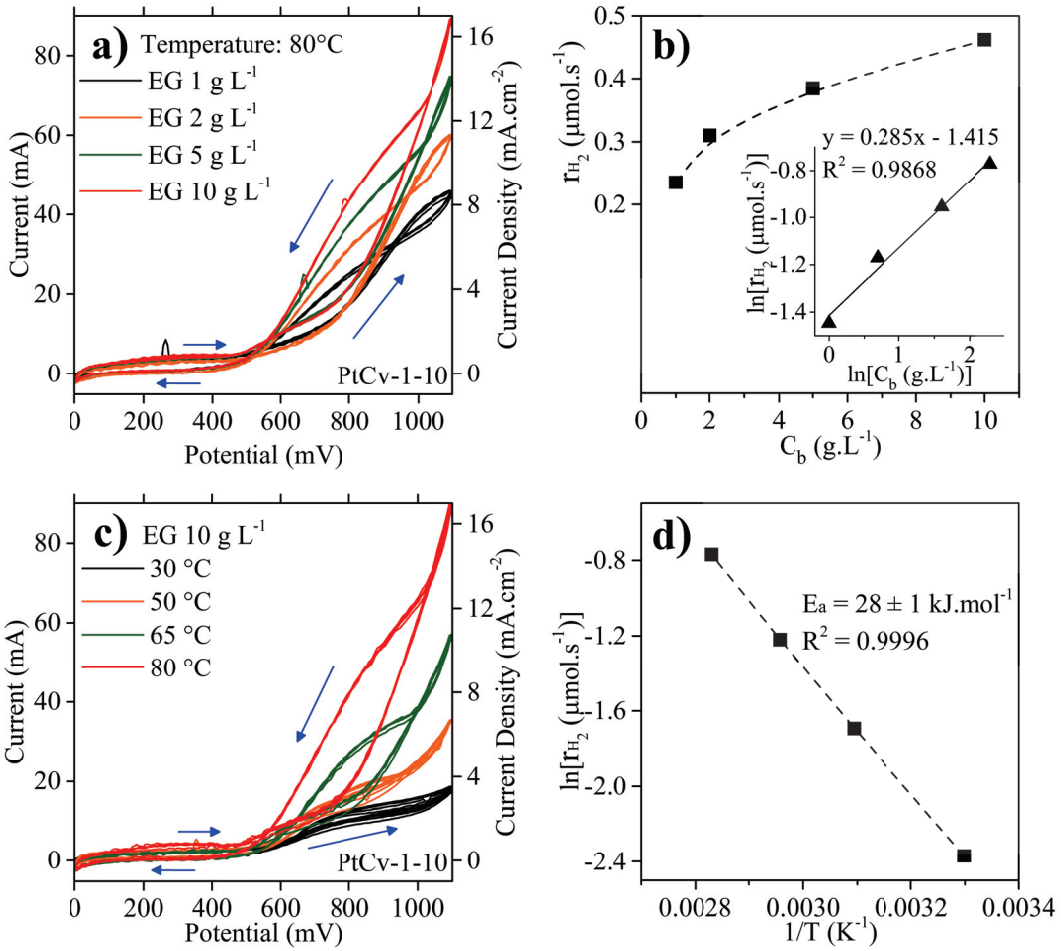

Figure 5.3: Effect of the EG initial concentration (C_b) and the reaction temperature on the EG electro-oxidation in a PEM cell: a) CVs with different C_b, b) Influence of C_b on the H_2 production and reaction order calculated from a) at 1100 mV (inset), c) CVs at different temperatures, d) Arrhenius plot: $ln(r_{H_2})$ vs. $1/T$ and activation energy calculated from c) at 1100 mV. (Cyclic voltammetries from 0 to 1100 mV, scan rate 10 mV s^{-1}, 10 cycles, plotted only 2nd, 4th, 6th, 8th and 10th cycles).

to a batch system, where the overall rate law can be simplified as follows [40, 41]:

$$r_{H_2} = kC^a_{H_2O}C^n_b = k_{obs}C^n_b \tag{5.2}$$

Where k is the rate constant, C_{H_2O} and C_b are the initial H_2O and EG concentrations (the species involved in the anodic reactions), a and n are the respective apparent reaction orders. Assuming an almost constant water concentration because of the excess in the aqueous solution, k_{obs} comprises the rate constant, together with the concentration of water. Then, by performing the calculation from Eq. (5.1), it becomes possible to plot r_{H_2} vs. C_b (Figure 5.3b). Thus, Eq. (5.2) could be linearised to produce a line with the form $ln(r_{H_2})$ vs. $ln(C_b)$ that leads to the reaction order (inset of Figure 5.3b). We found a value of $n \approx 0.285$, in agreement with values previously reported for the electro-oxidation of EG on noble metal-based electrodes

(0.2 – 0.4) [14]. An apparent reaction order near 1 was obtained in our previous study dealing with the electro-oxidation of methyl pivalate on a Pt-based electrode [41]. A lower apparent reaction order for EG probably indicates that there is a competitive adsorption between EG and intermediate species on the catalyst active sites at the selected potential of 1100 mV. Another possibility is the influence of the O_{ads} species at this potential, but it is less likely due to the low currents registered during the blank experiment with distilled water (Figure 5.2). One could think that similar issues would be found for higher molecular weight compounds (e.g. PEG).

On the other hand, as observed in Figure 5.3c, the temperature mainly affects the behaviour of the electrochemical system above 500 mV, i.e., after the onset potential. This suggests that this applied potential corresponds to the thermodynamic potential necessary for the first electro-oxidation step. However, the temperature increase considerably improves the kinetics. In addition, it is well known that the proton conductivity of the Nafion® membrane is also favoured by the increase of temperature over that range [42]. In order to go further on the basic kinetic parameters of the electro-oxidation of EG, the activation energy of the system can be calculated by taking the electrical current values at 1100 mV by the Arrhenius equation (Eq. (5.3)).

$$k = Ae^{(-E_a/RT)} \tag{5.3}$$

Where k is the rate constant, A is a pre-exponential factor, E_a is the activation energy, T is the temperature, and R is the gas constant. By combining Eq. (5.2) and (5.3), and knowing the hydrogen production rates calculated from Eq. (5.1) for each temperature at 1100 mV, it is possible to obtain an Arrhenius plot ($ln(r_{H_2})$ vs. $1/T$). Figure 5.3d shows the corresponding linearisation of the data, resulting in an activation energy of 28 ± 1 kJ mol^{-1}. E_a values of 18 kJ mol^{-1} have been reported in literature for the electro-oxidation of EG in a PEM system over Pt/C-based electrodes at 700 mV [16, 17]. In their studies, Stuve and Spies attribute this low E_a value to the initial steps of the electro-oxidation of EG (production of glycolaldehyde and glycolic acid), but they also point out that Ea can reach 43 kJ mol^{-1} for the final steps involving the production of CO_2 from CO. The EG electro-oxidation mechanism is complex and several intermediate reactions and paths are involved, which of course, could be affected by the reaction temperature. The general anodic EG electro-oxidation proposed by the same authors can be found in Eq. (5.4) [16, 17], but a more detailed and mechanistic path is also proposed. The anodic semi-reaction is completed by the cathodic hydrogen evolution semi-reaction (Eq. (5.5)).

$$Anode: C_2H_6O_2 + (2-x)H_2O \rightarrow C_2H_yO_{4-x} + (10-2x-y)(H^+ + e^-) \tag{5.4}$$

$$Cathode: (10-2x-y)(H^+ + e^-) \rightarrow (5-x-y/2)H_2 \tag{5.5}$$

Depending on the reaction conditions, *x* and *y* could take a variety of values that finally represent all the partial oxidation products of EG, which includes glycol aldehyde ($C_2H_4O_2$), glycolic acid ($C_2H_4O_3$), oxalic acid ($C_2H_4O_4$), glyoxal ($C_2H_2O_2$), and glyoxylic acid ($C_2H_2O_3$) [10, 11, 16, 17]. The complete oxidation of 1 molecule of EG would produce 2 molecules of CO_2, as well as 10 protons that would be reduced at the cathode to produce 5 molecules of H_2 [12]. The activation energy found here is placed between the two values reported in the literature. Considering previous studies dealing with the electro-oxidation of EG in the same range of applied potentials and reaction temperatures, one could assume that, under our employed conditions, the overall reaction entails the generation of a combination of all the above-mentioned reaction products, as well as a certain fraction that goes until carbon dioxide. In fact, the production of CO_2 is probable, as it was witnessed the presence of gas bubbles in the outlet of the anodic chamber under high applied potentials. To draw a better picture of the reaction path followed in our system, a series of chrono-amperometries (CA) was performed at different applied potentials.

Figure 5.4 shows the CAs at 80 °C under applied potentials of 700, 900 and 1100 mV with an initial EG concentration of 10 g L^{-1}. The experiment at 700 mV can be directly compared with the one reported in literature with a similar PEM configuration [16], where is reported a current density of ∼10 mA cm^{-2} for an anode with a Pt loading of 4 mg cm^{-2} after less than 1 min of stabilisation (∼2.5 mA mg_{Pt}^{-1}). This value is near to the one found in this study of ∼2 mA cm^{-2} (or ∼2 mA mg_{Pt}^{-1}). The same authors reported the production of glycol aldehyde, glycolic acid and oxalic acid as liquid products, as well as a high production of CO_2 (∼70% of the total mass products), measured by high performance liquid chromatography (HPLC) and mass spectrometry (MS), respectively. The application of higher potentials is expected to enhance the production of CO_2. As observed, when a potential of 900 mV was applied, the current achieved values of around 7 mA cm^{-2} with a gradual slow decrease starting after 1 h polarisation. For an applied potential of 1100 mV, higher currents were registered (>8 mA cm^{-2}), but no stabilisation was found. Instability of the system at potentials over 900 mV can be related with the Pt poisoning by CO_{ads} or other reaction intermediates, as already reported for Pt-based and other noble metals employed for the electroforming of EG [12–14, 16, 17]. This behaviour is especially noticeable in the case of 1100 mV, but also detectable at 900 mV after 1 h of experience. Eventually, the oxidation of Pt might contribute to such deactivation phenomenon, as evidenced for the electro-oxidation of other small organic molecules at potentials over 800 mV [29, 36].

The experiments performed with EG could allow to better understand the performance of the proposed electrochemical system for the electro-oxidation of PEG.

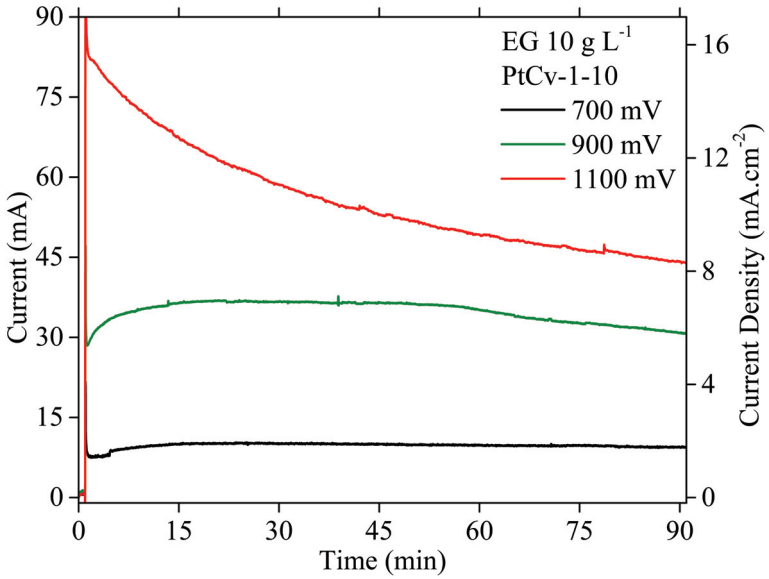

Figure 5.4: Effect of the applied potential on the performance for EG electrolysis in a PEM cell (Temperature = 80 °C, C_b = 10 g L^{-1}, chrono-amperometries at different applied potentials for 90 min).

Hence, a first series of electrochemical experiments was carried out aiming for the PEG electrolysis, by using the same MEA formulation as the one used for EG. As it was seen that the electro-oxidation of EG was enhanced with the temperature, such a parameter was fixed at 80 °C. Figure 5.5 shows some initial findings about the impact of the concentration and the molecular weight of PEG on the overall electrochemical performances. However, higher PEG concentrations were used compared to EG, on account of the slight impact of that variable at low values. The following conclusions could be obtained from these experiments:

(i) PEG with low molecular weights (≤400 g mol^{-1}) can be electro-oxidised and the concentration of PEG affects the overall electrochemical performance similarly than it does for EG, since higher currents are produced at higher PEG concentrations. One can assume that no transport limitations are taking place for these small macromolecules.

(ii) CVs profiles are different between PEG200 and PEG400, suggesting different reactions paths.

(iii) Lower currents are produced for the same range of applied potentials compared with EG, meaning a more sluggish electro-oxidation process.

(iv) Molecular weights over 1000 g mol^{-1} seriously hinder the electro-oxidation of the macromolecules, as noticed from the very low current densities for Figure 5.5c-d.

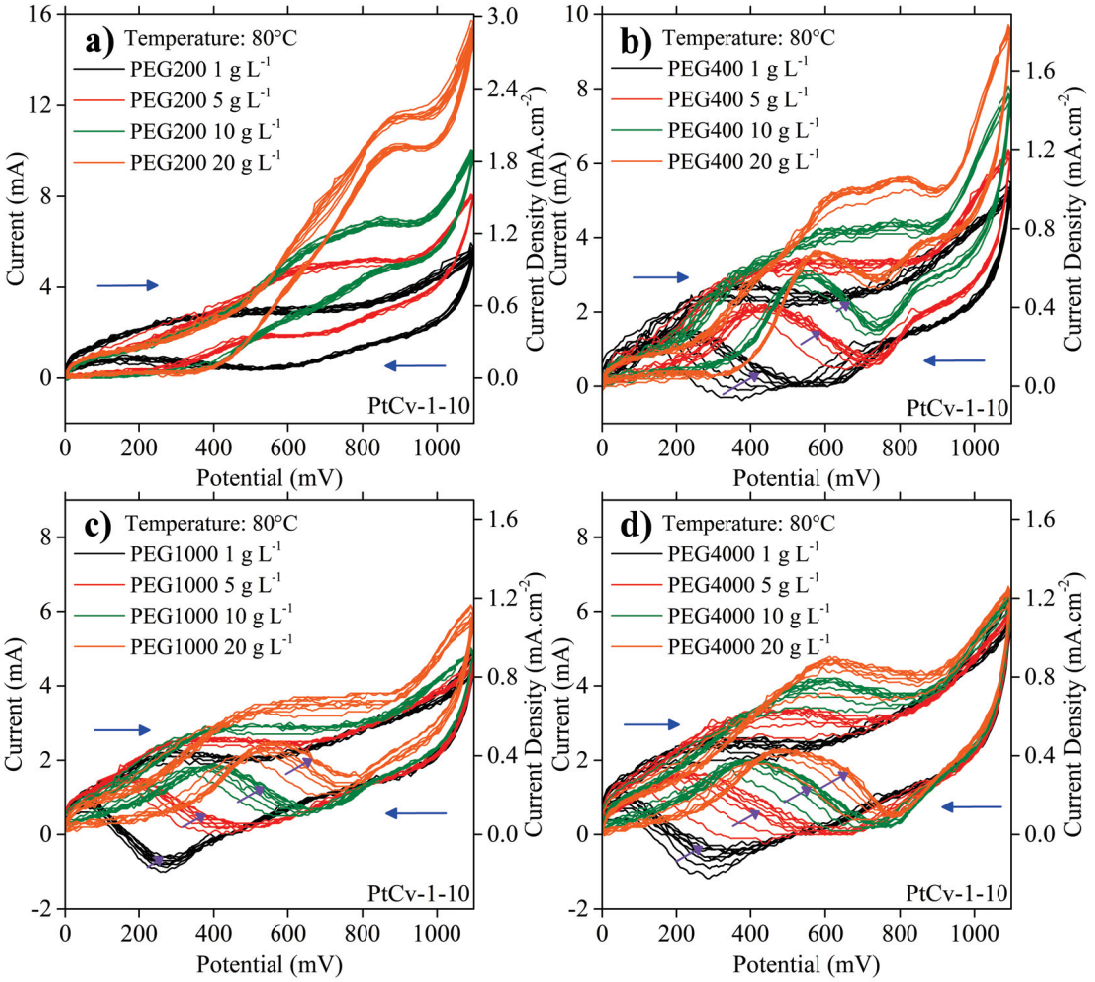

Figure 5.5: Effect of the initial concentration (C_b) and the molecular weight (M_w) on the PEG electrolysis in a PEM cell: a) PEG200, b) PEG400, c) PEG1000, and d) PEG4000. (Temperature = 80 °C, cyclic voltammetries from 0 to 1100 mV, scan rate 10 mV s^{-1}, 10 cycles).

In view of these conclusions, it seems evident the need to optimise the formulation and physicochemical properties of the anode in order to avoid further limitations for the bigger macromolecules. In this sense, the following section describes the optimisation process to develop a more suitable electrode formulation aiming to treat the complete series of PEG samples with better performances.

5.3.3 Optimised anode formulation for the PEG electro-oxidation

To enhance the electrochemical activity for the electro-oxidation of PEG, we decided to optimise the adhesion and the coverage of the catalytic layer onto the GDL carbon fibres in order to maximise the PEG solution/active sites interface. To achieve this goal, we varied the catalyst/ionomer ratio in the inks and the thickness of the carbon paper GDL. Two different catalysts were also used to determine the effect of the Pt particle size and dispersion, as well as on the concentration of active Pt

sites. The experiments reported in this section were performed only on PEG1000 solutions, since an important loss of activity became clearer from this molecular weight (Figure 5.5).

Initially, the influence of the Nafion®/catalyst mass proportion was studied to find a compromise between the porosity of the carbon paper GDL and preserving the advantages that the ionomer provides. Figure 5.6 shows CV and CA experiments performed with different electrode formulations prepared over the same carbon paper GDL (AvCarb MGL280) with different Nafion®/catalyst proportions (see Table 5.2 for details). The code notation used for the anodes corresponds to PtCv-1-*yy* (where *yy* refers to the content of Nafion®, as the catalyst charge was kept constant at 1 mg cm^{-2}). In this way, the anode used for the above described preliminary study with EG relates to the PtCv-1-10, and from that point, the content of the ionomer was reduced. The CV experiences depicted in Figure 5.6a seemed to indicate that a lower content of Nafion® in the electrode enhanced the electrochemical performance of the anode, where more pronounced peaks were observed for applied potentials over 450 mV. The case of the formulation without ionomer (PtCv-1-00) illustrates the negative effect of eliminating the ionomer from the anode formulation, probably by strongly decreasing the catalytic layer coverage on the carbon fibres due to the delamination phenomenon above mentioned. In addition, Nafion can also enhance the transport of H^+ through the triple-phase boundaries, leading to higher current production [30, 31]. The best result was accomplished by using 10 times more catalyst than Nafion® (PtCv-1-01). A broad oxidative peak appeared between 600 – 800 mV on both the forward and backward scans, and the maximum current production was obtained at 1100 mV. This could

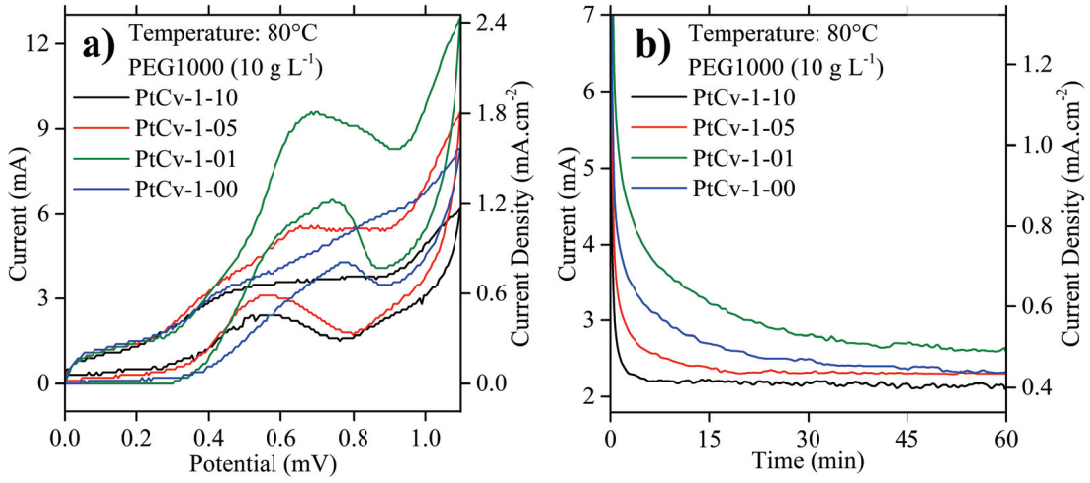

Figure 5.6: Influence of the ionomer (Nafion®) content in the anode for the PEG1000 electrolysis: a) CV experiences (only the 10^{th} cycle), and b) Chrono-amperometries at 1000 mV for 60 min. (Temperature = 80 °C, cyclic voltammetries from 0 to 1100 mV, scan rate 10 mV s^{-1}, 10 cycles).

represent a multistep electro-oxidation process, potentially involving the production of molecules smaller than PEG1000. Afterwards, the stability during longer polarisation time was evaluated at 1000 mV (Nafion®). The anodes with lower content of the ionomer showed higher currents over time (except for that with no ionomer) and took more time to attain stable values. The slow degradation could be attributed to the poisoning of the catalyst, which takes more time for the anode formulations with more availability of exposed active sites. In all the cases, the current densities after 45 min of polarisation were $\leq$0.5 mA cm^{-2}, a value that should be further improved to consider a real application of such electrochemical technology.

To better understand the impact of the Nafion®/catalyst proportion, the morphology of the fresh anodes coated surface (before contact with PEG) was observed by scanning electron microscopy (SEM) (Figure D.2). Please note that we observed the surface of the GDL, where the ink was sprayed. These images showed the major effect of the ionomer on the anode morphology and porosity, and a possible representation of the anode's section can be found in Figure 5.7. The two formulations richer in ionomer (PtCv-1-10 and PtCv-1-05, Figure 5.6a) barely presented available paths for the PEG to penetrate through the anode's bulk volume, as the pores between the carbon fibres were mostly blocked by the Nafion®/catalyst coating. The fact of having this dense coating could hinder the activity for two reasons: *(i)* a high number of catalyst particles are completely covered by the ionomer, making impossible for the PEG to reach the active sites, and *(ii)* the electro-oxidation is more likely to happen in the interface between the anode and the Nafion® membrane, as most of the catalyst is deposited in that face of the anode.

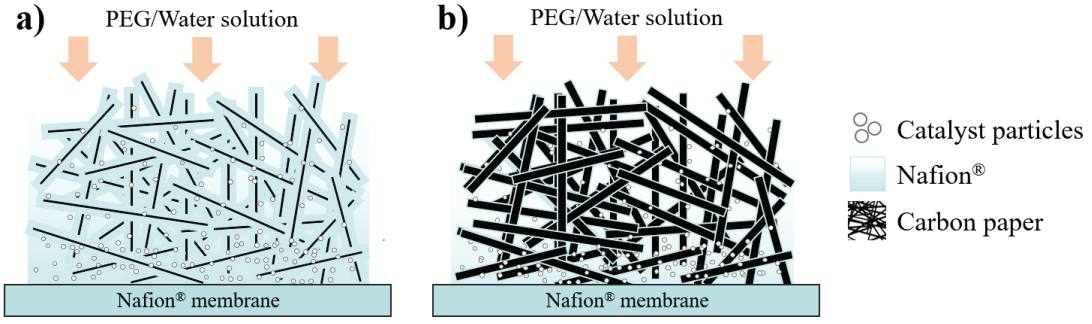

Figure 5.7: Schema of the influence of the Nafion®/catalyst proportion: high (a) and low (b) content of ionomer in the coating.

On the opposite, in the PtCv-1-00 formulation the catalytic layer is deposited on the carbon fibres surface, keeping the original macroporosity (in the order of tens of microns) of the carbon paper GDL, but it also sacrifices the stability that Nafion® provides as a binder between the catalyst and carbon fibres, as well as the enhanced H^+ transport through the triple-phase boundaries. Finally, the anode PtCv-1-01

(represented in Figure 5.7b) offers a better compromise between the macroporosity and the quantity of Nafion®, making more catalyst particles available for the reaction, and it also preserves the advantages of having an ionomer in the coating formulation. As a better performance was registered for this Nafion®/catalyst proportion, it was preserved for the following anode formulations.

The subsequent step was to study the influence of the thickness of the carbon paper GDL. SEM and optical microscopy (Figure D.1) confirm that all the carbon papers are made of overlapped carbon fibres with different thickness and, subsequently, different volumes. Cyclic voltammetries with PEG1000 were performed using the ink with the optimised Nafion®/catalyst mass proportion (0.1 : 1) over three carbon paper GDLs of different thickness (190, 280 and 370 μm). Figure 5.8 depicts the 10 consecutive cycles of each of the CV experiences. A more important difference was expected for the different thickness, but still a slightly better performance was found for the thinner configuration (Figure 5.8a). The electrode PtCv-2-01 helps to achieve the stability in a lesser number of cycles compared with the initial carbon support material (Figure 5.8b). The thicker anode (Figure 5.8c) presented lower currents over the complete range of applied potential. Nevertheless, the small impact of this variable could be attributed to the fact that the ionomer/catalyst coating is deposited to a similar depth in all cases, generating an equivalent bulk activity. The slight improvement of the thinner anode (PtCv-2-01) is possibly explained by the lesser volume that PEG should pass through to reach the active zone. Furthermore, the carbon paper GDL of 190 μm will be employed for the following experiences, as less material is required for this formulation. Observations of the cross-section of the electrodes could be very interested to determine the depth profile of the catalytic deposition in the GDL volume.

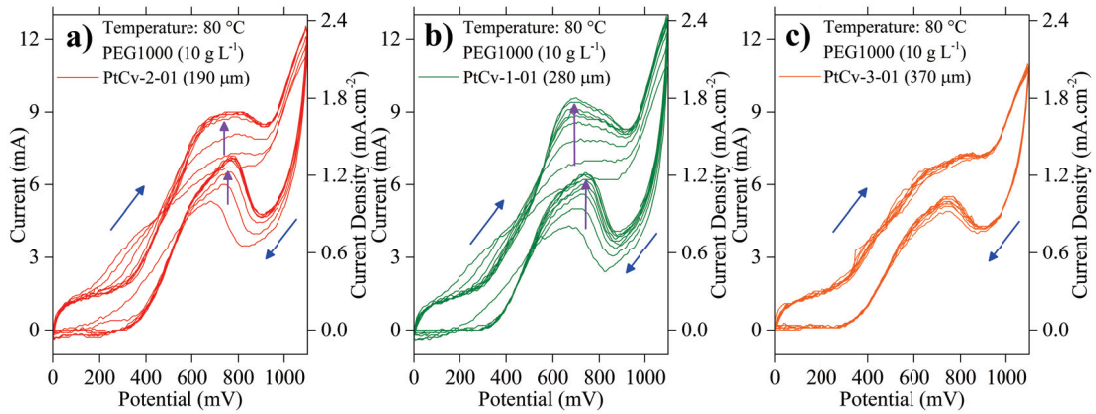

Figure 5.8: Influence of the thickness of the carbon paper GDL on the PEG1000 electrolysis: a) PtCv-2-01 (190 μm), b) PtCv-1-01 (280 μm), and c) PtCv-3-01 (370 μm). (Temperature = 80 °C, cyclic voltammetries from 0 to 1100 mV, scan rate 10 mV s^{-1}, 10 cycles).

The last variable that was modified for the anode formulation was the employed electrocatalyst. In fact, during the previously presented characterisations (Figure D.2), it was possible to see that our homemade catalyst presented a high degree of Pt nanoparticle agglomeration (bright spots in the SEM images). This fact could be detrimental for the overall electrochemical activity, as a better dispersed catalyst assures a higher number and availability of active sites. Subsequently, a commercial catalyst (20% wt. Pt supported on C_{black}, HiSPEC® 3000, Alfa Aesar) was tested. Then, a new anode formulation (PtCcom-2-01) was prepared by using the best performing carbon paper GDL (AvCarb MGL190) and the optimum Nafion®/catalyst mass proportion (0.1 : 1), according to the previous experiments. Low magnification SEM characterisation of the fresh anodes based on the home-made (PtCv-2-01) and the commercial (PtCcom-2-01) catalyst are presented in Figure 5.9, together with transmission electron microscopy (TEM) images at higher magnification of the Pt/C catalyst powders before deposition. The bright spots in Figure 5.9a (SEM) correspond to Pt agglomerates of our homemade catalyst, which cannot be observed in the anode impregnated with the commercial catalyst (Figure 5.9b). Another important feature is the more homogeneous coating of the ionomer/catalyst mixture over the surface of the carbon fibres. This could be attributed to a better dispersion of the catalyst in the ink that was used for the coating, which could be favoured by the nature of the mesoporous carbon used for the commercial catalyst. In fact, an initial idea of the reason for the better ionomer/catalyst deposition over the carbon support GDL can be obtained from the higher magnification TEM images.

The TEM micrographs of the catalyst powders (Figure 5.9c-d) confirmed that Pt nanoparticles (dark spots) are smaller and better dispersed in the case of the commercial catalyst. Average Pt particle diameter was calculated from the TEM images, and it is reported in Table 5.3. Overall, the metallic particle size of the commercial Pt/C_{black} catalyst is around half of the home-made one, and it presents a lower standard deviation, which is related to the more homogenous particle size dispersion (absence of bright spots on the SEM images). From our knowledge, it is likely that the mesoporous black carbon used as support for the commercial catalyst corresponds to Carbon Vulcan XC-72R, one of the most widely employed supports for electrochemical applications (used in around 80% of the electrocatalyst [43]). This support is also known for enhancing the catalyst dispersion [44], which may explain the more homogenous coating for the PtCcom-2-01 electrode. Therefore, working with the commercial catalyst could allow to develop a better electrode in terms of creating a more uniform catalyst layer, with no accumulation of metal in specific points, and well distributed over the carbon-paper fibres. Table 5.3 also summarises the results of the chemical analysis for both of the Pt/C catalysts. The ICP-OES analysis allowed to verify the Pt loading. A slight minor quantity of the

active metal is present in the home-made catalyst, a feature to have in mind when comparing the electrochemical activity of both anodes.

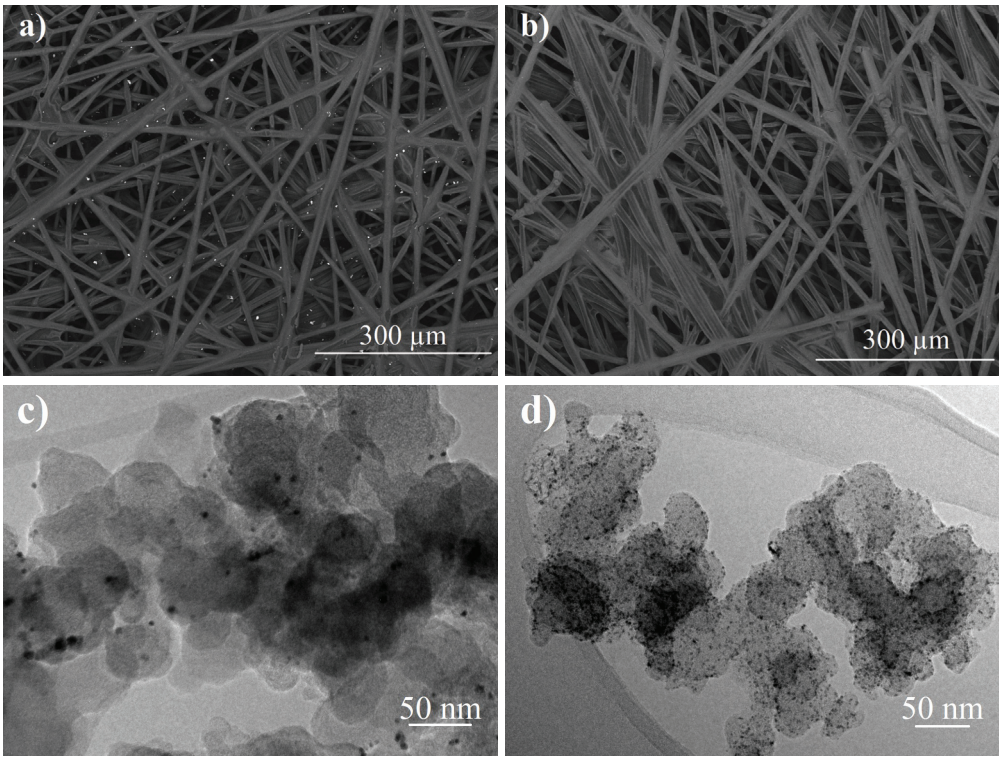

Figure 5.9: Characterisation of the fresh prepared anodes: SEM micrographs of the electrode surface at low magnification (a-b), and TEM micrographs of the catalysts powders before deposition (c-d). a) Anode PtCv-2-01 with the home-made electrocatalyst (c), and b) Anode PtCcom-2-01 with the commercial electrocatalyst (d).

Table 5.3: Characterisation of the home-made and commercial electrocatalysts: ICP-OES and TEM images.

Catalyst	ICP-OES analysis	TEM images
	Average Pt content (% wt.)	Average Pt particle size (nm)
Pt/C_{vulcan} (home-made)	16.5 ± 0.8	5.3 ± 1.4
Pt/C_{black} (commercial)	19.5 ± 1.0	2.6 ± 0.6

The electrochemical performance of the new anode formulation based on the commercial catalyst (PtCcom-2-01) was tested as previously. Figure 5.10 exhibits the results of CV and CA for both anodes (PtCcom-2-01 and PtCv-2-01), with a drastic improvement of the registered current and a change in the electro-oxidation trend for the electrode that uses the commercial catalyst. The CV plot showed that the electro-oxidation of PEG1000 can produce important current densities, especially between 700 – 800 mV. The application of an electrical potential larger than 900 mV seems to be detrimental. This may be due, as previously explained, to more complex electro-oxidation steps occurring at higher polarisations. It is worth noting

that the forward scan produces larger currents than the backward scan. A possible explanation for the deterioration during the negative sweep could be the poisoning of the catalytic surface by CO_{ads}, which may be an option on account of the high reached currents. This assumption can be supported by the fact that the onset potential (∼480 mV) during the forward scan is higher than the terminal potential (∼380 mV), potential at which the electro-oxidation finishes during the backward scan, which is usually a typical marker of this phenomenon [16]. Much smaller difference between these two potentials can be observed for the electro-oxidation of EG (Figure 5.3), but with PEG1000 it is more significant. In fact, CO_{ads} is a partial oxidation product that could be produced below 600 mV, but can be oxidised at potentials just over that value [16]. Here, the produced CO_{ads} seems to remain adsorbed during the negative sweep. Then, it could be fully oxidised when the following forward scan exceeds 600 mV, generating more significant currents. Similar behaviour was registered in the literature during the electro-oxidation of EG in a similar PEM arrangement [16]. Of course, as observed in previous studies, the partial deactivation of the system during the backward scan could also be also attributed to the oxidation of Pt at high polarisations [36, 41], but it is less likely as negligible loss of activity was registered for a blank experiment in presence of distilled water using the same electrode (Figure D.3). Figure 5.10b depicts the current densities achieved with the new electrode formulation upon application of 1000 mV. For the anode based on the Pt/C commercial catalyst, the current is at least 6 times higher than that for the electrode based on the home-made Pt/C_{vulcan} catalyst. Both systems still present a significant deactivation when a potential of 1000 mV is applied, but it can be equally explained by the combined effect of the

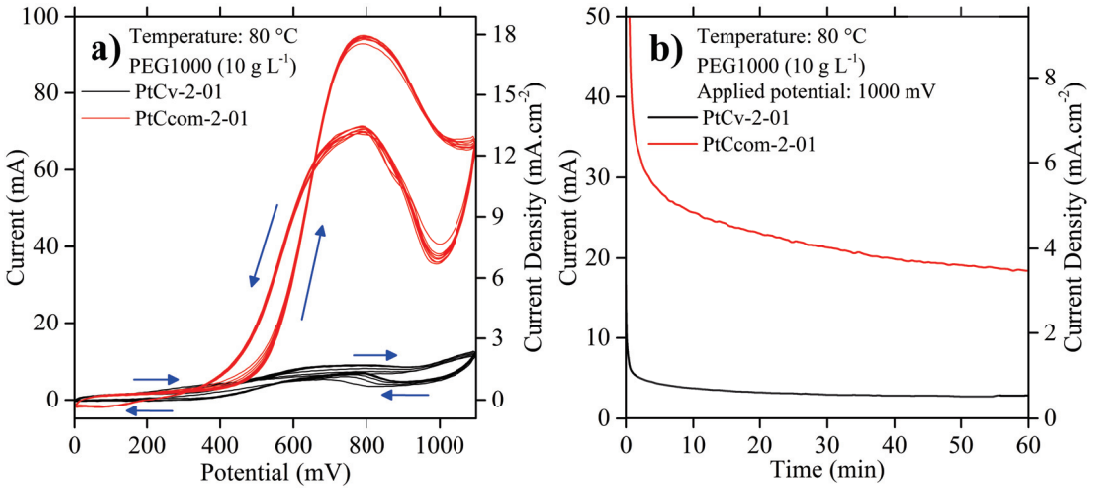

Figure 5.10: Effect of the electrocatalyst on the PEG1000 electrolysis: a) CV experiences, and b) Chrono-amperometries at 1000 mV for 60 min. (Temperature = 80 °C, cyclic voltammetries from 0 to 1100 mV, scan rate 10 mV s^{-1}, 10 cycles).

CO_{ads} persistence and the Pt oxidation. In any case, the application of potentials in the range of 700 – 800 mV might avoid the observed decrease on the electrochemical performance.

Even though the metal loading observed by ICP-OES for the home-made catalyst is slightly lower than that for the commercial material, this difference is not high enough to justify such a change in the anode activity. Another important point to have in mind is that no important difference could be attributed to the micro/mesoporosity of commercial catalyst. In fact, both catalysts present similar supports (Vulcan XC-72 for the home-made catalyst and Vulcan XC-72R for the commercial one) with BET surface area around 250 m^2 g^{-1} and pore sizes <10 nm. The only difference reported for these materials is morphological (XC-72 presents a beaded form while the XC-72R is in powder form) [43–47]. Therefore, the considerable different performance of the electrodes PtCv-2-01 and PtCcom-2-01 can be explained by the impact of three inter-dependent factors: the more homogenous catalyst/ionomer coating well covering the carbon fibres, the smaller Pt nanoparticles, and their better dispersion over the mesoporous carbon support. These characteristics guarantee the availability of a higher number of active sites uniformly present over the anode's surface, which finally explains the higher registered currents. Another possibility is a deeper catalyst/ionomer coating in the GDL volume, but further analysis of the cross section of the anode is necessary to conclude about that factor.

With the series of modifications presented so far, the anode formulation should reach high performance for the electro-oxidation of both EG and the whole series of molecular weights of PEG. For the rest of the present study, we will use an ink composed of 1 mg cm^{-2} of the commercial catalyst and 0.1 mg cm^{-2} of Nafion®, deposited by spray-coating on AvCarb MGL190 carbon paper. It has been found that this electrode (PtCcom-2-01) offers much important performance than the home-made catalyst-based electrode, besides an enhanced stability. This optimisation study could continue, for example, by using other types of supports (with greater porosity), and a wide variety of catalysts (based on noble and non-noble metals).

5.3.4 Electro-oxidation of EG/PEG using an optimised electrode

The optimised electrode formulation based on the commercial catalyst (PtCcom-2-01) was tested for the electro-oxidation of both EG and PEG. The electrochemical experiments (CVs and CAs) were performed under the same conditions as those described in the initial part of the study. Figure 5.11 depicts the electrochemical performance for EG electro-oxidation. The experiments are similar to those shown in Figure 5.3, but using the optimised anode formulation. It was possible to confirm,

as expected, an enhanced activity compared with the initial electrode (PtCv-1-10). For a EG concentration of 10 g L^{-1} and 80 °C, the current density at 1100 mV with the optimised anode is at least 6 times as high as that of the initial one. Not only the overall activity but also the trend of the CV curves differed from the curves presented in Figure 5.3. This suggests that the optimised anode (PtCcom-2-01) leads to a more advanced electro-oxidation process favoured by multiple factors, including a higher availability of catalyst active sites, as previously discussed.

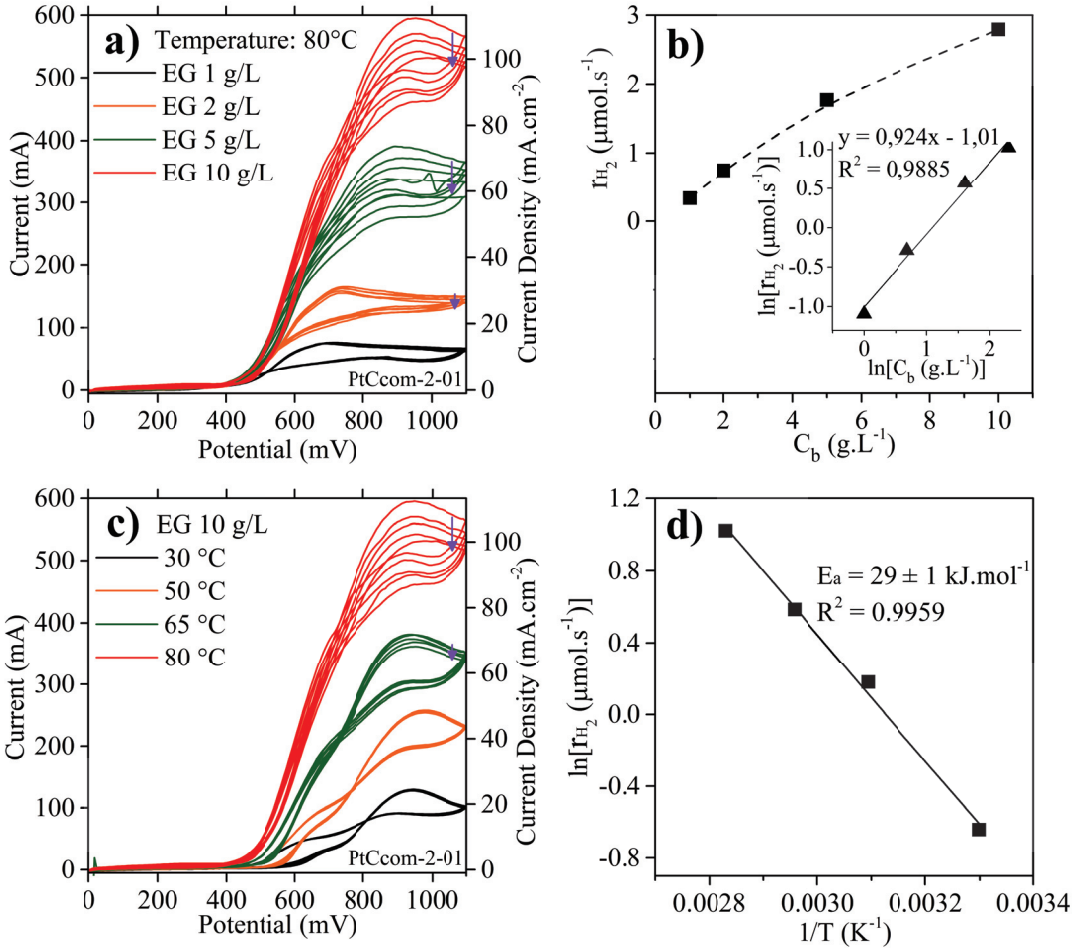

Figure 5.11: Effect of the initial concentration (C_b) and the reaction temperature on the EG electrolysis in a PEM cell using a PtCcom-2-01 anode: a) CVs with different C_b, b) Influence of C_b on the H_2 production and reaction order calculated from a) at 1100 mV (inset), c) CVs at different temperatures, d) Arrhenius plot: $ln(r_{H_2})$ vs. $1/T$ and activation energy calculated from c) at 1100 mV. (Cyclic voltammetries from 0 to 1100 mV, scan rate 10 mV s^{-1}, 10 cycles, plotted only 2nd, 4th, 6th, 8th and 10th cycles).

On the other hand, it is worth mentioning the loss of electrochemical activity along the cycles, which could be attributed to the poisoning by CO_{ads} and/or CO-like carbonaceous species and can be influenced by a combination of several factors: *(i)* Higher currents could lead to a higher probability of arriving to the final steps of the EG multiple-step reaction mechanism, being CO_{ads} part of the interme-

diary products prior the production of CO_2 [17, 38]. *(ii)* The smaller size of the Pt nanoparticles of the commercial catalyst makes the metal prone to deactivation because of the stronger interaction of the adsorbates (e.g. H, OH and CO) with the metallic surface, as documented for the electro-oxidation of low molecular weight alcohols and CO [29, 48, 49]. *(iii)* The degradation of the Nafion® membrane due to chemical stress and species crossover [50, 51]. However, further research should be carried out to further confirm the extent of each of those phenomena.

Despite of the important loss of activity at high concentration and temperature, it was possible to calculate the overall reaction order and the activation energy using the same procedure explained before. An average value of the currents obtained at 1100 mV was used for the calculations of both E_a and n. The same applied potential for the calculations (as in Figure 5.3b-d) was kept for comparison, also having into account the almost negligible currents registered for the blank CV in presence of distilled water (Figure D.3). Comparable results should be obtained at different polarisations, since a proportional increment with the concentration and temperature was registered over the range of 700 – 1100 mV. Having this in mind, the reaction order for the new system was found to be n ≈ 0.92 (slope of the inset in Figure 5.11b). A value near the unity is typical for systems that are not governed by diffusional limitations and does not present competitive adsorption of reaction intermediates. Similarly, such reaction order means that the H_2 production directly depends on the EG concentration.

Regarding the influence of the temperature on the electrochemical activity (Figure 5.3c-d), a similar effect than in the initial case was noticed (Figure 5.3c). A generalised improvement of the current is registered for potentials over the onset, but a more relevant difference between the onset and terminal potentials is registered. As explained before, this feature explains a possible poisoning by CO_{ads} species, being that difference almost negligible at 80 °C (both onset and terminal potentials ∼450 mV) and more important at 30 °C (with a difference of ∼180 mV). The reduction of the difference between the onset and terminal potentials as the temperature increases could be related to a higher likelihood of a complete EG electro-oxidation at higher temperatures. A similar behaviour was previously reported for EG electro-oxidation in PEM systems [16, 17]. Therefore, the E_a calculations (Figure 5.11d) gave a value of 29 ± 1 kJ mol^{-1}, which is very similar to the one calculated with the initial electrode. This suggests that a similar reaction path is taking place in both cases, since a similar energetic barrier needs to be overcome to start the electrochemical reactions.

The electro-oxidation of PEG was studied by using PEG4000 as a representative of this polymer family. Considering this is the highest molecular weight molecule

of those proposed in this study, the performance obtained could be further extrapolated to a series of PEG polymers with lower molecular weights. As observed in Figure 5.12, as expected, the electro-oxidation of PEG seems to be a much more complex process compared to EG. Regarding the CV experiments, several oxidation peaks were observed over the whole range of potentials, with maximum values between 700 and 800 mV. Even if lower current densities are registered around 1100 mV, no loss of activity (i.e., no deactivation) took place. On the contrary, a slight augmentation occurs along the cycles. The values of current density are significantly diminished in comparison with the EG curves, and the reason is quite obvious: the PEG macromolecules are more difficult to electro-oxidise on account of their size. The upward trend by effect of the concentration is clear for the range of 1-10 g L^{-1}, but the system attained a saturation level at higher concentrations. This

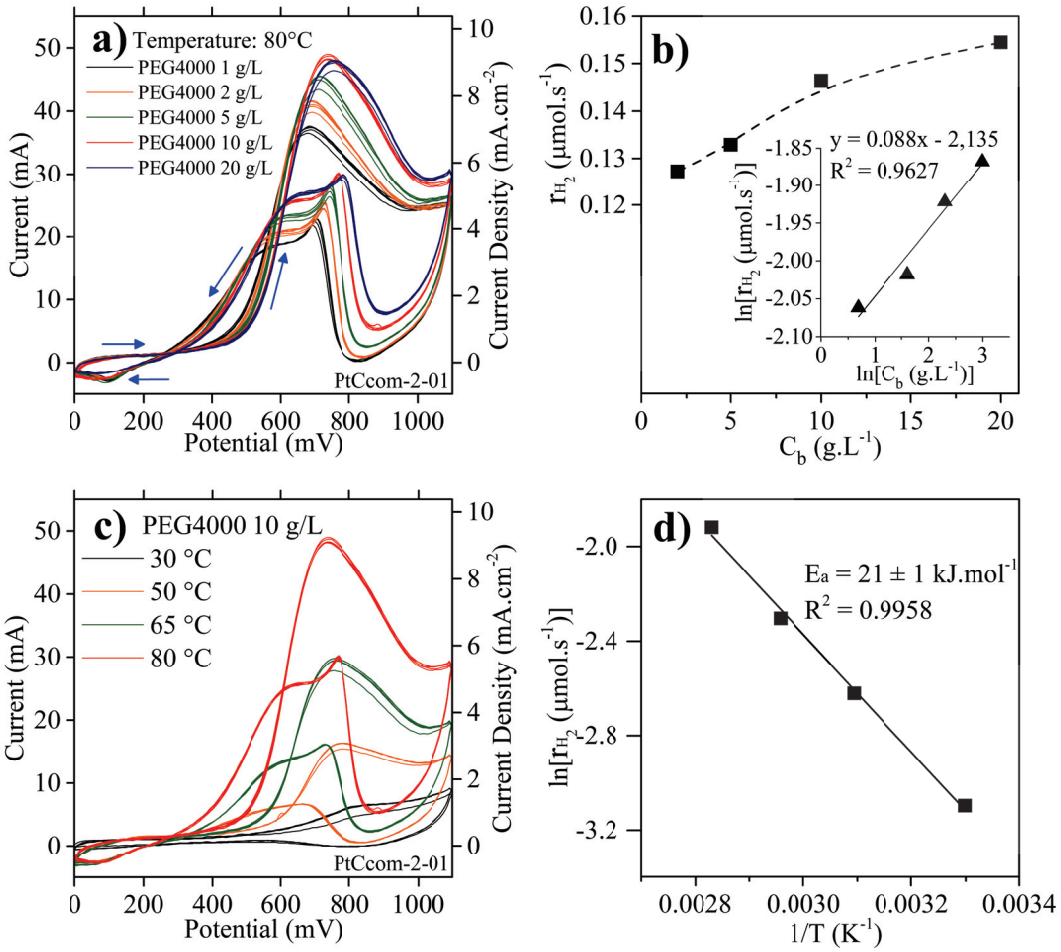

Figure 5.12: Effect of the initial concentration (C_b) and the reaction temperature on the PEG4000 electrolysis in a PEM cell using a PtCcom-2-01 anode: a) CVs with different C_b, b) Influence of C_b on the H_2 production and reaction order calculated from a) at 1100 mV (inset), c) CVs at different temperatures, d) Arrhenius plot: $ln(r_{H_2})$ vs. $1/T$ and activation energy calculated from c) at 1100 mV. (Cyclic voltammetries from 0 to 1100 mV, scan rate 10 mV s^{-1}, 10 cycles, plotted only 2nd, 4th, 6th, 8th and 10th cycles).

may indicate a saturation of the system above that range (transport limitations). In consequence, the kinetic parameters calculated below should be considered as indicative values, as a possible transport limitation could take place for PEG4000 at high concentrations.

Regarding the calculation of the kinetic parameters, an n value of 0.088 was calculated following the same procedure as before (the r_{H_2} value for 1 g L^{-1} was slightly out of the trend and was not considered). Such a reaction order suggests that the system is governed by diffusional limitations. In fact, the physical properties of the system PEG/water are strongly affected by the macromolecule length and the polymer concentration, because of the complex structural and molecular interactions between water/macromolecule and inter/intramolecular [52–54]. Characteristics such as the molar volume, the density and viscosity can be affected to a large extent by a higher M_w, changing the rheological and transport properties of the solution [55, 56]. Thus, the macromolecules travelling through the anode volume are equally affected. By comparing the onset potentials of the EG and PEG4000 curves on this system, one can see that both present values of ∼450 mV. This suggests that a similar initial energy input is necessary to start the electro-oxidation of both molecules, most likely because of the electro-oxidation of the terminal groups of the macromolecules chain. A comparable behaviour was reported by our group for the electro-oxidation of lignin (a complex natural polymer) and a representative model molecule (2-phenoxyethanol) in alkaline media [57, 58].

The impact of the reaction temperature on the overall behaviour of the system follows a similar trend as that observed with EG. Even if the electro-oxidation of PEG can take place at low temperatures, with likewise low current densities, an important improvement of the current densities is registered over the complete range of temperatures. The activation energy was calculated at 1100 mV, as previously explained. A value of 21 ± 1 kJ mol^{-1} may reveal the occurrence of a slightly less energy demanding reaction, compared with the values previously calculated for EG. This could offer mechanistic information, as it was explained in literature by Stuve and Spies [16, 17]. The complete oxidation of PEG could go as far as the production of CO_2, but the complexity of the molecule hinders the total oxidation of the polymer. We believe the currents measured for PEG4000 are mainly produced by the initial steps of the electro-oxidation of the macromolecule, and this can take place in two ways: *(i)* the attack of the terminal groups, or *(ii)* the partial depolymerisation and oxidation of the macromolecule by electrolysis of the −C−O−C− bonds. The competition of these mechanisms will be further discussed in the following section.

Finally, as observed in Figure 5.12, the difference between the onset and termi-

nal potentials does not follow the same trend as for EG. For the model molecule, it was observed a reduction of such a difference as the temperature increases. Here, the difference between the two potentials seems to be stable. It suggests that the lower activity obtained during the backward scan could be due to the adsorption of other molecules, rather than CO. For instance, it has been reported in the literature that PEG ($M_w \geq$600 g mol^{-1}) is strongly adsorbed on the surface of Pt-based electrodes in an acid medium (0.5 M H_2SO_4). The PEG macromolecules may take the form of collapsed spheres, making difficult the electrochemical transformations [24]. This is also supported by another study dealing with the electro-deposition of Cu in the presence of PEG, which employed a Quartz Crystal Microbalance (QCM) to study the surface coverage by the macromolecules [23]. Other study on the electro-oxidation and adsorption of oligoelthylene glycols (OEG or low M_w PEG, 2-4 repetitive units) on Pt electrodes [26] stated that higher molecular weights of OEG generate adsorbates more difficult to oxidise, as well as a concomitant blocking of the electrode surface, which hinders the overall reaction rate. The authors also affirm that OEG follows two routes of oxidation: *(a)* via strongly chemisorbed species with low reaction rate, and *(b)* via weakly adsorbed species present in low quantities at the catalytic surface but with higher reactivity [26]. The studies conclude that higher molecular weight macromolecules promote the predominant accumulation of hard-to-oxidise adsorbates on the electrode surface [25, 26]. Thus, one can image that lighter macromolecules could have a tendency to follow the path of weakly adsorbed species, as they are less likely to cover a large extend of the catalytic surface, avoiding the concomitant blocking of the active sites. Therefore, the reaction orders that were calculated in the present work for EG ($n \approx 0.92$) and PEG4000 ($n \approx 0.088$) are in agreement with these publications. The reactions involved in the calculations for EG probably follow the mechanism of weakly adsorbed species, but high molecular weight PEG is likely to be strongly adsorbed at the catalytic surface, generating the subsequent loss of activity. This fact also agrees with the results of our previous study on the electro-oxidation of dissolved PMMA, which demonstrated that these macromolecules also had the tendency to attach strongly to the electrode's surface, hindering the electrochemical activity [29].

5.3.5 Impact of the PEG molecular weight on the possible reaction path

As previously discussed, the size of the macromolecules could directly impact the electrochemical behaviour of the PEM system. The aim of this section was to deepen into the influence of this variable. Figure 5.13a shows the CV curves for the different PEG molecules with the same total mass concentration (20 g L^{-1}). It can be easily

noticed that the lighter PEG samples produced higher current densities. This could be attributed to two main factors: *(i)* the ease of smaller molecules to travel through the anode volume to meet the active sites and be therefore electro-oxidised, and *(ii)* the higher concentration of molecules that could follow the weakly adsorbed reaction route. The first factor was early detected with the initial electrode material (Figure 5.5), as a significant increase in the current was registered with the increasing concentration only for the low M_w polymers, i.e. PEG200 and PEG400. However, as previously discussed, the mass transport of molecules of high M_w is more complex, as it can be affected by both the macrostructure of the anode materials. Facilitated mass transport is of major importance to generate higher current densities, but the electro-chemical reforming is rather determined by the interactions between the involved species and the active sites. The second factor is more relevant in order to understand the reaction mechanism followed by the different polymer chain sizes.

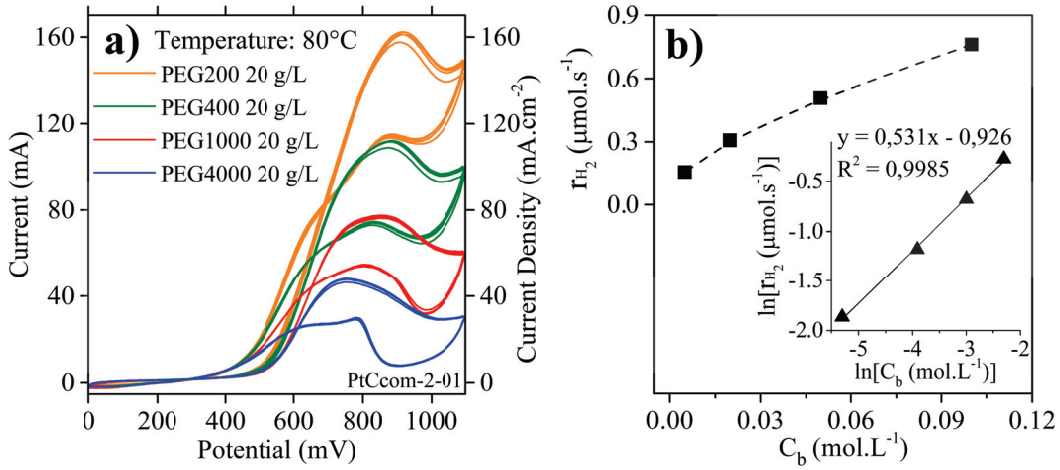

Figure 5.13: Influence of the molecular weight (M_w) on the PEG electrolysis in a PEM cell using PtCcom-2-01 anode: a) CVs using PEG of different M_w (20 g L^{-1}), and b) Influence of PEG molar concentration on the H_2 production and reaction order calculated from a) at 1100 mV (inset). (Temperature = 80 °C, cyclic voltammetries from 0 to 1100 mV, scan rate 10 mV s^{-1}, 10 cycles, plotted only 2nd, 4th, 6th, 8th and 10th cycles).

To better understand the information given in Figure 5.13a, it is necessary to interpret the data using a different basis. Until here, the concentration was always presented on total mass bases (g L^{-1}), but the effect of the molecular weight is more clear if it is presented in molar bases. Figure 5.13b presents the results of the hydrogen production rate (calculated at 1100 mV) vs. the solution concentration in mol L^{-1}. The reaction rate is directly affected by the molar concentration of PEG in the solution, and the most plausible reason for this behaviour is the higher concentration of molecules that could potentially follow the weakly adsorbed species oxidation route, with a reaction order n ≈ 0.531.

From the mechanistic point of view, two electro-oxidation paths could be proposed for the electro-oxidation of PEG: one involving only the terminal groups, and another that would implicate the breaking of a –C–O–C– bond. A complex multistep reaction is the most probable answer, as it was previously discussed for EG [16, 17], but here we will only consider the complete oxidation for simplicity. Therefore, Eq. (5.6) shows the case of the complete electro-oxidation of the terminal repetitive unit of a PEG_n at the anode to produce a PEG_{n-1}, assuming that the PEG only bears hydroxyl terminal groups.

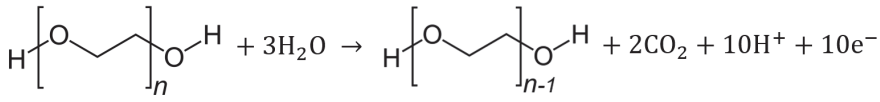

(5.6)

The second reaction mechanism is the one that involves the depolymerisation of a PEG macromolecule to produce two shorter polymeric chains. Here, a first step involving the adsorption and breaking of the –C–O–C– bond on the catalytic surface is necessary, followed by the electro-oxidation of the repetitive unit containing that bond. Eq. (5.7) shows how the complete electro-oxidation reaction would happen.

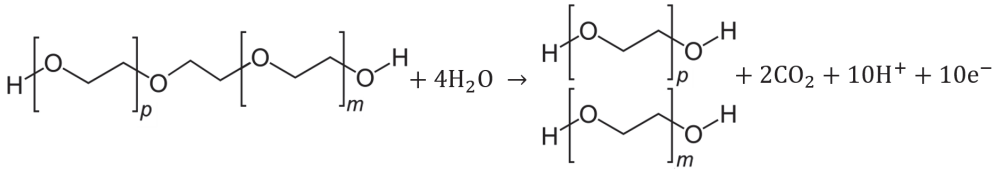

(5.7)

The latter mechanism could be essentially interpreted as the consumption of the terminal group of a PEG_{m+1} macromolecule that has been previously produced by depolymerisation of a PEG_{p+m+1}. Then, this pathway seems more complicated on account of the hindered intimate contact of the random –C–O–C– bond with the catalytic active sites. This reaction seems less likely and the contribution to the total current is probably lesser than the one coming from the oxidation of terminal groups.

To have a clearer idea of the occurrence of both reaction mechanisms, long-run electro-oxidation experiments were performed to allow the accumulation of products in the anodic solution reservoir. Figure 5.14 shows the results of the chronoamperometric experiments. An applied potential of 800 mV was employed to avoid the probable poisoning of the Pt/C_{black} commercial catalyst at higher potentials. The initial concentration of PEG was fixed at 5 g L^{-1} to avoid any possible transport limitation. The overall performance follows the same trend as previously showed by the CV experiments, where a direct impact of the molar PEG concentration can be observed. The system seems to need a longer time to stabilise as the molecular weight is reduced. Following the previous discussion, this can be attributed

to the consumption of the smaller macromolecules, which might follow the weak adsorption route previously explained. The curve of PEG4000 could be interpreted as the current produced by the contribution of reactions following the route of the strongly chemisorbed species [25, 26], and the additional current for the samples with molecular weight of 400 and 1000 g mol^{-1} is probably generated by a combination of both oxidation routes.

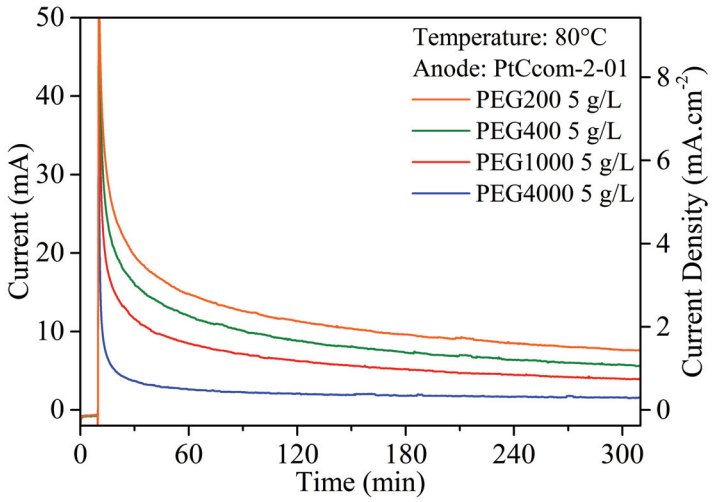

Figure 5.14: Effect of the molecular weight (M_w) on the PEG long-run electrolysis using a PtCcom-2-01 anode: Chrono-amperometries at 800 mV for 5 h using PEG of different M_w (5 g L^{-1}). (Temperature = 80 °C).

In order to have more insights into the oxidation mechanism, samples of the PEG solutions used for the CA experiences (Figure 5.14) were taken prior and after 5 h polarisation of the PEM cell. They were analysed by Size-Exclusion Chromatography (SEC). Figure 5.15 present the results for the samples of PEG200, PEG400, PEG1000 and PEG4000 (where 1 Da = 1 g mol^{-1}). It was possible to confirm that the electro-oxidation of PEG involves the reduction of the molecular weight distribution over the complete set of samples after electrolysis for 5 h. It is worth noting that the current densities registered during the CA experiences for all the PEG series were in the order of some mA cm^{-2}, but they were high enough to produce a tangible reduction in the molecular weights. From the SEC experiments, it is possible to calculate the number-average molecular weight ($M_n = \frac{\sum(N_i.M_i)}{\sum(N_i)}$, sum of the molecular weight of all the molecules divided by the total number of molecules) and the weight-average molecular weight ($M_w = \frac{\sum(N_i.M_i^2)}{\sum(N_i.M_i)}$, sum of the weight times the molecular weight of all the molecules divided by the total weight of the mixture), where N_i is the number of molecules with molecular weight M_i. Successively, the polydispersity ($PDI = \frac{M_w}{M_n}$) is calculated. If *PDI* equals the unity, then the polymer sample is a monodisperse sample [59]. On the contrary, an elevated *PDI* value indicates the existence of macromolecules with a large variety of molecular weights.

These values are presented in Table 5.4, for the samples before and after the electrochemical treatment.

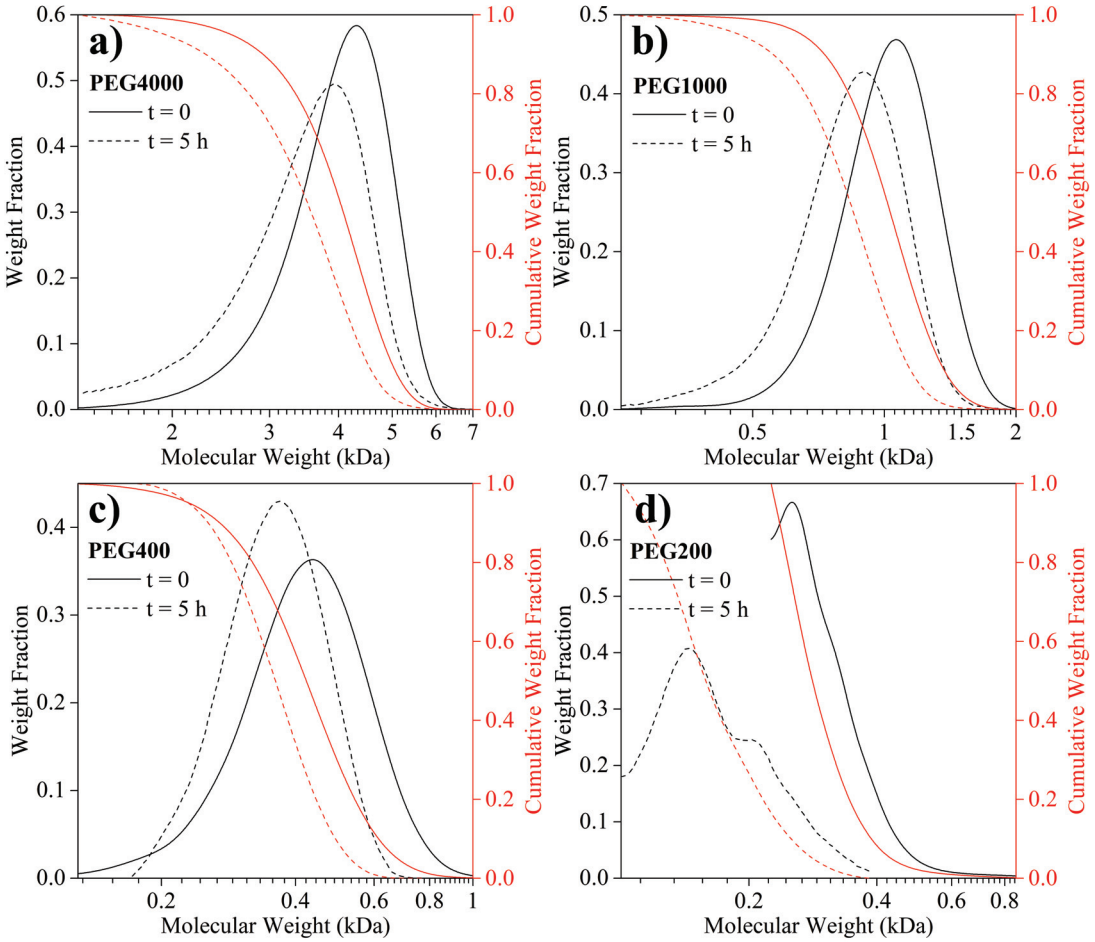

Figure 5.15: Molecular weight distribution from SEC characterisation of PEG of different molecular weights before and after long-run electrolysis using an optimised anode: CA at 800 mV for 5 h (Figure 5.14).

From the shape of the molecular weight distribution curves, it is possible to infer some similarities between PEG4000 and PEG1000, which may undergo a similar balance between both reaction mechanisms defined by Eq. (5.6) and (5.7). Both samples present a slight increase in the low molecular weight zone of the distribution, and small augmentation of the polydispersity. The latter suggests that some of the initial macromolecules may have followed a division step, to form smaller PEG chains. These two could be attributed to the influence of the electro-oxidation mechanism involving the depolymerisation step to produce lighter macromolecules. In fact, these results do not agree with one of the studies reported on electro-oxidation of PEG [25], which affirmed that the electrochemical transformations mainly involve the terminal groups of polymeric chains. In the case of PEG400, one may think, from the curve and the decrease of the *PDI* value, that the mechanism involving the oxidation of the terminal repetitive unit may be more important.

This is in good agreement with the observed reduction in M_w, of about ∼67 g mol^{-1}, which is in the same order of magnitude than a repetitive unit of the polymeric chain (∼62 g mol^{-1}). For PEG200 is complicated to establish which mechanism is predominant, as no clear trend can be attired from the curves, nor the calculations. This latter sample could be further studied by other chromatographic techniques in order to have a clearer idea of the reaction products, as the resolution of the SEC technique presents some limitations at low molecular weight range.

Table 5.4: Average PEG molecular weights and polydispersity calculated from the SEC characterisation before and after long-run electrolysis (Figure 5.15).

Sample	CA time (h)	M_n (Da)	M_w (Da)	PDI
PEG4000	0	3833	4023	1.049
	5	3204	3479	1.086
PEG1000	0	970	1036	1.069
	5	778	851	1.093
PEG400	0	389	433	1.113
	5	344	366	1.064
PEG200	0	288	301	1.045
	5	158	172	1.089

The results of SEC showed for the first time the possibility of reducing the average molecular weight of polymeric molecules by pure electrochemical methods at low temperature. In fact, a similar behaviour could be expected for PEG of higher molecular weight, but the current densities will be surely lower than the ones obtained in this work. Further characterisation of the samples needs to be carried out in order to define the real influence of each reaction mechanism, also including a larger range of molecular weights. The analysis presented here constitutes a first approach based on the electrochemical results and the SEC characterisation. Different spectroscopic techniques could give more insights about the electro-oxidation mechanism at the anodic surface. Finally, these results represent a very relevant outcome, as this may represent a first step into the electro-oxidation of other C–O bond-containing polymers.

Finally, we characterised the gas outlet of the cathodic side of the PEM system, aiming to analyse the purity of the hydrogen produced by electro-reforming of PEG, as well as to establish if the electrochemical system follows the behaviour dictated by the Faraday's Law (Eq. (5.1)). Hence, a cyclic voltammetry experiment was performed with a fresh anode with a solution of PEG1000 (10 g L^{-1}), while the gas products were online measured by mass spectrometry (MS) with a similar protocol as the one used in Chapter 2. Figure 5.16 shows the dynamic plot of the CV curves (red line), as well as the MS results registered in the same time frame (blue line). The gas bubbles produced at the cathode of the PEM cell were found to be pure

hydrogen, as negligible quantities of CO_2 were measured. No H_2 production was detected when the system was under open circuit potential. Consequently, the hydrogen production follows the form of Eq. (5.5), where 2 protons get reduced by 2 electrons to produce a H_2 molecule. In other words, the hydrogen production rates calculated from Eq. (5.1) throughout this work are correct. In addition, the H_2 flow measured by MS followed the same trend as the CV curves. The H_2 flow rate calculated assuming normal pressure and temperature conditions is in the same order of magnitude as the one calculated for the CV by the Faraday's Law. Slightly lower values are registered for the MS curve, probably because of the accuracy and the slow response of the system.

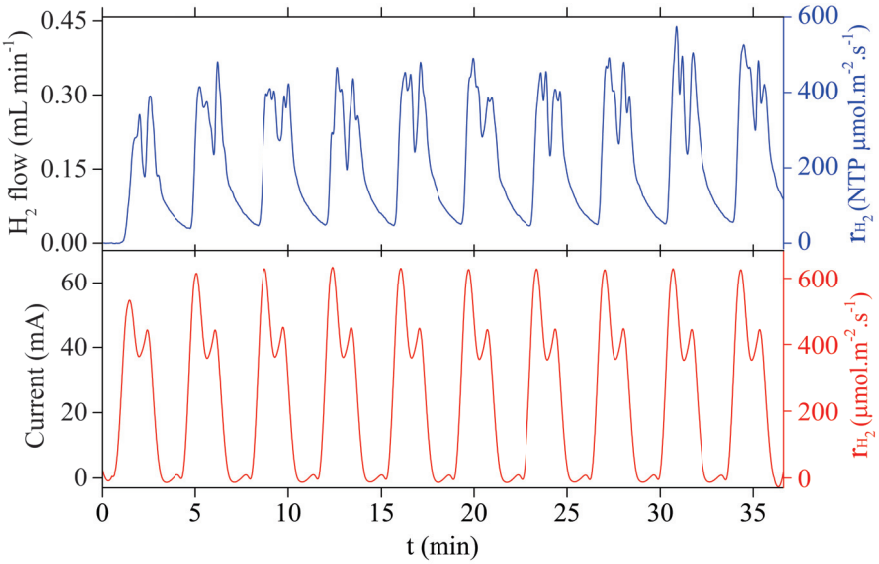

Figure 5.16: In-situ H_2 measuring by mass spectrometry (N_2 dilution flow of 70.6 mL min^{-1}) during a CV experience with PEG1000 using a PtCcom-2-01 anode. (C_b = 20 g L^{-1}, temperature = 80 °C, cyclic voltammetry from 0 to 1100 mV, scan rate 10 mV s^{-1}, 10 cycles, plotted in dynamic mode).

To conclude, the Faraday's Efficiency of the system was calculated from Eq. (5.8) [60], where r'_{H_2} and $r^0_{H_2}$ refer to the experimental hydrogen production rate measured upon polarisation and under open circuit potential conditions, respectively; and r_{H_2} is the value calculated by the Faraday's Law from the total current during the polarisation experiment.

$$\Lambda = \frac{r'_{H_2} - r^0_{H_2}}{r_{H_2}} \cdot 100 \tag{5.8}$$

Both curves were integrated to have a total H_2 production (for the MS curve, a longer time of 45 min was employed for the calculation, as H_2 was detected long after the polarisation stopped). From the CV curve, a value of 261.5 ± 13.1 μmol_{H_2} was calculated from the total produced current. Similarly, the MS measurements

gave a value of 260.9 ± 13.0 μmol_{H_2}. Then, Λ was calculated to be ∼99.8%, for the experiment shown in Figure 5.15, which points out that almost 100% of all the protons and electrons are transformed into molecular H_2 at the cathodic chamber.

5.4 Conclusions

A thorough series of experiments was carried out to get the first insights about the electro-oxidation of polyethylene glycol (PEG) in an aqueous solution in a Proton Exchange Membrane (PEM) reactor using Pt/C based anode materials. The anode formulation and nanostructure were improved to maximise the concentration and availability of Pt active site. With the optimised anode composition and nanostructure, we studied the impact of concentration and molecular mass of PEG molecules (from 200 up to 4000 g mol^{-1}) as well as of the temperature on the performance of the system. The results demonstrate that PEG can be electro-oxidised at low potentials, from around 0.4 V, with current densities larger than 100 mA cm^{-2} at 0.8 V and 80 °C for low molecular weight molecules (200 and 400 g mol^{-1}). Furthermore, the size-exclusion chromatography evidenced a decrease of the PEG molecular weight in the anodic solution after a chrono-amperometry at 0.8 V and 80 °C for 5 h, confirming the electrocatalytic attack of the polymers. The electro-oxidation process could follow two main routes, involving weakly adsorbed or strongly chemisorbed species. Nevertheless, further characterisations of the system are needed to propose a more detailed reaction mechanism. The production and purity of hydrogen in the cathode compartment was verified by MS, and a faradaic efficiency of 100 % was calculated. The authors believe that this study may represent a first contribution towards the low-temperature electro-oxidation of other types of polymers containing C−O bonds in their main chain. The application of this concept for the production of hydrogen by electrochemical means seems promising, but further research should be carried out in view of its further practical application.

Supplementary Information

Figure D.1

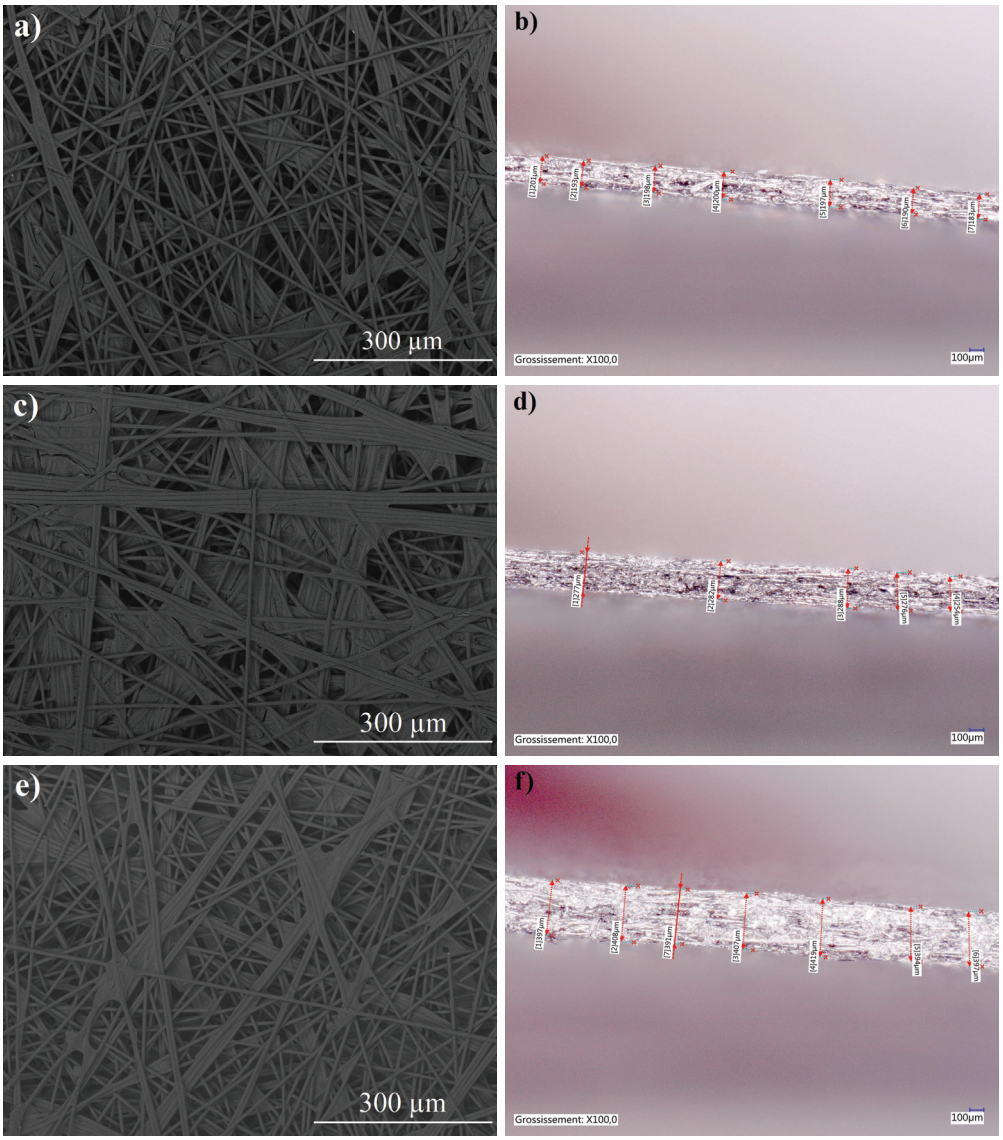

Figure D.1: Characterisation of the carbon paper supports used for the different electrodes: a-b) MGL 190 μm, c-d) MGL 280 μm, and e-f) MGL 370 μm. SEM micrographs of the surface at low magnification (a, c, d) and optical micrographs of the cross section (b, d, e).

Figure D.2

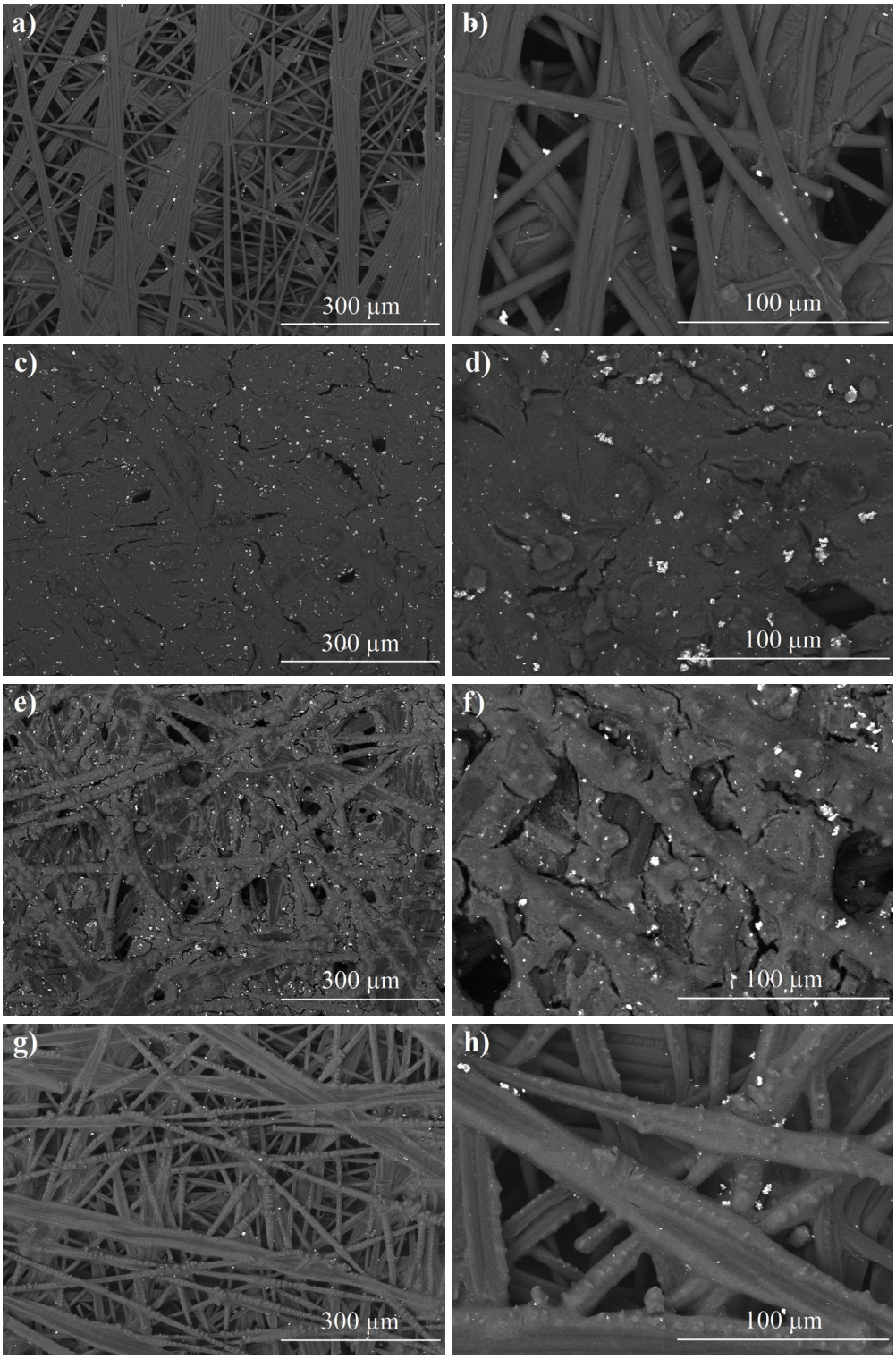

Figure D.2: SEM micrographs at low magnification of the anodes coated surface with different Nafion® content: a-b) PtCv-1-00, c-d) PtCv-1-10, e-f) PtCv-1-05, and g-h) PtCv-1-01.

Figure D.3

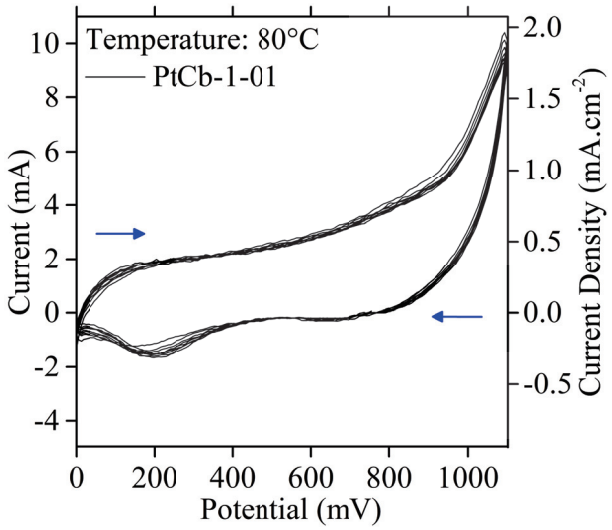

Figure D.3: Electrochemical performance of the PtCcom-2-01 anode in presence of distilled water in a PEM cell. (Temperature = 80 °C, cyclic voltammetry from 0 to 1100 mV, scan rate 10 mV s^{-1}, 10 cycles).

References

[1] D'souza, A.A. and Shegokar, R. Polyethylene glycol (PEG): a versatile polymer for pharmaceutical applications. *Expert Opinion on Drug Delivery*, 13(9): 1257–1275, 2016. doi: 10.1080/17425247.2016.1182485.

[2] Hamta, A. and Dehghani, M.R. Application of polyethylene glycol based aqueous two-phase systems for extraction of heavy metals. *Journal of Molecular Liquids*, 231:20–24, 2017. doi: 10.1016/j.molliq.2017.01.084.

[3] Wu, Y., Wang, Q. and Libera, M. PEG-based microgels to modify biomaterials surfaces. *Macromolecular Symposia*, 329:35–40, 2013. doi: 10.1002/masy.201200106.

[4] Chen, J., Spear, S.K., Huddleston, J.G. et al. Polyethylene glycol and solutions of polyethylene glycol as green reaction media. *Green Chemistry*, 7:64–82, 2005. doi: 10.1039/b413546f.

[5] Grand View Research. Polyethylene Glycol Market Size, Share and Trends Analysis Report By Application (Medical, Personal Care, Industrial), By Region (North America, Europe, Asia Pacific, Row), And Segment Forecasts, 2015 - 2020. Technical report, 2015.

[6] Pietrelli, L., Ferro, S., Reverberi, A.P. et al. Removal of polyethylene glycols from wastewater: A comparison of different approaches. *Chemosphere*, 273: 129725, 2021. doi: 10.1016/j.chemosphere.2021.129725.

[7] Huang, Y.L., Li, Q.B., Deng, X. et al. Aerobic and anaerobic biodegradation of polyethylene glycols using sludge microbes. *Process Biochemistry*, 40:207–211, 2005. doi: 10.1016/j.procbio.2003.12.004.

[8] Eriksson, E., Auffarth, K., Eilersen, A.M. et al. Household chemicals and personal care products as sources for xenobiotic organic compounds in grey wastewater. *Water SA*, 29(2):135–146, 2003. doi: 10.4314/wsa.v29i2.4848.

[9] Ulbricht, J., Jordan, R. and Luxenhofer, R. On the biodegradability of polyethylene glycol, polypeptoids and poly(2-oxazoline)s. *Biomaterials*, 35: 4848–4861, 2014. doi: 10.1016/j.biomaterials.2014.02.029.

[10] De Lima, R.B., Paganin, V., Iwasita, T. et al. On the electrocatalysis of ethylene glycol oxidation. *Electrochimica Acta*, 49(1):85–91, 2003. doi: 10.1016/j.electacta.2003.05.004.

[11] De Lucas-Consuegra, A., Calcerrada, A.B., De La Osa, A.R. et al. Electrochemical reforming of ethylene glycol. Influence of the operation parameters, simulation and its optimization. *Fuel Processing Technology*, 127:13–19, 2014. doi: 10.1016/j.fuproc.2014.06.010.

[12] Lamy, C., Belgsir, E.M. and Léger, J.M. Electrocatalytic oxidation of aliphatic

alcohols: Application to the direct alcohol fuel cell (DAFC). *Journal of Applied Electrochemistry*, 31(7):799–809, 2001. doi: 10.1023/A:1017587310150.

[13] Demarconnay, L., Brimaud, S., Coutanceau, C. et al. Ethylene glycol electrooxidation in alkaline medium at multi-metallic Pt based catalysts. *Journal of Electroanalytical Chemistry*, 601:169–180, 2007. doi: 10.1016/j.jelechem.2006.11.006.

[14] Habibi, E. Kinetics of ethylene glycol electrooxidation on the noble metal-based nano-catalysts. *Journal of the Iranian Chemical Society*, 14(9):1983–1991, 2017. doi: 10.1007/s13738-017-1136-7.

[15] An, L. and Chen, R. Recent progress in alkaline direct ethylene glycol fuel cells for sustainable energy production. *Journal of Power Sources*, 329:484–501, 2016. doi: 10.1016/j.jpowsour.2016.08.105.

[16] Stuve, E.M. and Spies, K.A. Reaction Pathways and Current Efficiency for Electrooxidation of Ethylene Glycol at Intermediate Temperatures. *ECS Transactions*, 58(1):1723–1731, 2013. doi: 10.1149/05801.1723ecst.

[17] Stuve, E.M. and Spies, K.A. Hydrogen Generation by Electrocatalyic Reforming of Biomass-Related Compounds: Ethylene Glycol. *ECS Meeting Abstracts*, 53(9):21–28, 2013. doi: 10.1149/05309.0021ecst.

[18] Silva, J.C.M., Ntais, S., Rajaraman, V. et al. The Catalytic Activity of Pt:Ru Nanoparticles for Ethylene Glycol and Ethanol Electrooxidation in a Direct Alcohol Fuel Cell. *Electrocatalysis*, 10(3):203–213, 2019. doi: 10.1007/s12678-019-00515-8.

[19] Serov, A. and Kwak, C. Recent achievements in direct ethylene glycol fuel cells (DEGFC). *Applied Catalysis B: Environmental*, 97:1–12, 2010. doi: 10.1016/j.apcatb.2010.04.011.

[20] Xu, C., Paone, E., Rodríguez-Padrón, D. et al. Reductive catalytic routes towards sustainable production of hydrogen, fuels and chemicals from biomass derived polyols. *Renewable and Sustainable Energy Reviews*, 127(109852):1–11, 2020. doi: 10.1016/j.rser.2020.109852.

[21] Zhao, Z., Jiang, J., Zheng, M. et al. Advancing development of biochemicals through the comprehensive evaluation of bio-ethylene glycol. *Chemical Engineering Journal*, 411(128516):1–12, 2021. doi: 10.1016/j.cej.2021.128516.

[22] Minteer, S.D. 11 - Biochemical production of other bioalcohols: Biomethanol, biopropanol, bioglycerol, and bioethylene glycol. In Luque, R., Campelo, J. and Clark, J., editors, *Handbook of Biofuels Production: Processes and Technologies*, pages 258–265. Woodhead Publishing Limited, 2011. doi: 10.1533/9780857090492.2.258.

[23] Bahena, E., Méndez, P., Meas, Y. et al. An EQCM study of polyethyleneglycol 8000 adsorption and its coadsorption with Cl- ions on Pt in perchloric acid

solutions. *Electrochimica Acta*, 49:989–997, 2004. doi: 10.1016/j.electacta.2003.10.010.

[24] Keily, J.J. and Wesr, A.C. Copper Deposition in the Presence of Polyethylene Glycol: I. Quartz Crystal Microbalance Study. *Journal of The Electrochemical Society*, 145(10):3472–3476, 1998.

[25] Safonova, T.Y., Smirnova, N.V. and Petrii, O.A. Adsorption of polyethylene glycol on platinum electrode from acidic solutions. *Russian Journal of Electrochemistry*, 42(9):995–1000, 2006. doi: 10.1134/S1023193506090163.

[26] Smirnova, N.V. and Kazakova, A.Y. Electrooxidation and adsorption of oligoelthylene glycols on platinized platinum electrode. *Russian Journal of Electrochemistry*, 44(3):353–356, 2008. doi: 10.1134/s1023193508030154.

[27] Hori, T., Kobayashi, K., Teranishi, S. et al. Fuel cell and electrolyzer using plastic waste directly as fuel. *Waste Management*, 102:30–39, 2020. doi: 10.1016/j.wasman.2019.10.019.

[28] Shi, R., Liu, K.S., Liu, F. et al. Electrocatalytic reforming of waste plastics into high value-added chemicals and hydrogen fuel. *Chem. Commun.*, 57: 12595–12598, 2021. doi: 10.1039/D1CC05032J.

[29] Grimaldos-Osorio, N., Sordello, F., Passananti, M. et al. From plastic-waste to H2: A first approach to the electrochemical reforming of dissolved Poly(methyl methacrylate) particles. *International Journal of Hydrogen Energy*, pages 1–15, mar 2022. doi: 10.1016/j.ijhydene.2022.02.229.

[30] O'Hayre, R. and Prinz, F.B. The Air/Platinum/Nafion Triple-Phase Boundary: Characteristics, Scaling, and Implications for Fuel Cells. *Journal of The Electrochemical Society*, 151(5):A756–A762, 2004. doi: 10.1149/1.1701868.

[31] Jiménez-García, J.C., Olmos-Asar, J.A., Franceschini, E.A. et al. Effect of Nafion content and hydration level on the electrochemical area of a Pt nanocatalyst in the triple-phase boundary. *Physical Chemistry Chemical Physics*, 23:27543–27551, 2021. doi: 10.1039/d1cp03731e.

[32] González-Cobos, J., Baranton, S. and Coutanceau, C. A Systematic in Situ Infrared Study of the Electrooxidation of C3 Alcohols on Carbon-Supported Pt and Pt-Bi Catalysts. *Journal of Physical Chemistry C*, 120(13):7155–7164, 2016. doi: 10.1021/acs.jpcc.6b00295.

[33] Sasikumar, G., Ihm, J. and Ryu, H. Dependence of optimum Nafion content in catalyst layer on platinum loading. *Journal of Power Sources*, 132(1-2):11–17, 2004. doi: 10.1016/j.jpowsour.2003.12.060.

[34] Bard, A.J. and Faulkner, L.R. *Electrochemical methods: Fundamentals and Applications*. John Wiley & Sons, Inc., 2nd edition, 2001.

[35] Coutanceau, C. and Baranton, S. Electrochemical conversion of alcohols for

hydrogen production: a short overview. *Wiley Interdisciplinary Reviews: Energy and Environment*, 5(4):388–400, 2016. doi: 10.1002/wene.193.

[36] Wang, H., Jusys, Z. and Behm, R. Ethanol Electrooxidation on a Carbon-Supported Pt Catalyst: Reaction Kinetics and Product Yields. *The Journal of Physical Chemistry B*, 108(50):19413–19424, 2004. doi: 10.1021/jp046561k.

[37] Khouchaf, A., Takky, D., Chbih, M.E.M. et al. Electrocatalytic Oxidation of Methanol on Glassy Carbon Electrode Modified by Metal Ions (Copper and Nickel) Dispersed into Polyaniline Film. *Journal of Materials Science and Chemical Engineering*, 4:97–105, 2016. doi: 10.1016/j.electacta.2007.10.004.

[38] Kim, H.J., Choi, S.M., Green, S. et al. Highly active and stable PtRuSn/C catalyst for electrooxidations of ethylene glycol and glycerol. *Applied Catalysis B: Environmental*, 101:366–375, 2011. doi: 10.1016/j.apcatb.2010.10.005.

[39] Li, Y., Gao, W., Ci, L. et al. Catalytic performance of Pt nanoparticles on reduced graphene oxide for methanol electro-oxidation. *Carbon*, 48:1124–1130, 2010. doi: 10.1016/j.carbon.2009.11.034.

[40] Caravaca, A., Jones, W., Hardacre, C. et al. H2 production by the photocatalytic reforming of cellulose and raw biomass using Ni, Pd, Pt and Au on titania. *Proceedings of the Royal Society A: Mathematical, Physical and Engineering Sciences*, 472(2191), 2016. doi: 10.1098/rspa.2016.0054.

[41] Grimaldos-Osorio, N., Sordello, F., Passananti, M. et al. From plastic-waste to H2: Electrolysis of a Poly(methyl methacrylate) model molecule on polymer electrolyte membrane reactors. *Journal of Power Sources*, 480:228800, 2020. doi: 10.1016/j.jpowsour.2020.228800.

[42] Sone, Y., Ekdunge, P. and Simonsson, D. Proton Conductivity of Nafion 117 as Measured by a Four[U+2010]Electrode AC Impedance Method. *Journal of The Electrochemical Society*, 143(4):1254–1259, 1996. doi: 10.1149/1.1836625.

[43] Tang, S., Sun, G., Qi, J. et al. Review of New Carbon Materials as Catalyst Supports in Direct Alcohol Fuel Cells. *Chinese Journal of Catalysis*, 31(1):12–17, 2010. doi: 10.1016/s1872-2067(09)60034-6.

[44] Raghuveer, V. and Manthiram, A. Mesoporous carbon with larger pore diameter as an electrocatalyst support for methanol oxidation. *Electrochemical and Solid-State Letters*, 7(10):A336–A339, 2004. doi: 10.1149/1.1792264.

[45] Assumpção, M.H., De Souza, R.F., Rascio, D.C. et al. A comparative study of the electrogeneration of hydrogen peroxide using Vulcan and Printex carbon supports. *Carbon*, 49(8):2842–2851, 2011. doi: 10.1016/j.carbon.2011.03.014.

[46] Carmo, M., dos Santos, A.R., Poco, J.G. et al. Physical and electrochemical evaluation of commercial carbon black as electrocatalysts supports for DMFC applications. *Journal of Power Sources*, 173:860–866, 2007. doi: 10.1016/j.jpowsour.2007.08.032.

[47] Raghuveer, V. and Manthiram, A. Mesoporous Carbons with Controlled Porosity as an Electrocatalytic Support for Methanol Oxidation. *Journal of The Electrochemical Society*, 152(8):A1504–A1540, 2005. doi: 10.1149/1.1940767.

[48] Li, X., Qiu, X., Yuan, H. et al. Size-effect on the activity of anodic catalysts in alcohol and CO electrooxidation. *Journal of Power Sources*, 184:353–360, 2008. doi: 10.1016/j.jpowsour.2008.03.058.

[49] Mukerjee, S. and McBreen, J. Effect of particle size on the electrocatalysis by carbon-supported Pt electrocatalysts: An in situ XAS investigation. *Journal of Electroanalytical Chemistry*, 448:163–171, 1998. doi: 10.1016/S0022-0728(97)00018-1.

[50] Okonkwo, P.C., Ben Belgacem, I., Emori, W. et al. Nafion degradation mechanisms in proton exchange membrane fuel cell (PEMFC) system: A review. *International Journal of Hydrogen Energy*, 46:27956–27973, 2021. doi: 10.1016/j.ijhydene.2021.06.032.

[51] Tang, Q., Li, B., Yang, D. et al. Review of hydrogen crossover through the polymer electrolyte membrane. *International Journal of Hydrogen Energy*, 46 (42):22040–22061, 2021. doi: 10.1016/j.ijhydene.2021.04.050.

[52] Azri, A., Giamarchi, P., Grohens, Y. et al. Polyethylene glycol aggregates in water formed through hydrophobic helical structures. *Journal of Colloid and Interface Science*, 379:14–19, 2012. doi: 10.1016/j.jcis.2012.04.025.

[53] Azri, A., Privat, M., Grohens, Y. et al. Linear rheological properties of low molecular weight polyethylene glycol solutions. *Journal of Colloid and Interface Science*, 393:104–108, 2013. doi: 10.1016/j.jcis.2012.10.059.

[54] Almásy, L., Artykulnyi, O.P., Petrenko, V.I. et al. Structure and Intermolecular Interactions in Aqueous Solutions of Polyethylene Glycol. *Molecules*, 27 (2573):1–9, 2022. doi: 10.3390/molecules27082573.

[55] Begum, S.K., Ratna, S.A., Clarke, R.J. et al. Excess molar volumes, refractive indices and transport properties of aqueous solutions of poly(ethylene glycol)s at (303.15-323.15) K. *Journal of Molecular Liquids*, 202:176–188, 2015. doi: 10.1016/j.molliq.2014.12.025.

[56] Shulyak, I.V., Grushova, E.I. and Semenchenko, A.M. Rheological properties of aqueous solutions of polyethylene glycols with various molecular weights. *Russian Journal of Physical Chemistry A*, 85(3):419–422, 2011. doi: 10.1134/S0036024411030265.

[57] Beliaeva, K., Elsheref, M., Walden, D. et al. Towards Understanding Lignin Electrolysis: Electro-Oxidation of a β-O-4 Linkage Model on PtRu Electrodes. *Journal of The Electrochemical Society*, 167(134511):1–8, 2020. doi: 10.1149/1945-7111/abb8b5.

[58] Beliaeva, K., Grimaldos-Osorio, N., Ruiz-López, E. et al. New insights into lignin electrolysis on nickel-based electrocatalysts: Electrochemical performances before and after oxygen evolution. *International Journal of Hydrogen Energy*, pages 1–13, 2021. doi: 10.1016/j.ijhydene.2021.01.224.

[59] Mori, S. and Barth, H.G. *Size exclusion chromatographie*. Springer-Verlag GmbH, Berlin, Heidelberg, 1 edition, 1999. doi: 10.1007/978-3-662-03910-6.

[60] Ruiz-López, E., Caravaca, A., Vernoux, P. et al. Over-faradaic hydrogen production in methanol electrolysis cells. *Chemical Engineering Journal*, 396 (125217), 2020. doi: 10.1016/j.cej.2020.125217.

Conclusions and Perspectives

Conclusions and Perspectives

The energy crisis and environmental issues that are currently arising must be addressed from combined approaches. For this reason, the production of hydrogen by co-electrolysis of water with organic wastes seems to be a promising technology since, in theory, it would allow to reduce the energetic needs (compared with the state-of-the-art water electrolysis process), while employing a feedstock that otherwise is considered as a waste. The different works presented throughout this thesis manuscript are a proof-of-concept of the valorisation of plastic wastes by electrochemical methods. A strategical choice about the polymeric molecules was the reason for employing both polymethyl methacrylate (PMMA) and polyethylene glycol (PEG). These two polymers allowed us to understand the different phenomena involved in their electro-oxidation, the main advantages and drawbacks, as well as the possible research paths that could be followed to overcome the limitations of this technology. The most important results, the final conclusions and the possible research paths are described below.

Four main studies were performed to understand the electrolysis of organic macromolecules in low temperature electrochemical devices. The first three chapters presented preliminary findings on the electro-oxidation of PMMA. Initially, a model molecule (methyl pivalate, MP) was used to establish a starting point towards the treatment of more complex samples of PMMA. The results presented in Chapter 2 using a proton exchange membrane (PEM) reactor and commercial state-of-the-art electrode materials (0.2 mg cm^{-2} of 20% Pt/C_{vulcan} on carbon cloth), allowed us to evaluate the impact of the concentration and the temperature in the kinetics of the electrochemical oxidation of MP. Low temperatures (<80 °C) and applied potentials below the Oxygen Evolution Reaction (OER) (<1.2 V) seemed to promote the cleavage of the ester group of the model molecule. This reaction likely led to the production of the corresponding carboxylic acid (pivalic acid, PA) and methoxy-like species. The further electro-oxidation of the latter would lead to the production of carbon dioxide on the anodic side and pure hydrogen on the cathodic side of the PEM cell. In the same way, a progressive decrease of the overall activity of the system was observed, probably to the accumulation on active Pt sites of chemisorbed species produced by the partial oxidation of MP. These preliminary results allowed to get more insights regarding the potential reaction paths of the PMMA electro-oxidation.

To go a step further into the treatment of real PMMA samples, an approach using a dissolution strategy was the research subject of the Chapter 3. The intention of that study was to explore the electro-oxidation of low molecular weight PMMA (10 kg mol^{-1}), which is a solid at room temperature and atmospheric pressure. To limit

the transport issues of the solid material in the working electrode (the anode), a binary solvent composed of isopropanol/water was used to dissolve the PMMA chains by taking advantage of their polarities. The electro-oxidation of the PMMA/binary solvent solutions was investigated in a two-electrode cell arrangement with an acid liquid electrolyte, initially employing the same commercial electrode as the MP study. It was found that the electrochemical oxidation of isopropanol (the main component of the binary solvent) took place in the range of applied potentials (0 – 1.4 V). Moreover, the presence of PMMA hindered the overall behaviour of the system, likely because of the accumulation of macromolecular species at the anodic surface. In order to overcome this problem, a macroporous anode support (by using carbon paper instead of carbon cloth) with a higher loading of a home-made catalyst (1 mg cm^{-2} of 20% Pt/C_{vulcan}, prepared by the polyol method) was developed and tested. This new electrode showed a slightly better performance regarding the electrochemical transformation of PMMA, as confirmed by Fourier-Transform Infrared Spectroscopy (FTIR) measurements. The electro-oxidation of PMMA under these conditions may happen by the same mechanism proposed for the case of MP, but further studies should be performed to better conclude about the involved mechanisms. Even if the results present in Chapter 3 established a series of first findings on the electro-oxidation of low molecular weight PMMA samples, the deactivation of the anode material is a problem that should be overcome.

A preliminary series of experiments were also performed using synthesised samples of PMMA nanoparticles in suspension. The synthesis of nanoparticle colloids was carried out by the emulsifier free-emulsion polymerisation method. The ratio of monomer/initiator was investigated aiming to obtain PMMA samples of different molecular weights (100 – 750 kg mol^{-1}). These colloids were further studied for the generation of hydrogen, seeking for a system closer to the real-life application where PMMA samples may undergo a preliminary selection and grinding process. At the electrochemical level, a poor activity was registered. This may be due to the same limitations that were exposed for the electro-oxidation of dissolved PMMA samples. In both cases, it seemed that the electrochemical performance was likely dominated by mass-transport phenomena. Therefore, the use of low porosity anode materials is not the best option for these applications. We found that the concentration nor the molecular weight of the polymer affected the general electrochemical behaviour. In view of these results, a second approach with a more porous anode and an aggressive pre-treatment (both in acid and alkaline conditions) of the polymer was tested in a broader range of applied potentials. Unfortunately, no significant improvements were observed either. We believe that the fact that PMMA presents only C–C bond in the main chain coupled with transport limitations in the mesopores of the anode make the electro-oxidation a highly complex process.

Further studies on the morphology of the anode materials are required to avoid the mass transport issues.

Until here, PMMA was the only polymeric material studied. In order to get more insights into the understanding of the reaction pathways that other polymeric materials can follow, a complete series of experiments was carried out dealing with the electro-oxidation of polyethylene glycol (PEG), a macromolecular compound that presents C–O bonds in the main chain. For the final chapter of this thesis, a Proton Exchange Membrane (PEM) reactor using Pt/C-based anode materials was employed. The anode formulation was optimised to maximise the activity by investigating the thickness of the Gas Diffusion Layer and the ionomer content in the coating. Similarly, we found that the use of a better dispersed Pt-based commercial catalyst enhanced the obtained current. The influence of the reaction temperature, as well as the impact of concentration and molecular weight of PEG molecules (in a low M_w range, from 200 to 4000 g mol^{-1}) was studied. Furthermore, the products of electro-oxidation were analysed by size-exclusion chromatography. A significant reduction of the PEG molecular weight in the anodic solution was evidenced after a chrono-amperometry at 0.8 V and 80 °C for 5 h. To the best of our knowledge, this is the first time that the reduction of the macromolecules size by electrochemical mean was reported. The process may undergo by two main routes, involving weakly adsorbed or strongly chemisorbed species, although further characterisations of the system and reaction products (in the liquid and gas phases) are required in order to propose a more detailed reaction mechanism. Finally, the production and purity of hydrogen in the cathode compartment was verified by mass spectrometry, and a faradaic efficiency of ∼100% was calculated.

The works presented throughout this manuscript are an exploratory attempt to propose a new method to take advantage of the organic nature of polymeric materials to produce hydrogen. The production of hydrogen from these macromolecular compounds was shown to be possible, but it was proved to be a complex process that is affected by several factors. Nevertheless, the results provide valuable information about the limitations of this approach and the paths to follow in the future. To significantly improve the overall activity of the electrochemical systems for the oxidation of macromolecules, we propose to address several breakthroughs. The first one is the design of more porous and active anode materials, specifically conceived to favour the diffusion of macromolecules. One can image, for example, materials such as metallic foams or carbon-based macroporous supports loaded with advanced catalytic materials for these specific processes.

Another important factor to consider is the nature of the polymeric materials appropriate for the electrochemical treatment. Macromolecules with C–O bonds

in their main chain seem to be more appropriate, as a reduction of the size of the polymer-chain is possible. Here we investigated a water-soluble polymer (PEG), a study that could be continued by exploring a larger range of molecular weights. This would allow to clarify the reaction mechanism for the electro-oxidation of this family of compounds. It is also important to perform a deeper characterisation of the anodic products, for example, by using a variety of spectroscopic techniques to get more insights about the intermediate species and the different interactions taking place at the catalyst active sites. In this sense, it would also be interesting to analyse the gas phase on that side of the PEM reactor, in order to quantify the production of volatile organic compounds, as well as CO and CO_2. Once a more specific mechanism has been established, further research with other C – O bond-containing polymers could be considered. Materials such as polyurethanes and polyethylene terephthalate could be possible options for future investigations, but a dissolution strategy may have to be considered for reducing the technical limitations.

The results presented here can be considered therefore as a starting point for the production of hydrogen by the electrochemical treatment of plastic wastes. Of course, further research should be carried out in view of its practical application. The literature on the applicability of electrochemical strategies for the treatment of plastic waste is still very limited, but we believe we are in the right path towards the valorisation of these residues to produce hydrogen, aimed to be the most relevant energy vector of the near-future.